CHEMICAL STUDY OF THE BLACKLEG FUNGUS: METABOLITES, PHYTOTOXINS AND PHYTOALEXINS

A thesis submitted to the

College of Graduate Studies and Research

In partial fulfillment of the requirements

For the degree of

Doctor of philosophy in the

Department of Chemistry

University of Saskatchewan

Saskatoon

by

Paulos Barbe Chumala

Permission to use

In presenting this thesis in partial fulfillment of the requirements for a postgraduate degree from the University of Saskatchewan, the author has agreed that the libraries of this University may make it freely available for inspection. The author further agrees that permission for copying of this thesis in any manner, in whole or in part, for scholarly purposes may be granted by the professor who supervised the thesis work or, in her absence, by the Head of the Department of Chemistry, or the Dean of the College of Graduate Studies and Research. It is understood that copying or publication or use of this thesis or parts thereof for financial gain shall not be allowed without the author's written permission. It is also understood that due recognition shall be given to the author and to the University of Saskatchewan in any scholarly use which may be made of any material in my thesis.

Requests for permission to copy or to make other use of material in this thesis in whole or part should be addressed to:

The Head
Department of Chemistry
University of Saskatchewan
Saskatoon, Saskatchewan, CANADA
S7N 5C9

Abstract

New isolates Mayfair 2 and Laird 2 of the blackleg fungus [*Phoma lingam*, perfect stage *Leptosphaeria maculans* (Desm.) Ces. et de Not.] cause blackleg on the traditionally resistant brown mustard (*Brassica juncea*). Mayfair 2/Laird 2 isolates of the blackleg fungus produce a diverse array of secondary metabolites in liquid cultures in minimal media. The isolation (FCC, RP-FCC, prep TLC) and characterization (NMR, MS, X-ray) of these metabolites resulted in the identification of four groups of compounds: polanrazines, sesquiterpenes, phomapyrones, and depsilairdin, where eleven of them were new. Phytotoxic assays conducted with these metabolites on *B. napus* (resistant), *B. juncea* (susceptible), and *S. alba* (resistant) indicated depsilairdin (**122**) to be a host-selective toxin. Studies on the biosynthetic origin of phomapyrone A suggested phomapyrones to be of polyketide origin.

Sixteen Thlaspi isolates of blackleg fungus originating from Saskatchewan were characterized on the basis of their secondary metabolite profiles, and it was determined that two of them were Polish type isolates and the remaining fourteen were weakly virulent type isolates.

The investigation of *Thlaspi arvense* (stinkweed) for phytoalexins led to the isolation of two phytoalexins: arvelexin (**142**) and wasalexin A (**38**). The structures of these phytoalexins as well as that of isovitexin, a secondary metabolite of *T. arvense*, were established based on spectroscopic methods and by synthesis. Arvelexin, as a phytoalexin, was reported for the first time here, but wasalexin A was previously reported from wasabi (*Wasabia japonica*, syn. *Eutrema wasabi*). Arvelexin (**142**) exhibited similar antifungal activity as indole-3-acetonitrile against *L. maculans*/*P. lingam*.

The secondary metabolites potentially involved in mediating the interactions between *Brassica* species and the new blackleg isolates Mayfair 2 and Laird 2 were analysed in infected plant tissues by HPLC. The host-selective toxins phomalairdenone A

(**55**) and depsilairdin (**122**), and phytoalexins, brassinin (**35**), rutalexin (**137**) and spirobrassinin (**138**) were detected in *B. napus*, whereas brassilexin (**139**) and sinalexin (**140**) were detected in *S. alba*, and brassilexin (**139**) was detected in *B. juncea*.

Acknowledgements

First of all, I am very grateful to God for the successful completion of my Ph.D. program. I would like to sincerely thank my supervisor, Professor M. Soledade C. Pedras for her excellent supervision and consistent support in the course of this work. Her persistent guidance and open mindedness immensely contributed to the successful completion of this work.

I would like to thank the members of my advisory committee: Prof. M. Majewski, Prof. H. B. Kraatz, Prof. J. R. Dimmock and Prof. W. Quail for their advice and help during the program. I also thank my external examiner, Dr. Paul Harrison for his suggestions and advice. Special thanks to Prof. W. Quail for performing crystallographic analysis.

I am very grateful to all past and present members of the Pedras group: Dr. P. W. K. Ahiahonu, Dr. R. Gadagi, Dr. N. Ismail, Dr. S. Montaut, Dr. O. Okeola, Dr. M. Suchy, Dr. V. Uppala, Dr. Y. Xu, Dr. I. L. Zaharia, Dr. Q. A. Zheng, Dr. Y. Zhou, C. Biesenthal, V. Cekic, M. Hossain, M. Jha, J. Liu, L. Liu, D. Okinyo, C. Nycholat, G. Sarwar, and Y. Yu. Special thanks to C. Biesenthal for introducing me to the microbiological preparations.

I wish to thank the Department of Chemistry and the University of Saskatchewan for financial support. Special thanks to Dr. Keith Brown and Mr. Ken Thoms for their technical assistance.

Finally I express my deepest gratitude to my wife Yeshi Ele Yaya, to families and friends for their encouragement and support in prayer.

Dedication

To my parents,

Arbe Uta and Barbe Chumala

To my wife,

Yeshi

TABLE OF CONTENTS

Permission to use ..... **i**

Abstract ..... **ii**

Acknowledgements ..... **iv**

Dedication ..... **v**

Table of contents ..... **vi**

List of tables ..... **ix**

List of figures ..... **xi**

List of abbreviations ..... **xiii**

List of Structures ..... **xvi**

CHAPTER ONE **1**

1. Introduction **1**

1.1 General objectives 1

1.2 The Blackleg fungus 2

1.2.1 Life cycle and infection strategies 2

1.2.2 Classification 3

1.3 Secondary metabolites 10

1.3.1 Major classes of secondary metabolites 11

1.3.2 Chemotaxonomy 12

1.3.3 Plant metabolites: chemical defenses 14

1.3.4 Microbial metabolites 23

1.3.4.1 Metabolites from the blackleg fungus 24

1.3.4.2 Host-selective toxins 27

1.4 Conclusion: plant-fungal interactions 55

CHAPTER TWO **58**

2. Results and Discussion **58**

2.1 Metabolites from *Phoma lingam/Leptosphaeria maculans* 58

2.1.1 Metabolites produced in minimal medium (MM) 58

2.1.1.1 Isolation of metabolites 58

2.1.1.2 Structure determination 64

2.1.2 Metabolites produced in PDB medium 121

2.2 Phytotoxicity bioassays 124

2.3 Analysis and classification of Thlaspi isolates and avirulent isolates from France 128

2.4 Biosynthetic studies of phomapyrones 133

2.5 HPLC analysis of metabolites produced in infected plants 141

2.6 Phytoalexins from the wild species *Thlaspi arvense* 145

2.6.1 Elicitation, isolation and chemical structure determination of metabolites from Thlaspi arvense (stinkweed) 145

2.6.2 Antifungal bioassays of elicited metabolites 152

CHAPTER THREE **155**

3. Conclusions and Future Work **155**

CHAPTER FOUR **158**

4. Experimental **158**

4.1 General methods 158

4.2 The Blackleg fungi 160

4.2.1 Fungal cultures (MM) and extractions 160

4.2.2 Isolation of metabolites 161

4.2.3 Hydrolysis of despilairdin 170

4.2.4 Determination of the absolute stereochemistry of **123** by synthesis 171

4.3 Metabolites from the cultures of Mayfair 2 in PDB medium 180
4.4 Biosynthetic studies of Phomapyrones 182
4.4.1 A preliminary study 182
4.4.2 Feeding experiment using [2-^{13}C]acetate 183
4.4.3 Feeding experiment using [1,2-^{13}C]acetate 184
4.4.4 Feeding experiment using sodium[2-^{13}C]malonate 184
4.4.5 Feeding experiment using [3,3,3-d_3]propionate 185
4.5 Phytotoxicity assays 185
4.6 Brine shrimp lethality assay 186
4.7 HPLC analysis of cultures of Thlaspi isolates 187
4.8 Phytoalexins from *Thlaspi arvense* 187
4.8.1 Time-course study for the production of phytoalexins 187
4.8.2 Elicitation of phytoalexins with Laird 2 and Thlaspi isolates 188
4.8.3 Elicitation, extraction and isolation of phytoalexins from *T. arvense* plants 188
4.8.4 Preparation of 4-methoxyindole-3-acetonitrile 191
4.8.5 Mycelial radial growth bioassays 192
4.8.6 Spore germination bioassays 192
4.9 The plant-fungal interaction studies 193
5. References 194

List of tables

Table 2.1 ^{1}H NMR (500 MHz) data (ppm) of phomapyrones D (**100**), E (**101**), F (**102**), G (**104**), phomenin B (**105**), and infectopyrone (**103**) ($CDCl_3$)..... 77

Table 2.2 ^{13}C NMR (125 MHz) data of phomapyrones D (**100**), E (**101**), F (**102**), G (**104**), phomenin B (**105**), and infectopyrone (**103**) ($CDCl_3$)..... 78

Table 2.3 ^{1}H (500 MHz) and ^{13} C NMR (125 MHz) data (ppm) of phomalairdenone D (**114**) and 3-oxosilphinene (**115**) (C_6D_6)..... 86

Table 2.4 ^{1}H NMR (500 MHz) data of phomalairdenols B (**116**), A (**117**), C (**118**), and D (**119**) (C_6D_6)..... 97

Table 2.5 ^{13}C NMR (125 MHz) data (ppm) of phomalairdenols B (**116**), A (**117**), C (**118**), and D (**119**) (C_6D_6)..... 98

Table 2.6 ^{1}H NMR (500 MHz) and ^{13}C NMR (125 MHz) data (ppm) of **120** and **121** (C_6D_6)..... 104

Table 2.7 ^{1}H NMR (500 MHz) and ^{13}C NMR (125 MHz) data (ppm) of depsilairdin (**122**) (C_6D_6)..... 112

Table 2.8 ^{1}H NMR (500 M Hz) and ^{13}C NMR (125 MHz) data (ppm) of 3,6-diisopropyl-4-methyl-2,5-morpholinedione (**123**) (C_6D_6)..... 116

Table 2.9 ^{1}H NMR (500 MHz) and ^{13}C NMR (125 MHz) data of compound A (**136**) (CD_3CN) 123

Table 2.10 Results of phytotoxicity assays of metabolites produced by isolate Mayfair 2. 127

Table 2.11 Toxicity of some metabolites isolated from Mayfair 2 to brine shrimp .. 128

Table 2.12 Classification of Thlaspi isolates based on the secondary metabolite profiles 132

Table 2.13 Conditions for feeding labeled precursors to cultures of Mayfair 2 135

Table 2.14 Incorporation data from sodium [2-^{13}C] acetate and sodium [2-^{13}C] malonate feeding experiments based on the ^{13}C NMR (125 MHz) of phomapyrone A (**49**). 140

Table 2.15 Secondary metabolites detected in infected *B. napus*, *B. juncea* and *S. alba*143

Table 2.16 Elicitation of phytoalexins in leaf tissue of *Thlaspi arvense* using $CuCl_2$ as elicitor 147

Table 2.17 ^{1}H NMR and ^{13}C NMR of 4-methoxyindole-3-acetonitrile (**142**) 150

Table 2.18 ^{1}H NMR and ^{13}C NMR data in DMSO-d_6 of isovitexin (**143**) 151

Table 2.19 Antifungal activity of metabolites isolated from *Thlaspi arvense* (stinkweed) 153

Table 2.20 Spore germination bioassay results on *Leptosphaeria maculans*/*Phoma lingam* (BJ 125 and Thl 9) with wasalexin A (**38**) after 30 hr incubation 154

List of figures

Figure 1. Proposed chemical markers of virulent isolates of *Leptosphaeria maculans*. 8

Figure 2. Proposed chemical markers of avirulent isolates of *Leptosphaeria maculans*.8

Figure 3. Proposed chemical markers of avirulent Polish type isolates of *Leptosphaeria maculans*. 9

Figure 2.1 Selected HMBC and NOE correlations of phomapyrone D (**100**) 65

Figure 2.2 Selected HMBC and NOE correlations of phomapyrone E (**101**)..... 67

Figure 2.3 Selected HMBC and NOE correlations of phomapyrone F (**102**)..... 69

Figure 2.4 Selected NOE correlations of infectopyrone (**103**) 71

Figure 2.5 Selected HMBC and NOE correlations of phomapyrone G (**104**) 73

Figure 2.6 Selected HMBC and NOE correlations of phomenin B (**105**) 75

Figure 2.7 A: Fragment; B: selected HMBC correlations; C: NOE correlations of **114**83

Figure 2.8 A: Fragment; B: selected HMBC correlations; C: NOE correlations of **115**84

Figure 2.9 Fragments A, B and C of phomalairdenol B (**116**)..... 87

Figure 2.10 A: selected HMBC correlations; B: NOE correlations of **116** 88

Figure 2.11 Fragments A, B and C of phomalairdenol A (**117**) 90

Figure 2.12 A: selected HMBC correlations; B: NOE correlations of **117** 91

Figure 2.13 A: Fragment; B: selected HMBC correlations; C: NOE correlations of **118**93

Figure 2.14 Fragments A, B and C for compound **119**..... 94

Figure 2.15 A: selected HMBC correlations; B: NOE correlations of **119** 95

Figure 2.16 Fragments A, B and C for compound **120**..... 100

Figure 2.16 Fragment A and B of compound **121** 102

Figure 2.18 Fragments A, B and C for compound **122**..... 106

Figure 2.19 Fragment D with selected HMBC correlations for compound **122**..... 107

Figure 2.20 Fragment E with selected HMBC and $^{3}J_{1H\text{-}1H}$ correlations for compound **122** 108

Figure 2.21 Fragment F, G and H with HMBC and $^{3}J_{1H\text{-}1H}$ correlations for compound **122** 109

Figure 2.22 Fragment I with HMBC and $^{3}J_{H\text{-}H}$ correlations for compound **122**..... 110

Figure 2.23 Fragment A and B with HMBC and $^{3}J_{H\text{-}H}$ correlations for compound 123114

Figure 2.24 ^{1}H NMR signal(s) of H-6 for A) 2:1 mixture of 128 and 135; B) hydrolysis product, 123; C) 80:20 mixture of 123 and 128; d) 80:20 mixture of 123 and 135 120

Figure 2.26 Effect of depsilairdin (**122**) assayed at the concentration of 5×10^{-4} M on punctured leaves of two-week-old *Sinapis alba*, *Brassica juncea* and *Brassica napus* after one week of incubation in a growth chamber. 126

Figure 2.27 Chromatograms of extracts of cultures of Thl 23 and avirulent..... 130

isolates..... 130

Figure 2.28 Chromatograms of extracts of cultures of Thl 4 and Mayfair 2 isolates 130

Figure 2.29 Biosynthesis of phomapyrone A (**49**): A) incorporation of sodium [2-^{13}C]acetate, B) incorporation of sodium [1,2-$^{13}C_2$]acetate, C) incorporation of sodium [2-^{13}C]malonate..... 137

Figure2.30 Biosynthesis of phomapyrone A (**49**): A) incorporation of [Me-$^{2}H_3$]methionine; B) incorporation of 3,3,3-d_3-propionic acid..... 138

Figure 2.31 HPLC profile of extracts of elicited leaves of *Thlaspi arvense*, A: control extract; B: extract from elicited leaves (elicitation performed with $CuCl_2$, arrows indicate peaks of elicited compounds).....146

List of abbreviations

^{13}C NMR	carbon-13 nuclear magnetic resonance
^{1}H NMR	proton nuclear magnetic resonance
AFLP	amplified fragment length polymorphism
B. juncea	*Brassica juncea* (brown mustard)
B. napus	*Brassica napus* (canola)
BJ-125	virulent isolate of *Phoma lingam*
Boc	*tert*-butoxycarbonyl
br	broad
calcd.	calculated
Cbz	benzyloxycarbonyl
CDI	N,N'-carbonyldiimidazole
CI	chemical ionization
COSY	correlation spectroscopy
cv.	cultivar
DAOM 229269	avirulent isolate of *P. lingam*
DAOM 229270	avirulent isolate of *P. lingam*
DMSO	dimethyl sulfoxide
EI	electron impact
Et_2O	diethyl ether
EtOAc	ethyl acetate
EtOH	ethanol
FAB	fast atom bombardment

FCC	flash column chromatography
FTIR	Fourier transformed infrared
h	hours
HMBC	heteronuclear multiple bond correlation
HMQC	heteronuclear multiple quantum correlation
HPLC	high performance liquid chromatography
Hz	Hertz
J	coupling constant
L. maculans	*Leptosphaeria maculans* (blackleg fungus)
m/z	mass/charge ratio
MeI	methyl iodide
MHz	megaHertz
min	minute(s)
MM	minimal medium
mmol	millimole
MS	mass spectrum
NOE	nuclear Overhauser enhancement
P. lingam	*Phoma lingam* (blackleg fungus)
PDA	potato dextrose agar
PDB	potato dextrose broth
ppm	parts per million
prep.TLC	preparative thin layer chromatography
RFLP	restriction fragment length polymorphism
RP-FCC	reverse phase flash column chromatography
rpm	revolutions per minute
R_t	retention time
s	seconds

T. arvense	*Thlaspi arvense* (stinkweed)
THF	tetrahydrofuran
Thl # 9	Thlaspi isolate
TLC	thin layer chromatography
TMS	tetramethylsilyl
UV	ultraviolet
v	volume
wt	weight

List of Structures

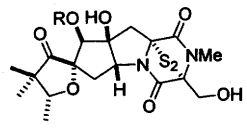

1 R = Ac
2 R = H

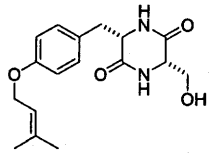

3

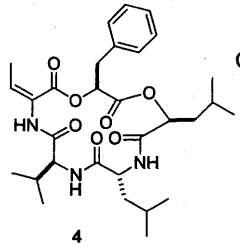

4

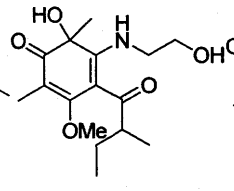

5

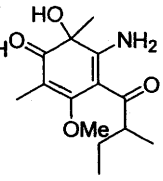

6

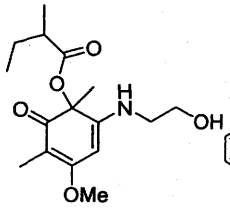

7

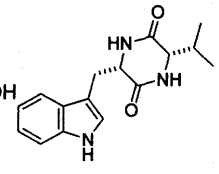

8

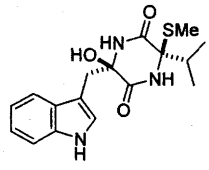

9

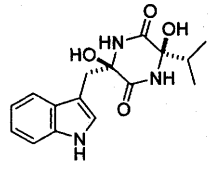

10

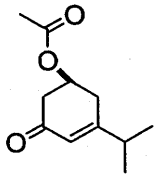

11

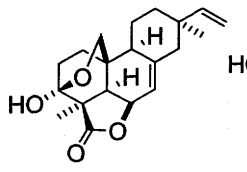

12

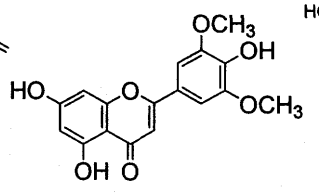

13

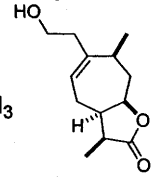

14

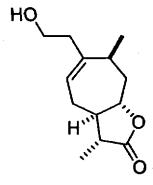

15

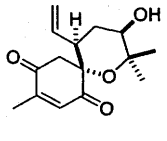

16

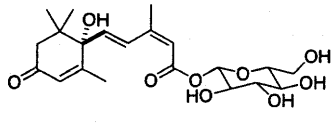

17

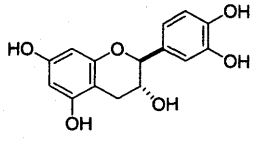

18

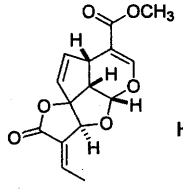

19

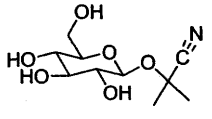

20

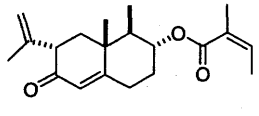

21

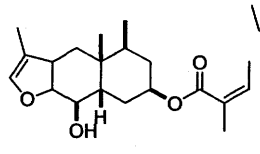

22

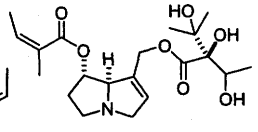

23

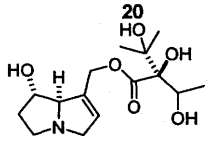

24

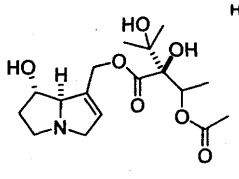

25

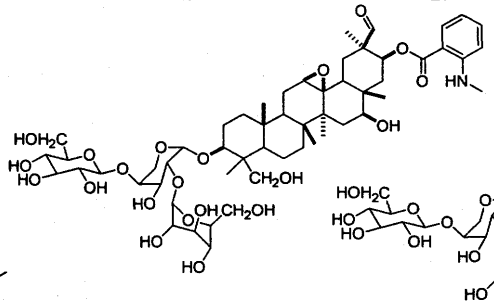

26

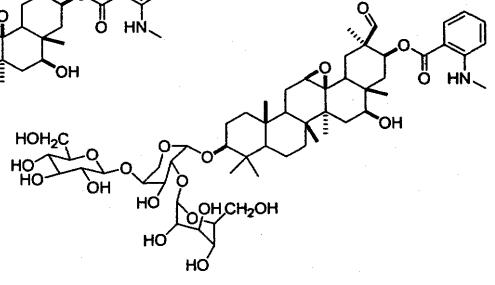

27

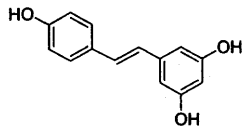

28

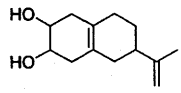

29

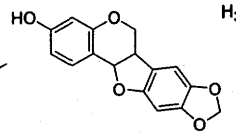

30

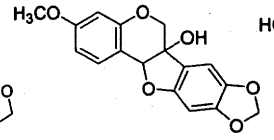

31

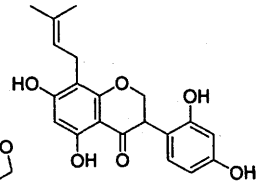

32

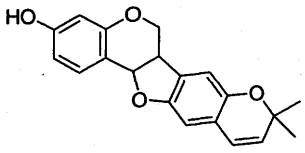

33

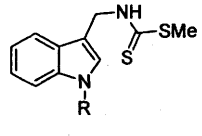

34 R = OMe
35 R = H

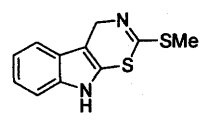

36

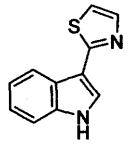

37

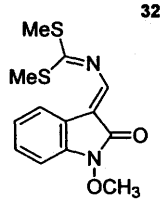

38

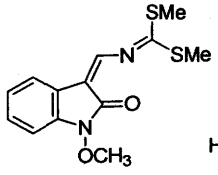

39

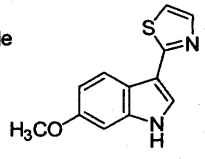

40

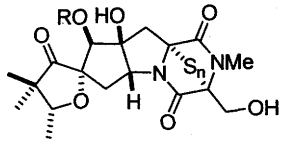

41 R = Ac n=1
42 R = Ac n=3
43 R = Ac n=4

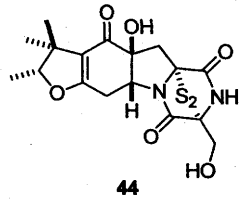

44

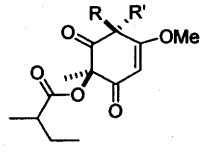

45 R = CH_3, R' = OH
46 R' = CH_3, R = OH

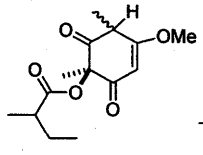

47

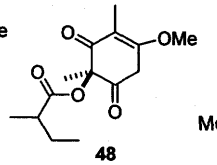

48

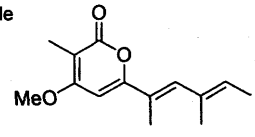

49

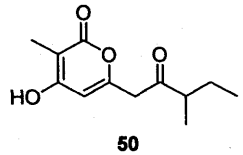

50

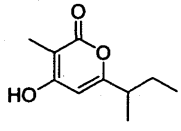

51

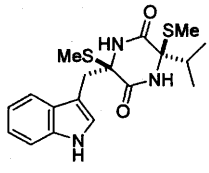

52

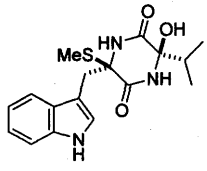

53

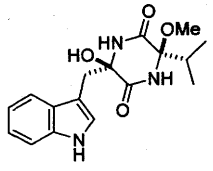

54

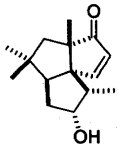

55

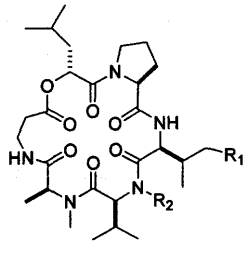

	R1	R2
56	CH_3	H
57	CH_3	CH_3

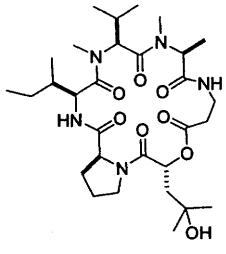

58

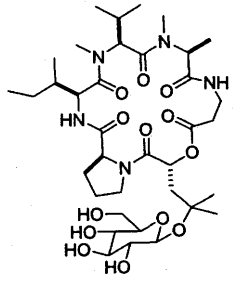

59

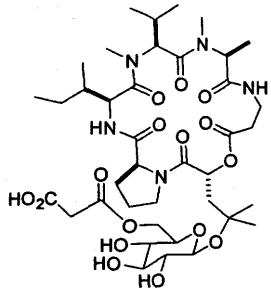

60

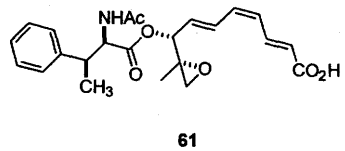

61

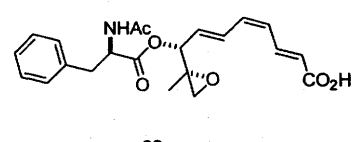

62

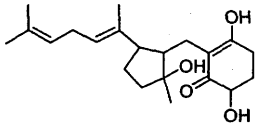

63

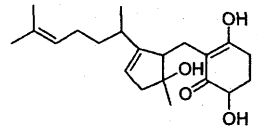

64

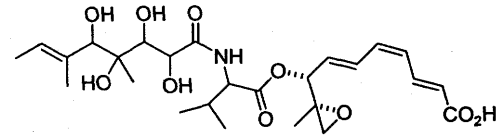

65

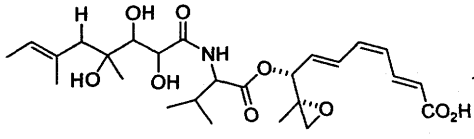

66

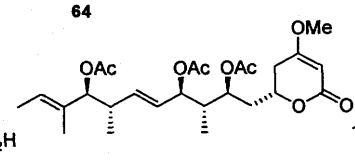

67

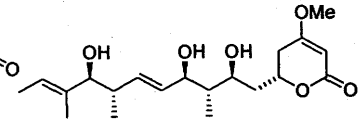

68

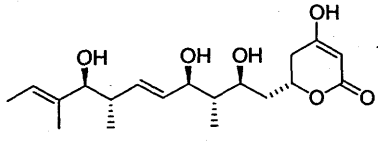

69

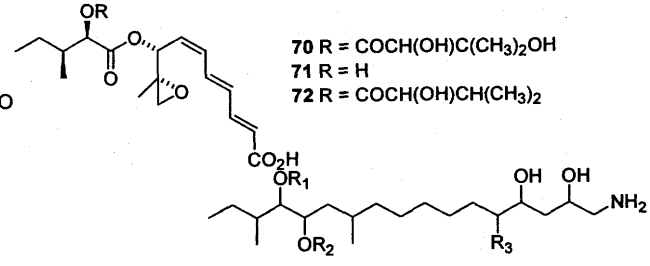

70 R = $COCH(OH)C(CH_3)_2OH$
71 R = H
72 R = $COCH(OH)CH(CH_3)_2$

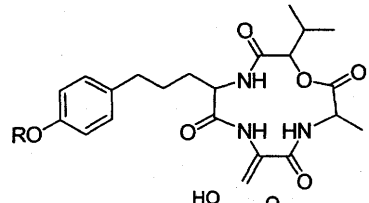

73 R = OCH_3
74 R = H
75 R = OH

		R1	R2	R3
T_A	76	H	Y	OH
	77	Y	H	OH
T_B	78	H	H	H
	79	Y	Y	H

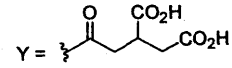

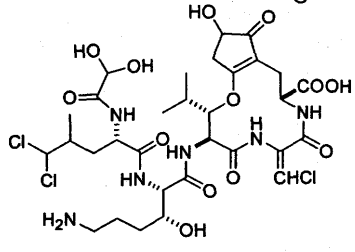

80

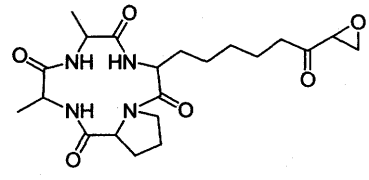

81

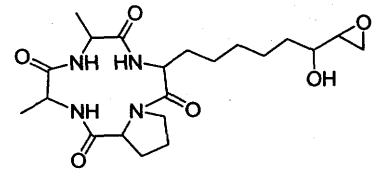

82

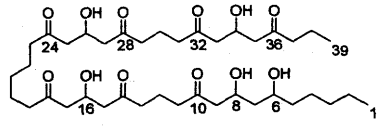

83

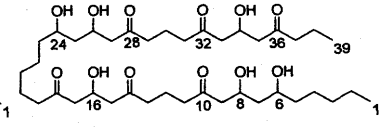

84

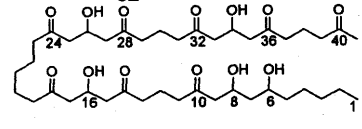

85

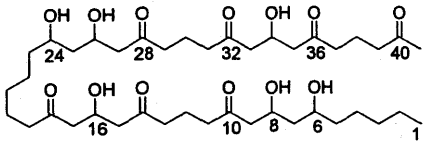

86

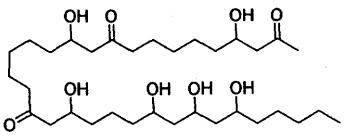

87

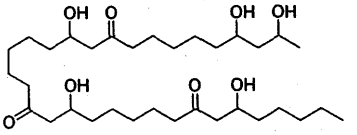

88

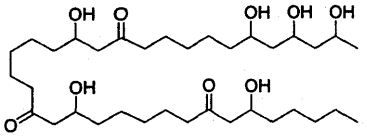

89

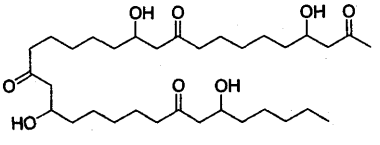

90

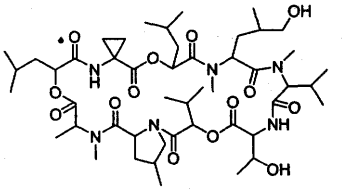

91

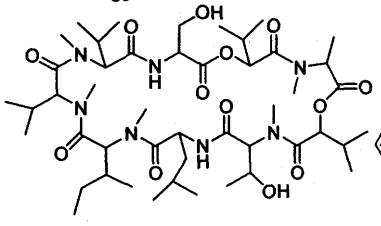

92

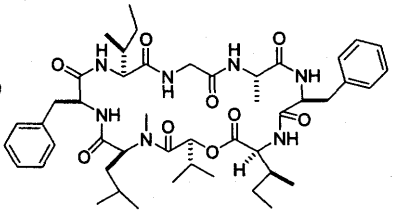

93

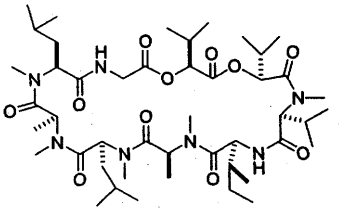

94

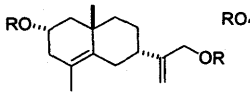

95

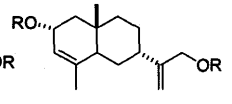

96

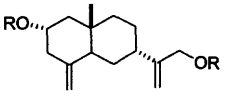

97

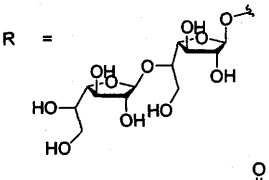

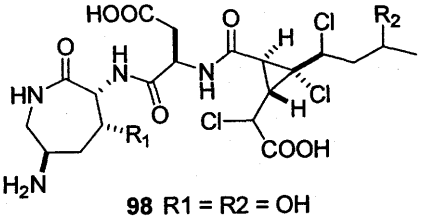

98 R1 = R2 = OH

99 R1 = OH, R2 = H

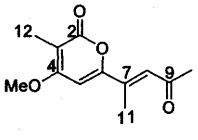

100

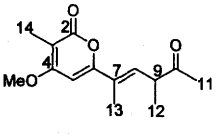

101

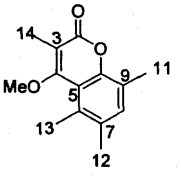

102

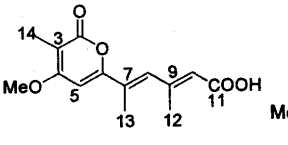

103

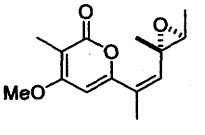

104

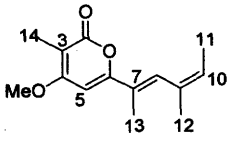

105

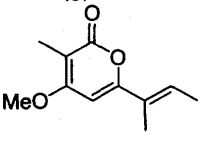

106

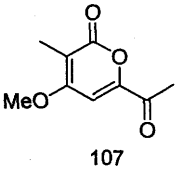

107

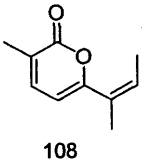

108

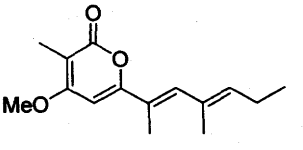

109

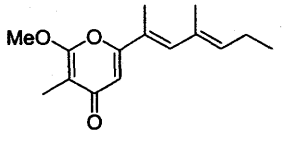

110

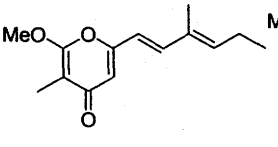

111

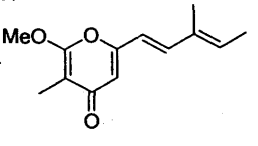

112

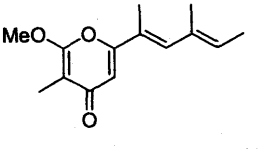

113

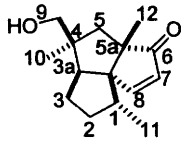

114

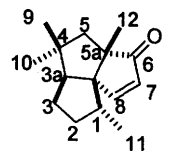

115

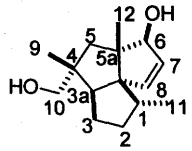

116

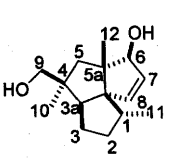

117

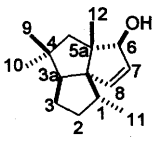

118

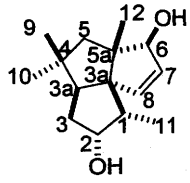

119

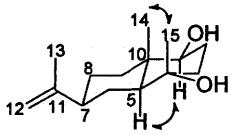

120

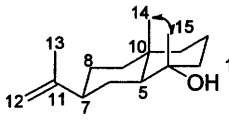

121

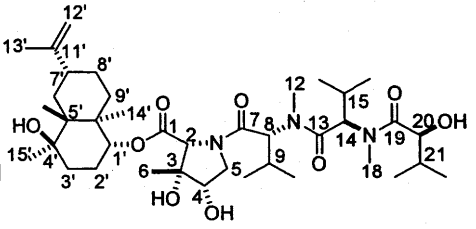

122

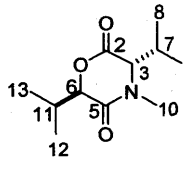

123

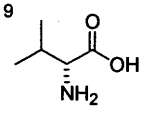

124

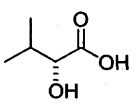

125

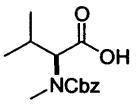

126

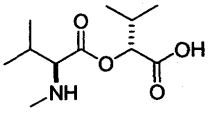

127

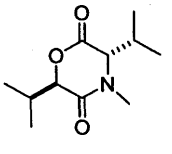

128

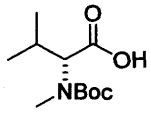

129

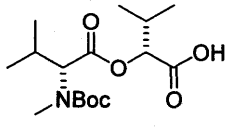

130

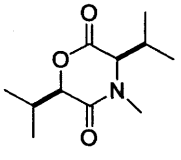

131

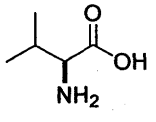

132

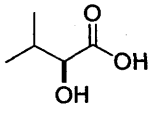

133

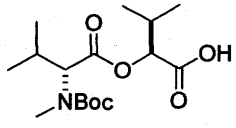

134

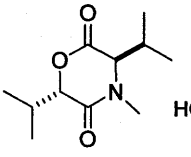

135

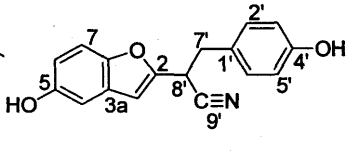

136

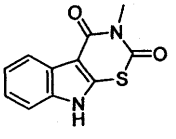

137

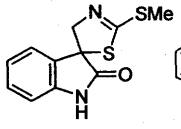

138

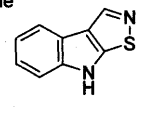

139

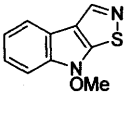

140

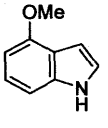

141

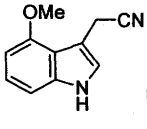

142

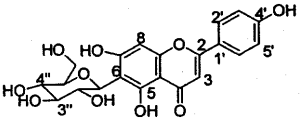

143

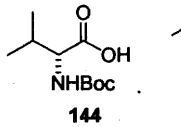

144

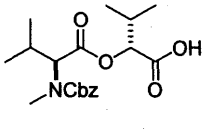

145

CHAPTER ONE

1. Introduction

1.1 General objectives

This thesis describes and discusses the secondary metabolites of new blackleg fungal isolates Mayfair 2 and Laird 2 (*Phoma lingam*, perfect stage *Leptosphaeria maculans* (Desm.) Ces. et de Not.), the use of secondary metabolite profiles in differentiation and grouping of blackleg isolates, and the interaction of new blackleg isolates Mayfair 2 and Laird 2 with susceptible and resistant cruciferous plants from cultivated and wild species. The susceptible cruciferous plants were *Brassica juncea* and *Sinapis alba*, whereas the resistant cruciferous plants were *B. napus* and *Thlaspi arvense*. The research involved:

(1) Establishing the secondary metabolite profiles of new blackleg fungal isolates that will assist in the chemotaxonomic reclassification of the species *P. lingam/L. maculans*.

(2) Determination of the phytotoxic activity of new metabolites against resistant and susceptible plant species.

(3) Studies of the biosynthetic origin of secondary metabolites.

(4) Elicitation and isolation of phytoalexins from the resistant wild crucifer *Thlaspi arvense*.

(5) Investigation of metabolites produced in infected plant tissues.

This work is part of ongoing research to understand the mechanism of blackleg disease development and its control in *Brassica* species. It is hoped that results of this work will provide valuable information for understanding the pathogen and the disease.

1.2 The Blackleg fungus

The blackleg fungus [*Phoma lingam*, perfect stage *Leptosphaeria maculans* (Desm.) Ces. et de Not.] is the causative agent of one of the most devastating diseases of cruciferous crops which is commonly called blackleg or stem canker disease (Gugel and Petrie 1992). In particular, it is a devastating disease for rapeseed and canola (*Brassica napus* and *B. rapa*) oilseed crops worldwide. The disease has caused enormous yield losses in many parts of the world including Canada, UK, France, Germany, and Australia. For instance, in Canada alone, crop losses caused by blackleg disease exceed tens of millions of dollars annually (Gugel and Petrie 1992; Howlett et al., 2001). The increasing epidemics of blackleg in many parts of the world have been a major problem for expanding oilseed industries during the last two decades. These problems plus the complexity of the blackleg fungus attracted the attention of many researchers to investigate its biology and pathogenicity, as well as differentiation methods (Williams, 1992; Howlett et al., 2001).

1.2.1 Life cycle and infection strategies

The blackleg fungus survives as a saprophyte colonizing the dead tissues of previously infested crop debris. Pseudothecia on infested crop debris release ascospores under suitable conditions of temperature, radiation and high relative humidity (Williams, 1992). The ascospore production from infested crop debris continues until complete decomposition of the debris, which usually takes about four years (Williams, 1992; Gabrielson, 1983). The ascospores spread mainly by wind from one field to another field. These airborne ascospores are therefore the primary inoculum of blackleg epidemics. The ascospores landing on young leaves or cotyledons gain entry into host plant tissues through stomates and wounds (Hammond and Lewis, 1987; Williams, 1992). Once the fungus invade the host cell, it induces cell death in leaves resulting in grayish to dirty

white colored lesions with variable size and shape. Leaf lesions usually contain large numbers of speckled small, black asexual fruiting bodies called pycnidia. These pycnidia produce pink or purple masses of pycnidiospores when humidity and temperature are conducive. Pycnidiospores are a secondary inoculum which usually spread by rain-splash and wind to neighboring plants in the field, causing more infections (Gabrielson, 1983; Howlett et al., 2001). Following leaf infection, the fungus continues colonizing the petiole and then stem tissues. After colonization of stem cells, the fungus induces cell death that results in blackened stem lesions or stem cankers. Stem cankers that are formed at an early stage of crop growth may girdle the base and cause premature ripening, lodging and plant death, resulting in a large yield loss (Gabrielson, 1983; Howlett et al., 2001). The fungus also infects pods forming pod lesions. Pods with lesions shatter prior to harvest resulting in yield losses. Crop residues from these infested plants become a source of inoculum for the following seasons. In addition, another source of inoculum for blackleg epidemic is infected seed. The pathogen can be introduced into areas previously uninfested through infected seed (Gabrielson, 1983).

Disease control strategies are mainly focused on disrupting the sequence of events necessary for establishing the disease. Since infected seed is the source of seedborne inoculum, use of clean seed can avoid spreading of the disease to areas previously not infested. Another source of primary inoculum could be spores arising from infested host residues. Thus, the proper management of plant residues reduces the risk of epidemics during the following seasons. Additionally, the use of disease-resistant varieties of crops and use of a systemic fungicide are among others means of controlling the disease (Gabrielson, 1983; Gugel and Petrie, 1992).

1.2.2 Classification

The blackleg fungus known as *Phoma lingam*, perfect stage *Leptosphaeria maculans* (Desm.) Ces. et de Not. is a species complex comprised of several pathotype

groups and subgroups. Initially, it was classified into two groups, namely: a virulent strain (also called aggressive, highly virulent, or "A" group) and an avirulent strain (also called non-aggressive, weakly virulent, or "B" group) on the basis of virulence and cultural characterstics (McGee and Petrie, 1978; Williams and Fitt, 1999). The pathogenicity tests of isolates of *L. maculans* isolated from rapeseed plants (*Brassica* species) revealed the presence of two pathotype groups, virulent and avirulent strains. The isolates collected from rapeseed plants from Saskatchewan, Australia and Wisconsin were analyzed based on their pathogenicity to *B. napus* cultivar Midas; most of the isolates from Australia and Wisconsin were virulent, whereas those from Saskatchewan were avirulent (McGee and Petrie, 1978). Similarly, 117 isolates of *L. maculans* collected from a range of brassica seed crops from south-east England were characterized as avirulent and virulent strains using pathogenicity tests conducted on cabbage cv. January King (Humpherson-Jones, 1983). Additional isolates collected from cruciferous weeds, *Thlaspi arvense* (stinkweed), *Sisymbrium* spp., *Descurania* spp., *Lepidium* spp., and *Erysimum* spp., were also classified as *L. maculans* (Williams and Fitt, 1999). Isolates classified in the Thlaspi strain were isolated from stinkweed (*T. arvense*) and are nonpathogenic to rapeseed but highly pathogenic to stinkweed (*T. arvense*), a cruciferous weed known to be resistant to virulent and avirulent strains (McGee and Petrie, 1978).

The culture characteristics also distinguish the two pathotype groups virulent and avirulent. In general, virulent isolates grow slowly and irregularly on V-8 juice agar and produce no water-soluble pigments in Czapek's broth medium. On the contrary, avirulent isolates grow fast and evenly on V-8 juice agar and produce brownish-yellow pigments in Czapek's broth medium (McGee and Petrie, 1978, Humpherson-Jones, 1983; Koch et al., 1989). Moreover, the cultures of virulent isolates are characterized by production of phytotoxic compounds, which were identified as sirodesmins. On the other hand, the production of sirodesmins was not detected in the cultures of avirulent isolates (Koch et

al., 1989; Pedras and Séguin-Swartz, 1990). In most cases, these cultural characteristics are closely correlated with pathogenicity ranking of the two pathotype groups.

Further studies on the taxonomy of *L. maculans* indicated the presence of subgroups within the virulent strains (Koch et al., 1991; Mengistu et al., 1991). Isolates of *L. maculans* collected from North America, Europe and Australia were analyzed for pathogenic variability on cotyledons of *B. napus* cultivars Westar, Quinta and Glacier. Three pathogenicity subgroups (PG2, PG3, and PG4) within the virulent strain were identified on the basis of differential reactions of *B. napus* cultivars. PG4 was highly virulent on Westar, Quinta and Glacier, whereas PG2 and PG3 were virulent on Westar, and Westar and Glacier, respectively. Australian virulent isolates exhibited variation in differential reactions toward the three *B. napus* cultivars; thus Australian virulent isolates of PG2, PG3 and PG4 groups were identified. Unlike Australian isolates, virulent isolates originating from Canada did not show pathogenicity variation within themselves, and all were classified into subgroup PG2. The subgroup PG1 comprised avirulent isolates of *L. maculans*, which were identified by the lack of pathogenicity to *B. napus* cultivars Westar and Quinta. PG1 caused no differential reactions on cotyledons of *B. napus* cultivars, suggesting the absence of pathogenic variability and hence subgroups within the avirulent strain (Koch et al., 1991; Mengistu et al., 1991).

Many genetic and biochemical studies indicated that virulent and avirulent isolates are distinct species (Johnson and Lewis, 1990; Koch et al., 1991; Taylor et al., 1991; Morales et al., 1993; Gall et al., 1995; Somda et al., 1996; Balesdent et al., 1998; Purwantara et al., 2000). For instance, restriction fragment length polymorphism (RFLP) analysis clearly differentiated the two pathotype groups and also subgroups within each group (Koch et al., 1991). The subgroups of virulent isolates resulting from RFLP analysis in some cases correlated to their pathogenicity subgroups. For instance, subgroups A2 and A3 composed isolates only from pathogenic subgroups PG4 and PG3, respectively. In the case of avirulent isolates, three genetically distinct subgroups NA1,

NA2 and NA3 were identified. Despite the great genetic diversity within avirulent isolates, there was no observed variation in pathogenicity. NA1 isolates are more prevalent in Europe, whereas NA2 isolates were common in Canada (Gall et al., 1995). Similarly, amplified fragment length polymorphism (AFLP) analyses of 100 isolates of *L. maculans* collected from Australia, Europe and North America discriminated readily virulent and avirulent isolates (Purwantara et al., 2000). In addition, AFLP profiles were distinct for isolates of NA1, NA2, and NA3 subgroups that were described using RFLP techniques (Koch et al, 1991). This distinction is also supported by analysis of the ITS of DNA and electrophoretic karyotyping (Taylor et al., 1991; Morales et al., 1993). Apart from these studies, isozyme and soluble protein analyses of *L. maculans* isolates also consistently differentiated between virulent and avirulent isolates (Gall et al., 1995; Somda et al., 1996; Balesdent et al., 1998).

Additional evidence indicating the need for reclassification of *L. maculans* was obtained from the chemical analysis of secondary metabolites of isolates of *L. maculans* (Pedras and Séguin-Swartz, 1990; Pedras et al., 1995; Pedras and Biesenthal, 2000; Pedras, 2001). In this study, cultures of isolates of *L. maculans* were grown in liquid medium and the extracts of cultures were analyzed by HPLC, equipped with a photodiode array detector. Standard phytotoxins and related metabolites were used for instrument calibration (retention time, and UV spectra) (Pedras and Biesenthal, 2000). The chemical structures of phytotoxins and other secondary metabolites were determined for representative isolates of the group and their secondary metabolite profiles established. Next, the differentiation and characterization of new isolates was carried out by comparison of the secondary metabolite profile of each isolate with those of the representative groups of isolates. Thus, this method appears to be simple and reliable as compared to other methods (Pedras and Biesenthal, 2000; Pedras, 2001).

The chemical analysis of cultures of virulent isolates indicated the production of metabolites unique to the group. The isolation and structure determination of these

metabolites allowed differentiation of virulent isolates. Of several metabolites produced by virulent isolates, sirodesmin PL (**1**, the major sirodesmin toxin), deacetylsirodesmin PL (**2**), phomamide (**3**) and phomalide (**4**) were proposed chemical markers of virulent isolates of *L. maculans* (Pedras, 1998, 2001; Pedras and Biesenthal, 2000) (fig.1). Similarly, avirulent isolates produced characteristic metabolites of polyketide origin in cultures grown in potato dextrose medium. The chemical investigation of metabolites led to the isolation of several metabolites including phomaligin A (**5**), wasabidienone B (**6**) and wasabidienone E (**7**), which impart a characteristic brownish-yellow color to avirulent cultures (Pedras et al., 1995; Pedras et al., 1996). Phomaligin A (**5**), wasabidienone B (**6**) and wasabidienone E (**7**) were thus metabolites proposed as chemical markers for avirulent isolates of *L. maculans* (fig. 2). Hence, the secondary metabolite profiles of virulent and avirulent isolates were quite distinctive and not overlapping, suggesting both are different species.

Further chemical investigation of cultures of avirulent Polish isolates showed a secondary metabolite profile different from those of virulent and avirulent isolates (Pedras and Biesenthal, 2000). Avirulent Polish isolates produce in minimal medium polanrazines and phomapyrones (Pedras and Biesenthal, 2000, 2001). Polanrazines are metabolites isolated only from avirulent Polish isolates, and therefore characteristic to the group (fig.3). Hence, polanrazine A (**8**), polanrazine C (**9**) and polanrazine F (**10**) were proposed as chemical markers for differentiation of avirulent Polish isolates. Avirulent Polish isolates unlike Canadian, European and Australian avirulent isolates are pathogenic and known to cause significant yield losses in Poland (Williams and Fitt, 1999). Pedras et al. (1999a) reported new blackleg isolates from Canada, Laird 2 and Mayfair 2, to exhibit similar secondary metabolite profiles to those of Polish isolates. Both Laird 2 and Mayfair 2 produce polanrazines, which are characteristic metabolites of Polish isolates (Pedras and Biesenthal, 2000). Consequently, Mayfair 2 and Laird 2 isolates were assigned to the group of avirulent Polish isolates. Laird 2 and Mayfair 2 are

closer genetically to avirulent isolates, however, unlike avirulent isolates, they are virulent to *B. juncea* (Taylor et al., 1995), a traditionally blackleg resistant species (Keri et al., 1997). Although Mayfair 2 and Laird 2 isolates are similar to Polish isolates in their secondary metabolite profiles, their relationship in pathogenicity remains to be established (Pedras and Biesenthal, 2000).

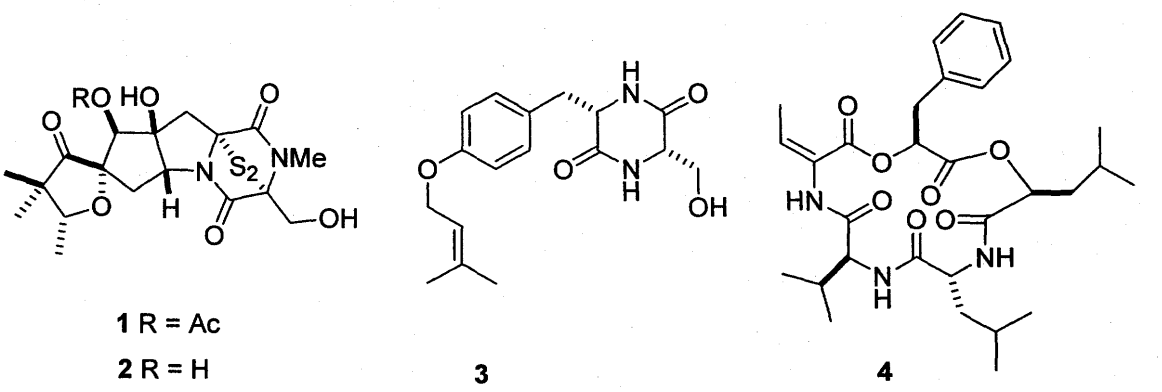

Figure 1: Proposed chemical markers of virulent isolates of *Leptosphaeria maculans*.

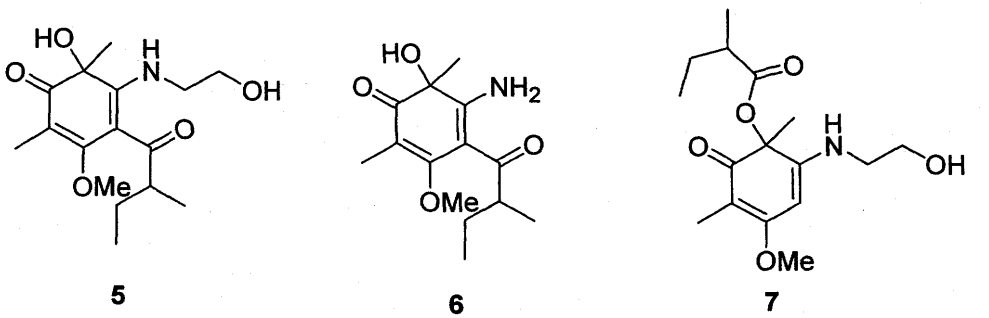

Figure 2: Proposed chemical markers of avirulent isolates of *Leptosphaeria maculans*.

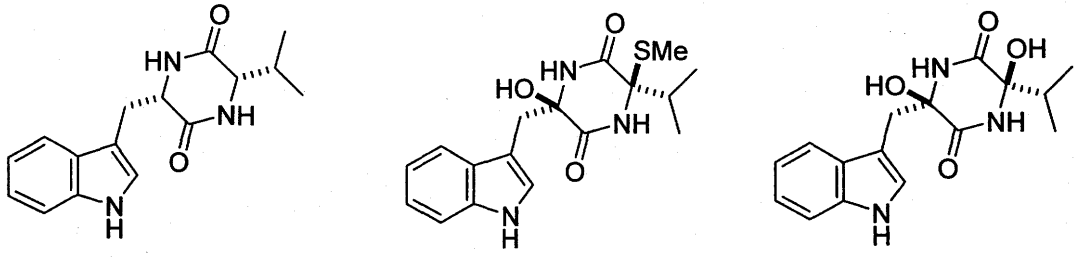

Figure 3: Proposed chemical markers of avirulent Polish type isolates of *Leptosphaeria maculans*.

In conclusion, three distinct groups of isolates of *L. maculans*, namely, virulent, avirulent and avirulent Polish isolates were identified on the basis of the secondary metabolite profiles (Pedras, 1998; Pedras and Biesenthal, 2000; Pedras, 2001). Similar to pathogenicity (McGee and Petrie, 1978), cultural (Koch et al., 1989), morphological (Shoemaker and Brun, 2001), biochemical (Sippell and Hall, 1995) and genetic (Koch et al., 1991; Morales et al., 1993; Patterson and Kapoor, 1995) studies, the analysis of the secondary metabolite profiles also indicated virulent and avirulent isolates to be distinct species (Pedras, 1998; Pedras and Biesenthal, 2000; Pedras, 2001). Further, avirulent isolates were shown to have similar secondary metabolite profiles as *Phoma wasabiae* (Pedras et al., 1995). On that basis, Pedras et al. (1995, 1996) proposed reclassification of avirulent isolates as *Phoma wasabiae*. Furthermore, the classification of avirulent isolates into *P. wasabiae* was supported by pathogenecity testing; both avirulent isolates of *P. lingam* and *P. wasabiae* are pathogenic to wasabi (*Eutrema wasabi* M.) plants and cause similar disease symptoms. In addition, electrophoretic karyotyping and analysis of ribosomal DNA ITS-1 and ITS-2 and 5.8*s* sequences showed close relationships between

avirulent isolates of *P. lingam/L. maculans* and *P. wasabiae* (Pedras et al., 1995, 1996; Taylor et al., 1995; Reddy et al., 1998).

Recently, Shoemaker and Brun (2001) classified avirulent isolates of *P. lingam/L. maculans* as *Leptosphaeria biglobosa* following morphological studies. However, this classification has a shortcoming because it did not incorporate evidence from previous studies. For instance, pathogenicity testing and genetic analysis showed close relationships between avirulent isolates of *P. lingam/L. maculans* and *P. wasabiae*. Such morphological studies, other than indicating that avirulent and virulent isolates are different species, were unable to establish relationships of avirulent isolates with other *Phoma/Leptosphaeria* species. Moreover, the isolates employed in the morphological study represent only the perfect stage of the species but no reference was made to the asexual stage. On the contrary, analysis based on secondary metabolite profiles (Pedras et al., 1995, 1996; Pedras and Biesenthal, 2000), pathogenicity testing (Soga, 1976) and genetic analysis (Pedras et al., 1995; Taylor et al., 1995; Reddy et al., 1998) showed that avirulent isolates belong to species different from virulent isolates but also showed close relationships between avirulent *L. maculans* and *P. wasabiae*. Consequently, formal reclassification needs to be revised so as to incorporate previous proposals referring to *P. wasabiae* (Pedras et al., 1995, 1996; Taylor et al., 1995; Reddy et al., 1998).

1.3 Secondary metabolites

In metabolic processes of living organisms, chemical compounds are synthesized as well as degraded by means of a series of biochemical reactions. The metabolic processes that commonly occur in all living organisms are part of the primary metabolism. The essential chemical classes such as carbohydrates, amino acids, common fatty acids, and nucleotides, are synthesized and utilized by all living organisms through primary metabolic processes. Living organisms do have other metabolic pathways, called

secondary metabolism, by which they produce compounds non-essential for life, that are however, important for their fitness and survival. These compounds are known as secondary metabolites, and are produced by living organisms during a particular stage of growth and development or during periods of stress caused by nutritional limitation or microbial attack (Mann, 1994). For example, secondary metabolites are involved in mediating the interactions between living organisms including plant-insect, insect-insect, plant-plant, plant-microbial, and animal-animal (Mann, 1994).

A large number of secondary metabolites of diverse structures have been isolated, most of which are of plant and microbial origin. Secondary metabolites are usually classified according to their structures and biosynthetic origins.

1.3.1 Major classes of secondary metabolites

Polyketides are metabolites widely distributed both in plants and microorganisms. Biogenetically, they are derived from acetyl CoA and malonyl CoA. The skeletal, which are formed from polymerization of C_2 units, undergo further transformations which include cyclization, oxidation, reduction, ring cleavage, alkylation, etc. (Mann, 1994).

Terpenoids are the largest and most widely distributed group of secondary metabolites especially in the plant kingdom. Biogenetically they are derived from 5-carbon (isoprene) units via the 1-deoxy-D-xylulose-5-phosphate (DOXP) pathway (Logan et al, 2000) or the mevalonate pathway. Condensation of 5-carbon units mediated by isoprenyl pyrophosphate synthetase produces geranyl pyrophosphate (GPP, C_{10}), farnesyl pyrophosphate (FPP, C_{15}) and geranylgeranyl pyrophosphate (GGPP, C_{20}). These acyclic terpenes, GPP, FPP, and GGPP, serve as immediate precursors of various terpenoid skeleta upon dimerization and/or cyclization and rearrangement. Terpenoids are classified according to the number of 5-carbon units as monoterpenes (C_{10}), sesquiterpenes (C_{15}), diterpenes (C_{20}), triterpenes (C_{30}), tetraterpenes (C_{40}) and polyterpenes (Mann, 1994).

Alkaloids are generally considered as non-peptidic and non-nucleosidic compounds containing nitrogen. Their distribution is predominant in higher plants; about 20% of species of flowering plants metabolize to produce alkaloids. Alkaloids are also found in animals, insects, and marine invertebrates and microorganisms. Most alkaloids are biosynthesized in plants from a restricted group of α-amino acids such as ornithine (Orn), lysine (Lys), phenylalanine (Phe), tyrosine (Tyr), and tryptophan (Trp). Over 12000 alkaloids of great structural diversity have been isolated. In spite of the structural diversity, alkaloids are usually classified according to the carbon skeleton, e. g. quinoline, isoquinoline, indole, etc (Mann, 1994; Roberts and Wink, 1998).

Shikimate derived metabolites are one of the major groups of secondary metabolites widely distributed in plants and in microorganisms. These include lignins, suberin, styrylpyrones, stilbenes, coumarins, furanocoumarins, hydrolyzable tannins, condensed tannins and flavonoids. In plants, they are biosynthesized from phenylalanine by the phenylpropanoid pathway. In this biosynthetic pathway, phenylalanine is converted to cinnamate, which serves as precursor for biosynthesis of thousands of phenolic compounds (Mann, 1994).

Metabolites of mixed biosynthetic origin are known from plants and microorganisms. These metabolites have skeleta derived from at least two biosynthetic pathways. This class of compounds comprises large number of compounds mainly derived from acetate and mevalonate, acetate and shikimate, and mevalonate and shikimate pathways. The distribution of most of these compounds is limited to one species or to closely related species, however, metabolites such as flavonoids and polyisoprenyl quinones commonly occur in higher plants (Mann, 1994).

1.3.2 Chemotaxonomy

Secondary metabolites are products of genetic make-up of the organism (Mann, 1994). Their biosynthetic relationships therefore reflect the biological relationships of the

producing species. The distribution of secondary metabolites is restricted within the group having common descent; that is, those secondary metabolites have taxonomic significance. Thus, chemotaxomy was introduced in systematic classification of the plant kingdom early in the 20th century (Hadacek, 2002). A remarkable contribution to the practical application of chemotaxonomy was that of Mirov (1965). In this work, pine terpenoid patterns were established for about 100 or so known pine species, and used as taxonomic markers for separating many species of the genus *Pinus* from each other. Since that landmark study, several classes of compounds of interest in plant taxonomy including alkaloids, flavonoids, iridoids, cyanogenic glycosides, and terpenoids have been studied (Harborne and Turner, 1984, Bohm and Stuessy, 2001). In many studies of systematic classification of angiosperms, several types of alkaloids have been considered as taxonomic markers. For instance, tropane alkaloids are common constituents in the family Solanaceae. Particularly, those tropane alkaloids such as hyoscyamine, scopolamine and other esters of tropane are characterstic of the genera *Datura*, *Brugmansia*, and *Duboisia* of the Solanaceae. Tropane alkaloids were also found distributed outside the Solanaceae in unrelated families such as the Erythroxylaceae, Proteaceae, Euphorbiaceae, Rhizophoraceae, Convolvulaceae and Cruciferae. Since many tropane alkaloids' distribution is restricted to particular families, they appear to have taxonomic significance only within the family. Many plant species have been surveyed, and relatively large amounts of phytochemical data accumulated for flavonoids (Harborne, 1988; Harborne et al, 1975). The pattern of flavonoid distribution in several plant families indicated their taxonomic significance. Recently, Williams et al. (2001) demonstrated the use of flavonoind as taxonomic markers in the classification of Anthemideae. The representative temperate species of seven genera, *Anthemis*, *Chrysanthemum*, *Cotula*, *Ismelia*, *Leucanthemum*, *Tripleurospermum* and *Tanacetum*, of Anthemideae were surveyed for their flavonoid constituents. Thus, *Anthemis* and *Tanacetum* on one hand and *Chrysanthemum*, *Cotula*, *Ismelia*, *Leucanthemum* and

Tripleurospermum on the other were distinguished based on their flavonoid profiles. For the same tribe Anthemideae, flavonoid glycosides served as taxonomic markers for differentiation at the generic level (Harborne et al., 1970).

Although chemotaxonomy is of considerable importance in plant systematics, some limitations exist in its practical application. For example, chemical markers may occur in unrelated taxa, and conclusive data on secondary metabolites of taxonomic value requires numerous phytochemical studies; thus there is a lack of completeness. The distribution of secondary metabolites may vary within tissues of a particular plant species, between identical tissues of individuals within a population, and between populations of the same species. Therefore, the metabolite data need to be interpreted carefully (Roberts and Wink, 1998; Wink, 2003; Hadacek, 2002).

Chemotaxonomic methods are employed in the classification of microorganisms as well. Müller and Hallaksela (1998) classified 1740 isolates of endophytic fungi into 81 groups based on combined fatty acid and sterol profiles (FAST-profiles). Moreover, lipid profiles were employed in the classification of a new cyanobacterium in the *Spirulina* genus (Romano et al., 2000). Chemotaxonomic methods appear to be useful also for the determination of diversity; for instance, in fungal species the characterization based on chemotaxonomic methods is less ambiguous even compared to that of morphological characterization (Müller and Hallaksela, 1998).

1.3.3 Plant metabolites: chemical defenses

Plants in their ecosystems are always under heavy pressure caused by competing plants, herbivores, and microorganisms. In the course of their struggle for survival, plants have evolved chemical defenses, which are part of their secondary metabolites. Plants utilize chemical defenses to overcome the stress caused in their interactions with the environment including plant-plant, plant-herbivore, and plant-microbial interactions

(Bennett and Wallsgrove, 1994; Hadacek, 2002; Wink, 2003). Plants release toxic compounds to inhibit germination or growth of other competing plant species. This phenomenon was termed allelopathy by Molisch in 1937 (Weston and Duke, 2003). These toxic compounds, which are called allelochemicals, are released into the environment through root exudation, foliar leaching, residue decomposition and volatilization. Allelochemicals introduced into the soil rhizosphere have defensive roles by inhibiting germination or growth of susceptible plant species in the vicinity. Several allelochemicals have been reported after allelopathy received great attention among many researchers because of its potential impact on agriculture. In recent years, different crop species with allelopathic traits have been investigated for allelochemicals.

Rice (*Oryza sativa*) was shown to be allelopathic; it suppresses effectively the growth of aquatic weeds (Weston and Duke, 2003). The chemical analysis of root exudates of *O. sativa* led to the isolation of the growth inhibitor momilactone B (**12**). In bioassays, momilactone B (**12**) showed growth inhibition of cress (*Lepidium sativum* L.) and lettuce (*Lactuca sativa* L.) seedlings at concentrations greater than 3 μM and 30 μM, respectively. In addition, the rice seedlings were shown to release momilactone B (**12**) from their roots to the environment (Kato-Noguchi et al., 2002; Kato-Noguchi, 2004). Kong et al., (2004b) also reported the isolation of momilactone B (**12**) and two growth inhibitors, 5,7,4'-trihydroxy-3',5'-dimethoxyflavone (**13**) and 3-isopropyl-5-acetoxy-2-cyclohexen-1-one (**11**), from the above-ground part of an allelopathic rice cultivar. Compounds **11-13** exhibited growth inhibitory activity on the weeds *Echinochloa crusgalli* and *Cyperus difformis* associated with rice. Moreover, the growth inhibitory effect was found to be much higher for mixtures of **11**, **12**, and **13** than for individual compounds. Thus, rice allelopathy appears to result from the total concentrations of **11**, **12**, and **13** released through rice seedlings into the soil (Kong et al., 2004a).

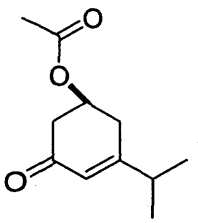

11

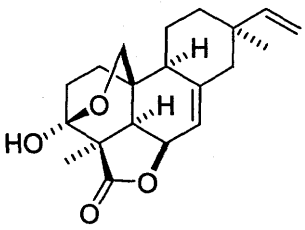

12

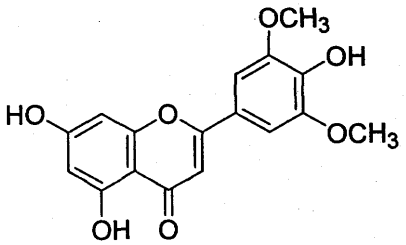

13

Sunflower (*Helianthus annuus* L.) is allelopathic, and inhibits weed-seedling growth of several weeds including velvet leaf, thorn apple, morning glory, and wild mustard (Leather, 1987). Macías et al. (1998) reported heliespinore A (**16**), a potential allelopathic agent from leaves of a cultivar of sunflower (variety SH-222). Additionally, the chemical investigation of the exudate of germinating sunflower seeds yielded the allelopathic compound sundiversifolide (**14**). Bioassays indicated that **14** inhibited shoot and root growth of cat's-eyes (*Veronica persica* Poiret) by about 50% at a concentration of 30 ppm (Ohno et al., 2001). Allelopathy in cultivar sunflower var. SH-222 (*H. annuus*) therefore resulted from allelochemicals released into the environment (Vyvyan, 2002).

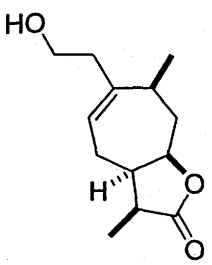

14

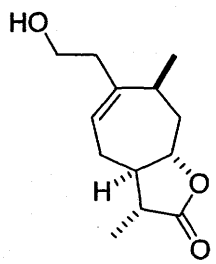

15

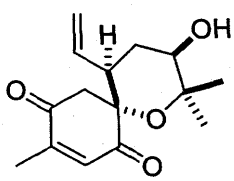

16

Allelopathy is also known to contribute to the success of some invasive weeds such as *Centaurea maculosa* (spotted knapweed) (Weston and Duke, 2003). *C. maculosa* causes large economic damage in North America since it replaces native plant species. The chemical investigation of root exudates from *C. maculosa* yielded the allelopathic compound (-)-catechin (**18**). Further analysis of soil extracts from a *C. maculosa*-invaded field showed the accumulation of a substantial quantity of (-)-catechin (**18**) in soil rhizospheres. In bioassays, (-)-catechin (**18**) exhibited growth and germination inhibition of native plant species at its natural concentrations in rhizospheres. These facts suggested that *C. maculosa* releases (-)-catechin (**18**) into the environment to enhance its invasiveness (Bais et al., 2002; 2003). Kato-Noguchi et al. (2002) have reported the isolation of the allelopathic compound abscisic acid-β-D-glucopyranosyl ester (**17**) from *Citrus junos* peel. Bioassays showed abscisic acid-β-D-glucopyranosyl ester (**17**) caused 50% inhibition of the hypocotyl and root growth of lettuce seedlings at concentrations of 2.3 μM and 1.4 μM, respectively. Additionally, abscisic acid-β-D-glucopyranosyl ester (**17**) was reported to be found in soils from agricultural fields in which several crop plants were grown (Kato-Noguchi et al., 2002).

In a highly competitive environment, like in forests, plants utilize chemical defenses to inhibit the germination and growth of other plant species. For instance, *Duroia hirsuta* is an allelopathic tree in the forests of the western Amazon, and has no vegetation in its surroundings. The chemical investigation of chemical traits responsible for allelopathic interactions of *D. hirsuta* with other plant species led to the isolation of plumericin (**19**). Bioassays indicated that plumericin (**19**) is a strong inhibitor of lettuce radicle elongation at a concentration (IC_{50}) of 123 μM. The observed allelopathy is attributed to plumericin (**19**) mediated interactions of *D. hirsuta* with competing plants (Page et al., 1994).

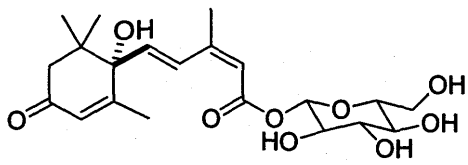

17

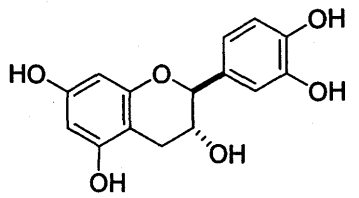

18

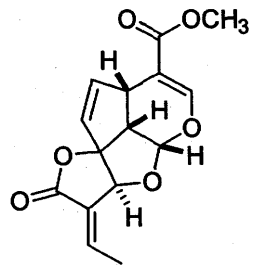

19

Moreover, plant secondary metabolites play defensive roles against herbivores. Many plants exhibit toxicity, deterrence/anti-feeding activity or oviposition deterrence to herbivores; as a result, plants are protected from herbivore attack. An illustrating example is plants producing cyanogenic glucosides. In damaged plant tissues, cyanogenic glucosides undergo subsequent hydrolysis leading to the release of hydrogen cyanide, a respiratory inhibitor, and an aldehyde or ketone, a toxic compound. Linamarin (**20**), a cyanogenic glucoside from cassava (*Manihot esculenta*), protects cassava tubers from cassava root borer (Rosenthal and Berenbaum, 1991; Bennett and Wallsgrove, 1994). Petasin (**21**) and furanopetasin (**22**) are sesquiterpenes from *Petasites hybridus* plants having a defensive function. Both petasin (**21**) and furanopetasin (**22**) deter slugs and snails from feeding on *P. hybridus* plants. The leaves contain a high concentration of these sesquiterpenes, enough to cause feeding deterrence; the composition of petasin (**21**) in leaves (0.07-0.71% of dry weight) is higher than its level of deterrence (0.05%). Thus, the chemical defenses of *P. hybridus* against herbivores feeding on it are attributed to petasin (**21**) and furanopetasin (**22**) (Haëgele et al., 1998). Further pyrrolizidine alkaloids such as heliosupine (**23**), echinatine (**24**) and 3'-acetylechinatine (**25**) from *Cynoglossum officinale* are antifeedants against generalist herbivores. The concentration of pyrrolizidine alkaloids in *C. officinale* is higher in the youngest leaves than in old leaves; thus, the youngest leaves suffer less damage from generalist herbivores (Van Dam et al., 1995).

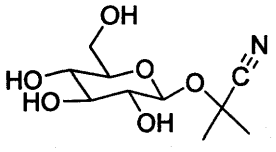

20

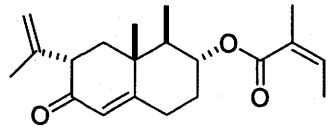

21

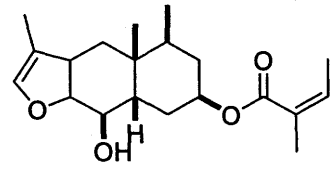

22

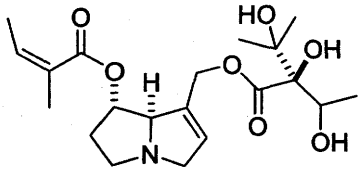

23

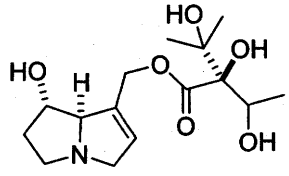

24

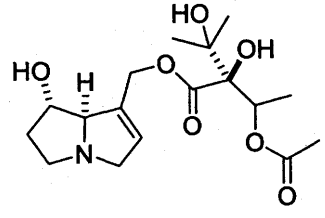

25

Plant chemical defenses contribute to their resistance toward pathogenic microbial attack or stress. Hence, plants produce antimicrobial secondary metabolites, which may be either constitutive defense metabolites (also called phytoanticipins, VanEtten et al., 1994) or induced defense metabolites (also called phytoalexins, Paxton, 1981; Smith, 1996). Phytoanticipins are produced by plants during their normal program of growth and development, and occur in healthy plants representing inbuilt chemical barriers to infection. Phytoanticipins are stored in the inactive forms, however, they are readily converted into biologically active forms by plant enzymes during pathogenic attacks. They include classes of compounds such as saponins, benzoxazinoids and cyanogenic glycosides (Ingham, 1973; Morrissey and Osbourn, 1999). The saponins, avenacins A-1 (**26**) and B-1 (**27**), are constitutive defense metabolites from oat (*Avena* species). Both avenacins A-1 (**26**) and B-1 (**27**) exhibited fungal growth inhibitory activity toward *G.*

graminis var. *tritici*, a pathogenic fungus of oats. In oat plants, the defensive role of avenacins was shown in studies carried out on the fungal disease susceptibility of oat varieties. Oat plants producing avenacins were resistant to *G. graminis* var. *tritici*, whereas the avenacin deficient oat species, *Avena longiglumis*, was susceptible. Thus, avenacins play important roles as chemical defenses in oats (Osbourn et al., 1994).

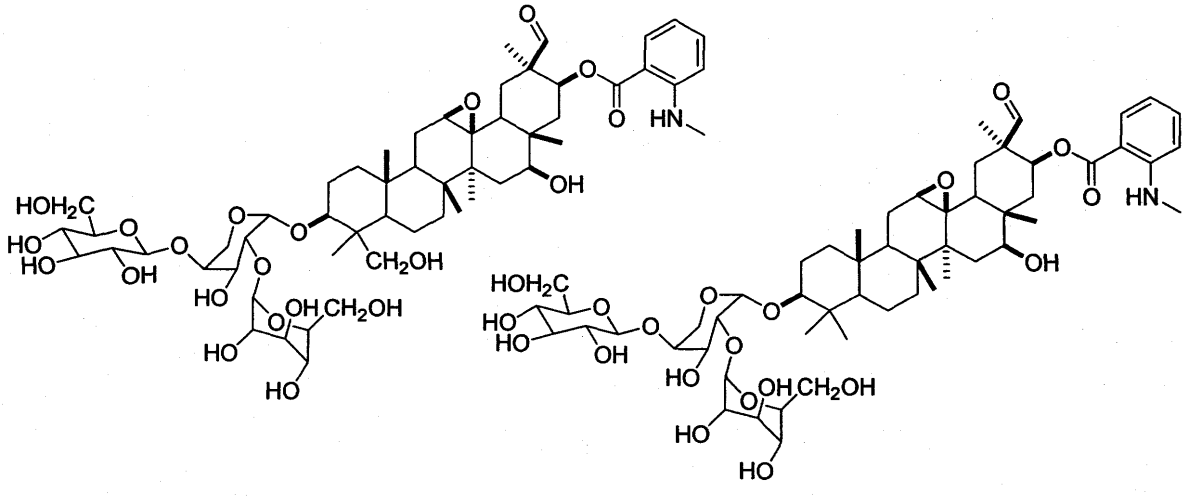

26 **27**

In plant-pathogen interactions, induced chemical defenses appear to play a major role in plant disease resistance. Plants respond to microbial attack by synthesizing *de novo* antifungal metabolites, phytoalexins. Both susceptible and resistant plants accumulate phytoalexins at the site of infection, however, the accumulation of phytoalexins takes place more rapidly and to higher levels in resistant plants as compared to that in susceptible plants (Morrissey and Osbourn, 1999; Pedras et al., 2000). The extent of resistance of plants toward pathogenic attack is related to the timing, rate of

accumulation, and relative amount of phytoalexins (Pedras, 1998; Pedras et al, 2000; 2002). The defensive role of phytoalexins in plants against microbial attack was demonstrated first for the phytoalexin resveratrol (**28**) by Hain et al., (1993). In this work, a stilbene synthase gene responsible for the biosynthesis of resveratrol (**28**) was isolated from grapevine and transferred into tobacco susceptible to *Botrytis cinerea*. As a result, transgenic tobacco plants acquired higher disease resistance than wild type tobacco (Hain et al., 1993).

Several phytoalexins have been reported from many plant families since Müller first hypothesized the production of phytoalexins by infected plants in 1940 (Hammerschmidt, 1999; Morrissey and Osbourn, 1999; Pedras et al., 2000). Rishitin (**29**), a phytoalexin from resistant potato tubers, appears to be a resistance factor in potato plants. Rishitin (**29**) was found to accumulate at infection sites in resistant potato tubers to a concentration of 120 μg rishitin per g of tissue within 48 h. The concentration of rishitin (**29**) that was found at infection sites is enough to retard hyphal growth of the pathogenic fungus *Phytophthora infestans* (Tomiyama et al., 1968). Legumenous plants are known to produce isoflavonoid phytoalexins in response to the pathogenic fungi. Pisatin (**30**) was the first phytoalexin to be reported from pea (*Pisum sativum)*, followed by the minor isoflavonoid phytoalexin maackiain (**31**). Both pisatin (**30**) and maackiain (**31**) were antifungal, and inhibited mycelial growth of pathogenic fungi of pea (*P. sativum*). Isoflavonoid phytoalexins, phaseollin (**33**) and kievitone (**32**) have been reported from infected *Phaseolus vulgaris* L. These phytoalexins accumulated faster at infection sites in concentrations essential for the inhibition of fungal growth; phaseollin concentration was determined to be 829 μg/g fresh tissue after 72h of inoculation (Ingham, 1979, Gnanamanickam, 1979).

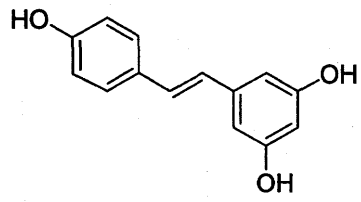

28

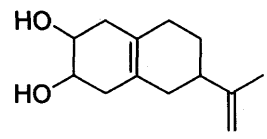

29

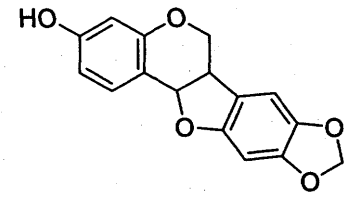

30

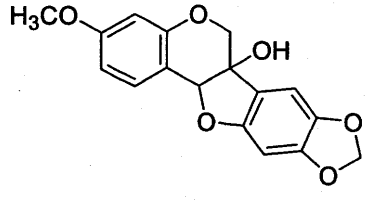

31

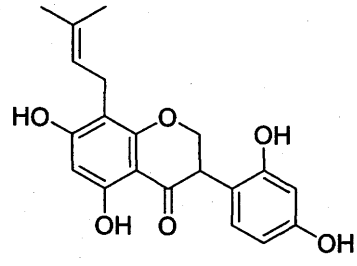

32

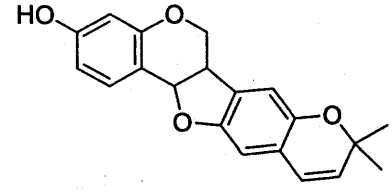

33

Plant chemical defenses have been investigated for the cruciferous family with over thirty phytoalexins reported (Pedras et al., 2003b). The first crucifer phytoalexins were reported by Takasugi et al. (1986) from Chinese cabbage (*Brassica campestris* L.ssp. *pekinensis*). The elicitation of phytoalexins from Chinese cabbage (*Brassica campestris* L. ssp. *pekinensis*) using the bacterium *Pseudomonas cichorii* led to the isolation of phytoalexins such as methoxybrassinin (**34**), brassinin (**35**), and cyclobrassinin (**36**). Wasabi (*Wasabia japonica*, syn. *Eutrema wasabi*), a plant resistant to virulent isolates of the blackleg fungus (*L. maculans*/*P. lingam*) was found to produce antifungal compounds such as wasalexin A (**38**) and B (**39**) in response to fungal infection (Pedras et al., 1999b). Both wasalexin A (**38**) and B (**39**) showed antifungal activity against *P. lingam*; they inhibited both spore germination and mycelial growth *in vitro*. The wild crucifer *Camelina sativa* (false flax) is resistant to different *Brassica* pathogens including *Alternaria brassicae*. The investigation of phytoalexins of *Camelina sativa* using biotic or abiotic elicitors resulted in isolation of two induced metabolites, camalexin (**37**) and 6-methoxycamalexin (**40**) (Browne et al., 1991). These compounds

were the first examples of thiazoyl substituted indole phytoalexins whose structures were established on the basis of NMR and X-ray data. Both camalexin (**37**) and 6-methoxycamalexin (**40**) exhibited antifungal activity against *Alternaria brassicae*.

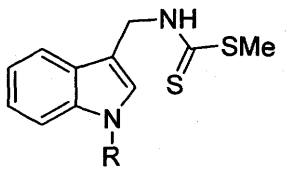

34 R = OMe
35 R = H

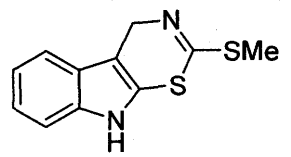

36

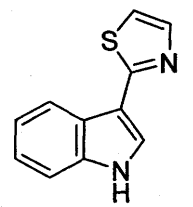

37

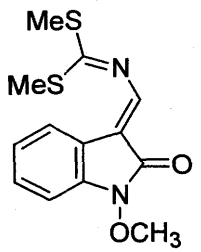

38

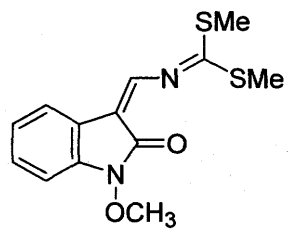

39

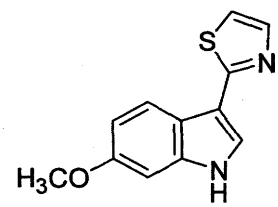

40

1.3.4 Microbial metabolites

Secondary metabolites of microbial origin are large in number and have diverse structures, classified into major groups on the basis of their biosynthetic origins as mentioned in section 1.3. Most secondary metabolites of microbial origins reported so far are from phytopathogenic fungi. Based on the toxicity range to plants these metabolites are classified into non-host selective and host selective phytotoxins. In several studies of the plant diseases caused by host-selective fungi, many host-selective toxins have been

reported to be involved in disease (Kohmoto and Otani, 1991; Pedras, 2001; Hadacek, 2002).

1.3.4.1 Metabolites from the blackleg fungus

The blackleg fungus (*Leptosphaeria maculans/Phoma lingam*) is known to produce structurally diverse metabolites derived from acetyl coenzyme A and malonyl coenzyme A, mevalonic acid, shikimic acid and mixed biosynthetic origins. Each pathotype group of *L. maculans* produces metabolites characteristic of the group. The virulent pathotype group biosynthesizes different classes of compounds, namely: epipolythiodioxopiperazines (ETPs) and a depsipeptide, in liquid cultures in minimal medium (Pedras, 1998). ESPs include metabolites such as sirodesmin PL (**1**, the major sirodesmin toxin), deacetylsirodesmin PL (**2**), sirodesmin H (**41**), sirodesmin J (**42**), sirodesmin K (**43**), phomalirazine (**44**) and phomamide (**3**) (Férézou et al., 1977; Pedras et al., 1988; Pedras et al., 1989; Pedras et al., 1990). Sirodesmins and phomalirazine are non-host selective toxins which cause necrosis and cell death to host and non-host plants (Pedras et al., 1989). Sirodesmins are biosynthesized from phomamide (**3**), a non-phytotoxic metabolite isolated together with sirodesmins (Férézou et al., 1980). Further, phomalirazine (**44**) was proposed to be an intermediate between phomamide and sirodesmins (Pedras et al., 1989). Sirodesmins differ from one another by the size of the sulphur bridge. Initially, sirodesmin PL (**1**) and deacetylsirodesmin PL (**2**) were reported from unrelated fungal species, *Sirodesmium diversum* (Curtis et al., 1977). Further investigation of host-selective toxins from virulent isolates led to the isolation of phomalide (**4**), whose structure was determined by a combination of spectroscopic methods and chemical degradation. Chemically, phomalide (**4**) is a 15-membered cyclic depsipeptide composed of five residues, dehydrothreonine (DhThr), (*S*)-valine [(*S*)-Val], (*R*)-Leucine [(*R*)-Leu], (*S*)-3-phenyllactic acid [(*S*)-O-Phe)], and (*S*)-2-hydroxyisovaleric

acid [(*S*)-O-Leu)], in a sequence of cyclo (DhThr-Val-Leu-O-Leu-O-Phe) (Pedras et al., 1993b, Pedras, 1997). Phomalide (**4**) is produced in *vitro* earlier than sirodesmine PL (**1**), which inhibits the biosynthesis of **4** (Pedras, 1998). Moreover, phomalide (**4**) was detected in extracts of infected plant tissues suggesting its production *in planta* (Pedras and Biesenthal, 1998). Host-selective toxins such as phomalide (**4**) could serve as a useful tool for the rapid screening and selection of disease-resistant plants (Pedras et al., 1993b; Pedras, 1997).

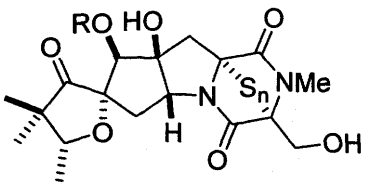

1 R = Ac n=2
41 R = Ac n=1
42 R = Ac n=3
43 R = Ac n=4

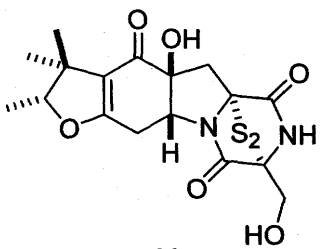

44

Similarly, avirulent isolates grown in Cove's liquid media produce metabolites of polyketide origin, which are characteristic of the pathotype group. Pedras et al. (1993a) reported phomaligols A (**45**) and A1 (**46**), and phomaligadiones A (**47**) and B (**48**) from cultures of avirulent strain grown in potato dextrose or Cove's media. The structures of phomaligols and phomaligadiones were established by spectroscopic methods and chemical derivatization. Phomaligadiones A (**47**) and B (**48**) are tautomeric forms (Pedras et al., 1993a). Further, the chemical analysis of liquid cultures of avirulent isolates producing yellow pigments led to isolation of phomapyrone A (**49**), B (**50**) and C (**51**), whose structures were determined by spectroscopic methods (Pedras et al., 1994). Additionally, three yellow compounds, **5**, **6** and **7**, imparting yellow color to cultures of avirulent isolates in Cove's liquid media have been reported. These yellow compounds

are characteristic of avirulent isolates; as a result, they have chemotaxonomic significance (Pedras et al., 1995).

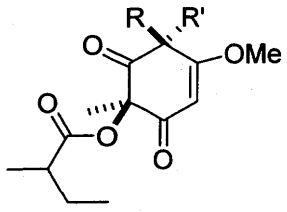

45 R = CH_3, R' = OH
46 R' = CH_3, R = OH

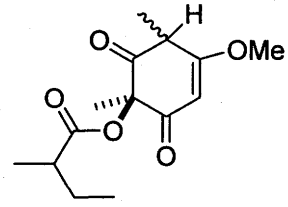

47

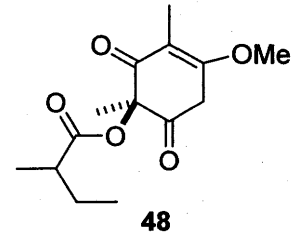

48

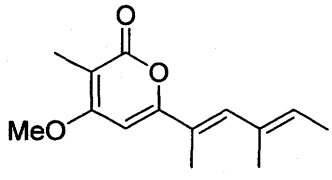

49

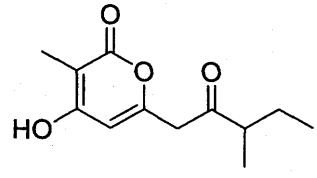

50

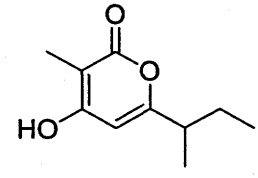

51

On the other hand, avirulent Polish type isolates produce secondary metabolites characterizing the pathotype group. The chemical investigation of Laird 2 /Mayfair 2 isolates led to identification of metabolites such as polanrazine A (**8**), phomapyrone A (**49**) and phomalairdenone A (**55**) (Pedras et al., 1999a). Phomalairdenone A (**55**) is a host-selective toxin, and it is the first example of a host-selective toxin representing a silphinene type sesquiterpenoid. The toxin causes necrotic, chlorotic, and reddish lesions on susceptible cultivars at a concentration of 5×10^{-4} M, whereas it has no effect on the resistant cultivar. In these respects, phomalairdenone A (**55**) appeared to mimic the pathogenicity range of Polish type isolates (Pedras et al., 1999a). Further chemical analysis of liquid cultures of avirulent isolates from Poland showed the production of similar metabolites to those of Mayfair and Laird 2 isolates. Pedras and Biesenthal (2001)

reported polanrazines B (**52**), C (**9**), D (**53**) E (**54**) and F (**10**) from liquid cultures of Polish isolate IBCN 19. Biosynthetically, polanrazines are derived from condensation of L-tryptophan and L-valine (Pedras, 2001). Polanrazines are unique metabolites to avirulent Polish type isolates, which were proposed as chemical markers of the pathotype group (Pedras and Biesenthal, 2000).

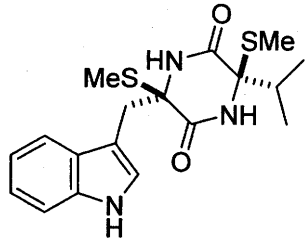

52

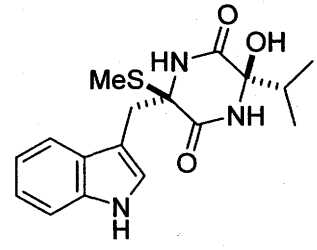

53

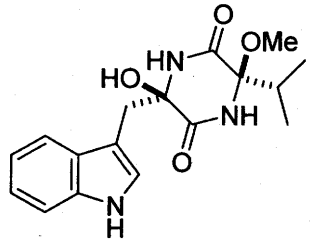

54

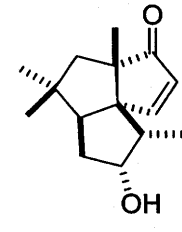

55

1.3.4.2 Host-selective toxins

Since fungal diseases cause enormous economic losses, several studies are focused on plant-fungal interactions resulting in disease. Initially, the idea of involvement of chemical factors in plant diseases caused by pathogenic fungi evolved in the second half of the 19th century (Graniti, 1991). Since then, many reports have shown that the phytopathogenic fungi utilize chemical signals to facilitate invasion and colonization. The first plant disease known to be mediated by a fungal metabolite was the blackspot

disease of the Japanese pear caused by *Alternaria alternata* (Scheffer, 1997). Many phytopathogenic fungi produce phytotoxins in culture and in their host plants. Several of these phytotoxic metabolites have been reported but only a few were documented as host-selective (Walton, 1996). Host-selective toxins (HSTs) are secondary metabolites produced by phytopathogenic fungi that affect selectively only certain varieties or genotypes of a plant species. They are toxic to host plants at very low concentrations ranging from 10 pM to 1 μM. HSTs comprise classes of compounds such as polyketides, cyclic peptides, terpenoids, saccharides, and compounds of uncertain biogenesis (Walton, 1996; Liakopoulou-Kyriakides et al., 1997).

Host-selective toxins produced by phytopathogenic fungi facilitate fungal invasion and colonization of the host. These HSTs mimic the pathogenicity range of the toxin-producing pathogen, reproducing the disease symptoms in the absence of the pathogen. They determine the virulence and specificity of pathogenic fungi. Knowledge of the mechanism of action of HSTs and their targets in the host cells enables the understanding of the molecular basis of fungal diseases (Kohmoto and Otani, 1991; Scheffer, 1997). Several studies have been carried out to understand the role of HSTs in the development of the disease. Of more than twenty host-selective toxins known to date, most of them were reported from two fungal genera, *Cochliobolus* and *Alternaria*. These HSTs include victorin, T-toxin and HC-toxin from Cochliobolus, and AF-toxin, ACT-toxin, and ACTG-toxin. Few HSTs have also been reported from other fungal genera including *Phyllostica maydis, Periconia circinata*, and *L. maculans*.

I) Host-selective toxins from *Phoma lingam/Leptosphaeria maculans*

Although blackleg (*Phoma lingam/Leptosphaeria maculans*) is a devastating disease of economically important cruciferous crops, not as much work has been done on it regarding the biochemistry and molecular genetics of disease development and disease resistance as compared to plant diseases caused by the fungal genera *Cochliobolus* and

Alternaria. However, blackleg appears to be one of the toxin-mediated diseases since the causative agent, *P. lingam/L. maculans*, like the species and pathotypes of *Cochliobolus* and *Alternaria*, is a host-selective pathogen. So far, two host selective toxins, phomalide (**4**) and phomalairdenone A (**55**), were reported from this fungal pathogen (*P. lingam/L. maculans*).

Phomalide (**4**) was isolated from 24-60-h-old cultures of virulent isolates of *P. lingam/L. maculans* and its structure was elucidated by combination of both spectroscopic methods and chemical degradation (Pedras et al., 1993b; Pedras, 1997). Chemically, phomalide (**4**) is a 15-membered cyclic depsipeptide composed of five residues, dehydrothreonine (DhThr), (*S*)-valine [(*S*)-Val], (*R*)-leucine [(*R*)-Leu], (*S*)-3-phenyllactic acid [(*S*)-O-Phe], and (*S*)-2-hydroxyisovaleric acid [(*S*)-O-Leu], in a sequence of cyclo(DhThr-Val-Leu-O-Leu-O-Phe). The chemical structure was confirmed by total synthesis (Ward et al., 1996; 1999). Phomalide (**4**) was also identified to be produced *in planta* by virulent isolates of *P. lingam/L. maculans* (Pedras, 1998; Pedras and Biesenthal, 1998). The host-selectivity of phomalide (**4**) correlated to the pathogenicity range of the pathogen; both phomalide (**4**) and the pathogen cause damage on leaves of *Brassica napus*, *B. rapa*, and other susceptible species. Phomalide (**4**) exhibited phytotoxicity at a concentration of 5×10^{-5} M to *B. napus* (susceptible to the pathogen), whereas no effect was observed on *B. juncea* (resistant to the pathogen). From the structure-activity relationships studies of phomalide (**4**), the (*E*)-double bond configuration of phomalide (**4**) appears to be essential for the observed host-selective phytotoxicity (Ward et al., 1996; 1999). Moreover, phomalide (**4**) causes disease symptoms on susceptible plants similar to the pathogenic fungus, *P. lingam/L. maculans*. Therefore, phomalide (**4**) appears to be essential for host-selectivity and virulence of the pathogenic fungus *P. lingam/L. maculans*. However, much work remains to be done to establish the role of phomalide (**4**) in the disease development (Pedras, 1998; Pedras and Biesenthal, 2000).

Phomalairdenone A (**55**) is another host-selective toxin produced in the liquid cultures of Polish type isolates of *P. lingam/L. maculans* (Pedras et al, 1999a). Polish type isolates are pathogenic to *B. juncea* (brown mustard), but not to rapeseed (*B. napus* and *B. rapa*) (Taylor et al., 1995). Phomalairdenone A (**55**) is the first example of a host-selective toxin representing a silphinene-type sesquiterpenoid. The toxin caused necrotic, chlorotic, and reddish lesions on susceptible cultivars at a concentration of 5×10^{-4} M, whereas no effect on resistant cultivars were observed. In these respects, phomalairdenone A (**55**) appeared to mimic the pathogenicity range of Polish type isolates. However, the phytotoxicity of phomalairdenone A (**55**) appears to be lower as compared to most-host selective toxins. Furthermore, not much else is known about the role of phomalairdenone A in infection and disease development (Pedras et al, 1999a).

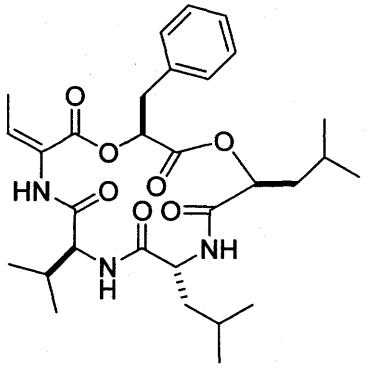

4

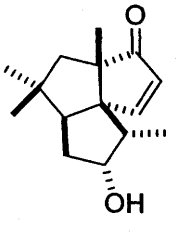

55

II) HSTs from genera Alternaria

The HSTs are the determinant factors of the pathogenicity and host-selectivity of species and pathotypes in the genus *Alternaria*. The genus *Alternaria* is well known to cause plant diseases mediated by host-selective toxins. These HST-mediated diseases

have been studied for establishing the biochemical basis of disease development and resistance in host plants. However, the role of HSTs in the development of diseases caused by *Alternaria* is only little known. One of the reasons is that the sexual stage of the fungus *Alternaria* is not known, making the genetic analysis of HSTs production difficult. Several host-selective toxins have been reported from species and pathotypes of the genus *Alternaria* (Scheffer, 1997).

HSTs from *Alternaria brassicae*

Destruxin B (**56**) and homodestruxin B (**57**) are cyclodepsipeptides characterized as HST from Alternaria brassica, the causative agent of blacklegspot disease of *Brassica* species (Ayer and Pena-Rodriguez, 1987; Bains and Tewari, 1987). The structures and absolute stereochemistry of destruxin B (**56**) and homodestruxin B (**57**) were established based on chemical and spectroscopic methods and comparison with previous work (Ayer and Pena-Rodriguez, 1987). Destruxin B (**56**) caused necrotic and chlorotic symptoms in different plant species, of which *Brassica* species was the most sensitive. Moreover, the sensitivity also varied in degree within the *Brassica* species, suggesting that destruxin B (**56**) is a host-selective but not host-specific compound (Buchwaldt and Green, 1992; Pedras et al., 2001). Additionally, destruxin B (**56**) mimics the pathogenicity range of *A. brassica*, and causes similar disease symptoms on host plants. The detection of destruxin B (**56**) in infected *B. napus* suggests its production *in planta* as well (Buchwaldt and Jensen, 1991; Pedras and Smith, 1997). Furthermore, Buchwaldt and Green (1992) identified the production of destruxin B (**56**) by germinating conidia of *A. brassicae* at early stages of the infection process, which suggests the importance of destruxin B (**56**) in the initial colonization of plant tissue (Buchwald and Green, 1992). Homodestruxin B (**57**) also appears to have a role in facilitating colonization of plant tissue; it was found to be produced *in planta* as well (Buchwaldt and Jensen, 1991; Pedras and Smith, 1997).

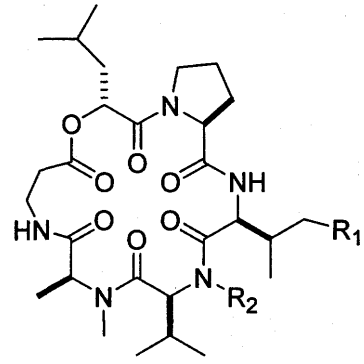

	R1	R2
56	CH_3	H
57	CH_3	CH_3

Evidence that destruxin B (**56**) and homodestruxin B (**57**) play important roles in the development of Alternaria blackspot disease was observed from their metabolism by plants (Pedras et al., 1999c, 2001, 2003c). Plant detoxification of destruxin B (**56**) and homodestruxin B (**57**) was observed both in resistant and susceptible plants but at different rates, being faster in resistant plants than in susceptible. Pedras et al. (2001, 2003c) studied the detoxification pathway by feeding ^{14}C-labeled destruxin B (**56**) to leaves of blackspot-resistant (*Sinapis alba*, *Camelina sativa*, *Capsella bursa-pastoris* and *Eruca sativa*) and susceptible plants (*Brassica napus*, *B. juncea* and *B. rapa*). Destruxin B (**56**) was found to undergo subsequent transformation to hydroxydestruxin B (**58**), β-D-glucosyl hydroxydestruxin B (**59**), and then to (6'-*O*-malonyl)hydroxydestruxin B β-D-glucopyranoside (**60**) as shown in scheme 1. The structures of hydroxydestruxin B (**58**), β-D-glucosyl hydroxydestruxin B (**59**) and (6'-*O*-malonyl)hydroxydestruxin B β-D-glucopyranoside (**60**) were determined by spectroscopic data and confirmed by total synthesis. In these subsequent detoxification steps, hydroxylation was the rate limiting step in susceptible plants whereas glucosylation was the rate limiting step in the resistant

species. Moreover, the detoxification product, hydroxydestruxin B (**58**) induced production of phytoalexins in resistant plants, which was not observed in susceptible plants. Similarly, the detoxification reaction converted homodestruxin B (**57**) to hydroxyhomodestruxin B at a faster rate in resistant plants as compared to susceptible plants (Pedras et al., 1999c, 2001, 2003c).

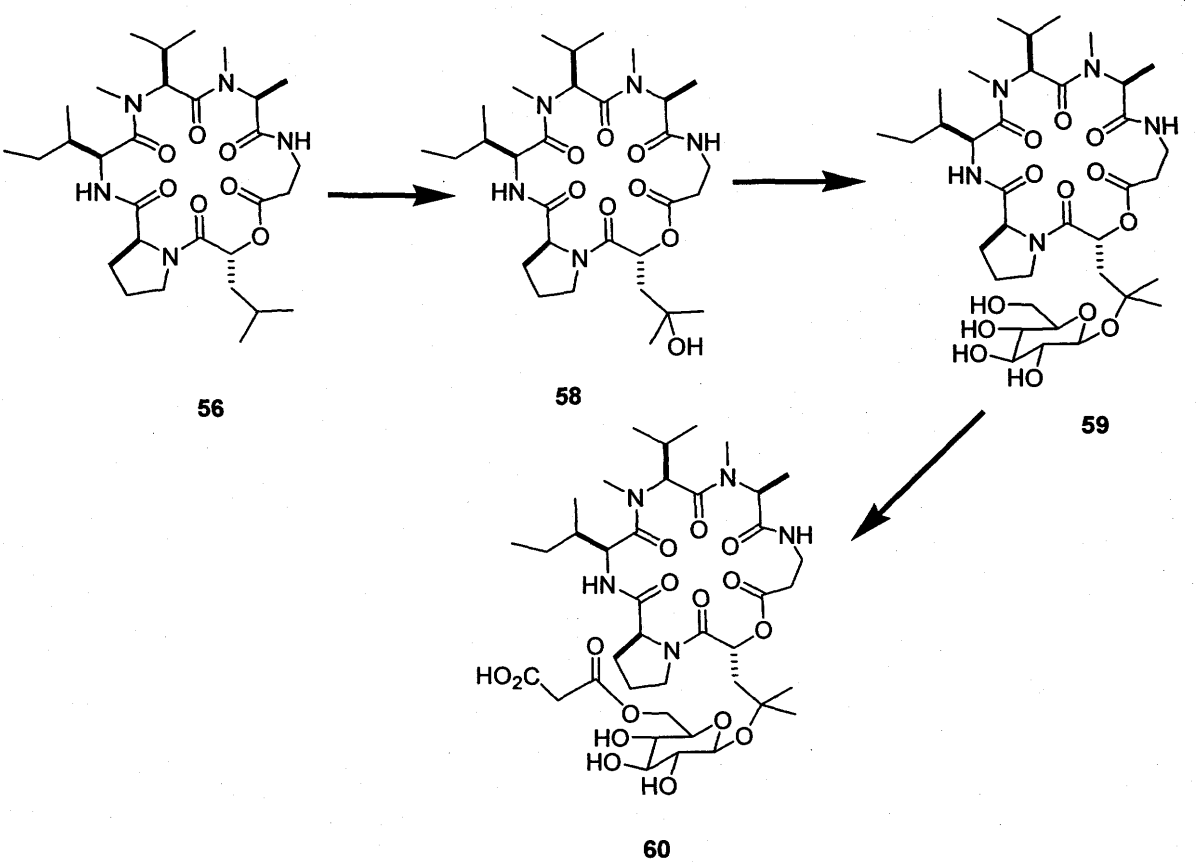

Scheme 1. Detoxification of destruxin B (**56**) by crucifers (Pedras et al., 1999c, 2001, 2003)

HSTs from *Alternaria alternata* (Fr.) Keissler

Alternaria alternata has seven pathotypes, which are pathogenic to susceptible plants such as Japanese pear, rough lemon, tangerine, strawberry and tomato. Each pathotype produces host-specific phytotoxins that appear to mediate disease caused by pathotype group (Park et al., 1987; Kohmoto and Otani, 1991; Walton, 1996).

Pathotype pathogenic to Japanese pear (*A. alternata* f. sp. kikuchiana)

Two host-specific phytotoxins, AK-toxin I (**61**) and II (**62**), have been reported from *A. alternata* f. sp. kikuchiana, a causative agent of backspot disease of Japanese pear. AK-I (**61**) and II (**62**) were isolated from a culture broth of *A. alternata* f. sp. kikuchiana (Nakashima et al., 1982), and their structures were characterized as 8-[(2'S,3'S)-2-acetylamino-3'-methyl-3'-phenylpropionyloxy]-(8R,9S)-9,10-epoxy-9-methyl-deca-(2E,4Z,6E)-trienoic acid (**61**) and 8-[(2'S)-2-acetylamino-3'-phenylpropionyloxy]-(8R,9S)-9,10-epoxy-9-methyl-deca-(2E,4Z,6E)-trienoic acid (**62**), respectively (Nakashima et al., 1985). These AK-toxins were reported to affect the Nijisseiki pear, a susceptible Japanese pear. These toxins cause symptomatic lesions on the susceptible pear cultivar, Nijisseiki, at a low concentration (10^{-8} M). The host-specific phytotoxicity observed for AK-toxin I (**61**) and II (**62**) was similar to that of the causal fungus itself. Consequently, AK-toxin I (**61**) and II (**62**) were considered determinants of pathogenicity of *A. alternata* and mediators of blackspot disease of Japanese pear (Nakashima et al., 1985; Scheffer, 1997).

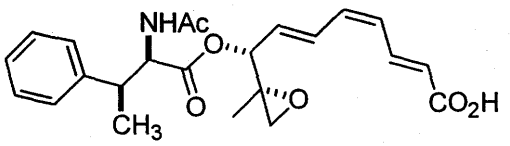

61

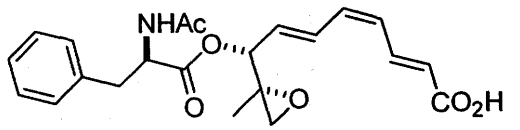

62

Biosynthetic studies showed that these AK-toxins are biosynthesized from (8R,9S)-9,10-epoxy-8-hydroxy-9-methyldecatrienoic acid (Feng et al., 1990; Nakatsuka et al., 1990). Moreover, two genes, AKT1 and AKT2, controlling the biosynthesis of AK-toxins were characterized (Tanaka et al., 1999). The mutants (Tox^-) without these genes were unable to biosynthesize AK-toxins and were not pathogenic, confirming that AK-toxins are essential factors in pathogenicity of the Japanese pear pathotype (Tanaka et al., 1999). Further study on the infection mechanism of blackspot pathogen in Japanese pear indicated that AK-toxins are essential for infection to occur. In addition, it was shown that inhibition of AK-toxin production in germinating spores of the pathogen decreased the infection (Otani et al, 2002). The primary site of action of AK-toxins is on the plasma membrane of susceptible pear cells, causing changes in the permeability of the plasma membrane. Moreover, AK-toxins released by germinating spores appear to suppress defensive mechanisms of susceptible pear. These facts support AK-toxins as virulence factors of *A. alternata* f. sp. kikuchiana (Park et al, 1987; Otani et al, 2002).

Host-specific toxins from *A. alternate* f. sp. citri

A. alternata f. sp. *citri* is a pathogenic fungus which causes brownspot disease of two closely related cultivars, Dancy tangerine and Emperor mandarin (Scheffer, 1997; Kono et al., 1986). Two host-selective phytotoxins, ACTG-toxins A (**64**) and B (**63**) were isolated from the culture broth of *A. alternata* f. sp. *citri*. Structurally these toxins are

related by having in common a six-membered ring connected via a methylene group to a five-membered ring having an alkenyl substituent. ACTG-toxins A (**64**) and B (**63**) were toxic to susceptible plants such as *Dancy tangerine* (*Citrus reticulata*) and other mandarin species. Four different bioassays showed ACTG-toxins to be active on susceptible plants at a concentration of 0.1μg/mL (Kohmoto and Otani, 1991). However, the selectivity of ACTG-toxins varied in degree depending on the bioassay method carried out on the host plants. The observed selectivity of ACTG-toxins to *Dancy tangerine* was greater in leaf puncture and cutting uptake bioassays, but it was low in the assays based on loss of electrolytes. These toxins were shown to affect non-host citrus species, whereas the pathogen producing ACTG-toxins infects only mandarin and grapefruit (Gardner et al., 1986). That is, the selectivity range of ACTG-toxins and the pathogenicity range of the tangerine pathotype of *A. alternata* f. sp. *citri* are not directly correlated (Kohmoto et al., 1979; Gardner et al., 1986). In fact, whether ACTG-toxins have a role in the development of brownspot disease is not known (Kohmoto and Otani, 1991). Additional reports also indicate doubts about ACTG-toxins as host selective toxins (Liebermann et al., 1994; 1997; and 2000).

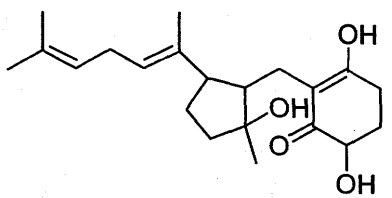

63

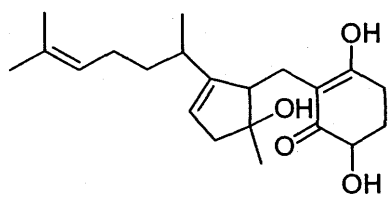

64

Kohmoto et al. (1993) also reported two additional host-selective toxins, ACT-toxins Ib (**65**) and IIc (**66**), from *A. alternate* f. sp. *citri* affecting tangerines and mandarins. These host-selective toxins are structurally similar to AK-toxins in having 9,10-epoxy-8-

hydroxy-9-methyl-decatrienoic acid as a common structural moiety (Nakashima et al., 1982; 1985). (8R,9S)-9,10-epoxy-8-hydroxy-9-methyldecatrienoic acid was also determined to be the biosynthetic intermediate of AK-toxins, suggesting ACT-toxins to share the same biosynthetic pathway with AK-toxins (Kohmoto et al., 1993; Masunaka et al., 2000). Moreover, the homologs of AKT genes, the genes responsible for biosynthesis of (8R,9S)-9,10-epoxy-8-hydroxy-9-methyldecatrienoic acid, were also found in the ACT-toxins producing pathogen (Tanaka et al., 1999; Masunaka et al., 2000; Hatta et al., 2002). Unlike ACTG-toxins, ACT-toxins are host-specific toxins exhibiting the same host range as the producing fungal isolates. ACT-toxins are selectively toxic to host plants at concentrations of μM or less. Moreover, the tangerine pathotype produces ACT-toxin Ib (**65**) as the major toxin at the site of infection, indicating ACT-toxin Ib (**65**) to be essential for disease development in susceptible citrus. Furthermore, addition of ACT-toxin Ib (**65**) to the site of infection allowed a toxin-minus isolate to colonize host plants (Kohmoto et al., 1993). ACT-toxin IIc (**66**) was also detected in trace amounts in extracts of spore germination fluids; however, the authors suggested ACT-toxin IIc (**66**) to be an artifact of isolation resulting from ACT-toxin Ib (**65**), perhaps from exposure of ACT-toxin Ib to light (Kohmoto et al., 1993).

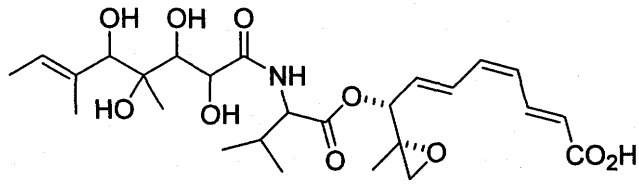

65

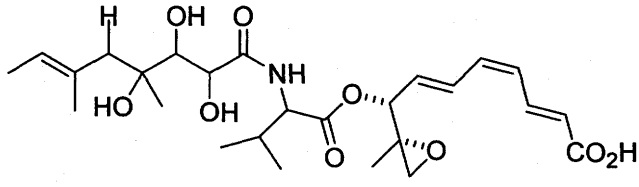

66

Another pathotype of *A. alternata* f. sp. *citri*, which causes brownspot disease of rough lemon (*Citrus jambhiri* Lush.) and Rangpur lime (*C. limonia* Osbeck), produces host-specific ACRL-toxins, I (**69**), II (**67**) and III (**68**), in which ACRL-toxin I (**69**) is the major toxin (Gardner et al., 1985; Kono et al, 1985). The chemical structures and absolute stereochemistry of ACRL-toxins were determined on the basis of NMR, circular dichroism (CD) and X-ray crystallography (Kono et al., 1986). The major toxin, ACRL-toxin I (**69**), was determined to be a 19 carbon polyalcohol with an α-dihydropyrone ring whereas the minor ACRL-toxins are analogous compounds of different chain lengths with a 2-pyrone moiety. These ACRL-toxins cause serious damage on susceptible cultivars of rough lemon and Rangpur lime, and exhibit therefore the same plant specificity as the fungus itself. Consequently, ACRL-toxins were thought to be determinants of the specificity in the interaction between rough lemon and the fungal pathogen *A. alternata* rough lemon pathotype. Although host-plant specificity is the same for all ACRL-toxins, they differ in strength of toxicity, with ACRL-toxin I (**69**) being the most toxic toxin of all (ED_{50}, 18-30 ng/mL) (Kono et al., 1986; Gardner et al., 1985). Moreover, the primary site of action for these ACRL-toxins in the plant-pathogen

interaction is the mitochondria of foliar cells of the susceptible host plant (Akimitsu et al., 1989; Ohtani et al., 2002).

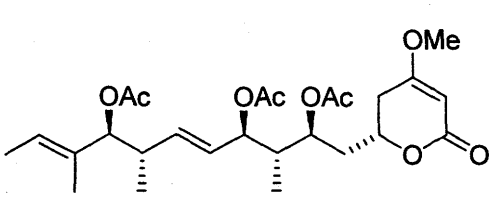

67

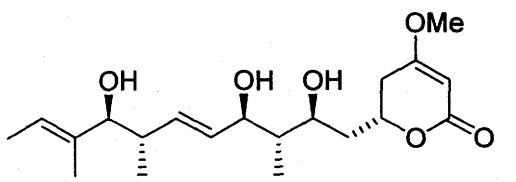

68

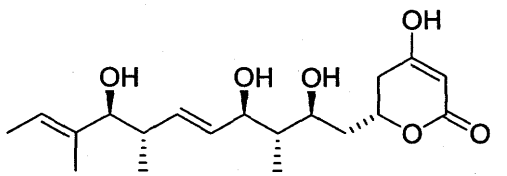

69

Host selective toxins from strawberry pathotype of *Alternaria alternata*

The strawberry pathotype of *A. alternata*, a causative agent of Alternaria blackspot disease of strawberry cv. Morioka-16, produces a series of analogous host-selective toxins, AF-toxin I (**70**), II (**71**) and III (**72**), whose structures were determined by means of chemical and spectroscopic methods (Nakatsuka et al., 1986). AF-toxin I (**70**), II (**71**) and III (**72**) are stereoisomeric compounds with (2*E*,4*E*,6*Z*), (2*E*,4*Z*,6*E*) and (2*E*,4*E*,6*E*) stereochemistry, respectively. These toxins are structurally similar to those of AK-toxins of the Japanese pear pathotype and ACT-toxins of the tangerine pathotype in having a common 9,10-epoxy-8-hydroxy-9-methyldecatrienoic acid moiety. Thus, AF-, AK-, and ACT-toxins producing pathogens should share genes required for the biosynthesis of this common moiety (Nakatsuka et al., 1990; Hatta et al., 2002). For these stereoisomeric toxins, their biological activity appears to be correlated with slight differences in chemical structures (Scheffer, 1997). For instance, AF-toxin I (**70**) causes leaf necrosis

both on Morioka-16 strawberry and Nijisseiki pear, AF-toxin II (**71**) on Nijisseiki pear only, and AF-toxin III (**72**) strong on strawberry and slight on pear (Scheffer, 1997). Of these, the host selectivity of AF-toxin I (**70**) fits exactly with the pathogenicity range of strawberry pathotype. Additionally, AF-toxin I (**70**) is also released by germinating spores of the strawberry pathotype during the early stage of infection. Moreover, a mutant of the strawberry pathotype lacking capability to produce AF-toxin I (**70**) was found to be avirulent to strawberry (Ito et al., 2004). Thus, AF-toxin I is the determinant factor of the pathogenicity of strawberry pathotype (Hayashi et al, 1990). AF-toxin II (**71**) and III (**72**) are minor products present in cultures of the strawberry pathotype, and appear to be isomerization products of AF-toxin I (**70**) (Nakatsuka et al., 1986).

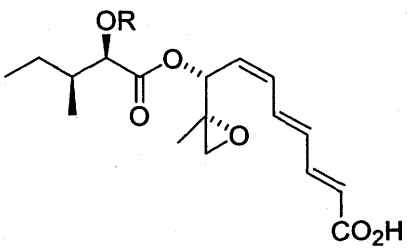

70 R = $COCH(OH)C(CH_3)_2OH$
71 R = H
72 R = $COCH(OH)CH(CH_3)_2$

Host selective toxins from *A. alternata* f. sp. mali

Alternaria blotch of apple caused by *A. alternata* f. sp. *mali* is a disease mediated by host-selective toxins. Multiple host-selective toxins, AM-toxin (**73**), (**74**), and III (**75**), have been isolated from the culture filtrates of *A. alternata* f. sp. *mali*, and the chemical structures were determined by spectroscopic methods and total synthesis (Ueno et al, 1975a, 1975b). AM-toxins are four-membered cyclic depsipeptides consisting of a

molecule of L-α-hydroxyisovaleric acid, L-alanine, α-amino acrylic acid, and derivatives of L-α-amino-δ-phenylvaleric acid. The major toxin of the three derivatives, AM-toxin I (**73**) is described as [cyclo(α-hydroxyisovaleryl-α-amino-p-methoxyphenylvaleryl-α-aminoacryl-alanyl-lactone)] (Ueno et al., 1975a, 1975b). These AM-toxins showed extremely potent biological activity; for instance, AM-toxin I (**73**) at a concentration of 10^{-8} M caused an increase in electrolyte loss and necrosis in susceptible apple tissue. Moreover, they exhibit host-selectivity that corresponds to the pathogenicity range of *A. alternata* f. sp. *mali*, indicating that AM-toxins play an important role in host recognition during the early stages of infection (Kohmoto et al., 1976; Scheffer, 1997). Further, the mutants of *A. alternata* apple pathotype that do not produce AM-toxin were unable to cause disease symptoms on susceptible apple cultivars. Thus, AM-toxins are a primary determinant of virulence and specificity in the *A. alternata* apple pathotype-apple interaction (Johnson et al., 2000; Johnson et al., 2001).

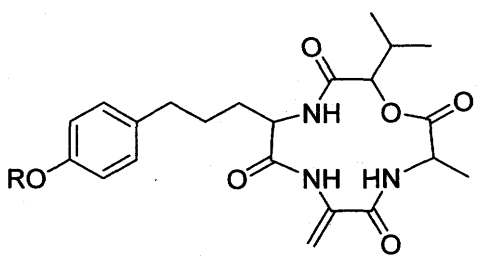

73 R = OCH_3
74 R = H
75 R = OH

Host-selective toxins from *A. alternata* f. sp. lycopersici

A. alternata f. sp. *lycopersici*, a cusative agent of Alternaria stem canker disease in tomato, produces multiple host-selective toxins, AAL-toxins, **76-79** (Bottini et al., 1981;

Caldas et al., 1994). Regioisomeric AAL toxins, which were grouped in T_A and T_B, have been reported from the liquid cultures of *A. alternata* f. sp. *lycopersici*. Chemically, AAL toxins are esters of 1-amino-11,15-dimethylheptadeca-2,4,5,13,14-penthol (Caldas et al., 1994). These AAL toxins are also produced by the pathogen during disease development and were detected in extracts of necrotic leaves of tomato plants infected with the pathogenic fungus (Siler and Gilchrist, 1983). AAL toxins affect only those tomato species susceptible to *A. alternata* f. sp. *lycopersici*, and reproduced the necrotic symptoms of the disease (Gilchrist and Grogan, 1975; Mesbah et al., 2000). Thus, AAL toxins appear to function as chemical determinants of the Alternaria stem canker disease in tomato. Moreover, the study on structure-activity relationship of AAL toxins revealed that the amine function of the toxin is essential for biological activity (Siler and Gilchrist, 1983). However, the detailed mechanism of action of AAL toxins in the development of Alternaria stem canker disease is not well understood (Kohmoto and Otani, 1991; Scheffer, 1997).

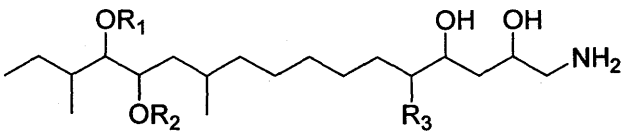

		R1	R2	R3
T_A	**76**	H	Y	OH
	77	Y	H	OH
T_B	**78**	H	H	H
	79	Y	Y	H

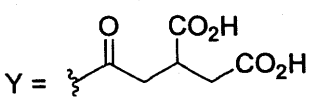

III) Host selective toxins from genus *Cochliobolus*

Pathogenic species of the genus *Cochliobolus* are known to cause toxin-mediated plant diseases (Scheffer, 1997). Of these diseases, Victoria blight of oats, maize leaf spot and maize blight, which are caused by *C. victoriae*, *C. carbonum* and *C. heterostrophus*, respectively, are the most studied diseases in regard to the biochemistry of disease development and disease resistance. Each of the pathogenic species of *Cochliobolus* produces host-specific toxins that act as host recognition and virulence factors (Kohmoto and Otani, 1991; Walton, 1996).

Host selective toxins from *C. victoriae*

The pathogenic fungus *C. victoriae*, the causative agent of Victoria blight of oats, produces in culture several host selective toxins, of which victorin C (**80**) is the major host selective toxin (Scheffer and Pringle, 1963; Macko et al., 1985; Wolpert et al., 1986). A long time after the isolation of victorin C (**80**) (Scheffer and Pringle, 1963), Macko et al. (1985) established its chemical structure by chemical degradation and spectroscopic methods. Victorin C (**80**) belongs to a chemical class of cyclic peptides and is constituted by glyoxylic acid, 5,5-dichloroleucine, erythro-β-hydroxyleucine, victalanine, threo-β-hydroxylysine, and α-amino-β-chloroacrylic acid. The biological activity of victorin C (**80**) is quite remarkable; for instance, growth of susceptible oat (*Avena sativa*) roots was inhibited at a concentration of 0.1 ng/mL (Walton and Earle, 1983). Additionally, victorin C (**80**) affects selectively susceptible oats (*Avena sativa* L.), reproducing disease symptoms caused by the pathogenic fungus. The studies on the structure-activity relationships of victorin C revealed that the glyoxylic acid residue particularly the hydrated aldehyde group is essential for biological activity. For instance, victorin C (**80**) tested for its effect on dark CO_2 fixation in susceptible oat leaf slices showed inhibition of dark CO_2 fixation, whereas a victorin C derivative without the

glyoxylic acid residue had no effect on dark CO_2 fixation. Moreover, several studies have showed that specificity in toxicity of victorin C (**80**) is correlated with its specificity in binding to victorin C receptor, which is only available in susceptible oat (*Avena sativa* L.) (Wolpert et al., 1994; Wolpert and Macko, 1989; Navarre and Wolpert, 1999). Importantly, those mutants that did not produce victorin C were found to be nonpathogenic (Scheffer et al., 1967). Consequently, victorin C (**80**) appears to determine host-specificity and virulence of *C. victoriae*.

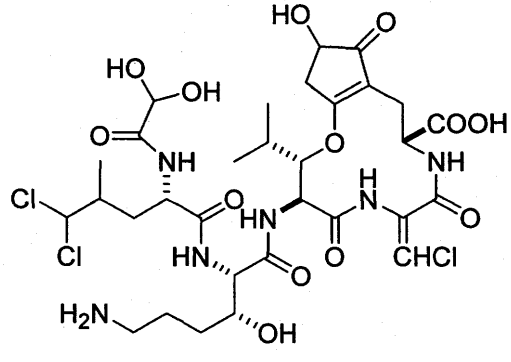

80

Host-selective toxins from *Cochliobolus carbonum* race 1

Northern leaf spot of maize caused by *C. carbonum* race 1 is a toxin-mediated disease (Kohmoto and Otani, 1991; Walton, 1996; Scheffer, 1997). The fungus, *C. carbonum* produces in culture HC-toxin (**81**), a host-selective toxin (Scheffer and Ullstrup, 1965). HC-toxin (**81**) contains a cyclic tetrapeptide, which is composed of four amino acids (cyclo-[(L-2-amino-9,10-epoxy-8-oxodecanoyl)-D-prolyl-L-alanyl-L-alanyl]) (Walton et al., 1982, Pope et al., 1983). HC-toxin (**81**) caused necrosis and inhibited growth of seedlings of susceptible maize whereas it had no effect on resistance maize (Scheffer and Ullstrup, 1965). The observed selectivity of HC-toxin (**81**) therefore

correlated with the pathogenicity range of *C. carbonum* race 1. Moreover, HC-toxin (**81**) is essential for *C. carbonum* race 1 colonization of susceptible maize as demonstrated by Comstock and Scheffer (1973). Non-pathogenic *C. carbonum* and *C. victoriae*, which are unable to colonize *C. carbonum* race 1 susceptible maize, were found to successfully colonize *C. carbonum* race 1-susceptible maize in the presence of HC-toxin (**81**). Thus, genetic variants of the pathogen unable to biosynthesize HC-toxin (**81**) are not pathogenic. They also lack genes required for the biosynthesis of HC-toxin (**81**) and pathogenicity, which are characterized for the pathogenic fungus. HC-toxin (**81**) is therefore the determinant factor of host-selectivity and pathogenicity of *C. carbonum* race 1 (Comstock and Scheffer, 1973; Cheng et al., 1999).

Studies of structure-activity relationships of HC-toxin (**81**) showed that reduction of the keto group of 2-amino-8-oxo-9,10-epoxydecanoic acid moiety of the HC-toxin to the corresponding alcohol resulted in a HC-toxin derivative, which completely lost its toxicity to maize which was sensitive to HC-toxin (Kim et al., 1987). Similarly, HC-toxin lost its biological activity by converting the epoxide of the 2-amino-8-oxo-9,10-epoxydecanoic acid moiety to the corresponding dihydroxy derivative (Ciuffetti et al., 1983; Walton and Earle, 1983). Additionally, HC-toxin treated with 2-mercaptoethanol, which modified the keto group of the 2-amino-8-oxo-9,10-epoxydecanoic acid moiety, was found to lose reversibly the inhibitory activities on histone deacetylases (HD1-A, HD1-B, and HD2) of *C. carbonum* race 1 susceptible maize in *vitro*. The conversion of the epoxide group by hydrolysis caused similar loss of inhibitory activity on histone deacetylases (Brosch et al., 1995). As these studies indicated, both epoxy and keto groups are essential for the biological activity of HC-toxin (**81**). Interestingly, HC-toxin was found to be detoxified in *vivo* by *C. carbonum* race 1 resistant maize by enzymatic conversion of the 8-keto group of 2-amino-8-oxo-9,10-epoxydecanoic acid moiety to the 8-hydroxy derivative of HC-toxin (**82**) (Meeley and Walton, 1991). Occurrence of the detoxifying enzyme, NADPH dependent HC-toxin reductase, in the resistant maize

cultivar (genotype Hm/Hm or Hm/hm) was attributed to be the biochemical basis of resistance to infection by *C. carbonum* race 1 (Johal and Briggs, 1992; Meeley et al., 1992).

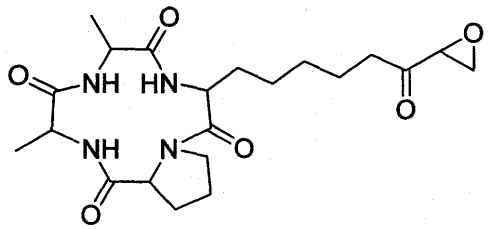

81

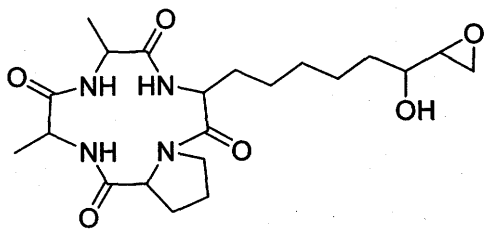

82

Host-selective toxins from *C. heterostrophus* race T (telemorph, *Bipolaris maydis*, = *Helminthosporium maydis*)

C. heterostrophus race T, the causative agent of Southern corn blight disease of maize (*Zea mays*), produces a host-selective toxin complex (HmT-toxins) in liquid culture (Kono and Daly, 1979). The structure determination of the major host-selective toxins by chemical and spectroscopic methods allowed the identification of two pairs of structurally isomeric HmT-toxins, Band 3-toxin (**83**) and Band 1'-toxin (**84**), and Band 1-toxin (**85**) and Band 2-toxin (**86**) of C_{39} and C_{41} polyketo-polyhydroxy compounds, respectively. The structural isomers differ from each other at C-24 in both C_{39} and C_{41} polyketo-polyhydroxy compounds, where one isomer contains a hydroxy group and the other a keto group. HmT-toxins represent a class of polyketides and HmT-toxins with C_{39} appear to be biogenetic intermediates in the production of HmT-toxins with C-41 (Kono et al., 1980; Kono et al., 1981). HmT-toxins exhibit high toxicity, toxic at concentrations of 10^{-8}-10^{-9} M, and biological specificity toward Texas male sterile maize (Suzuki et al.,

1982). Hence, both HmT-toxins and pathogenic *C. heterostrophus* race T are correlated in host-selectivity. These HmT-toxins are biosynthesized in the pathogenic *C. heterostrophus* race T, and the genes (Tox1A and Tox1B) responsible for HmT-toxins biosynthesis have also been characterized. By contrast, the genetic variant of the pathogen, race O, is unable to biosynthesize HmT-toxin. Thus, HmT-toxins are determinant factors of virulence and host-selectivity of *C. heterostrophus* race T (Kodama et al., 1999; Rose et al., 2002).

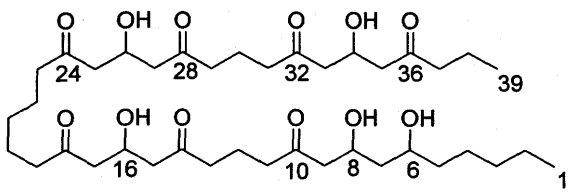

83

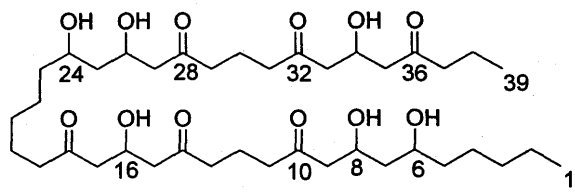

84

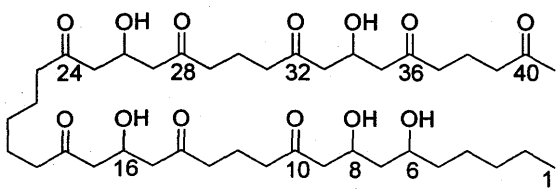

85

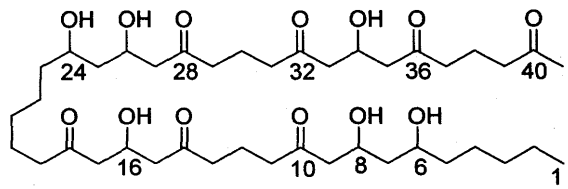

86

Host-selective toxins from *Bipolaris zeicola race* 3

Bipolaris zeicola race 3, the causative agent of leaf spot disease in maize, produces host-selective toxins, namely BZR-cotoxin I (**92**), II (**91**), III (**94**) and IV (**93**), in liquid culture and in spore-germination fluids. Chemically BZR-cotoxins are cyclic depsipeptide compounds, whose structures were established by both spectroscopic and chemical methods (Ueda et al., 1992; 1994; 1995a; 1995b). BZR-cotoxins are

biologically less active when assayed separately, but in combination they exhibit potent phytotoxicity and host-selectivity. Their host-selectivity correlated to the pathogenicity range of *B. zeicola* race 3, and caused disease symptoms on susceptible rice and maize plants. Interestingly, a non-pathogenic fungus like *Bipolaris victoriae* that could not penetrate alone into maize tissues, was found penetrating and colonizing maize tissues in the presence of BZR-cotoxins. On the other hand, mutants not producing BZR-cotoxins were also unable to infect host-plants compared to wild *B. zeicola* race 3. During infection, the germinating spores release BZR-cotoxins to facilitate colonization of host tissues of the toxin producing fungus. These facts indicate that BZR-cotoxins are the determinant factors of virulence and host selectivity of *B. zeicola* race 3 (Xiao et al., 1991; 1992).

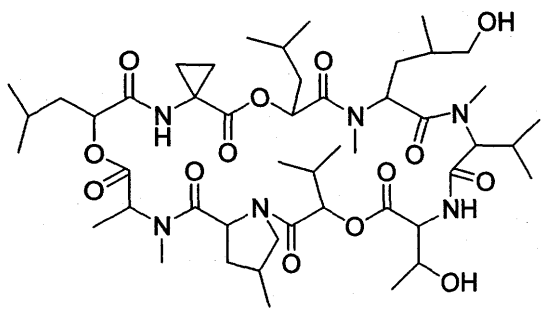

91

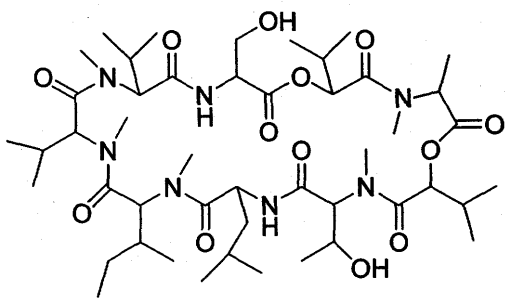

92

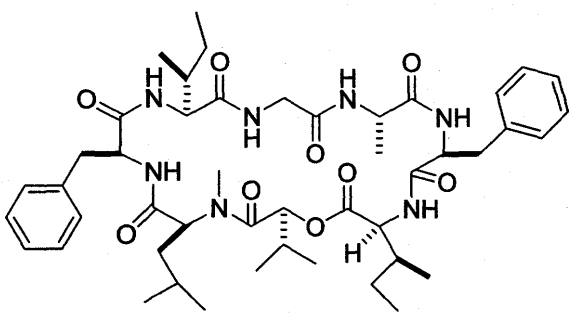

93

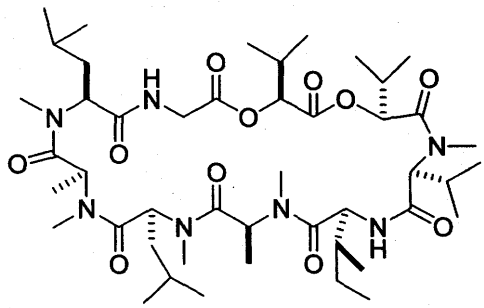

94

Host-selective toxins from *Bipolaris sacchari* (= *Helminthosporium sacchari*)

Three host-selective toxins, HS-toxin A (**95**), B (**97**) and C (**96**), have been reported from *B. sacchari*, a causative agent of eyespot disease of sugarcane. HS-toxins are structural isomers composed of a sesquiterpene linked to two residues of 5-O-(β-galactofuranosyl)-β-galactofuranoside (Steiner and Byther, 1971; Macko et al., 1981, 1983). Additionally, HS-toxins were also isolated from the leaves of sugarcane infected by *B. sacchari* (Strobel and Stainer, 1972). HS-toxins all exhibited selective toxicity towards *B. sacchari*-susceptible sugarcane cultivars, but had no effect on resistant sugarcane (Steiner and Byther, 1971). These toxin isomers were found to differ in toxicity toward *B. sacchari*-susceptible sugarcane cultivar; HS-toxin C (**96**) was the

highest and HS-toxin A (**95**) was the lowest in toxicity (Livingston and Scheffer, 1984). In several biological activities, HS-toxins also exhibit similar selectivity. For instance, in the investigation of HS-toxins effect on dark CO_2 fixation in HS-susceptible sugarcane leaf slices, maximum inhibition of dark CO_2 fixation was observed for HS-toxin A (**95**), B (**97**), and C (**96**), at concentrations of 4, 6, and 0.7 μM, respectively (Dubick et al., 1984). In addition, HS-toxins induced electrolyte losses from tissues of susceptible sugarcane cultivar at a concentration of 0.01 μg/mL. On the other hand, resistant sugarcane cultivar remained unaffected upon exposure of tissues at concentrations of 100 μg/mL (Scheffer and Livingston, 1980).

HS-toxins reproduce disease symptoms caused by the pathogenic fungus on host sugarcane cultivars (Steiner and Byther, 1971). A further study of the role of HS-toxins in eyespot disease development revealed that the primary site of action of HS-toxins is at the toxin receptor on the plasma membrane. Treatment of tissues of susceptible and resistant cultivars with C-14 labeled HS-toxin showed that only tissues of susceptible cultivars bound to the toxin, indicating the absence of a toxin receptor in resistant sugarcane cultivars. Therefore, the susceptibility of the sugarcane cultivars to the HS-toxins correlated to the availability of a toxin receptor. Thus, the absence of a HS-toxin receptor in resistant sugarcane was attributed to be the biochemical basis of the resistance of sugarcane to eyespot disease. HS-toxins are therefore essential for infection and disease development (Strobel, 1973; Strobel and Hess, 1974; Strobel et al., 1975; Kenfield and Strobel, 1981).

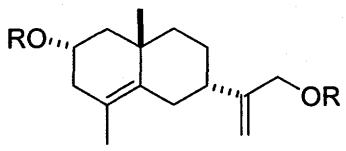

95

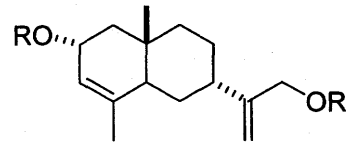

96

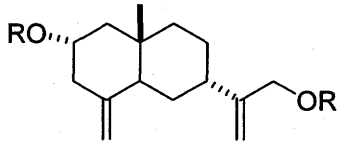

97

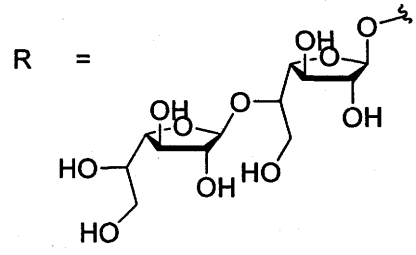

IV) Host-selective toxins from *Phyllostica maydis*

Yellow leaf blight of maize is a disease that appears to be mediated by host-selective toxins. The causative agent of the disease, *Phyllostica maydis*, produces a series of 10-12 PM-toxins in liquid culture (Comstock and Scheffer, 1973; Yoder, 1973). The structure determination of PM-toxins showed that the major four toxins, PM-toxin A (**90**), B (**88**), C (**89**) and D (**87**), are linear C_{33} and C_{35} polyketol compounds (Kono et al., 1983, Danko et al., 1984). PM-toxins are highly toxic (10^{-8}-10^{-9} M) and very selective for Texas male sterile maize (*Zea mays*). The biological assays showed that these toxins selectively inhibit seedling root growth, induce leaf chlorosis, and also cause an increased leakage of electrolytes on susceptible maize leaves, whereas no such effect was observed on resistant maize cultivar (Comstock and Scheffer, 1973). This host-selectivity of PM-toxins is similar to that observed for HmT-toxins; both are selective for Texas male sterile maize (Zea mays). Moreover, both PM-toxins and HmT-toxins are highly toxic (10^{-8}-10^{-9} M), and structurally similar, except that PM-toxins have shorter chain length than HmT-toxins. Like most host-selective toxins, PM-toxins mimic the pathogenicity range of the producing fungal isolate, and appear to be the determinants of host-

specificity and pathogenicity of *P. maydis* (Kono et al., 1983). Several studies were conducted to establish structure-activity relationships of PM-toxins. In these studies, many synthetic analogs of natural PM-toxins having 4β-ketol groups spaced by varying lengths of CH_2 chains or by a 1,3-diene chain were employed. The structural features contributing to biological activity of PM-toxins were shown to be the presence of four β-ketol groups with a spacing of chains equal to or longer than penta-methylene (Suzuki et al., 1987; 1988; 1991).

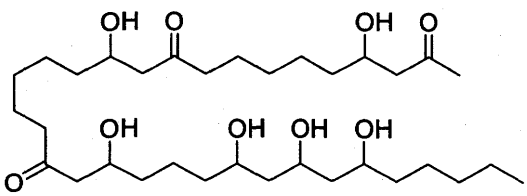

87

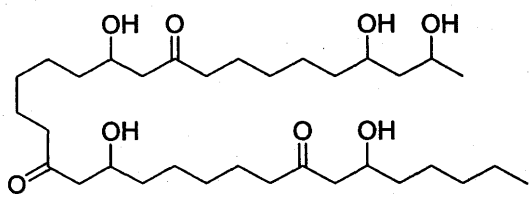

88

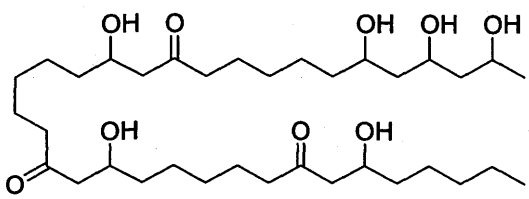

89

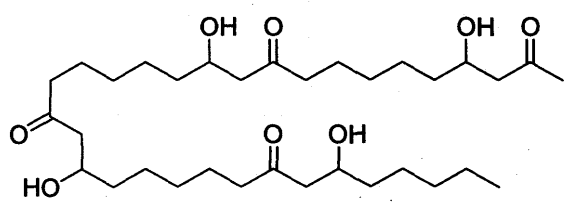

90

Host-selective toxins from *Periconia circinata*

The milo disease, a root and crown rot of the grain *Sorghum bicolor*, is a plant disease that also appears to be mediated by host-selective toxins. The host-selective toxins PC-toxin A (**98**) and B (**99**) were isolated from liquid cultures of *Periconia*

circinata, the causative agent of milo disease (Scheffer and Pringle, 1961; Pringle and Scheffer, 1963; 1967). Later on, Macko et al. (1992) established the chemical structures of PC-toxin A (**98**) and B (**99**) by a combination of spectroscopic methods and chemical degradation. PC-toxins are metabolites of mixed biosynthetic origin, consisting of two amino acids, a cyclic D-lysine and a D-aspartic acid, attached to a C_{10} polyketide unit (Churchill et al., 2001). Biological assays showed both culture filtrate and pure toxins (PC-toxins) to be selectively toxic to susceptible genotypes of sorghum, but not to the resistant genotypes. Similarly, PC-toxins exhibited selectivity in causing inhibition of primary root growth and in inducing electrolyte leakage in susceptible genotypes of sorghum at low concentrations (5 - 500 nM). Thus, the host-selectivity of PC-toxins correlated to the pathogenicity range of the pathogen (Gardner et al., 1972, Dunkle and Macko, 1995). Further, Macko et al (1992) established structure-activity relationships for PC-toxins based on comparison studies of PC-toxins and their derivatives. The free amino group at C-5 and the free hydroxy group at C-3 of the caprolactam ring of PC-toxins are crucial structural requirements for host-selective toxicities. For colonization of sorghum tissue by the pathogenic fungus, production of PC-toxins is essential. As the pathogenicity studies of isolates of *P. circinata* indicated, only toxin-producing isolates (Tox^+) were pathogenic to susceptible genotypes of sorghum, but not non-toxin-producing isolates (Tox^-). PC-toxins appear to be the determinant of host-selectivity and virulence of the fungus *P. circinata*. However, the role of PC-toxins in the disease development requires further investigation (Scheffer and Pringle, 1961; Churchill et al., 2001).

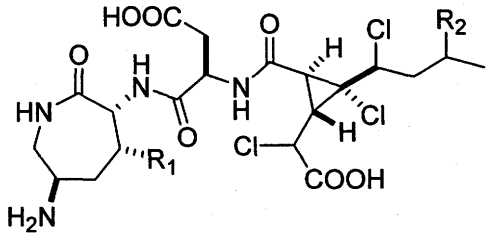

98 R1 = R2 = OH

99 R1 = OH, R2 = H

1.4 Conclusion: plant-fungal interactions

The virulence of the pathogen is decisive for establishment of the plant disease. Many studies indicated that host-selective toxins are essential for virulence of phytopathogenic fungi. The pathogenic fungus releases host-selective toxins at an infection site during the early stages of the infection process. These host-selective toxins disrupt the normal cell function and facilitate the successful infection of host tissues. Toxin deficient mutants (Tox^-) of pathogenic fungi are usually unable to cause infection, and can be shown to elicit successful infection of host tissues when inoculated with host-selective toxins of the pathogen. Thus, secretion of host-selective toxins is critical for the virulence of the fungus. Moreover, Dewey et al. (1988) demonstrated that HC-toxin, a host-selective toxin from *B. maydis*, is a virulence factor of the pathogen. The basis of susceptibility of maize species to *B. maydis* is secretion of HC-toxin; HC-toxin interacts with 13-kD maize mitochondrial protein to cause inhibition of whole cell respiration of susceptible maize species (Dewey et al., 1988).

Additional contributing factors to the virulence of a pathogenic fungus may be its ability to detoxify antifungal metabolites produced by plants. Several studies demonstrated that the phytoalexin and/or phytoanticipin detoxifying capability of a fungus correlated with its pathogenicity (VanEtten et al., 1989; Delserone et al., 1999; Bouarab et al., 2002). VanEtten and coworkers demonstrated this in their work on a pisatin detoxifying enzyme (VanEtten et al., 1989). The comparative studies with a strain producing pisatin detoxifying enzyme and a strain deficient in pisatin detoxifying enzyme indicated the existence of the correlation between the ability of the fungus to detoxify pisatin and its virulence. Only the strains with pisatin detoxifying enzyme were able to elicit successful infection of pea (*Pisum sativum* L.) (Delserone et al., 1999, George and VanEtten, 2001).

In plant-fungal interactions, initially the fungal infection triggers plant defenses, which include chemical defenses (Knogge, 1996). Plant chemical defenses are comprised of both constitutive antifungal compounds (phytoanticipins) and induced compounds (phytoalexins). Phytoanticipins play a defensive role during the early infection process by inhibiting fungal penetration (Osbourn, 1996). In addition, some reports indicated that disease resistance in plants correlated with the defensive role of phytoanticipins. For instance, oat species (*Avena strigosa*) producing the phytoanticipin avenacin A-1 exhibited resistance toward *G. graminis* var. *tritici*. On the contrary, avenacin A-1 deficient mutants were found to be susceptible to *G. graminis* var. *tritici*, supporting avenacin A-1 as a determinant of resistance in wild-type oat species (Osbourn et al., 1994; Papadopoulou et al., 1999). Further fungal infection triggers induced chemical defense causing the accumulation of phytoalexins. This accumulation of phytoalexins occurs at the site of infection within a short time and inhibits further fungal growth. Many studies suggested that phytoalexins are a resistance factor of plants, however, this was demonstrated in only few of these studies (Hammerschmidt, 1999; Pedras et al., 2003b). The first example to illustrate phytoalexins as a disease resistance factor was the works of Hain and coworkers (1993) on the stilbene phytoalexin. In this work, stilbene phytoalexin synthetase genes isolated from grapevine (*Vitis vinifera*) were transferred into phytoalexin deficient tobacco. As a result, transgenic tobacco showed increased disease resistance compared to that of wild-type tobacco (Hain et al., 1993). Thus, phytoalexins play an important role in protecting plants from fungal invasion. In addition, plant resistance against fungal infection can be attributed to their ability to detoxify host-selective toxins from the pathogen. For instance, the fungal pathogen *Cochliobolus carbonum* race 1, a causative agent of leaf spot disease of maize, is unable to infect a genotype of maize possessing HC-toxin reductase. The HC-toxin reductase detoxifies the HC-toxin, a virulence factor of *C. carbonum* (Johal and Briggs, 1992; Meeley et al.,

1992). Thus, plant resistance to fungal invasion and colonization largely arises from chemical defenses as well as from fungal toxin detoxifying enzymes of plants.

The factors involved in plant-fungal interactions, which are decisive for the pathogenicity of fungus on one hand and disease resistance in plants on the other hand, determine plant disease development. Factors such as host-selective toxins and antifungal compound detoxifying enzymes increase the virulence of the fungus, and thereby plant disease development. On the other hand, factors such as phytoanticipins, phytoalexins and phytotoxin detoxifying enzymes, which are involved in plant defense reactions, are crucial for plant resistance. Therefore, plant-fungal interactions end up in disease development if the chemical arsenal of the fungus overwhelms that from the plant. Such plant-fungal interactions are called compatible. On the contrary, strong plant defenses which cause disfunction of fungal invasive strategies hinder the disease development and such interactions are called incompatible (Ueno, 1990, Hadacek, 2002; Schulz et al., 2002).

CHAPTER TWO

2. Results and Discussion

2.1 Metabolites from Phoma lingam/Leptosphaeria maculans

This section describes and discusses the isolation and structure determination of metabolites from new isolates of *Phoma lingam/Leptosphaeria maculans* (Mayfair 2 and Laird 2) produced in MM as well as PDB medium. In addition, studies of the biogenetic origin of some of these metabolites are described. Phytotoxicities of the isolated metabolites were determined using phytotoxic assays carried out on oilseed crucifers: canola (*Brassica napus*, cv. Westar), brown mustard (*B. juncea*, cv. Cutlass), and white mustard (*Sinapis alba*, cv. Ochre). This study was conducted to establish interrelationships between isolates Mayfair 2 and Laird 2 and other isolates of *P. lingam/L. maculans* by their secondary metabolite profiles.

2.1.1 Metabolites produced in minimal medium (MM)

2.1.1.1 Isolation of metabolites

The fungal isolates Mayfair 2 and Laird 2 were grown on V8 agar medium to collect pycnidiospores. Pycnidiospores were employed for initiating liquid cultures. Liquid cultures of Mayfair 2 isolate were grown in a chemically defined medium, minimal medium (MM), under conditions indicated in the Experimental section. Broth and mycelium were separated by filtration. From previous work, since EtOAc extracts of

mycelium were found to be non-phytotoxic and its examination led only to the isolation of D-mannitol (Pedras et al., 1998), further chemical analysis was not carried out. The broth obtained from six-day-old cultures was combined (110 L) and concentrated by freeze-drying (22 L). The extraction of broth with EtOAc yielded on average 110 mg residue per 1 L of concentrated broth. As the TLC and HPLC analysis of EtOAc extracts indicated, a wide variety of secondary metabolites is produced by isolate Mayfair 2 in the minimal medium.

The residue was fractionated by flash column chromatography (FCC) using as eluent CH_2Cl_2-MeOH, as described in the experimental section and summarized in Scheme 2.1-2.3. The fractions were analyzed by TLC and HPLC, and combined accordingly. Fractions F1 and F2, the least polar fractions, contained mainly fatty acids and lipids, as shown by their ^1H NMR spectra, hence further purification was not carried out on this material.

Fractions F3 to F6 were combined and were subjected to PTLC, developed with CH_2Cl_2-MeOH (98:2), to yield phomalairdenol C (**118**, 12 mg) and phomapyrone F (**102**, 4 mg), and a non-homogenous fraction. This fraction was further subjected to PTLC, developed with hexane-EtOAc (80:20) to afford 3-oxosilphinene (**115**, 3 mg) and selin-11-en-4α-ol (**121**, 3 mg).

Fraction F7 (from EtOAc extract) was further fractionated by FCC, eluting with CH_2Cl_2-EtOAc. Prep. TLC on sub-fractions F2 and F3, yielded compounds phomapyrone A (**49**, 36 mg) and phomenin B, (**105**, 28 mg). Again sub-fractions F6 to F9 from FCC on F7 (from FCC on EtOAc extracts) were combined and subjected to PTLC, developed with CH_2Cl_2-MeOH (98:2), to yield phomalairdenone A (**55**, 12 mg) and phomapyrone D (**100**, 10 mg) and a PTLC fraction of non-homogenous material. The non-homogenous PTLC fraction was further subjected to PTLC, developed with hexane-EtOAc (60:40), to yield phomalairdenone D (**114**, 8 mg) and polanrazine B (**52**, 5 mg), and a non-homogenous PTLC fraction. Further separation of this non-homogenous fraction was

achieved by PTLC (hexane-Et_2O, 50:50) to afford phomapyrone G (**104**, 7 mg) and phomapyrone E (**101**, 4 mg).

The combined fractions F8-F9 (from FCC of EtOAc extracts) were subjected to RP-FCC and eluted with CH_3CN-H_2O (40:60) to obtain eight fractions. Sub-fractions F5 and F6 were combined and further purified by RP-FCC (CH_3CN-H_2O, 20:80) to yield depsilairdin (**122**, 22 mg).

The combined polar fractions F10-F12 (from FCC on EtOAc extracts) were chromatographed on PTLC, developed with CH_2Cl_2-MeOH (97:3), to obtain infectopyrone (**103**, 4 mg) and polanrazine C (**9**, 21 mg), and UV inactive non-homogenous material. This non-homogenous material was further subjected to PTLC and developed several times with CH_2Cl_2-Et_2O (50:50) to yield phomalairdenol B (**116**, 24 mg) and lairdinol A (**120**, 18 mg) as well as a non-homogenous PTLC fraction. Again, this non-homogenous fraction was further subjected to PTLC and developed several times with hexane-EtOAc (70:30), which finally yielded, after this laborious isolation steps, two compounds, phomalairdenol A (**117**, 8 mg) and phomalairdenol D (**119**, 9 mg).

Altogether four different classes of metabolites were isolated from cultures of isolate Mayfair 2, namely: dioxopiperazines (polanrazines), sesquiterpenes, polyketides (phomapyrones) and depsipeptide (depsilairdin). Of these metabolites, six sesquiterpenes (**114**, **116-120**), four phomapyrones (**100-102**, **104**) and depsilairdin (**122**) were new metabolites, and three sesquiterpenes (**55, 115, 121**), three phomapyrones (**49, 103, 105**), and two polanrazines (**9, 52**) were metabolites previously reported.

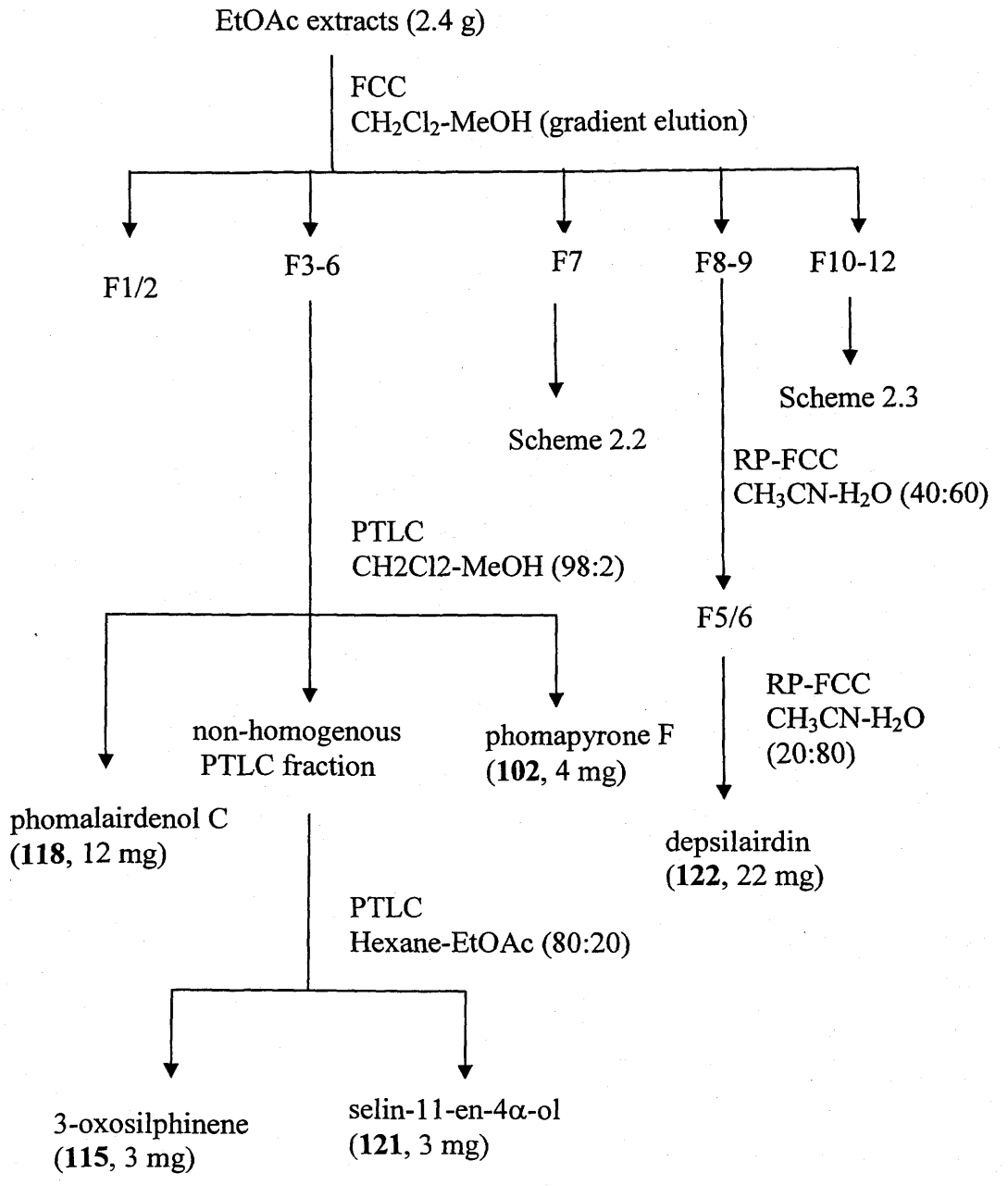

Scheme 2.1 Flow chart for separation of metabolites from EtOAc extracts of broth obtained from cultures of Mayfair 2

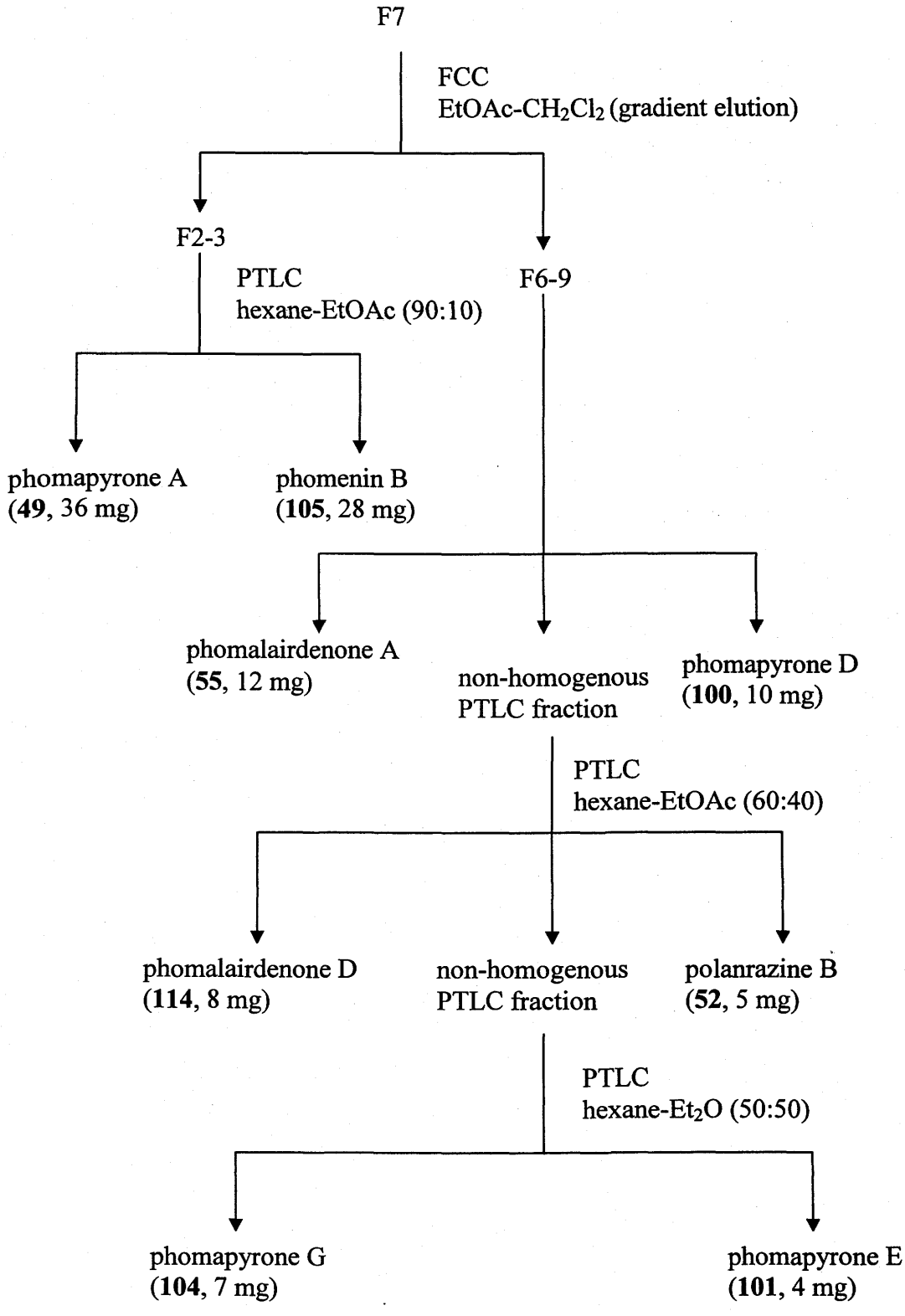

Scheme 2.2 Flow chart for separation of metabolites from EtOAc extracts of broth obtained from cultures of Mayfair 2

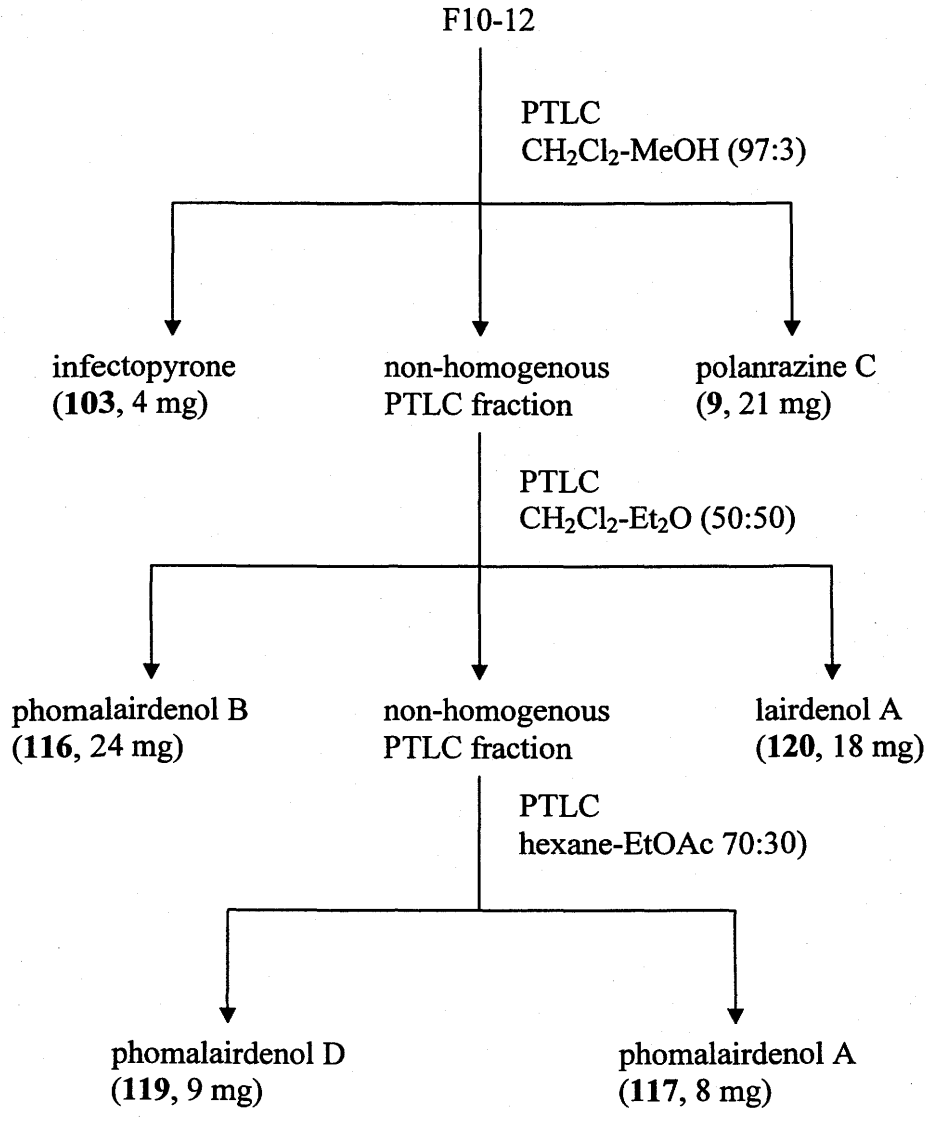

Scheme 2.3 Flow chart for separation of metabolites from EtOAc extracts of broth obtained from cultures of Mayfair 2

2.1.1.2 Structure determination

Polanrazines

Polanrazine B (**52**) and polanrazine C (**9**) were metabolites isolated previously from avirulent Polish isolates (Pedras and Biesenthal, 2001). Polanrazine B (**52**) and polanrazine C (**9**) were characterized by comparison of their ^{1}H NMR data and HPLC data (retention time and UV) with that of the authentic samples.

2-Pyrones

The molecular formula of compound **100** was determined to be $C_{12}H_{14}O_4$ (HREI-MS), indicating six degrees of unsaturation. The ^{1}H NMR indicated the presence of three methyl groups, one methoxy group, and two sp^2 hybridized CH protons, accounting for the total number of hydrogens. The proton decoupled ^{13}C NMR showed twelve resonances, three of which were due to methyl groups, one to a methoxy group, two to sp^2 methine groups, and seven to sp^2 hybridized quaternary carbons. For four of these carbons, the signals had chemical shifts suggesting oxygen-bearing carbons. From the ^{13}C NMR data it was evident that five of the six elements of unsaturation, indicated by the molecular formula of **100**, accounted for the presence of two carbonyl groups and three double bonds; the remaining one therefore required the presence of a ring. The carbon signal at δ_C 165.2 exhibiting a long-range correlation with a methoxy group at δ_H 3.95 was assigned to =C-OMe (C-4). Additional carbon signals at δ_C 199.7 and 164.5 were attributed to carbonyl carbons (C-9 and C-2) from a ketone and an ester, respectively. Another carbon at δ_C 158.2 was assigned to an oxygen attached to an olefinic carbon (C-6). The long-range correlations of the methyl group at δ_H 2.05 (H_3-12) with carbons at δ_C 164.5, 106.3 and 165.2, together with a long-range correlation of protons at δ_H 3.95 (OMe) with carbon at δ_C 165.2, allowed the assignment of carbons at δ_C 164.5, 106.3 and 165.2 as C-2, C-3 and C-4, respectively. Further, H-5 (δ_H 6.52) showed long-range

correlations with C-3 (δ_C 106.3) and C-4 (δ_C 165.2). The HMBC correlations of the proton at δ_H 6.52 (H-5) with carbons at δ_C 158.2 (C-6) and 139.8 (C-7), together with correlations of H_3-11 (δ_H 2.36) with C-6 (δ_C 158.2), C-7 (δ_C 139.8) and C-8 (δ_C 126.5) suggested the branching point to be at C-6 of the 2-pyrone unit. The long-range correlation of the olefinic proton at δ_H 7.15 (H-8) with the carbonyl carbon (δ_C 199.7, C-9) together with an intense C=O stretching IR band at 1681 cm^{-1} suggested the presence of an α,β-unsaturated carbonyl group in the side chain. Additionally, the methyl group at δ_H 2.36 showing a long-range correlation with this carbonyl carbon (δ_C 199.7, C-9) was assigned to H_3-10. On the basis of these assignments, structure **100** was proposed.

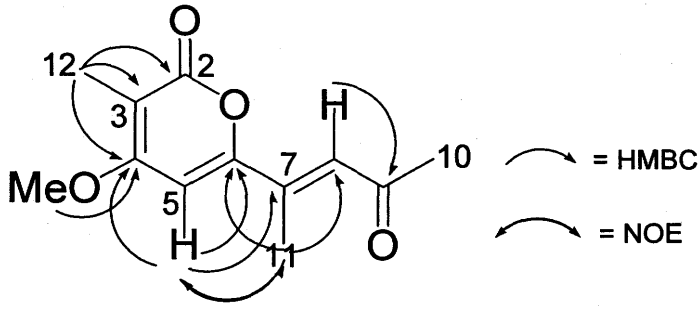

Figure 2.1: Selected HMBC and NOE correlations of phomapyrone D (**100**)

The assignment of the carbons (see table 2.2) of the 2-pyrone unit of **100** was confirmed by comparison with those reported for phomapyrone A (**49**) (Pedras et al., 1994). The configuration at the C-7-C-8 double bond was assigned based on NOE difference data as follows: irradiation of the protons at δ_H 2.36 (H_3-11) showed an NOE enhancement on the signal at δ_H 6.52 (H-5, 3.5%), and vice versa, but had no effect on the signal at δ_H 7.15 (H-8) (Fig. 2.1). These NOE difference data allowed assignment of the stereochemistry at the double bond as 7-*E*. Hence, the structure was unambiguously assigned to **100**, which was named phomapyrone D.

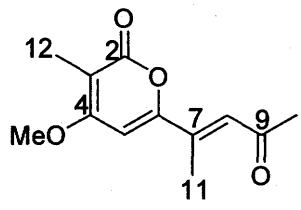

100

Compound **101** had a molecular formula of $C_{14}H_{18}O_4$ (HREI-MS), indicating six degrees of unsaturation. The ^1H NMR spectrum displayed signals for four methyl groups, one methoxy group, two olefinic protons and one sp^3 methine proton, accounting for the total number of protons in the molecular formula. ^{13}C NMR data together with HMQC data indicated the presence of four methyl carbons, a methoxy carbon, three methine carbons and six sp^2 hybridized quaternary carbons. From the ^{13}C NMR spectrum, four carbon signals at δ_C 208.0, 166.0, 165.2, and 159.4 were attributed to oxygen bearing sp^2 carbons. An intense IR band at 1707 cm^{-1} together with a ^{13}C NMR signal at δ_C 208.0 suggested the presence of a carbonyl carbon. Moreover, an intense IR band that was observed at 1692 cm^{-1} suggested the presence of an α,β-unsaturated carbonyl group. In agreement with this, the ^{13}C NMR signal observed at δ_C 165.2 indicated the presence of an α, β-unsaturated carbonyl carbon (ester). The HMBC correlation of a methoxy group at δ_H 3.94 with a carbon at δ_C 166.0 suggested its attachment to C-4. The long-range correlations observed between a methyl group at δ_H 1.97 (H-14) with carbons at δ_C 165.2, 103.3 and 166.0, allowed connecting C-14 to C-3, and C-3 further to C-2 and C-4. Additional HMBC correlations of a proton at δ_H 6.21 (H-5) with carbons at δ_C 103.3 (C-3) and 166.0 (C-4) suggested further bonding of C-4 to C-5. Additional long-range correlations of H-5 with δ_C 159.4 (C-6) and 128.8 (C-7), and correlation of a methyl group at δ_C 2.00 (H_3-13), with δ_C 159.4 (C-6) and 128.8 (C-7) indicated the direct connectivity between C-5 and C-6, C-6 and C-7, and C-7 and C-13. The connectivity of

C-6 to an oxygen atom, which is further linked to C-2, led to the 2-pyrone moiety with side branching at C-6. Additional connectivity between C-7 and C-8 was established based on HMBC correlations of H-8 (δ_H 6.51) with C-6 and C-13. Moreover, the spin system showing H-9 (δ_H 3.53) coupling to H-8 (δ_H 6.51, d, J =10 Hz), and H_3-12 (δ_H 1.30, d, J = 7 Hz) allowed the direct attachment of C-8 to C-9, and C-9 to C-12. The carbon signal at δ_C 208.0, showing a long-range correlation with H-8, was assigned to C-10. A further HMBC correlation observed between C-10 and a methyl group at δ_H 2.17 (H_3-11) suggested C-10 to bond to C-11. Finally, the structure **101** was deduced.

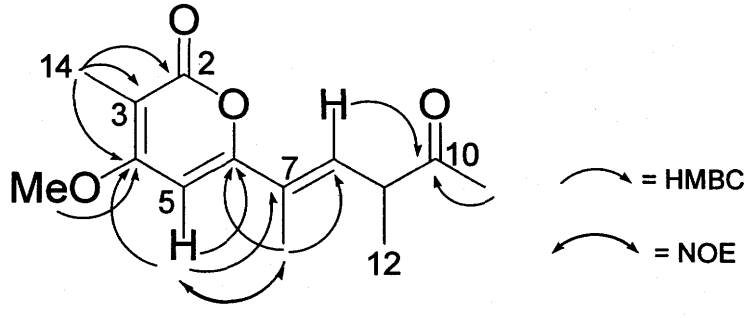

Figure 2.2: Selected HMBC and NOE correlations of phomapyrone E (**101**)

The assignment of the carbons of the 2-pyrone moiety of **101** was consistent with those reported for phomapyrone A (**49**) (Pedras et al., 1994). The stereochemistry at the C-7-C-8 double bond was deduced on the basis of NOE difference data (Fig. 2.2). Thus irradiation of the proton at δ_H 2.00 caused an NOE enhancement on the signal at δ_H 6.21 (H-5, 2%), and vice versa, but it had no effect on the proton at δ_H 6.51 (H-8). Based on these NOE difference data, the stereochemistry at C-7-C-8 was assigned as 7-*E*. Hence, the structure **101** was assigned unambiguously to the compound named phomapyrone E.

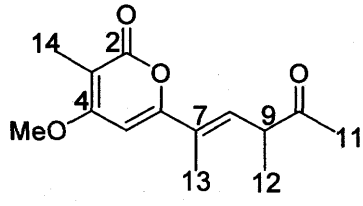

101

The molecular formula of **102** was established as $C_{14}H_{16}O_4$ on the basis of HREI-MS and NMR data. The ^1H NMR spectrum displayed signals for four methyl groups, one methoxy group, and one sp^2 hybridized CH, accounting for the total number of protons. The proton decoupled ^{13}C NMR spectrum displayed fourteen carbon resonances, of which three had chemical shifts above δ_C 150, suggestive of oxygen-bearing sp^2 carbons. From the ^{13}C NMR data, the presence of four C-C double bonds and one carbonyl group was evident. Therefore, five of the seven elements of unsaturation, indicated by the chemical formula of **102**, could be attributed to these four C-C double bonds and one carbonyl group; **102** is thus a bicyclic compound. The carbon signal at δ_C 164.5 correlating with the methyl group at δ_H 2.19 was assigned to carbon C-2 of an α,β-unsaturated carbonyl group. The observed intense IR band at 1711 cm^{-1} also corroborated the presence of a carbonyl group. Further, a methyl group at δ 2.19 (H-14) exhibited

long-range correlations with carbons at δ_C 114.1 and 167.1, which were assigned to C-3 and C-4, respectively. The carbon at δ_C 167.1 (C-4) also exhibited a long-range correlation with the methoxy group at δ_H 3.82. Diagnostic HMBC correlations of a methyl group at δ_H 2.61 (H_3-13) with δ_C 116.1 (C-5), 133.3 (C-6) and 131.1 (C-7) showed the C-C connectivity between C-5 and C-6, C-13 and C-6, and C-6 and C-7. Additional long-range correlations of a methyl group at δ_H 2.33 (H_3-12) with δ_C 133.3 (C-6), 131.1 (C-7) and 134.6 (C-8) indicated C-C bonding from C-12 to C-7, and C-7 to C-8. Further long-range correlations observed between a methyl group at δ_H 2.41 (H-11) and carbons at δ_C 134.6 (C-8), 123.5 (C-9), and 150.6 (C-10) as well as long-range correlations of a proton at δ_H 7.17 (H-8) with C-7, C-9, C-10, C-11 and C-12 suggested further connectivity between C-8 and C-9, C-9 and C-10, and C-9 and C-11. Additionally, NOE difference data allowed establishing the connectivity between C-4 and C-5 (Fig. 2.3).

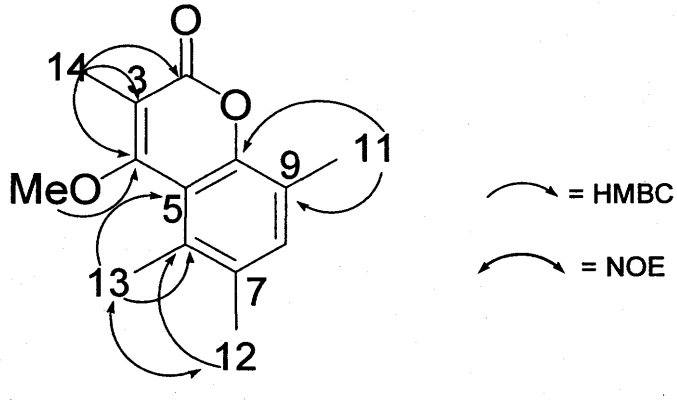

Figure 2.3: Selected HMBC and NOE correlations of phomapyrone F (**102**)

The observed NOE enhancement on the signal at δ_H 2.61 (H_3-13, 2%) upon irradiation of the methoxy group at δ_H 3.82, and vice versa, suggested the attachment of

C-4 to C-5. Further irradiation of a methyl group at δ_H 2.33 (H_3-12, 2%) caused an NOE enhancement on signals at δ_H 2.61 (H_3-13, 3%) and 7.17 (H-8, 3%), and vice versa. Likewise, irradiation of proton signal at δ_H 7.17 (H-8) caused an NOE enhancement on the signal of the methyl protons at δ_H 2.41 (H_3-11, 5%), and vice versa. Finally on the basis of these analyses, structure **102** was assigned unambiguously to the compound named phomapyrone F.

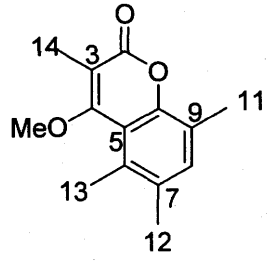

102

The molecular formula of **103** was determined to be $C_{14}H_{16}O_5$ by HREI-MS and NMR data, indicating seven degrees of unsaturation. The ^1H NMR spectrum displayed three sp^2 CH groups, one methoxy group, three methyl groups and one exchangeable proton. The proton decoupled ^{13}C NMR spectrum showed 14 resonances, of which the two most downfield resonances (δ_C 165.9 and 168.2) were assigned to carbonyl carbons of a carboxylic acid or its derivatives. The carbon signal at δ_C 165.9, correlating with the methyl group at δ_H 1.96 (H_3-14) was assigned to a lactone carbonyl (C-2). Additionally, long-range correlations exhibited between the methyl group at δ_H 1.96 (H_3-14) and carbons at δ_C 102.5 (C-3) and 167.5 (C-4) indicated a 2-pyrone moiety. Again, the latter carbon (C-4) exhibited long-range correlation with the methoxy group as well as with H-5 (δ_H 6.67). An additional long-range correlation of the proton δ_H 6.67 (H-5) with carbon at δ_C 159.6 allowed its assignment as C-6. The ^{13}C NMR chemical shift suggested C-6 to be connected to an oxygen atom, which was further bonded to C-2, confirming a 2-

pyrone moiety as a structural unit of **103**. The long-range correlation of δ_C 159.6 (C-6) with protons δ_H 7.02 (H-8) and 2.09 (H_3-13) as well as the correlation of δ_C 129.6 (C-7) with δ_H 6.67 (H-5) of the 2-pyrone moiety suggested the branching point is at C-6.

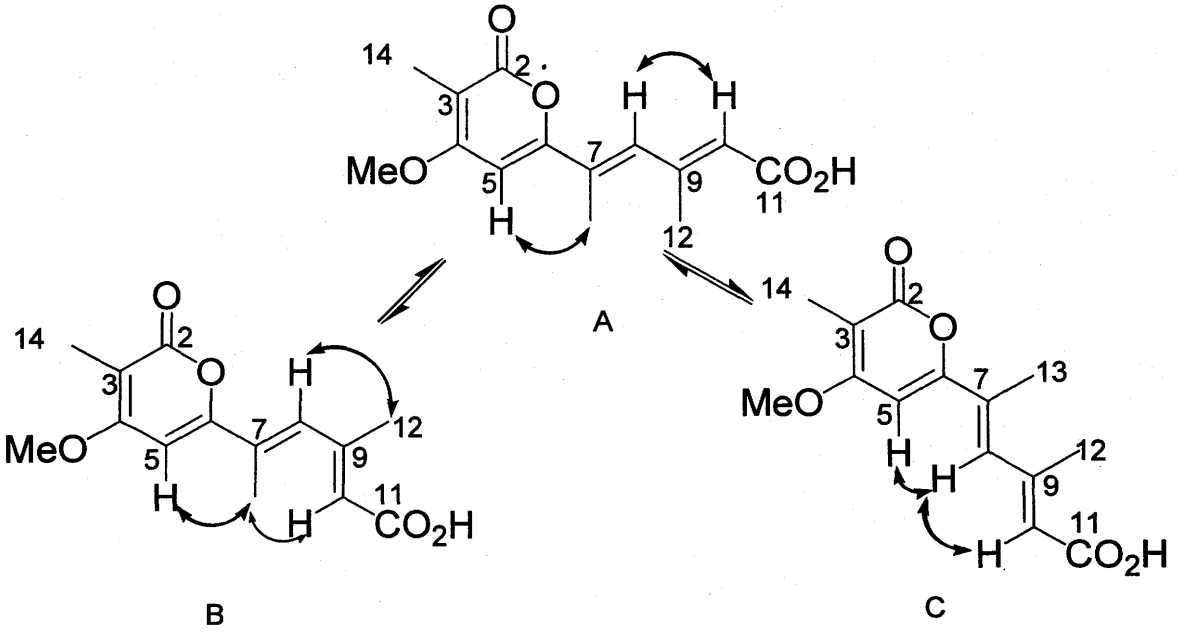

Figure 2.4: Selected NOE correlations of infectopyrone (**103**)

The structure of the side chain was established based on the HMBC and NOE data. One of the downfield carbon signals at δ_C 168.2 was assigned to an α,β-unsaturated carboxylic acid carbon (C-11). A broad OH stretching band at 3600-2800 cm^{-1} and an intense stretching C=O band at 1687 cm^{-1} observed in the IR spectrum corroborated the assignment of the carboxylic group. Irradiation of the methyl protons at δ_H 2.09 (H_3-13) resulted in an NOE enhancement on the signals at δ_H 6.67 (H-5, 4%) and δ 5.85 (H-10, 2%) whereas there was no change on the signals of the protons at δ_H 7.02 (H-8) and 2.31 (H_3-12). Again, irradiation of the proton at δ 6.67 (H-5) caused an NOE enhancement of the signals at δ_H 2.09 (H_3-13, 11%), 4.02 (OMe, 13%) and 7.02 (H-8, 3%). Additionally,

irradiation of the proton at δ_H 7.02 (H-8) showed an NOE enhancement of the signals at δ_H 5.85 (H-10, 3%), 2.31 (H_3-12, 4%) and 6.67 (H-5, 1%). In turn, the irradiation of the proton at δ_H 2.31 (H_3-12) caused an NOE enhancement only on the signal at δ_H 7.02 (H-8, 2%). These NOE data allowed the assignment of the configuration of the diene of the side branching as 7-*E*, 9-*E*. Moreover, the NOE data indicate occurrence of free rotation about C-6-C-7 and C-8-C-9 single bonds giving rise to s,s-*trans,trans* (A), s,s-*trans,cis* (B), and s,s-*cis,trans* conformations (C) (Fig. 2.4). Hence the structure was unambiguously assigned as **103**. A literature search showed that compound **103** was infectopyrone, a metabolite isolated previously from *Alternaria infectoria* (Larsen et al., 2003).

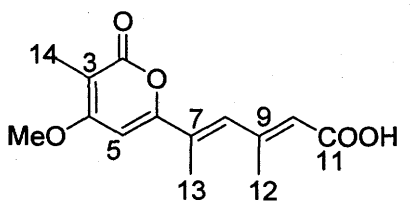

103

The molecular formula of **104** was established on the basis of HRMS and NMR data as $C_{14}H_{18}O_4$, indicating six degrees of unsaturation. The ^{1}H NMR spectrum displayed methine proton signals attached to two sp^2 hybridized carbons, one sp^3 hybridized carbon, four methyl groups and one methoxy group, which accounted for the total number of hydrogens. The proton decoupled ^{13}C NMR spectrum displayed fourteen carbon signals, three of which were assigned to sp^2 hybridized carbons attached to oxygen (δ_C 165.5, 164.8 and 158.9). One of these carbons at δ_C 164.8 displaying the only long-range correlation with a methyl group at δ_H 1.96 was assigned to an α,β-unsaturated carbonyl carbon (C-2). An intense IR band that observed at 1700 cm^{-1} also suggested the presence of a carbonyl group. Additional HMBC correlations of a methyl group at δ_H 1.96 (H_3-14) with carbons at δ_C 103.5 and 165.5 allowed their assignments as C-3 and C-

4, respectively. Further the carbon at δ_C 165.5 (C-4) showed a long-range correlation with the methoxy group at δ_H 3.88. In addition, long-range correlations of the proton at δ_H 6.19 (H-5) with C-3, C-4, and a carbon at δ_C 158.9, assigned to C-6, substantiated the presence of a 2-pyrone. The ^{13}C NMR chemical shift of C-6 indicated its attachment to an oxygen atom, which again connected to C-2 to complete the structure of the 2-pyrone moiety. Moreover, the additional long-range correlations of C-6 (δ_C 158.9) with a methyl group at δ_H 1.99 (H_3-13) and olefinic proton H-8 (δ_H 6.02) showed C-6 to be the branch point of the 2-pyrone moiety. The assignment of carbons of the 2-pyrone moiety was consistent with the NMR data (^{13}C NMR, HMBC, and HMQC) reported for **49** (Pedras et al., 1994). The chemical shifts of two sp^3 hybridized carbons, δ_C 60.3 (C-9) and δ_C 62.4 (C-10), suggested that these carbons were oxygen-bearing sp^3 carbons. Hence to satisfy the chemical formula, the presence of an oxirane moiety is required in the side chain.

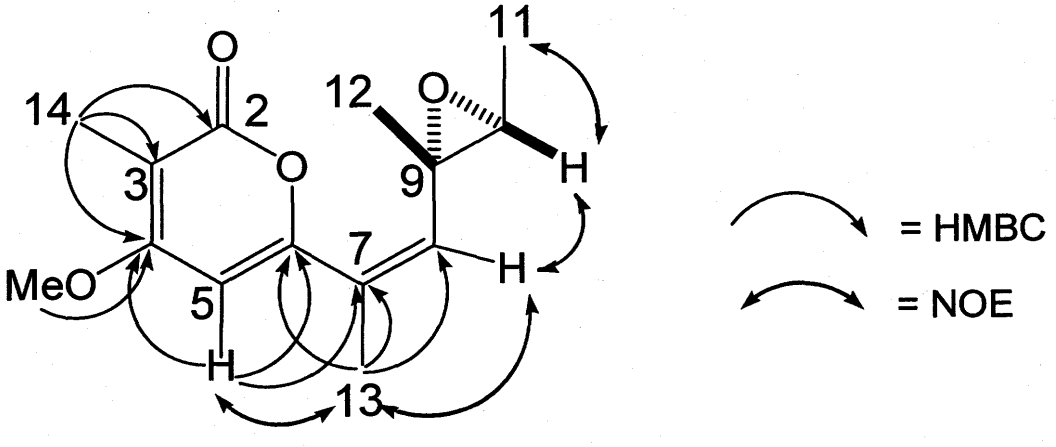

Figure 2.5: Selected HMBC and NOE correlations of phomapyrone G (**104**)

The stereochemistry of the side chain was determined on the basis of NOE data (Fig. 2.5). Irradiation of the proton signal at δ_H 1.99 (H_3-13) caused an NOE enhancement on the signal at δ_H 6.19 (H-5, 4%) and δ_H 6.02 (H-8, 4%). Furthermore, irradiation of the proton signal at δ_H 6.02 (H-8) caused an NOE enhancement on the

signal at δ_H 1.99 (H_3-13, 6%) and 3.06 (H-10, 2%), but had no effect on the signals at δ_H 1.96 (H_3-12) and 1.47 (H_3-11). These results of NOE difference experiments required that the stereochemical assignment at the C-7-C-8 double bond was *Z*. Irradiation of H-10 (δ_H 3.06) caused an NOE enhancement on the signals of H-8 (δ_H 6.02, 1%) and H_3-11 (δ_H 1.47, 5%). Similarly, irradiation of the proton at δ_H 1.47 (H_3-11) caused NOE enhancement on the signal of H-10 (δ_H 3.06, 3%), but had no effect on the signal of H-12 (δ_H 1.96). These results suggest a *trans* orientation of the methyl groups about two carbons (C-9, C-10) of the oxirane moiety. Therefore, structure **104** was assigned unambiguously and named phomapyrone G.

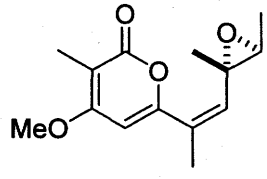

104

The molecular formula of compound **105**, $C_{14}H_{18}O_3$, indicating six degrees of unsaturation, was established on the basis of HRMS and NMR data. The ^{1}H NMR spectrum displayed signals for four methyl groups, one methoxy group and three sp^2 CH groups. These signals were similar to those of **49**, except for H-10 (δ_H 5.49) and H-11 (δ_H 1.54), which showed a slight up field shift relative to their chemical shift in the ^{1}H NMR spectrum of phomapyrone A (**49**) (Pedras et al., 1994). The proton decoupled ^{13}C NMR spectrum displayed fourteen signals, of which three were for four methyl groups, one for a methoxy group, three for sp^2 hybridized methine carbons, and six for sp^2 hybridized quaternary carbons. An intense IR band at 1680 cm^{-1} suggested the presence of an α,β-unsaturated carbonyl group. From HMBC data, the carbon signal at δ_C 165.3 showing the

only correlation with the methyl group at δ_H 1.99 (H_3-14) was assigned to C-2. Additionally, the methyl group (δ_H 1.99, C-14) showed long-range correlations with carbons at δ_C 102.9 and 166.2, which were assigned to C-3 and C-4, respectively. C-4 (δ_C 166.2) further correlated with a methoxy group at δ_H 3.94. Additional correlations of the olefinic proton at δ_H 6.20 (H-5) with C-3 (δ_C 102.9), C-4 (δ_C 166.2) and C-6 (δ_C 160.2) were displayed in the HMBC spectrum. The ^{13}C NMR chemical shift of C-6 required C-6 to be connected to an oxygen atom, which indicated a 2-pyrone moiety. The assignment of all carbons of the 2-pyrone moiety of **105** was in good agreement with those reported in the literature (Pedras et al., 1994). The long-range correlations of C-6 with a methyl group at δ_H 1.88 (H_3-13), bonded to C-7 (δ_C 126.8), and H-8 (δ_H 6.98) indicated that the side chain was connected to C-6. Further HMBC correlations of a methyl group at δ_H 1.88 (H_3-13) with C-8 (δ_C 133.2) indicated the connectivity between C-7 and C-8. Additionally, the observed long-range correlations of a methyl group at δ_H 1.83 (H_3-12) with C-9 (δ_C 132.9) and C-10 (δ_C 124.7) showed C-12 to be bonded to C-9, which was further bonded to C-10. The connectivity between C-8 and C-9 was also established on the basis of the observed long-range correlation between H-8 and C-10. Moreover, the coupling shown between H-10 (δ_H 5.49, q, J = 7 Hz) and methyl group H_3-11 (δ_H 1.54, d, J = 7 Hz) allowed direct attachment of C-10 to C-11. As a result, a diene moiety was proposed as a structural unit of the side chain.

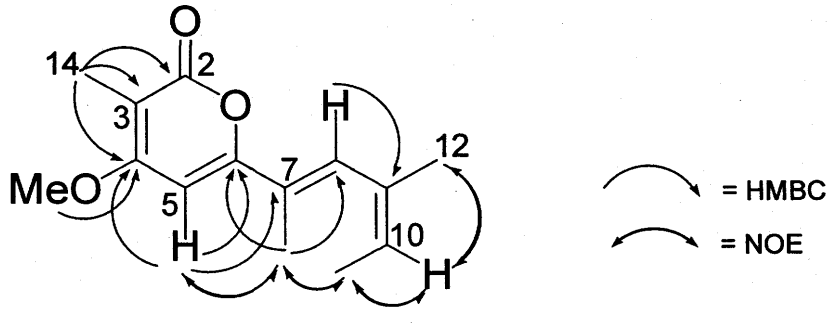

Figure 2.6: Selected HMBC and NOE correlations of phomenin B (**105**)

The stereochemistry of the diene was determined on the basis of NOE data (Fig. 2.6). Irradiation of the signal at δ_H 1.88 (H_3-13) caused an NOE enhancement on the signal at δ_H 6.20 (H-5, 5%) but no measurable NOE enhancement was observed on the signals at δ_H 6.98 (H-8) and δ_H 1.83 (H_3-12). Hence, these NOE data suggested the stereochemistry at the double bond (C7-C8) to be 7-*E*. Likewise, an NOE enhancement was observed on the signals at δ_H 1.54 (H_3-11, 7%) and 1.83 (H_3-12, 5%) when proton H-10 (δ_H 5.49) was irradiated. Additional irradiation of the proton at δ_H 1.54 (H-11) caused enhancement of proton signals at δ_H 1.88 (H-13, 1%) and 5.49 (H-10, 3%). These NOE data allowed the assignment of the stereochemistry at the double bond (C-9, C-10) as 9-*Z*. Therefore, the structure was unambiguously assigned as **105**. A literature search showed that compound **105** was isolated previously from *Phoma tracheiphila* and named phomenin B (Tringali et al., 1993).

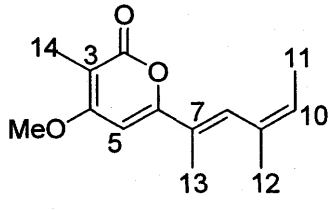

105

Table 2.1 ^{1}H NMR (500 MHz) data (ppm) of phomapyrones D (100), E (101), F (102), G (104), phomenin B (105), and infectopyrone (103) ($CDCl_3$)

H	**100** δ_H, m, *J*	**101** δ_H, m, *J*	**102** δ_H, m, *J*	**104** δ_H, m, *J*	**105** δ_H, m, *J*	**103** δ_H, m,
5	6.52 (s)	6.21	-	6.19 (s)	6.20 (s)	6.67 (s)
8	7.15 (s)	6.51, d, 9	7.17 (s)	6.02 (s)	6.98 (s)	7.02 (s)
9	-	3.53 (m)	-	-	-	-
10	2.36 (s)	-	-	3.05, q, 5	5.49, q, 7 Hz	5.85 (s)
11	2.36 (s)	2.17 (s)	2.41 (s)	1.46, d, 5	1.54, d, 7	-
12	2.05 (s)	1.30, d, 7	2.33 (s)	1.50 (s)	1.83 (s)	2.31 (s)
13		2.00 (s)	2.61 (s)	1.99 (s)	1.88 (s)	2.09 (s)
14		1.97 (s)	2.19 (s)	1.96 (s)	1.99 (s)	1.96 (s)
OMe	3.95	3.94	3.82	3.88	3.94	4.02

Table 2.2 ^{13}C NMR (125 MHz) data of phomapyrones D (100), E (101), F (102), G (104), phomenin B (105), and infectopyrone (103) ($CDCl_3$)

Carbon	δ_C **100**	δ_C **101**	δ_C **102**	δ_C **104**	δ_C **105**	δ_C **103**
2	164.5	165.2	164.5	164.8	165.3	165.9
3	106.3	103.3	114.1	103.5	102.9	102.5
4	165.2	166.0	167.1	165.5	166.2	167.5
5	97.5	93.3	116.1	95.4	92.9	95.3
6	158.2	159.4	133.3	158.9	160.2	159.6
7	139.8	128.8	131.1	127.1	126.8	129.6
8	126.5	132.8	134.6	137.7	133.2	134.2
9	199.7	48.2	123.5	60.3	132.9	152.2
10	33.0	208.0	150.6	62.4	124.7	120.9
11	13.9	28.3	16.1	14.5	15.6	168.2
12	9.4	16.9	20.9	17.9	23.7	18.2
13		13.3	16.7	21.0	14.3	13.2
14		9.2	10.9	9.0	9.1	7.6
OMe	56.7	56.6	60.7	56.6	56.5	56.7

A few C-6 substituted 2-pyrones have been isolated from phytopathogenic fungi as well as from fungi used as biological control agents, as for instance, *Gliocladium* and *Trichoderma* species (Avent et al., 1992b). The chemical examination of *Gliocladium vermoesenii* led to the isolation of two pyrones, nectriapyrone (**106**) and vermopyrone (**107**) (Avent et al., 1992b). Phytopathogenic fungi have been investigated for host-selective phytotoxins as well as for secondary metabolites. As discussed in the introduction, isolates of *Phoma lingam* have been investigated for secondary metabolites. Metabolites containing a 2-pyrone moiety, phomapyrone A (**49**), phomapyrone B (**50**), and phomapyrone C (**51**), were isolated from cultures of weakly virulent isolates of *P. lingam* grown in potato dextrose or in Cove's media (Pedras et al., 1994). Phomapyrone A (**49**) was isolated by an independent group from *P. tracheiphila* and named phomenin A (Tringali et al., 1993). Phomenin A (**49**) was reported along with phomenin B (**105**) from culture fluids of *P. tracheiphila*. Phomenin A (**49**) was both phytotoxic and active against *Artemia salina* whilst **105** was active only against *Artemia salina.* Similarly, chemical investigation of weakly virulent isolates of *P. lingam* originating from Poland also yielded phomapyrone A (**49**) (Pedras and Biesenthal, 2001). Additionally infectopyrone (**103**) was reported from *Alternaria infectoria*, a phytopathogenic fungus that infects barley in temperate regions. Moreover, **103** was found to be produced by *Stemphylium sp.* in infected tomatoes. Infectopyrone is a potential mycotoxin, but is not cytotoxic (Larsen et al., 2003).

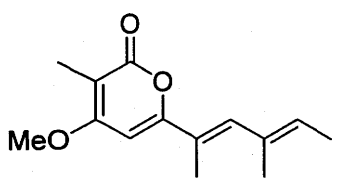

49

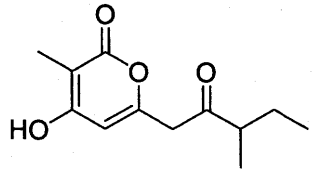

50

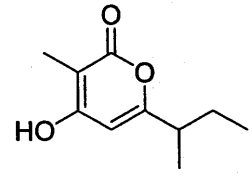

51

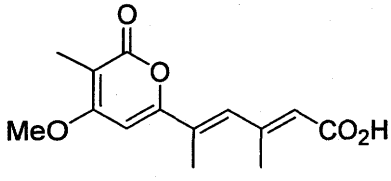

103

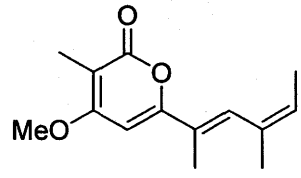

105

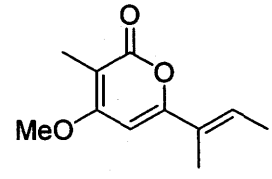

106

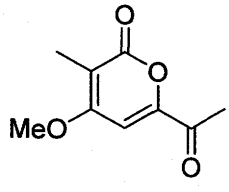

107

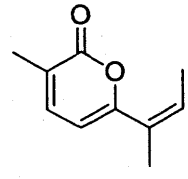

108

More C-6 substituted 2-pyrone and 4-pyrone compounds have been isolated from marine mollusks: ascoglossans, pulmonats, and cephalaspideans. A chemical study of *Ercolania funerea* led to the isolation of the 2-pyrone compounds **49** and **109**, and 4-pyrone compounds **110-113** (Vardaro et al., 1992). Pyrone compounds from mollusks possess ichthyotoxicity suggesting their potential role as defense allomones (De Marzo et al., 1993; Vardaro et al., 1992).

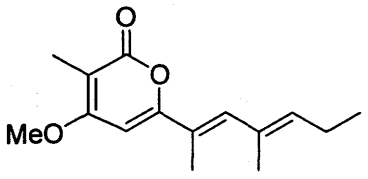

109

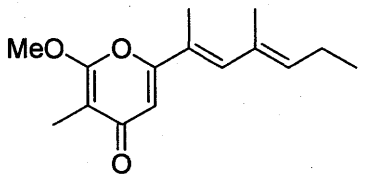

110

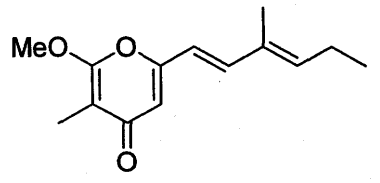

111

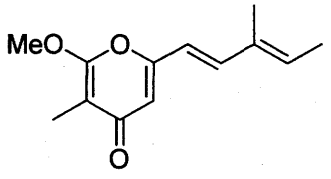

112

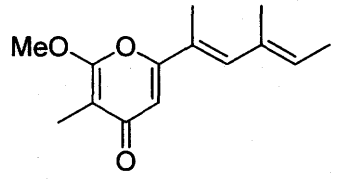

113

Sesquiterpenes

As described in the isolation of metabolites section, a total of nine sesquiterpenes were isolated from cultures of Mayfair 2 in minimal medium. The structure determination of these sesquiterpenes is discussed here.

Compound **55** was identified as phomalairdenone A by comparison of its ^{1}H NMR spectrum and HPLC data (both retention time and UV spectrum) with that of an authentic sample available in our library. Phomalairdenone A (**55**) was reported previously from Polish type isolate Laird 2 (Pedras et al., 1999a).

The molecular formula of **114**, $C_{15}H_{22}O_2$, indicating five degrees of unsaturation, was established on the basis of HREI-MS and NMR data. The ^{1}H NMR spectrum displayed signals for two methyl singlets, a methyl doublet, one isolated methylene group and one hydroxymethylene group. The proton decoupled ^{13}C NMR, together with J-mod NMR spectral data revealed the presence of three methyls, four methylenes, four methines and four quaternary carbons. The most downfield carbon signal at δ_C 215.0 in the ^{13}C NMR spectrum was assigned to a carbonyl carbon (C-6). An intense IR

absorption at 1697 cm^{-1} coupled with UV max at 235 nm confirmed the presence of an α,β-unsaturated ketone group. In agreement with this, carbon signals at δ_C 130.3 (C-7) and δ_C 168.8 (C-8), and the corresponding proton signals at δ_H 5.99 (H-7, d, J = 6 Hz) and δ_H 7.05 (H-8, d, J = 6 Hz) indicated a conjugated five-membered ring ketone moiety. The molecular composition, coupled with ^{13}C NMR data suggested a tricyclic system. Both ^1H-^1H COSY spectrum and selective spin decoupling revealed an isolated spin system containing a methyl doublet at δ_H 0.77 (H_3-11) coupled to H-1 (δ_H 1.70), which in turn coupled to methylene protons at δ_H 1.70 and 1.30 (H_2-2). These proton signals coupled to protons at δ_H 1.82 and 1.30 (H_2-3), which in turn coupled to δ_H 1.82 (H-3a). This spin system allowed establishing the fragment **A**, which was also in agreement with HMBC data (Fig. 2.7). All signals of proton-bearing carbons were assigned from HMQC correlation data. The connectivity of a methyl group (H_3-10, δ_H 0.99) and a hydroxymethylene group (H_2-9, δ_H 3.08, 3.25) to a quaternary carbon C-4 (δ_C 45.0) were established based on HMBC data. Additionally, isolated methylene proton signals at δ_H 1.32 and 2.13 exhibiting long-range correlations with quaternary carbons at δ_C 45.0 (C-4) and δ_C 56.7 (C-5a) and further with carbons at δ_C 21.2 (C-12), 25.1 (C-10) and 69.9 (C-9) were assigned as H_2-5. The connectivity of isolated groups and fragments was established from long-range correlations observed across the fragments and isolated groups in the HMBC spectrum, which gave a five membered tricyclic structure (Fig. 2.7). These data suggested that **114** had a skeleton similar to that of phomalairdenone A (**55**). The carbon assignments were consistent with those reported for **55** (Pedras et al., 1999a).

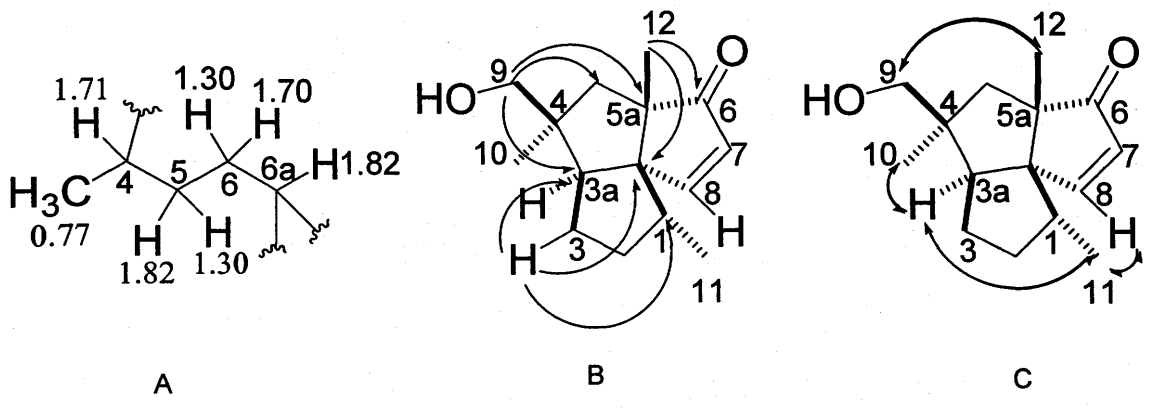

Figure 2.7 A: Fragment; B: selected HMBC correlations; C: NOE correlations of **114**

The relative configuration of the substituents at C-8a, C-1, C-3a, C-4 and C-5a was deduced from NOE difference spectral data (Fig. 2.7). Thus, irradiation of the signal at δ_H 7.05 (H-8) caused an NOE enhancement on the signals at δ_H 1.82 (H-3a, 3%) and 0.77 (H_3-11, 3%). Likewise, irradiation of the signal at δ_H 0.99 (H_3-10) caused an NOE enhancement on the signals at δ_H 1.82 (H-3a, 2%) and 2.13 (H-5, 1%). As a result, the spatial orientation of these protons H-3a, H_3-10 and H_3-11 was *cis*. Similarly, NOE difference data indicated H_3-12 to be *cis* to H_2-9. Consequently, the structure was unambiguously assigned for **114**, which was named phomalairdenone D. Phomalairdenone D is a new metabolite from the culture of Mayfair 2 isolate.

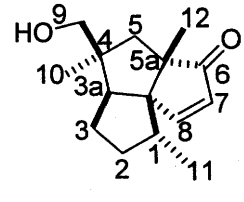

114

Compound **115** had a molecular formula of $C_{15}H_{22}O$, based on MS (HRMS, CI and FAB) and NMR (^1H, ^{13}C NMR, HMQC and HMBC) data. The analysis of ^1H NMR and ^{13}C NMR data (tables 1 and 2) of compound **115** suggested that it contained three methyl singlets and a methyl doublet, three methylenes, four methines and three quaternary carbons. The carbon signal at δ_C 214.9 in the ^{13}C NMR spectrum was assigned to a carbonyl carbon (C-6). The chemical shifts of two olefinic carbons at δ_C 130.2 and 168.3, which were assigned to C-7 and C-8, respectively, indicated that compound **115** had an α, β-unsaturated five membered ketone moiety, which was also corroborated by the UV Λmax at 235 nm. ^1H-^1H COSY revealed an isolated spin system where a methyl at δ_H 0.79 (H_3-11, d, J = 7 Hz) coupled to a methine proton at δ_H 1.87 (H-1, m), which correlated again to methylene protons at δ_H 1.11 (H_2-2, m) and1.69 (H-2, m). Decoupling of the proton signals of this methylene group (δ_H 1.11 and 1.69, H_2-2) showed further coupling with another methylene group at δ_H 1.03 and 1.51 (H_2-3, m), which in turn coupled to the methine proton at δ_H 1.71 (H-3a). Consequently, a fragment **A** was deduced (Fig. 2.8). The proton-bearing carbons in the fragment were assigned on the basis of HMQC data. The connectivity of isolated groups and fragments were established from long-range correlations observed in the HMBC spectrum, which led to a five membered tricyclic structure.

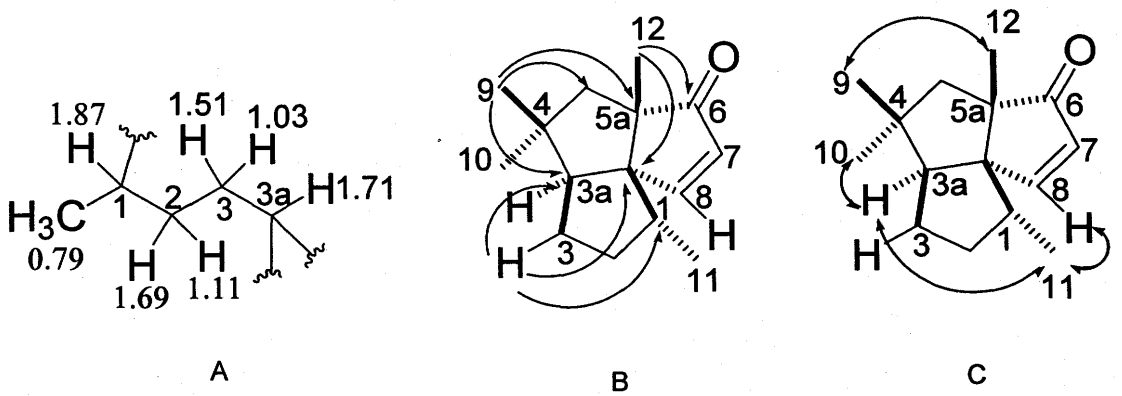

A B C

Figure 2.8 A: Fragment; B: selected HMBC correlations; C: NOE correlations of **115**

The relative stereochemistry of **115** was established on the basis of NOE difference spectral data (Fig. 2.8). Thus, irradiation of the proton at δ_H 0.79 (H_3-11) caused an NOE enhancement on signals at δ_H 7.07(H-8, 2%) and δ_H 1.70 (H-3a, 1%). Likewise, irradiation of protons at δ_H 0.91 (H_3-10) and 0.86 (H_3-9) caused an NOE enhancement on proton signals at δ_H 1.70 (H-3a, 2%) and 1.09 (H_3-12, 2%), respectively. These NOE results imply that the orientations of H-3a to H_3-11 and H_3-9 to H_3-12 are *cis*. Hence, the structure was assigned as **115**. Finally, a literature search revealed that **115** was a metabolite isolated previously from *Dugaldia hoopesii*, which was named 3-oxosilphinene (Bohlmann et al., 1984). The reported optical rotation data of 3-oxosilphinene, however, was not the same as that of **115**.

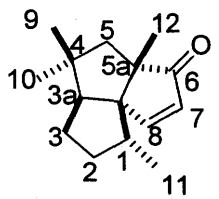

115

Table 2.3 ^{1}H (500 MHz) and ^{13}C NMR (125 MHz) data (ppm) of phomalairdenone D (114) and 3-oxosilphinene (115) (C_6D_6)

Carbon No.	114 δ_C	114 δ_H, m, J	115 δ_C	115 δ_H, m, J
1	38.6	1.70, m	38.6	1.87, m
2	36.6	1.82, m;1.30, m	36.6	1.69, m; 1.11, m
3	28.4	1.70, m; 1.30, m	29.2	1.51, m; 1.03, m
3a	59.1	1.82, m	61.2	1.71, m
4	45.0	-	40.0	
5	46.6	2.13, d, 13; 1.32, d, 13	51.2	1.47, d, 13 ; 2.25, d, 13
5a	56.7	-	68.2	-
6	215.1		215.1	-
7	130.3	5.99, d, 6	130.3	5.97, d, 6
8	168.8	7.05, d, 6	168.8	7.70, d, 6
8a	67.9		67.9	-
9	69.9	3.25, d, 10; 3.08, d, 10	27.1	0.86, s
10	25.1	0.99, s	30.4	0.91, s
11	16.1	0.77, d, 7	16.2	0.79, d, 7
12	21.2	1.60, s	21.1	1.09, s

Compound **116** gave a parent ion in HREI-MS consistent with the molecular formula of $C_{15}H_{24}O_2$, indicating four degrees of unsaturation. The ^1H NMR spectrum revealed the presence of two methyl singlets, a methyl doublet, and two isolated methylene groups. The proton decoupled ^{13}C NMR and J-mod NMR displayed fifteen carbon signals, of which three are for methyl groups, four for methylenes, five for methines, and three for quaternary carbons. The two downfield carbon signals at δ_C 128.7 and 143.5 were assigned to olefinic carbons, C-7 and C-8, respectively. The carbon signals at δ_C 85.4 and 73.0 were attributed to oxygen-bearing sp^3 hybridized carbon atoms. On the basis of ^{13}C NMR data and the molecular formula, a tricyclic structure was presumed. In the ^1H-^1H COSY spectrum, an isolated spin system contained an olefinic proton at δ_H 5.70 (H-8, d, J = 6 Hz) coupled to another olefinic proton at δ_H 5.61 (H-7, dd, J = 6, 2 Hz), which in turn coupled to the proton at δ_H 4.21 (H-6, d, J = 2 Hz). These data, together with ^{13}C NMR data required the presence of structural subunit **A** (Fig. 2.9).

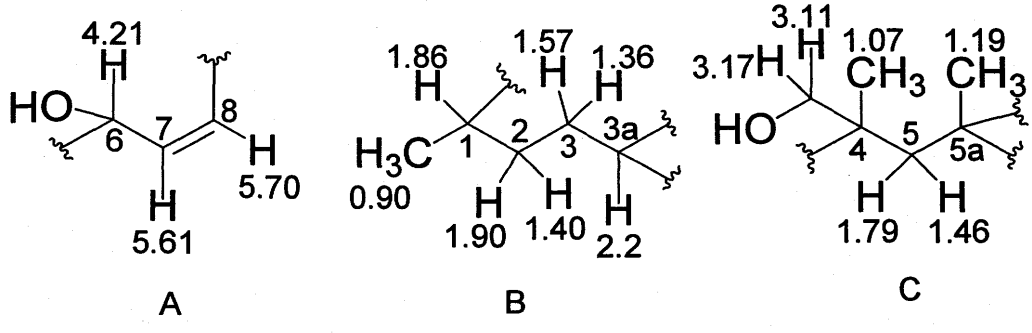

Figure 2.9: Fragments A, B and C of phomalairdenol B (**116**)

Analysis of the ^1H-^1H COSY data also revealed another spin system, in which a methyl doublet at δ_H 0.90 (H-11, J = 7 Hz) showed coupling to a methine proton at δ_H 1.86 (H-1). The latter showed further coupling to methylene protons at δ_H 1.90 and 1.40 (H_2-2), which in turn coupled to methylene protons at δ_H 1.57 and 1.36 (H_2-3), and these

coupled to a proton at δ_H 2.02 (dd, J = 9, 9 Hz, H-3a). Consequently, fragment **B** was deduced (Fig. 2.9). The HMBC correlations of an isolated methylene group at δ_H 3.11 and 3.17 (H_2-10) with carbons at δ_C 45.1 (C-4), 53.6 (C-5) and 22.9 (C-9), together with correlations of another isolated methylene group δ_H 1.46 and 1.79 (H_2-5) with carbons at δ_C 45.1 (C-4), 52.8 (C-5a), 19.6 (C-12), 73.0 (C-10), and 22.9 (C-9), suggested the presence of a structural subunit **C** (Fig. 2.9). Finally, the long-range correlations of the proton at δ_H 4.21 (H-6) with carbon at δ_C 53.6 (C-5), the proton at δ_H 1.86 (H-1) with carbon at δ_C 143.5 (C-8), and proton at δ_H 3.17 and 3.11 (H_2-10) with carbons at δ_C 53.6 (C-5) and 58.5 (C-3a) allowed one to assemble all the fragments and isolated groups, which resulted in a five membered tricyclic skeleton. This tricyclic skeleton was also corroborated by comparison of the NMR data of **116** with that of **55.**

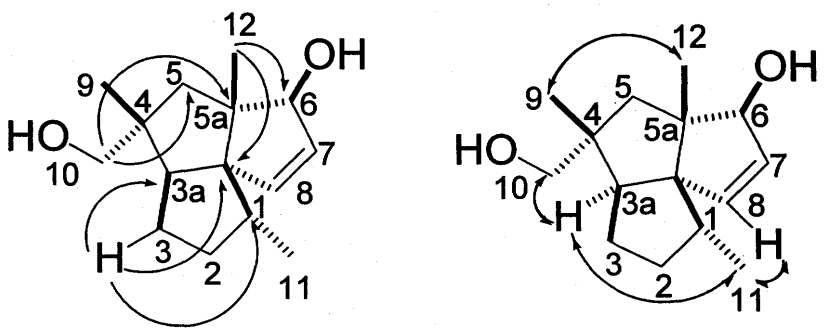

Figure 2.10: A) selected HMBC correlations; B) NOE correlations of **116**

The configuration was deduced from NOE difference spectral data as shown in fig. 2.10. Thus, irradiation of the signal at δ_H 5.70 (H-8) caused an NOE enhancement of the signals at δ_H 0.90 (H-11, 2%) and 2.02 (H-3a, 3%), and vice versa. Additionally, irradiation of H-3a (δ_H 2.02) caused an NOE enhancement of the signal at δ_H 3.17 and 3.11 (H_2-10, 4%), which in turn caused upon irradiation an NOE enhancement of the signals at δ_H 1.79 (H-5, 2%) and 4.21 (H-6, 1%), and vice versa. Hence, protons H-8, H-11, H-3a, H-10, and H-6 are all *cis* to one another. Likewise, the stereochemistry was

assigned for H-12 and H-9 to be also *cis*. Hence, the structure was unambiguously assigned for **116**, which was named phomalairdenol B.

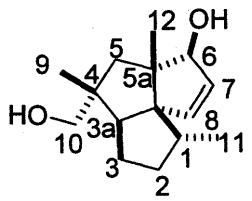

116

The molecular formula of compound **117** was determined as $C_{15}H_{24}O_2$ by analysis of HREI-MS and NMR data. In the ^1H NMR spectrum, signals for two methyl singlets, one methyl doublet, two isolated methylene protons and two olefinic methine protons were observed. The ^{13}C NMR spectrum displayed fifteen signals, and upon analysis of HMQC data, three of these signals were for methyl carbons, four for methylene carbons, five for methine carbons and three for quaternary carbons. These ^{13}C NMR data together with the molecular formula required three rings and two hydroxyl groups. Carbon signals at δ_C 129.0 and 143.3 were attributed to olefinic carbons (C-7 and C-8, respectively). An isolated spin system shown in the ^1H-^1H COSY spectrum indicated a proton at δ_H 5.71 (H-8, d, J = 6 Hz) coupling with a proton at δ_H 5.50 (H-7, dd, J = 6, 2 Hz), which showed in turn coupling to a proton at δ_H 4.37 (H-6, d, J = 2 Hz). Consequently, a structural subunit **A** was established (Fig. 2.11)

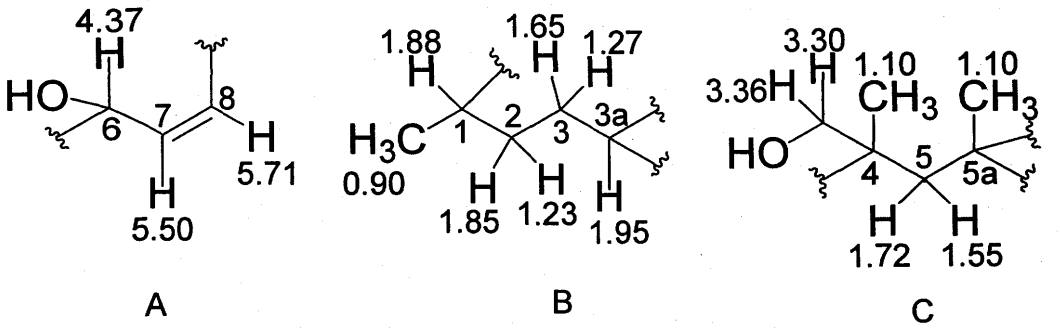

Figure 2.11: Fragments A, B and C of phomalairdenol A (**117**)

Additionally, ^{1}H-^{1}H COSY and selective proton decoupling experiments revealed another spin system in which a proton at δ_H 1.95 (H-3a, dd, J = 10, 8 Hz) coupled to methylene protons at δ_H 1.65 and 1.27 (H_2-3), which in turn coupled to δ_H 1.23 and 1.85 (H_2-2). In addition, the ^{1}H-^{1}H COSY spectrum displayed a coupling between the methine proton at δ_H 1.88 (H-1) and methyl protons at δ_H 0.90 (H_3-11, d, J = 7 Hz). The long-range correlation of the methyl group (H-11) to C-1 and C-2 indicated the connectivity between the spin systems leading to the sequence **B** (fig. 2.11). Moreover, long-range correlations of isolated methylene protons at δ_H 3.30 and 3.36 (H_2-9) with carbons at δ_C 44.3 (C-4), 70.0 (C-10), and 53.1 (C-5), together with long-range correlations of another isolated methylene group at δ_H 1.55 and 1.72 (H_2-5) with carbons at δ_C 44.3 (C-4), 53.8 (C-5a), 20.0 (C-12), 70.0 (C-10) and 26.8 (C-9) led one to deduce the sequence **C** (Fig. 2.11). The connectivity of fragments and isolated spin systems were established by detailed analysis of the HMBC data.

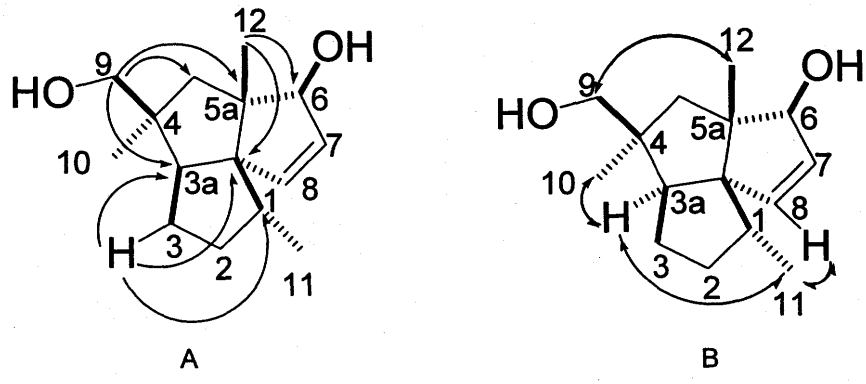

Figure 2.12: A) selected HMBC correlations; B) NOE correlations of **117**

The relative stereochemistry was determined on the basis of NOE difference spectral data (Fig. 2.12). Thus, irradiation of the signal at δ_H 5.71 (H-8) caused an NOE enhancement of the signals at δ_H 0.90 (H-11, 3%) and 1.95 (H-3a, 2%). Additionally, irradiation of the signal at δ_H 1.95 (H-3a) caused an NOE enhancement of the signals at δ_H 5.71 (H-8, 2%) and 1.11 (H-10, 2%), but had no effect on the methylene protons at δ_H 3.36 and 3.30 (H_2-9). These correlations suggest the *cis* stereochemistry for H-10, H-3a, H-8 and H-11. As well, NOE results suggested a *cis* orientation of H-6 relative to H-10, H-3a, H-8 and H-11. Likewise, the spatial relationships of protons H_3-10 to H-12 was determined to be *cis*, but *trans* relative to protons H-9, H-3a, H-8 and H-11. Hence, structure **117** was unambiguously assigned and named phomalairdenol A.

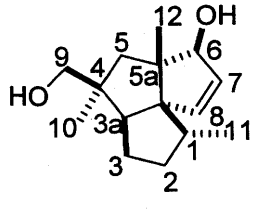

117

Compound **118** had a molecular formula of $C_{15}H_{24}O$ (HREI-MS and NMR data), indicating four degrees of unsaturation. The ^1H NMR spectrum displayed signals for three methyl singlets and one methyl doublet. Additional signals for protons bonded to two sp^2 hybridized carbons and an oxygen-attached sp^3 hybridized carbon were displayed. The proton decoupled ^{13}C NMR and J-mod NMR spectra displayed 15 resonances, of which four were assigned to methyl carbons, three to methylene carbons, five to methine carbons, and three to quaternary carbons. Two carbon signals at δ_C 128.7 and 143.5 were assigned to olefinic carbons (C-7 and C-8, respectively). Additionally, the signal at δ_C 85.9 was attributed to an oxygen-bearing sp^3 hybridized carbon (C-8). Both the ^1H NMR and ^1H-^1H COSY showed coupling of the proton at δ_H 5.61 (H-7, dd, J = 6 Hz, 2 Hz) with the protons at δ_H 5.74 (H-8, d, J = 6 Hz) and at δ_H 4.31 (H-6, d, J = 2 Hz)], indicating the presence of an allylic alcohol moiety. In addition, ^1H-^1H COSY spectrum displayed a coupling between the proton at δ_H 1.94 (H-3a, dd, J = 9, 9 Hz) and methylene protons at δ_H 1.60 and 1.34 (H_2-3), which in turn coupled to methylene protons at δ_H 1.34 and 1.84 (H-2). The latter methylene protons (H_2-2) showed coupling with the methine proton at δ_H 1.91 (H-1), which in turn coupled to methyl protons at δ_H 0.90 (H_3-11, d, J = 7 Hz). This spin system suggested the presence of fragment **A** (Fig. 2.13). In support of this assignment, HMBC also displayed correlations of the methyl group H_3-11 with C-1 and C-2, H_2-2 with C-1, C-3 and C-3a, and H_2-3 with C-2. Furthermore, the HMBC spectrum showed correlations of both methyl groups at δ_H 1.04 (H_3-10) and 1.03 (H_3-9) with δ_C 39.7 (C-4), and with each other, which suggested their connectivity to C-4. In support of this, NOE difference experiments indicated a close spatial relationship between these methyl groups (H-10 and H-9). Additionally, HMBC data revealed isolated methylene protons at δ_H 1.62 and 1.73 (H_2-5) correlating with carbons at δ_C 39.7 (C-4), 53.3 (C-5a), 19.4 (C-12), 32.3 (C-10) and 27.9 (C-9). Further, the long-range correlations observed among fragments and isolated groups allowed one to establish a five membered tricyclic framework.

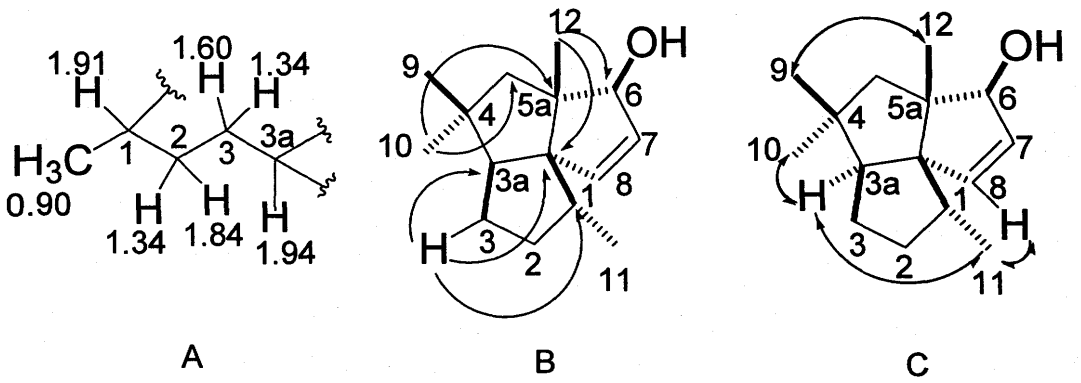

Figure 2.13: A) Fragment; B) selected HMBC correlations; C) NOE correlations of **118**

The relative configuration was determined by NOE difference experiments (Fig. 2.13). Thus, irradiation of signals at δ_H 5.74 (H-8) caused an NOE enhancement of the signals at δ_H 0.90 (H_3-11, 2%) and 1.94 (H-3a, 3%). Additionally, irradiation of the signal at δ_H 1.03 (H_3-9) caused an NOE enhancement of the signals at δ_H 4.31 (H-6, 1%) and 1.94 (H-3a, 2%). These NOE results imply that H-3a (δ_H 1.94), H-6 (δ_H 4.31) and H_3-10 (δ_H 1.03) all be *cis* to one another. Similarly, irradiation of the signal at δ_H 1.18 (H_3-12) showed an NOE enhancement on the signal at δ_H 1.04 (H_3-9), suggesting the *cis* relative orientation of H_3-12 to H_3-9. Consequently, structure **118** was unambiguously assigned and named phomalairdenol C.

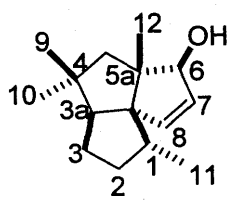

118

The molecular formula of compound **119** was determined as $C_{15}H_{24}O_2$ by HREI-MS and NMR data (^{13}C NMR and HMQC), indicating four degrees of unsaturation. The ^1H NMR spectrum displayed signals for four methyl protons, where three of them were methyl singlets and one was a methyl doublet. In addition, the ^1H NMR spectrum also displayed two olefinic methine protons, a low field methine proton and isolated methylene protons. Similarly, the ^{13}C NMR showed fifteen resonances, of which four were for methyls, two for methylenes, five for methine and three for quaternary carbons. The two most downfield signals at δ_C 128.5 and 143.2 were attributed to olefinic carbons and two other carbon signals at δ_C 85.3 and 80.3 were attributed to oxygen-bearing sp^3 hybridized carbons. ^{13}C NMR data, together with its molecular composition suggested a tricyclic framework for compound **119**. The presence of two isolated spin systems from H-6 to H-8 and from H-1 to H-3a through H-2 were elucidated by analysis of the ^1H-^1H COSY spectrum. An olefinic proton at δ_H 5.54 (H-8, d, J = 6 Hz) coupled to another olefinic proton at δ_H 5.58 (H-7, dd, J = 6, 2 Hz), which in turn coupled to the proton at δ_H 4.24 (H-6, d, J = 2 Hz) suggested structural subunit **A** (Fig. 2.14).

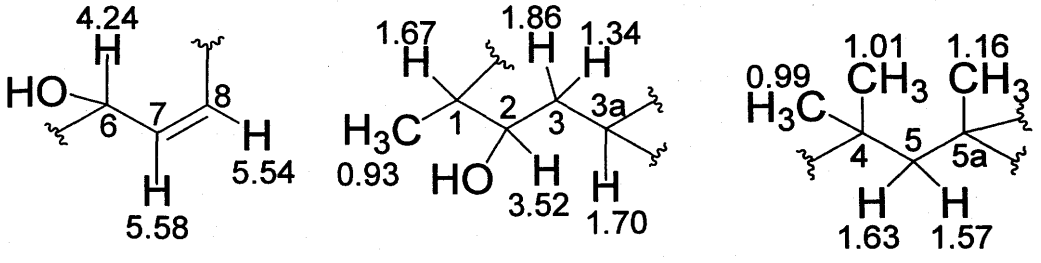

Figure 2.14: Fragments A, B and C for compound **119**

The carbon signals bearing these protons were assigned as C-6 (δ_C 85.3), C-7 (δ_C 128.5) and C-8 (δ_C 143.2). In another spin system, the proton at δ_H 1.67 (H-1, m) coupled

to methyl protons at δ_H 0.93 (H_3-11, d, J = 7 Hz) and to the proton at δ_H 3.52 (H-2, m). H-2 (δ_H 3.52, m) coupled further to the protons at δ_H 1.86 and 1.34 (H-3), which in turn coupled to H-3a (δ 1.70, m). These proton correlations suggested the presence of a structural subunit **B** (Fig. 2.14). All proton-bearing carbons in the structural subunit were assigned by one bond carbon-hydrogen correlation data. The HMBC spectrum showed correlations of the two methyl singlets at δ_H 1.01 (H_3-10) and 0.99 (H_3-9) with C-4 as well as with each other (C-9 to H-10 and C-10 to H-9). Furthermore, the HMBC data revealed the presence of isolated methylene protons δ_H 1.57 and 1.63 (H-5) flanked by carbons at δ_C 39.9 (C-4) and 54.0 (C-5a). Hence, structural subunit **C** was deduced (Fig. 2.14). Moreover, the connectivity of fragments and isolated groups was established by HMBC correlations and NOE difference data.

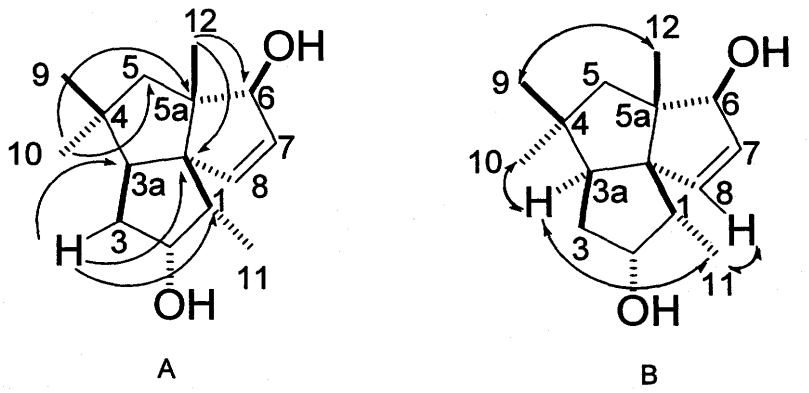

Figure 2.15: A) selected HMBC correlations; B) NOE correlations of **119**

The relative stereochemistry of compound **119** was determined on the basis of NOE difference experiments (Fig.2.15). Thus, irradiation of the signal at δ_H 5.54 (H-8) caused an NOE enhancement of signals at δ_H 1.70 (H-3a, 3%), 3.52 (H-2, 3%), and 0.93 (H_3-11, 1%), and vice versa. Irradiation of the signal at δ_H 0.99 (H_3-10) caused an NOE enhancement of the signal at δ_H 1.70 (H-3a, 3%), and irradiation of the signal at δ_H 4.24

(H-6) caused an NOE enhancement of the signal at δ_H 5.58 (H-7, 3%), but had no effect on δ_H 1.16 (H-12). These data suggested that protons H-8, H-3a, H_3-10 and H_3-11 are all *cis* to one another. Likewise, the relative orientation of H_3-12 to H_3-9 was determined to be *cis*, but *trans* to protons H-8, H-3a, H_3-10 and H_3-11. Hence, the structure was unambiguously assigned as **119** and the metabolite was named phomalairdenol D.

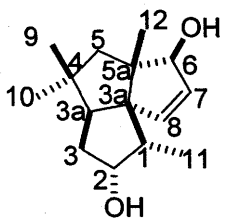

119

Table 2.4 ^{1}H NMR (500 MHz) data of phomalairdenols B (116), A (117), C (118), and D (119) (C_6D_6)

H	**116** δ_H, m, *J* (Hz)	**117** δ_H, m, *J* (Hz)	**118** δ_H, m, *J* (Hz)	**119** δ_H, m, *J* (Hz)
1	1.86	1.88, m	1.91, m	1.67,
2	1.90; 1.40	1.85, m; 1.23, m	1.34, m; 1.84, m	3.52, ddd, 10, 10, 6
3	1.57; 1.36	1.65, m; 1.27, m	1.60, m; 1.34, m	1.86, ddd, 11, 8, 6; 1.34, ddd, 11, 11, 10
3a	2.02, dd, 9, 9	1.95, dd, 10 , 8	1.94, dd, 9, 9	1.70, m
5	1.79, d, 13; 1.46, d, 13	1.72, d, 13; 1.55, d, 13	1.62, d, 13; 1.73, (13	1.63, d, 13; 1.57, d, 13
6	4.21, d, 2	4.37, d, 2	4.31, d, 2	4.24, br s
7	5.61, dd, 6, 2	5.50, dd, 6, 2	5.61, dd, 6, 2	5.58, dd, 6 , 2
8	5.70, d, 6	5.71, d, 6	5.74, d, 6	5.54, d, 6
9	1.07, s	3.36, d, 10; 3.30, d, 10	1.03, s	0.99, s
10	3.17, d, 10: 3.11, (10	1.10, s	1.04, s	1.01, s
11	0.90, d, 7	0.90, d, 7	0.90, d, 7	0.93, d, 7
12	1.19, s	1.10, s	1.18, s	1.16, s

Table 2.5 ^{13}C NMR (125 MHz) data (ppm) of phomalairdenols B (116), A (117), C (118), and D (119) (C_6D_6)

Carbon NO.	**116** δ_C (ppm)	**117** δ_C (ppm)	**118** δ_C (ppm)	**119** δ_C (ppm)
1	39.6	39.4	39.6	46.4
2	38.4	37.7	38.2	80.3
3	27.6	27.0	27.1	36.1
3a	58.5	61.5	63.0	57.0
4	45.1	44.3	39.7	39.9
5	53.6	53.1	58.8	57.9
5a	52.8	53.8	53.3	54.0
6	85.4	86.4	85.9	85.3
7	128.7	129.0	128.7	128.5
8	143.5	143.3	143.5	143.2
8a	72.4	72.5	73.0	70.3
9	22.9	26.8	27.9	32.5
10	73.0	70.0	32.3	28.0
11	16.6	16.8	16.7	13.7
12	19.6	20.0	19.4	19.4

The molecular formula of compound **120** was determined as $C_{15}H_{26}O_2$ on the basis of HREI-MS and NMR data, indicating three degrees of unsaturation. In the ^1H NMR spectrum, three methyl singlets (δ_H 0.88, 1.02, and 1.82), olefinic methylene protons (δ_H 4.96), and an oxymethine proton (δ_H 3.11) were disclosed. The proton decoupled ^{13}C NMR and J-mod NMR spectra revealed 15 carbon resonances, three methyl singlets, five methylenes and a methylidene, three methines and three quaternary carbons. Two low field carbon signals displayed at δ_C 152 and 110 in the ^{13}C NMR spectrum were assigned to olefinic carbons (C-11 and C-12, respectively). Furthermore, two sp^3 hybridized carbon signals at δ_C 79.5 (C-1) and 71.1 (C-4) in the ^{13}C NMR spectrum were attributed to oxygen attached carbons. The ^{13}C NMR, coupled with its molecular formula, suggested a bicyclic framework for compound **120**. The chemical shift of methyl protons H_3-13 (δ_H 1.82), together with its long-range correlations with C-11 (δ_C 150.6) and C-12 (δ_C 108.8) suggested it to be vinylic. In support of this assignment, the ^1H-^1H COSY also displayed a $^4J_{H\text{-}H}$ correlation of H_3-13 (δ 1.82) with the signal at δ_H 4.96 (H-12). The long-range correlation of methyl protons at δ_H 1.82 (H-13) and methylidene protons at δ_H 4.96 (H-12) with δ_H 46.4 (C-7) allowed connecting C-11 to C-7; consequently fragment **A** was deduced (Fig. 2.16). The ^1H-^1H COSY spectrum displayed correlations of the methine proton at δ_H 1.15 (H-5, dd, J = 12, 2 Hz) with methylene protons at δ_H 1.30 (H_2-6, ddd, J=12, 12, 12 Hz) and 2.03 (H-6, m). The long-range correlations of H-6 (δ_H 1.30, 2.03) with C-7, together with the proton decoupling experiments showing coupling of H-6 (δ_H 1.30, 2.03) with H-7 (δ_H 1.95, m) allowed connecting C-6 to C-7. Methylene protons at δ_H 1.05 (H-9, ddd, J = 13, 13, 3 Hz) and 1.85 (H-9, ddd, J = 13, 3, 3 Hz) showed coupling with the methylene protons at δ_H 1.47 (H-8, dddd, J = 13, 13, 13, 3 Hz) and 1.65 (H-8, m), which in turn coupled to H-7 (δ_H 1.95, m). Hence, these data established the structural subunit **B** (Fig. 2.16). Accordingly, the HMBC spectrum displayed carbon-hydrogen correlations supporting this fragment. Additionally, an oxymethine proton at δ_H 3.11 (H-1, dd, J = 11 Hz, 4 Hz) showed

coupling to protons at δ_H 1.44 (H-2, m) and 1.50 (H-2, m) in ^1H-^1H COSY spectrum, and proton decoupling experiments revealed further coupling of protons at δ_H 1.44 and 1.50 (H-2) to methylene protons at δ_H 1.38 and 1.67 (H_2-3), suggesting the presence of a fragment **C** (Fig. 2.16).

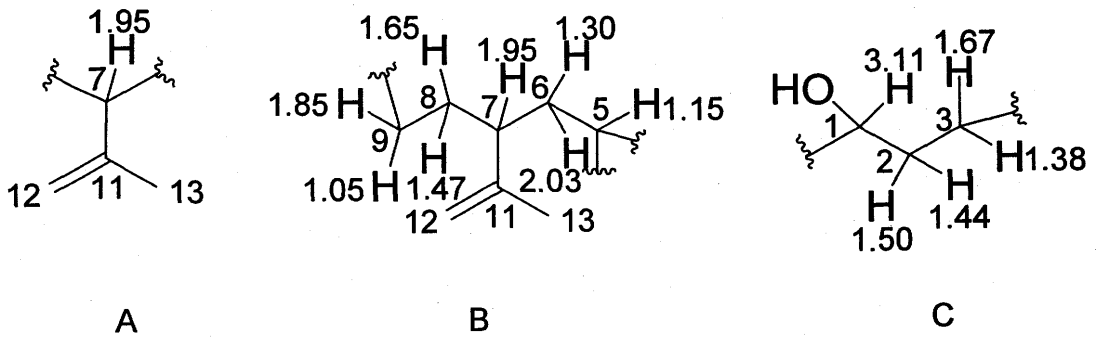

Figure 2.16: Fragments A, B and C for compound **120**

Finally, analysis of the HMBC data allowed connecting fragments and isolated groups to form a six membered bicyclic framework. A literature search showed that **120** had a selinene type skeleton (Thappa et al., 1979). The configuration of **120** was established on the basis of coupling constants and NOE difference spectral data. The coupling of the proton at δ_H 1.30 (H-6) to both H-5 and H-7 with J =12 Hz indicated its trans-diaxial orientation with respect to H-5 and H-7. Consequently, the isopropenyl group had to occupy an equitorial position at C-7. Additionally, the coupling constants of proton H-1 (δ_H 3.11, J = 11 Hz, 4 Hz) indicate its trans-diaxial orientation with one of the protons at C-2 (δ_C 29.2). In agreement with this, irradiation of the proton at δ_H 3.11 (H-1) resulted in an NOE enhancement of axial proton signals at δ_H 1.15 (H-5, 4%) and 1.05 (H-9, 3%), and vice versa. However, irradiation of either H-5 (δ_H 1.15) or H-1 (δ_H 3.11) never caused NOE enhancement of the methyl proton signals at δ_H 0.88 (H_3-14) and 1.02

(H_3-15). Further irradiation of the methyl protons at δ_H 0.88 (H_3-14) caused an NOE enhancement on the other methyl signal at δ_H 1.02 (H-15, 1%), and vice versa. These NOE difference spectral data suggested a *trans*-fused ring stereochemistry at the ring junction as well as diaxial relationship between CH_3-14 and CH_3-15. Thus, the structure **120** was unambiguously assigned for lairdinol A.

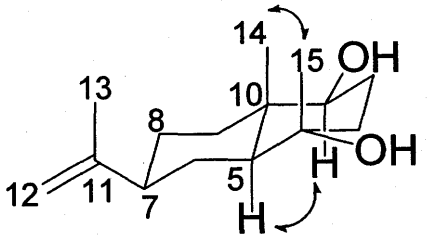

120

Compound **121** had the molecular formula of $C_{15}H_{26}O$ as determined by HREI-MS and NMR data, indicating three degrees of unsaturation. The ^1H NMR spectrum had signals for tertiary methyl groups at δ_H 1.07 (s, 3H) and 0.85 (s, 3H), and a vinylic methyl group at δ_H 1.84 (s, 3H). In addition, it displayed signals at δ_H 4.98 for olefinic methylene protons. The ^{13}C NMR and J-mod exhibited 15 signals, of which three were for methyl, seven for methylene, three for methine and three for quaternary carbons. The two farther downfield carbon signals at δ_C 150.6 and 108.8 were assigned to C-11 and C-12, respectively, and the carbon signal at δ_H 71.5 was assigned to an oxygen-bearing quaternary carbon (C-4). In addition to complement this assignment, an intense IR band at 3400 cm^{-1} indicated the presence of a hydroxyl group. Olefinic methylene protons (H_2-12) showed a coupling with the methyl group at δ_H 1.84 (H_3-13) in the ^1H-^1H COSY spectrum, suggesting the presence of an allylic moiety. Furthermore, the long-range correlation at δ_H 1.84 (H-13) with a carbon at δ_C 46.9 (C-7) indicated that the carbon at δ_C 150.8 (C-11) was connected with C-7. Proton decoupling experiments showed the correlations of H-7 (δ_H 2.00) to H-8 (δ_H 1.49, 1.62) and H-6 (δ_H 1.23, 2.13), H-6 to H-5

(δ_H 1.12), and H-8 (δ_H 1.49, 1.62) to H-9 (δ_H 1.40, 1.49). Consistent with these assignments, the HMBC spectrum displayed a correlation of H_2-6 with C-5 (δ_C 55.2), C-7 (δ_C 46.9) and C-11 (δ_C 150.8), indicating the presence of structural subunit **A** (Fig. 2.17).

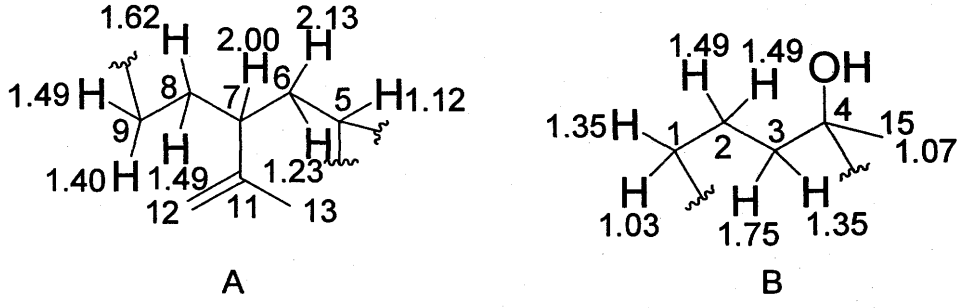

Figure 2.16: Fragment A and B of compound **121**

In addition, both the ^{1}H-^{1}H COSY spectrum and homodecoupling experiments revealed an isolated spin system which contains δ_H 1.03, 1.35 (H_2-1) coupled to δ_H 1.49 (H_2-2), which in turn coupled to δ_H 1.35, 1.75 (H_2-3). An HMBC correlation of H-3 with the quaternary carbon at δ_C 71.5 (C-4), together with correlations of H-15 (δ_H 1.07) with C-4 and C-3, suggested the structural subunit **B** (Fig. 2.17). The connectivity of fragments and isolated groups was established from hydrogen-carbon long-range correlations across the fragments and isolated groups, which indicated a selinene type framework for compound **121** (Thappa et al., 1979). The ^{1}H and ^{13}C NMR data of **121** were quite similar to those of **120**, except for the lack of the secondary hydroxyl group. The relative configuration of **121** was determined based on ^{1}H NMR and NOE difference data. The ^{1}H NMR spectrum displayed a ddd signal for H-6 (δ_H 1.23), which coupled to two vicinal methine protons, H-5 (δ_H 1.12) and H-7 (δ_H 2.00), and a geminal proton, H-6 (δ_H 2.13) with coupling constants of J = 12, 12, 12 Hz. These large coupling constants required the *trans*-diaxial orientation of H-6 (δ_H 1.23) to H-5 (δ_H 1.12), and H-6 (δ_H 1.23) to H-7 (δ_H 2.00), which implied an equatorial orientation for the isopropenyl group at C-

6. Furthermore, irradiation of the signal at δ_H 0.85 (H_3-15) caused an NOE enhancement on signal at δ_H 1.07 (H_3-14, 3%), but had no effect on signal at δ_H 1.12 (H-5). Hence, a *trans*-fused stereochemistry at the ring junction and a *cis* relative orientation for the two methyl groups at C-10 and C-4 was deduced leading to an unambiguous assignment of **121**. A literature search showed that compound **121** was identical with selin-11-en-4α-ol, a sesquiterpenoid report previously from the essential oil of *Podocarpus dacrydioides* (Corbett and Smith, 1967). However, the optical rotation data of **112** could not be compared with that of selin-11-en-4α-ol because the solvent used was not indicated for the reported optical rotation data.

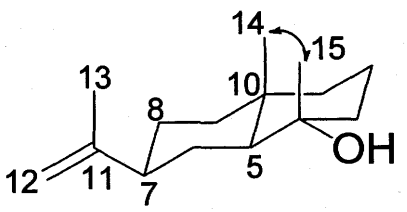

121

Table 2.6 ^{1}H NMR (500 MHz) and ^{13}C NMR (125 MHz) data (ppm) of 120 and 121 (C_6D_6)

Carbon No.	**120** δ_C (ppm)	**120** δ_H, m, J (Hz)	**121** δ_C (ppm)	**121** δ_H, m, J (Hz)
1	79.5	3.11, dd, 11, 4	46.6	1.35, m; 1.03, m
2	29.2	1.44, m; 1.50, m	20.7	1.49, m; 1.49, m
3	41.5	1.38, m; 1.67, m	44.0	1.75, m; 1.35, m
4	71.1	-	71.5	-
5	53.3	1.15, dd, 12, 2	55.2	1.12, m
6	26.3	2.03, m; 1.30, ddd, 12, 12, 12	26.5	2.13, m; 1.23, ddd, 12, 12, 12
7	46.4	1.95, m	46.9	2.00, m
8	27.0	1.65, m, 1.47, ddd, 13, 13, 13, 3	27.5	1.62, m; 1.49, m
9	41.0	1.05, ddd, 13, 13, 3 1.85, ddd, 13, 3, 3	45.1	1.40, m; 1.49, m
10	39.3	-	34.8	-
11	150.6	-	150.8	-
12	108.8	4.96, d, 15	108.8	4.98, br d, 20
13	21.2	1.82, s	21.3	1.84, s
14	13.3	0.88, s	18.9	0.85, s
15	22.9	1.02, s	22.9	1.07, s

Compounds **114-119** have the same skeleton as silphinene, which was first isolated from roots of *Silphium perfoliatum* (Bohlmann and Jakupovic, 1980). Sesquiterpenes **114, 116-119** are reported here for the first time, whereas **55** and **115** are known compounds. Phomalairdenone A (**55**) was reported previously by our research group from Polish type isolate (Laird 2) (Pedras et al., 1999a). Compound **55** is the first example of a host-selective phytotoxin from a phytopathogenic fungus containing a silphinene skeleton. The structure of phomalairdenone A (**55**) was determined by both NMR and X-ray crystallographic analysis of a single crystal. Compound **115** was identical to 3-oxosilphinene, which had been isolated from *Dugaldia hoopesii* (Bohlmann et al, 1984). Interestingly, tricyclic silphinene sesquiterpenes have not been reported yet from other phytopathogenic fungi (Pedras et al., 1999a, Cane et al., 1990). However, sesquiterpenes with a silphinene skeleton are common in plant species. For instance, the essential oils from the genus Artemisa are constituted largely of tricyclic silphinene sesquiterpenes (Marco et al., 1996; Weyerstahl et al., 1991). Some silphinene sesquiterpenes from plant species are insect antifeedants, for example, those obtained from *Cineraria geifolia* showed strong insect antifeedant activity (González-Coloma et al., 2002). In addition, sesquiterpenes **120** and **121** isolated from Mayfair 2/Laird 2 had the selinene skeleton (Corbett and Smith, 1967). Lairdinol A (**120**) is a new metabolite, whilst **115** was found to be identical with selin-11-en-4α-ol, which was first reported from the essential oil of *Podocarus dacrydioides* (Corbett and Smith, 1967).

Depsipeptide

Compound **122** had a molecular formula of $C_{38}H_{65}N_3O_9$, based on MS (HREI-MS and FAB) and NMR (^1H, ^{13}C NMR and HMQC) data, indicating eight degrees of unsaturation. The ^1H NMR spectrum displayed signals for six methyl singlets and six methyl doublets. Two methyl singlets at δ_H 3.36 (H-12) and 2.74 (H-18) were attributed to N-methyl groups. The ^{13}C NMR and J-mod NMR spectral data revealed the presence of twelve methyls, seven methylenes, eleven methines and eight quaternary carbons. The ^{13}C NMR spectrum displayed four carbon signals far down field at δ_C 171.7, 175.4, 170.1, and 171.1, suggestive of carbonyls of amide or ester groups. Additionally, two signals were displayed for olefinic carbons at δ_C 108.4 and 150.1 in the ^{13}C NMR spectrum. The four carbonyl groups and one olefinic double bond accounted for five of the eight degrees of unsaturation, indicated by the molecular formula. The remaining three unsaturations unaccounted for suggested the presence of three rings. The HMQC data allowed the assignment of all protons attached to carbon atoms with the exception of four protons, which were D_2O exchangeable. The ^1H-^1H COSY spectrum displayed several spin systems, of which three were designated as A, B and C. The spin system A contained a methine proton at δ_H 5.34 (H-14, d, J = 11 Hz) coupled with a proton at δ_H

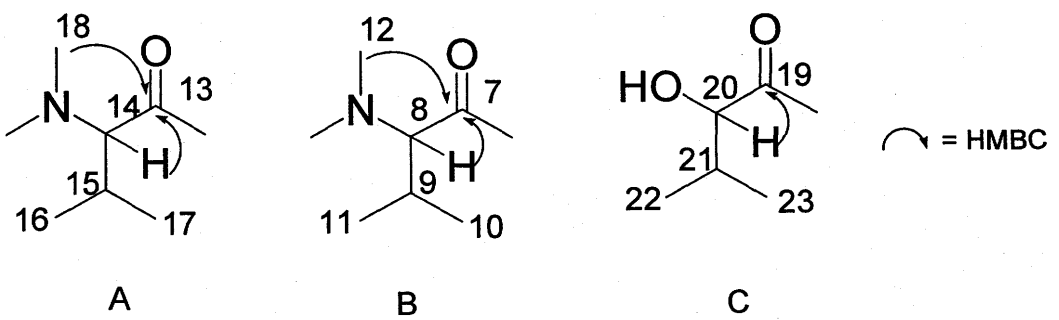

Figure 2.18: Fragments A, B and C for compound **122**

2.45 (H-15), which in turn coupled with two methyl groups at δ_H 0.92 (H_3-16, d, J = 7 Hz) and δ_H 0.81 (H_3-17, d, J = 7 Hz). The spin system B contained a methine proton at δ_H 5.29 (H-8, d, J = 11 Hz) coupled to a methine proton at δ_H 2.47 (H-9, m), which was coupled to two methyl groups at δ_H 1.18 (H_3-10, d, J = 7 Hz) and δ_H 0.83 (H_3-11, d, J = 7 Hz). The spin system C contained a proton at δ_H 4.22 (H-21, br d, J = 7 Hz) coupled to a proton at δ_H 1.80 (H-21, m), to a hydroxyl proton at δ_H 3.91(d, J = 7 Hz), and to H-21 (δ_H 4.22), which in turn was coupled to two methyl protons at δ_H 1.18 (H_3-22, d, J = 7 Hz) and δ_H 0.99 (H_3-23, d, J = 7 Hz). These proton spin systems, together with HMBC data allowed one to deduce fragments **A**, **B** and **C** (Fig. 2.18). Additionally, the HMBC spectrum displayed several long-range correlations; H-8 (δ_H 5.29) with C-13 (δ_C 171.1), C-12 (δ_C 31.0) and C-7 (δ_C 170.1), H-14 (δ_H 5.34) with C-18 (δ_C 29.8) and C-13 (δ_C 171.1), H-18 (δ_H 2.74) and H-22 (δ_C 19.5) with C-19 (δ_C 175.4). On the basis of these correlations, the fragments **A, B,** and **C** were connected to obtain fragment **D** as shown in Fig. 2.19.

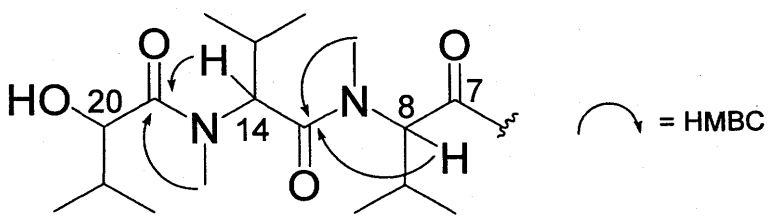

Figure 2.19: Fragment D with selected HMBC correlations for compound **122**

The ^{1}H-^{1}H COSY spectrum showed another isolated spin system which contained a proton at δ_H 3.68 (H-4) coupled with two methylene protons at δ_H 4.48 (H_2-5, dd, J = 6, 12 Hz) and 3.89 (H_2-5, dd, J = 4, 12 Hz). H-4 (δ_H 3.68) exhibited an HMBC correlation with a quaternary carbon at δ_C 76.4 (C-3), which showed a correlation with a methyl singlet at δ_H 1.28 (H-6), which in turn correlated with C-4, C-5, and a carbon at δ_C 67.2 (C-2). Thus, the connectivity of the proton at δ_C 24.8 (C-6) to C-3 (δ_C 76.4) was established. Furthermore, the HMBC spectrum displayed correlations of H-2 (δ_H 4.47, s) with C-3, C-5, C-6 and a carbon at δ_C 171.7 (C-1). The observed HMBC correlation between H-2 (δ_H 4.47, s) and C-5 (δ_C 52.8) suggested that this spin system contained a ring. In agreement with this, the ^{13}C NMR chemical shift of C-5 (δ_C 52.8) and C-2 (δ_C 67.2) as well as the absence of coupling between H-2 and H-5 clearly indicated that the connectivity of C-2 and C-5 was through a nitrogen atom. In addition, the ^{13}C NMR chemical shifts of C-3 (δ_C 76.4) and C-4 (δ_C 76.4) indicated the presence of hydroxyl groups, thus leading to substructure **E** (Fig. 2.20).

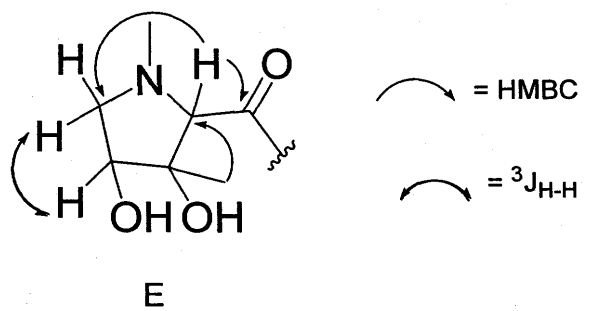

E

Figure 2.20: Fragment E with selected HMBC and $^{3}J_{1H-1H}$ correlations for compound **122**

The ^{1}H-^{1}H COSY spectrum displayed a correlation of the proton at δ_H 4.89 (H-1', dd, J = 12, 4 Hz) with methylene protons at δ_H 2.10 and 1.78 (H_2-2'), which in turn showed a further correlation with the proton at δ_H 1.44 (H-3'). These ^{1}H-^{1}H correlations

indicated C-C bonds to occur between C-1' and C-2', and C-2' and C-3'. Diagnostic HMBC correlations observed from the methyl singlet at δ_H 1.00 (H-15') to C-3' (δ_C 40.5), C-4' (δ_C 71.3) and C-5' (δ_C 53.1) showed C-15' to bond to the quaternary carbon C-4', which further bonded to C-3' and C-5'. Furthermore, diagnostic HMBC correlations were observed from a methyl singlet at δ_H 1.09 (H-14') to C-1' (δ_C 83.3), C-5' (δ_C 53.1), C-9' (δ_C 40.3) and C-10' (δ_C 38.9). As a result, the connectivity was established between C-15' and the quaternary carbon C-10', and also between C-10' and C-5', C-10' and C-1', and C-10' and C-9'. The ^{13}C NMR chemical shift of C-1' (δ_C 83.3) and C-4' (δ_C 71.3) suggested C-1' and C-4' to be connected to oxygen atoms. Consequently, the structural subunit **F** was deduced (Fig. 2.21). In addition, the HMBC spectrum displayed a methyl singlet at δ_H 1.80 (H-13') correlating with olefinic carbons at δ_C 108.4 (C-12') and 150.1 (C-11') was assigned to a vinyl methyl group. A further HMBC correlation of a vinyl methyl group (H-13') with a carbon signal at δ_C 46.1 (C-7'), and an additional correlation of this carbon (C-7') with a methylene proton at δ_H 4.93 (H-12'), indicated the presence of the structural subunit **G** (Fig. 2.21). Further correlations of H-7' (δ_H 1.94), in the ^1H-^1H COSY spectrum, with the methylene protons at δ_H 1.41 (H_2-8') and 1.28 (H_2-6') allowed an extension of fragment **G** into fragment **H** (Fig. 2.21).

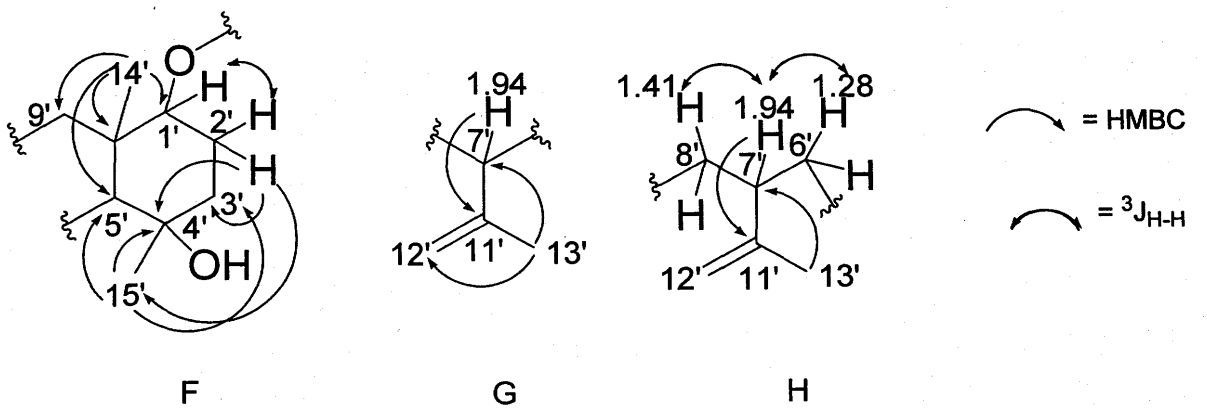

Figure 2.21: Fragment **F**, **G** and **H** with HMBC and $^3J_{1H\text{-}1H}$ correlations for compound **122**

The structural subunits **F** and **H** were assembled together on the basis of long-range correlations shown across the structural subunits. Thus, ^{1}H-^{13}C correlations were observed between H-5' (δ_H 1.26) and C-6' (δ_C 25.6), and H-9' (δ_H 2.05) and C-8' (δ_C 26.2), indicating a C-C bond between C-8' and C-9', and C-5' and C-6', respectively. As a result, the structural subunit **I** was established (Fig. 2.22). Interestingly, the skeleton of structural subunit **I** was similar to those of lairdinol A (**120**) and selin-11-en-4α-ol (**121**), discussed in the previous section.

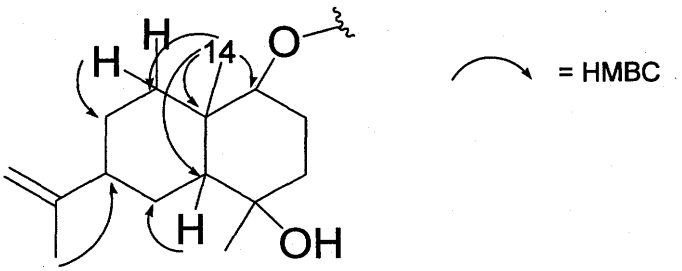

I

Figure 2.22: Fragment **I** with HMBC and $^{3}J_{H\text{-}H}$ correlations for compound **122**

The connectivity of the structural subunits **E** and **I** was established on the basis of HMBC correlations. Thus, the long-range correlation observed between proton H-1' (δ 4.89) from **I** and carbonyl carbon C-1 (δ 171.1) from **E** was a key correlation, establishing the connectivity between structural units **I** and **E**. Finally, structural subunit **D** was connected to the assembled unit from **E** and **I** to obtain the structure of **122**. Compound **122** was crystallized from a mixture of hexane/acetone (70:30) to yield crystals of monoclinic system of $P2_1$ space group. X-ray crystallographic analysis was conducted on a single crystal. This analysis confirmed and established unambiguously the assignment of the relative configurations of all stereogenic centres of compound **122**, which was named depsilairdin.

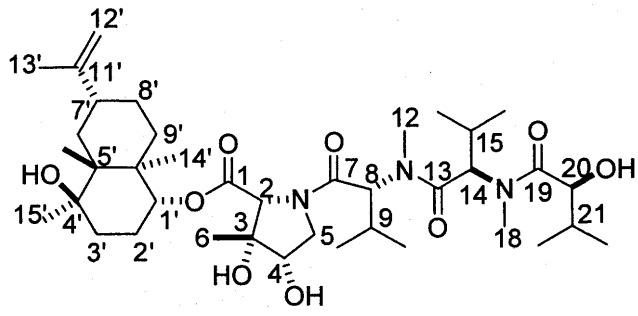
12'
13'
11'
8'
7'
9'
5'
14'
HO
15'
4'
1'
3'
2'
O
1
2
N
3
6
HO
4
OH
5
O
7
8
N
9
12
13
15
14
N
O
18
19
O
20
OH
21

122

Table 2.7 ^{1}H NMR (500 MHz) and ^{13}C NMR (125 MHz) data (ppm) of depsilairdin (122) (C_6D_6)

Carbon No:	δ_C (ppm)	δ_H (ppm), *J* (Hz)	Carbon No:	δ_C (ppm)	δ_H (ppm), *J* (Hz)
1'	83.3	4.89, dd, 12, 4	5	52.8	4.48, dd, 12, 6; 3.89, dd, 12, 4
2'	25.1	2.10, m; 1.78, m	6	24.8	1.28, m
3'	40.5	1.64, m; 1.44, m	7	170.1	-
4'	71.3	-	8	59.4	5.29, d, 11
5'	53.1	1.26, m	9	27.4	2.47, m
6'	25.6	2.08, m; 1.28, m	10	20.3	1.18, d, 7
7'	46.1	1.94, m	11	18.8	0.83, d, 7 Hz
8'	26.2	1.62, m; 1.41, m	12	31.0	3.36, s
9'	40.3	1.19, m; 2.05, m	13	171.1	-
10'	38.9	-	14	59.5	5.34, d, 11 Hz
12'	108.4	4.93, d, 12	15	27.2	2.45, m
11'	150.1	-	16	19.5	.92, d 7 Hz
13'	21.3	1.80, s	17	18.7	0.81, d 7 Hz
14'	22.7	1.00, s	18	29.8	2.74, s
15'	14.5	1.09, s	19	175.4	-
1	171.7	-	20	72.6	4.22, br d, 6
2	67.2	4.47, br s	21	31.0	1.80, d, 7 Hz
3	76.4	-	22	19.5	1.18, d, 7 Hz
4	76.4	4.47, m	23	15.0	0.99, d, 7

Once the relative stereochemistry of depsilairdin (**122**) was established, it remained to determine its absolute stereochemistry. To establish the absolute stereochemistry, a small amount of depsilairdin (**122**) was hydrolyzed in an NMR tube under acidic conditions (0.2 M DCl and MeOD) as described in the experimental section. The reaction progress was monitored by ^{1}H NMR spectroscopy. In particular, the proton signals at δ_H 5.29 (H-8) and 5.34 (H-14) in the ^{1}H NMR spectrum of depsilairdin (**122**) were examined during the reaction progress. The reaction was stopped after the disappearance of the reference proton signals [δ_H 5.29 (H-8) and 5.34 (H-14)] of depsilairdin (**122**). The reaction mixture was separated by prep. TLC and then by semi-prep. HPLC to obtain compound **123.**

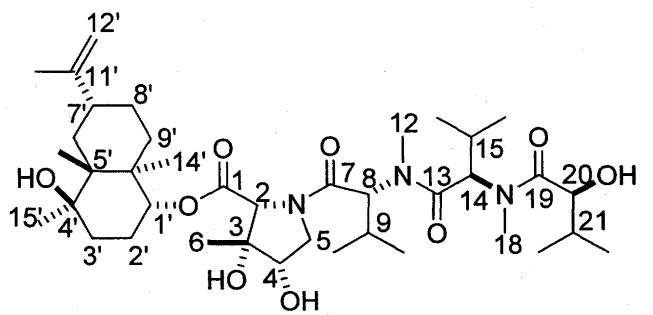

122

DCl (0.2M)
MeOD, r.t., 7 days

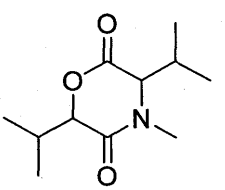

123

Scheme 2.4: Acid hydrolysis of depsilairdin (**122**)

Compound **123** had a molecular formula of $C_{11}H_{19}O_3N$ (HREI-MS), indicating three degrees of unsaturation. The ^1H NMR spectrum displayed signals for five methyl groups (4×d, 1s) and four methine protons. The ^{13}C NMR spectrum, together with HMQC data confirmed the presence of five methyl groups and four methine groups, as well as two carbonyl groups. The ^1H-^1H COSY spectra of **123** revealed the existence of two isolated spin systems, A and B. The spin system A contained H-3 (δ_H 3.34, d, J = 6 Hz) coupled with H-7 (δ_H 1.71, m), which in turn coupled with H-8 (δ_H 0.84, d, J = 7 Hz) and H-9 (δ_H 0.72, d, J = 7 Hz). In B, H-6 (δ_H 4.49, d, J = 2 Hz) showed coupling with H-11 (δ_H 2.77, m), which further coupled with H-12 (δ_H 1.10, d, J = 7 Hz) and H-13 (δ_H 1.09, d, J = 7 Hz). Consequently, fragments **A** and **B** were deduced (Fig. 2.23).

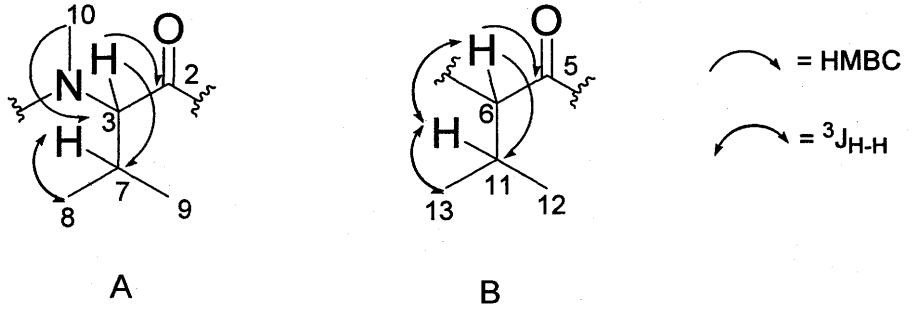

Figure 2.23: Fragment A and B with HMBC and $^3J_{H-H}$ correlations for compound **123**

Diagnostic long-range ^1H-^{13}C correlations observed between C-2 (δ_C 165.4) and H-3 (δ_H 3.22), H-7 (δ_H 1.60), and H-10 (δ_H 2.38) showed C-2 to bond to C-3 as well as C-3 to an N-Me group. Similarly, long-range ^1H-^{13}C correlations of C-5 (δ_C 165.3) with H-6 (δ_H 4.37) and H-10 (δ_H 2.38) suggested C-5 to bond to C-6 and N-Me. Consequently, HMBC data coupled with ^1H-^1H COSY data revealed the presence of a didepsipeptide. As was deduced from HRMS, **123** contained three degrees of unsaturation, of which two could be accounted for by the two carbonyl groups, and the additional unsaturation by a cyclic structure; as well the relative stereochemistry was assigned on the basis of NOE

difference experiments. Thus, irradiation of the proton at δ_H 1.60 (H-7) caused an NOE enhancement on the signal of the proton at H-6 (δ_H 4.37), and vice versa, suggesting the *cis* orientation for H-6 and the isopropyl group at C-3. This assignment was consistent with the relative configuration of the corresponding stereogenic centers of depsilairdin (**122**). Hence, the structure of this product was assigned unambiguously as 3,6-diisopropyl-4-methyl-2,5-morpholinedione (**123**).

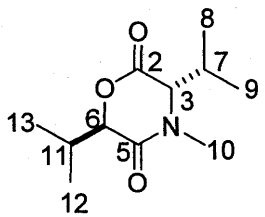

123

Table 2.8 ^{1}H NMR (500 M Hz) and ^{13}C NMR (125 MHz) data (ppm) of 3,6-diisopropyl-4-methyl-2,5-morpholinedione (123) (C_6D_6)

Carbon No.	δC (ppm)	δH (ppm),m, J (Hz)	HMBC
2	165.4	-	3, 7
3	67.2	3.22, d, 6	7, 8, 9, 10
5	165.3	-	6, 10
6	81.7	4.37, d, 2	12, 13
7	31.8	1.60, m	3, 8, 9
8	19.4	0.73, d, 7	3, 7, 9
9	18.2	0.61, d, 7	7, 8
10	33.5	2.38, s	-
11	30.97	2.66, m	6, 12, 13
12	15.7	0.99, d, 7	6, 13
13	18.7	0.98, d, 7	12

To establish the absolute configuration of **123**, three of its four stereoişomers, (3*S*,6*R*), (3*R*,6*S*) and (3*R*,6*R*)-3,6-diisopropyl-4-methyl-2,5-morpholinedione, were synthesized. The synthesis of (3*S*, 6*R*)-3,6-diisopropyl-4-methyl-2,5-morpholinedione (**128**) was carried out starting with (*S*)-Cbz-Me-val (**126**) and (*R*)-2-hydroxy-3-methylbutyric acid (**125**) (Koch et al., 2003) (Scheme 2.5). First, (*R*)-2-hydroxy-3-methylbutyric acid (**125**) was obtained from the reaction of (*R*)-valine (**124**) with nitrous acid followed by hydrolysis in 77% yield. The overall transformation of **124** to **125** occurs with retention of configuration (Li et al., 1990). Next, coupling of (*R*)-2-hydroxy-3-methylbutyric acid (**125**) with CDI-activated (*S*)-Cbz-MeVal (**126**) in THF gave (*S*)-

Cbz-MeVal-(*R*)-2-hydroxy-3-methylbutyric acid in 74% yield. Deprotection of this coupled product by catalytic hydrogenolysis using Pd/C in methanol led to (*S*)-Me-Val-(*R*)-2-hydroxy-3-methylbutyric acid (**127**) quantitatively. Finally, cyclization of (*S*)-Me-Val-(*R*)-2-hydroxy-3-methylbutyric acid (**127**) to (3*S*, 6*R*)-3,6-diisopropyl-4-methyl-2,5-morpholinedione (**128**) (69%) was achieved by treatment of **127** with Mukaiyama's reagent (2-chloro-1-methyl-pyridinium iodide) in the presence of triethylamine in refluxing CH_2Cl_2 (Koch et al., 2003). The synthesis of the enantiomer of **128**, (3*R*, 6*S*)-3,6-diisopropyl-4-methyl-2,5-morpholinedione (**135**), from (*R*)-BocMeVal (**129**) and (*S*)-2-hydroxy-3-methylbutric acid (**133**), and the diastereomer (3*R*,6*R*)-3,6-diisopropyl-4-methyl-2,5-morpholinedione (**131**), from (*R*)-BocMeVal (**129**) and (*R*)-2-hydroxy-3-methylbutyric acid (**125**), were also carried out following the same reaction sequence (Schemes 2.6 and 2.7). For these reactions, (*R*)-BocMeVal (**129**) was synthesized from (*R*)-valine (**124**) by first protecting the amino group with Boc_2CO (Campbell et al., 1998), followed by N-methylation (Cheung and Benoiton, 1977). The ^1H NMR spectra of both **128** and **135** were found to be identical with that of **123,** but that of **131** was different.

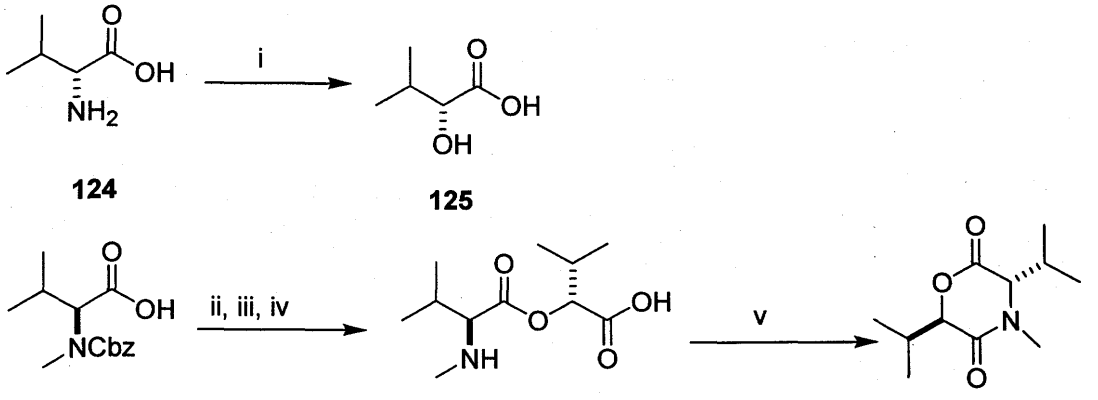

Scheme 2.5 Synthesis of (3S,6R)-3,6-diisopropyl-2,5-morpholinedione (**128**): i) 1 N H_2SO_4, $NaNO_2$, 77%; ii) CDI, THF; iii) **125**, THF, 74%; iv) H_2, Pd/C, EtOH; v) 2-chloro-1-methylpyridinium iodide, Et_3N, CH_2Cl_2, 69%.

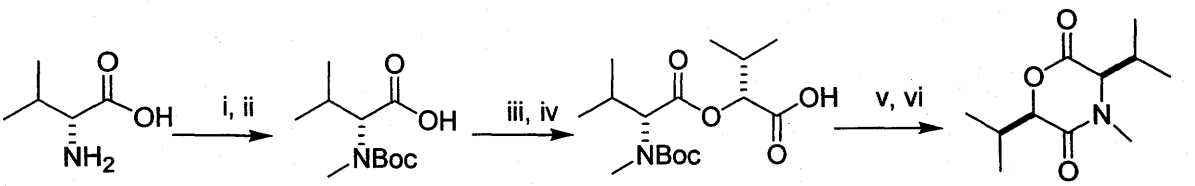

124 **129** **130** **131**

Scheme 2.6 Synthesis of (3R,6R)-3,6-diisopropyl-2,5-morpholinedione (**131**): i) Boc_2CO, dioxane, 1N NaOH, 78%; ii) NaH, MeI, THF; iii) CDI, THF; iv) **125**, THF, 63%; v) Formic acid (excess); vi) 2-chloro-1-methylpyridinium iodide, Et_3N, CH_2Cl_2, 40%.

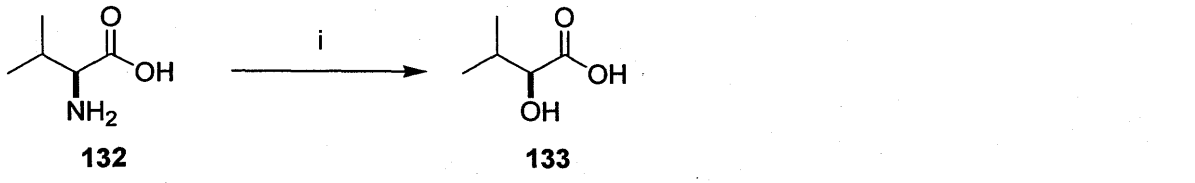

132 **133**

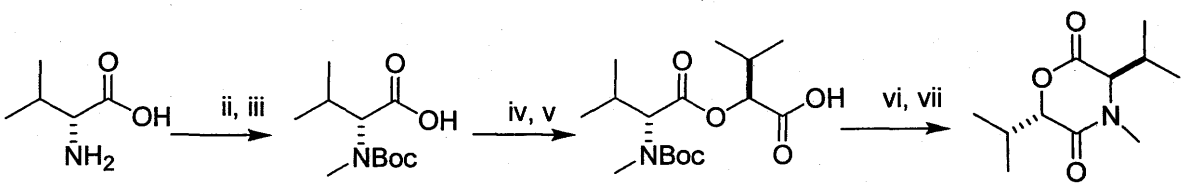

124 **129** **134** **135**

Scheme 2.7 Synthesis of (3R,6S)-3,6-diisopropyl-2,5-morpholinedione (**135**): i) 1 N H_2SO_4, $NaNO_2$, 78%; ii) Boc_2CO, dioxane, 1N NaOH; iii) MeI, THF; iv) CDI, THF; v) **133**, THF, 56%; vi) Formic acid (excess); vii) 2-chloro-1-methylpyridinium iodide, Et_3N, CH_2Cl_2, 47%.

To determine which enantiomer had the absolute configuration identical to that of **123,** ^{1}H NMR spectra were recorded for **123** and for the two enantiomers, **128** and **135,** in the presence of the chiral solvating agent, 1-(9-anthranyl)-2,2,2-trifluoroethanol (TFAE). The optimum concentration of the chiral solvating agent was established by gradual addition of (R)-(-)-TFAE until baseline separation of selected signals in the ^{1}H NMR spectrum was achieved (Hana and Lau-Cam, 1993). This optimum concentration was established to be 0.12 M. At this concentration, the ^{1}H NMR spectrum recorded for a 2:1 mixture of (3*S*,6*R*)-3,6-diisopropyl-2,5-morpholidenone (**128**) and (6*R*, 3*S*)-3,6-diisopropyl-2,5-morpholidenone (**135**) in $CDCl_3$ showed a baseline separation between the H-6 signals of each enantiomer. The observed chemical shift for the H-6 proton of the (3*S*, 6*R*)-enantiomer was at δ_H 4.55, whereas for the (6*R*, 3*S*)-(-)-enantiomer was at δ_H 4.52. Following these determinations, the ^{1}H NMR spectrum was recorded for **123** in $CDCl_3$ in the presence of (*R*)-(-)-TFAE (0.12 M). The ^{1}H NMR spectrum displayed the signal for the H-6 proton at δ_H 4.55 as shown in figure 2.24. This corresponded to the chemical shift of the H-6 proton of (3*S*,6*R*)-3,6-diisopropyl-2,5-morpholidenone (**128**). Further, this "natural" sample was spiked first with a solution of (3*S*,6*R*)-3,6-diisopropyl-2,5-morpholidenone (**128**) in $CDCl_3$ with 0.12 M (*R*)-(-)-TFAE. The recorded ^{1}H NMR spectrum of this mixture displayed a signal for H-6 again at δ_H 4.55, suggesting **123** to be identical with (3*S*,6*R*)-3,6-diisopropyl-2,5-morpholidenone (**128**). Further confirmation was obtained by spiking the same mixture with a solution of (3*R*,6*S*)-3,6-diisopropyl-2,5-morpholidenone (**135**) in $CDCl_3$ with 0.12 M (*R*)-(-)-TFAE. In this case, the ^{1}H NMR spectrum showed the separated signals at δ_H 4.55 and 4.52, for the H-6 protons of **123** and (3*R*,6*S*)-3,6-diisopropyl-2,5-morpholidenone (**135**), respectively. The resolved signals of the H-6 proton demonstrate **123** is the enantiomer of (3*R*,6*S*)-3,6-diisopropyl-2,5-morpholidenone (**135**). On the basis of the observed ^{1}H NMR chemical shifts, the absolute configurations of the stereogenic centers of **123** were assigned as 3*S* and 6*R*. Since **123** was a fragment composing depsilairdin (**122**), these assignments of absolute

configuration in **123** further allowed the assignment of the absolute configuration of the stereogenic centers of **122** as 2*S*, 3*S*, 4*R*, 8*S*, 14*S*, 20*R*, 1'*S*, 4'*S*, 5'*S*, 7'*S* and 10'*S*. Consequently, structure **122** was assigned unambiguously for depsilairdin (Pedras et al., 2004a).

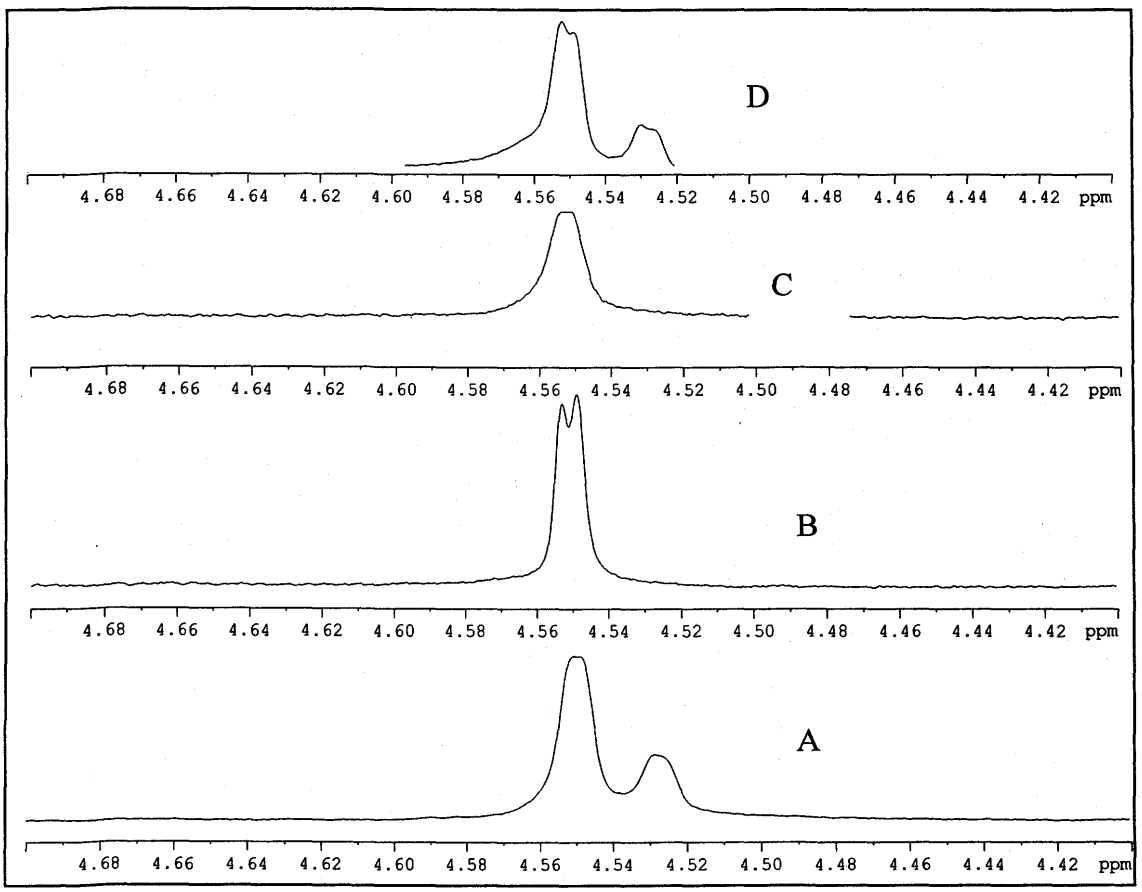

Figure 2.24: ^{1}H NMR signal(s) of H-6 for A) 2:1 mixture of **128** and **135**; B) hydrolysis product **123**; C) 80:20 mixture of **123** and **128**; d) 80:20 mixture of **123** and **135**

2.1.2 Metabolites produced in PDB medium

A total of 68 L culture was prepared in PDB medium. The six-day-old cultures were filtered (62 L) and were extracted with EtOAc (12.6 g). The EtOAc extracts (PDB) were fractionated on RP-FCC (350 mg per batch, 12.6 g) to yield twelve fractions, most of which were phytotoxic. Multiple fractionation of the phytotoxic fractions, however, resulted in loss of phytotoxicity. This loss was attributed to decomposition during the isolation procedure. The isolation attempted for the major phytotoxic metabolite (R_t = 24.4 min) even by HPLC column chromatography was unsuccessful. However, non-phytotoxic fractions F_2 and F_3 obtained by RP-FCC of EtOAc extracts yielded compound A (3.0 mg) after multiple FCC followed by prep. TLC and finally by HPLC, as described in the experimental section.

The molecular formula of **136** was determined to be $C_{17}H_{13}O_3N$ based on HREI-MS and NMR data. The ^1H NMR spectrum displayed proton signals, which integrated for a total of 11 protons, and additionally two D_2O exchangeable protons. The ^{13}C NMR spectrum displayed 17 carbon signals, two of which were sp^3 methine and methylene carbons, eight sp^2 methine, and seven tetrasubstituted sp^2 carbons. The four most down field carbon signals were attributed to tetrasubstituted sp^2 carbons attached to oxygen atoms. The FTIR spectrum showed characteristic absorptions at 3375cm^{-1} and 2256cm^{-1} which revealed the presence of hydroxyl and nitrile groups, respectively. Two aromatic proton signals at δ_H 7.09 (d, J = 8.5 Hz) and 6.75 (d, J = 8.5 Hz), each of which integrated for two protons, showed coupling with each other, and the coupling constant of these protons was suggestive of the *ortho* orientation. Moreover, this spin system indicated the presence of a *para* substituted benzene moiety. Consequently, the carbon signal at δ_C 130.7 was assigned to C-2' and C-6', and the other carbon signal at δ_C 115.6

to C-3' and C-5'. Two carbon signals at δ_C 127.9 and 156.6 displaying correlations with protons δ_H 7.09 (H-2'/6') and 6.75 (H-3'/5') were assigned to C-1' and C-4', respectively.

Another spin system showed the proton at δ_H 6.83 (dd, J = 9.0, 2.5 Hz) coupling with protons at δ_H 7.38 (d, J = 9.0 Hz) and 7.97 (d, J = 2.5 Hz). The coupling constants for this set of aromatic protons suggested that the proton at δ_H 6.83 was *ortho* to the proton at δ_H 7.38 and the proton at δ_H 6.83 was *meta* to the proton at δ_H 7.97. Consequently, the presence of a 1,3,4- trisubstituted benzene moiety was deduced. ^{1}H NMR and HMQC data allowed the assignment of carbons at δ_C 106.2, 113.8 and 111.8 to C-4, C-6, and C-7, respectively. Moreover, HMBC data allowed the assignment of the carbon signals at δ_C 129.1 (C-3a), 153.6 (C-5) and 149.9 (C-7a). Further, the analysis of HMBC and ^{1}H NMR data indicated a 2,5-disubstituted benzofuran moiety (Fig. 2.25).

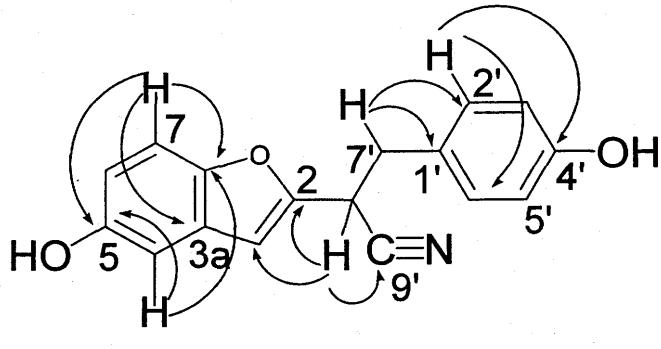

Figure 2.25: Selected HMBC correlations of **136**

An additional spin system contained the proton at δ_H 4.45 (H-8') coupling with methylene protons at δ_H 3.25 (H_2-7'). The latter protons, H_2-7' (δ_H 3.25) showed long-range correlations with C-1' (δ_C 127.9), C-2' (δ_C 130.7) and C-6' (δ_C 130.7), suggesting the connection of C-7' to C-1'. A further long-range correlation of the protons at δ_H 3.25 (H_2-7') with carbons at δ_C 118.7 (C-9') and 152.0 (C-2), together with a long-range

correlation of the proton at δ_H 4.45 (H-8') with carbons at δ_C 118.7 (C-9'), 152.0 (C-2) and 105.3 (C-3) allowed the connection of C-8' to C-9' and C-2. Finally these correlations led one to assemble all fragments to obtain structure **136**. Hence structure **136** was assigned unambiguously to compound A.

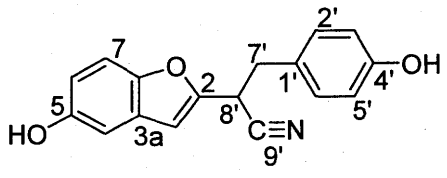

136

Table 2.9 ^{1}H NMR (500 MHz) and ^{13}C NMR (125 MHz) data of compound A (136) (CD_3CN)

C	δ_C	δ_H, m, *J*	C	δ_C	δ_H, m, *J*
C-2	152.0	-	C-2'	130.7	7.09, d, 8.5
C-3	105.3	6.62 (s)	C-3'	115.6	6.75, d, 8.5
C-3a	129.1	-	C-4'	156.6	-
C-4	106.2	7.97, d, 2.5	C-5'	115.6	6.75, d, 8.5
C-5	153.6	-	C-6'	130.7	7.09, d, 8.5
C-6	113.8	6.83, dd, 2.5, 9	C-7'	36.8	3.25, m
C-7	111.8	7.38, d, 9.0	C-8'	33.9	4.45, dd, 7.5 7.5
C-7a	149.9	-	C-9'	118.7	-
C-1'	127.9	-			

2.2 Phytotoxicity bioassays

The metabolites obtained from Mayfair 2 cultures were assayed for their phytotoxic activity on selected cruciferous species having various ranges of susceptibility toward blackleg fungus. The cruciferous species employed in the assays were *B. napus* (cv. Westar, susceptible to *P. lingam*), *B. juncea* (cv. Cutlass, resistant to *P. lingam* virulent), and *S. alba* (cv. Ochre, susceptible to *P. lingam*). Two-week-old plant leaves were inoculated with solutions of metabolites as described in the experimental section. After incubating of the plants for a week, leaves were visually inspected for lesions and the diameter of lesions was measured (see table 2.10). Plant leaves were not affected by phomapyrone A (**49**), phomapyrone D (**100**) and phomenin B (**105**), even at relatively high concentrations (e.g. 1×10^{-3} M). Therefore, these phomapyrones are not phytotoxic metabolites. Other phomapyrones such as phomapyrone E (**101**), phomapyrone G (**104**), infectopyrone (**103**) and phomapyrone F (**102**) were not assayed for their phytotoxic activity because these metabolites were isolated in very small quantities. For phomalairdenones and phomalairdenol compounds, the phytotoxic activity observed was not significant at a concentration of 5×10^{-4} M. However, at 1×10^{-3} M concentration metabolites such as phomalairdenone A (**55**), phomalairdenone D (**114**), lairdinol A (**120**) and phomalairdenol A (**117**) caused necrotic, chlorotic, and reddish lesions selectively on brown mustard leaves. Interestingly, one of these sesquiterpenes, phomalairdenone A (**55**), was detected in MeOH extracts of plant tissues infected by Mayfair 2 isolate, indicating also its production *in planta* as well. Phomalairdenone A (**55**) is a host-selective phytotoxin reported previously from Laird 2 isolate (Pedras et. al., 1999). On the other hand, the phytotoxicity of depsilairdin (**122**) was very selective and the highest among the metabolites of Mayfair 2. Depsilairdin (**122**) showed remarkable phytotoxicity

at concentrations as low as 5×10^{-6} M and selectivity at concentrations as high as 1×10^{-3} M toward brown mustard (*B. juncea*) (see fig. 2.26). Importantly, the selectivity of depsilairdin appeared to be similar to the pathogenicity range of isolate Mayfair 2 (Polish type isolate). Mayfair 2 isolate (Canadian Polish type isolate) is pathogenic to brown mustard (*B. juncea*), but not pathogenic to *B. napus* or *S. alba*. In addition, **122** was found in plant tissue extracts obtained from leaves infected by Mayfair 2 isolate, indicating its production *in planta*. Therefore, depsilairdin is a host-selective phytotoxin that may have an important role in plant-fungal interactions.

The cytotoxicity of metabolites **55**, **116**, **119**, **120** and **122** were determined using the brine shrimp lethality assays as described in the experimental part. Phomalairdenone A (**55**) and depsilairdin (**122**) showed little activity, whereas **116**, **119** and **120** were inactive (Table 2.11)

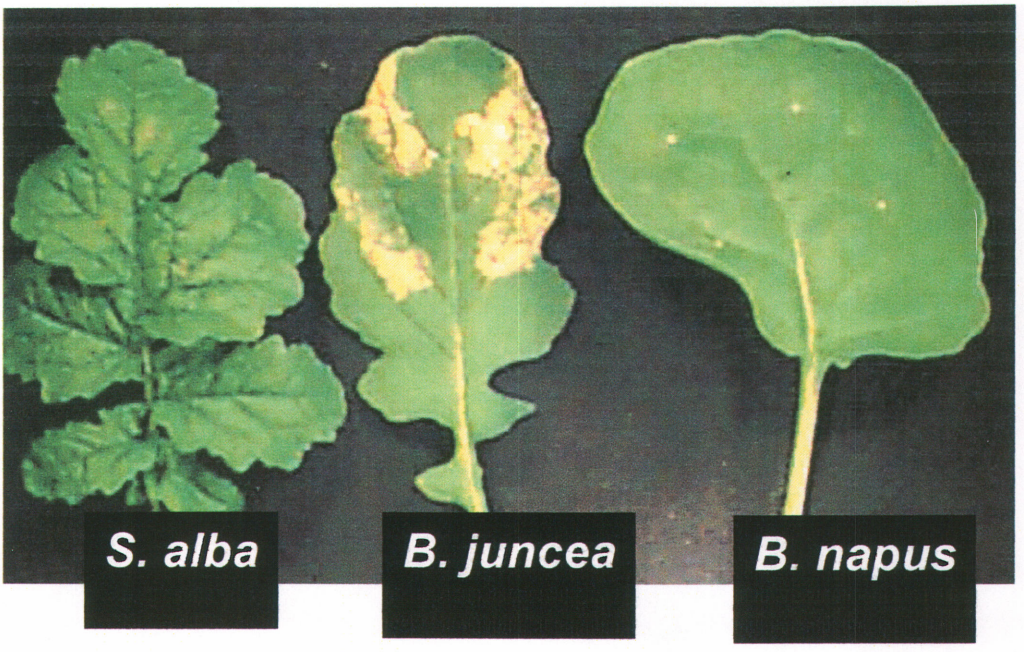

Figure 2.26:F Effect of depsilairdin (**122**) assayed at the concentration of 5×10^{-4} M on punctured leaves of two-week-old *Sinapis alba*, *Brassica juncea* and *Brassica napus* after one week of incubation in a growth chamber.

Table 2.10 Results of phytotoxicity assays of metabolites produced by isolate Mayfair 2.

Compound	B. napus		B. juncea		S. alba	
	A*	B*	A*	B*	A*	B*
phomalairdenone A (**55**)	0	0	0	1	0	0
phomalairdenone D (**114**)	0	0	0	1	0	0
phomalairdenol C (**118**)	0	0	0	0	0	0
phomalairdenol B (**116**)	0	0	0	0	0	0
lairdinol A (**120**)	0	0	0	1	0	0
phomalairdenol D (**119**)	0	0	0	0	0	0
phomalairdenol A (**117**)	0	0	0	1	0	0
phomapyrone A (**49**)	0	0	0	0	0	0
phomapyrone D (**100**)	0	0	0	0	0	0
phomapyrone G (**104**)	0	0	0	0	0	0
depsilairdin (**122**)	0	0	3	4	0	0

[a]Lesion diameter scale: 0=1-2 mm, 1=3-4 mm, 2=4-7 mm, 3=8-10 mm, 4=11-14 mm
Concentrations: A* = 5×10^{-4} M, B* = 1×10^{-3} M

Table 2.11 Toxicity of some metabolites isolated from Mayfair 2 to brine shrimp

Compound	concentration	% Mortality[a] ± SD
Phomalairdenol B (**116**)	5×10^{-4} M	0
Lairdinol A (**120**)	5×10^{-4} M	0
Phomalairdenone A (**55**)	5×10^{-4} M	42 ± 1
Phomalairdenol D (**119**)	5×10^{-4} M	0
Depsilairdin (**122**)	5×10^{-4} M	25 ± 2

[a] % Mortality = 100-[(number of live shrimp after 24h/number of live shrimp in control) × 100] ± standard deviation

2.3 Analysis and classification of Thlaspi isolates and avirulent isolates from France

Thlaspi isolates appear mostly on stinkweed (*Thlaspi arvense*) in canola fields in Saskatchewan and Alberta (Petrie and Vanterpool, 1968). The isolates are virulent on stinkweed (*T. arvense*) but not on rapeseed (McGee and Petrie, 1978, De March et al., 1986). Initially, these isolates were classified as part of the Thlaspi strain, a distinct strain from those of highly virulent and weakly virulent strains of *Phoma lingam* (*Leptosphaeria maculans*). This classification was based on pathogenicity tests (McGee and Petrie, 1978). Recently, as a result of methods developed for the differentiation of *P. lingam* (*L. maculans*), various reports suggested the need for revision of this classification. One of these methods of differentiation and grouping is based on secondary metabolite profiles (Pedras and Biesenthal, 2000; Williams and Fitt, 1999). Therefore, since the secondary metabolite profiles of Thlaspi isolates were unknown, the

chemical analysis of various Thlaspi isolates was carried out. For these analyses, a total of sixteen Thlaspi isolates originating from three regions of Saskatchewan (Melfort, Eastend and Saskatoon) were obtained from Agriculture and Agri-food Canada. These isolates were cultured as described in the experimental section. Culture samples were collected at various times, extracted with EtOAc and the extracts were analyzed by HPLC.

The analysis of chromatographic profiles of sixteen Thlaspi isolates suggested two different chromatographic profiles. Accordingly, Thlaspi isolates were divided into two groups, one group containing fourteen isolates and the other group containing two isolates. Figures 2.27 and 2.28 show the representative chromatograms of these groups of Thlaspi isolates. In cultures of sixteen Thlaspi isolates, the production of phomamide (**3**), sirodesmin PL (**1**) and deacetylsirodesmin PL (**2**) were not detected, indicating that none of these isolates were of the virulent type. A further comparison of the secondary metabolite profiles of the group of fourteen Thlaspi isolates with those established previously for isolates of *P. lingam* (Pedras and Biesenthal, 2000) revealed their similarity to weakly virulent isolates of *P. lingam* (Fig. 2.27). As a result, these fourteen Thlaspi isolates (see table 2.12) were assigned as weakly virulent isolates of *P. lingam*. This group of thlaspi isolates, like weakly virulent isolates (Pedras et al., 1994), produced metabolites of polyketide origin such as phomapyrone A (**49**). Phomapyrone A is one of the chemical markers for weakly virulent isolates (Pedras and Biesenthal, 2000). Thlaspi isolates were also found to produce tricyclic silphinene sesquiterpenes, which were not reported for weakly virulent isolates.

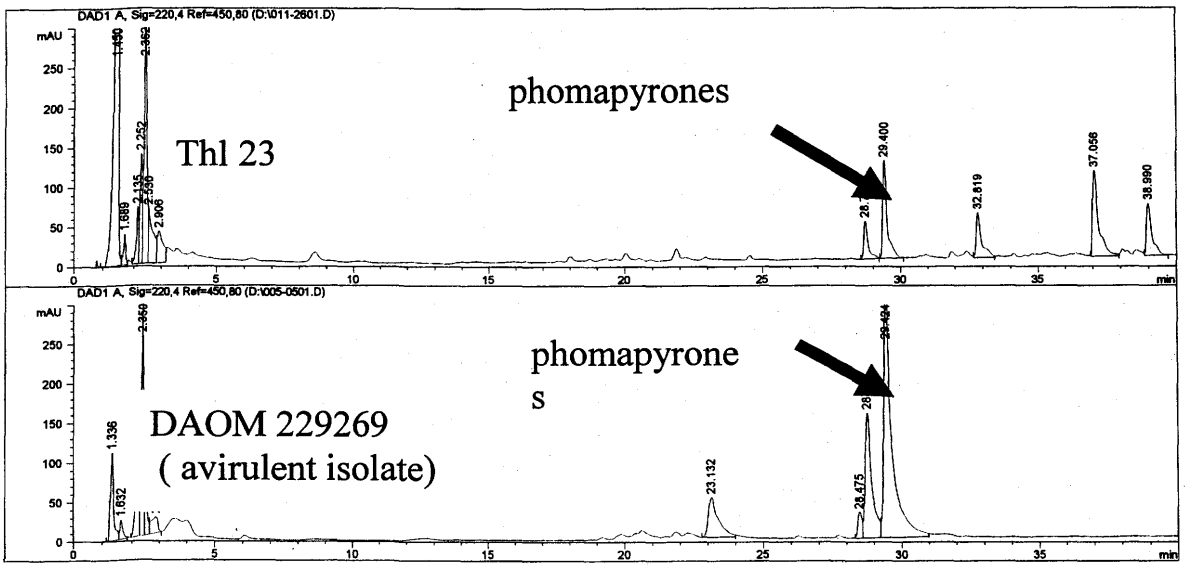

Figure 2.27: Chromatograms of extracts of cultures of Thl 23 and DAOM 229269 (avirulent isolate)

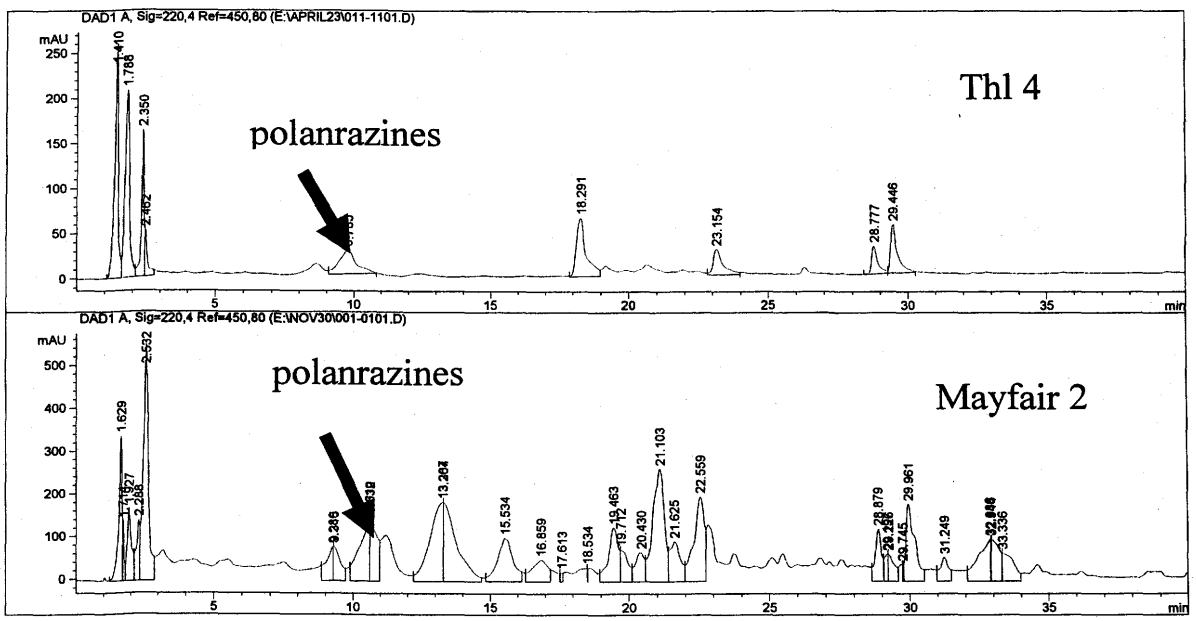

Figure 2.28: Chromatograms of extracts of cultures of Thl 4 and Mayfair 2 isolates

On the other hand, the chromatographic profiles of two Thlaspi isolates (Thl 4 and Thl 21) were found to be similar to those of Polish type isolates. Surprisingly, there are metabolite profile overlaps of Thl 4 and Thl 21 with those of Polish type isolates (see Fig. 2.28). On the basis of these metabolite profile similarities, Thl-4 and Thl-21 were characterized as weakly virulent Polish type isolates. Thl 4 and Thl 21 produce mostly metabolites such as polanrazines, polyketides and sesquiterpenoids. Polanrazines are the major metabolites produced by Polish type isolates. As a result, polanrazines were considered as chemical markers for characterizing Polish type isolates (Pedras and Biesenthal, 2000). The group of weakly virulent Polish type isolates had two isolates from Canada, Laird 2 and Mayfair 2 (Pedras and Biesenthal, 2000). Laird 2 and Mayfair 2 are new blackleg isolates, which were identified recently on the prairie of western Canada. These isolates are more pathogenic to *Brassica juncea* (brown mustard), a species traditionally known to be resistant to virulent blackleg isolates (Taylor et al., 1995). Earlier in western Canada, only weakly virulent and highly virulent isolates of blackleg fungus were prevalent. Mayfair 2 and Laird 2 isolates are suspected to originate from European countries and to have got into western Canada through imported seed (Pedras and Biesenthal, 2000). In addition to Mayfair 2 and Laird 2 isolates, the appearance of Thl 4 and Thl 21 isolates, in Saskatoon and Eastend, respectively, suggests the spreading of the Polish type isolates in the region. This group of blackleg isolates is a big concern to agricultural sectors, particularly those growing the new Prairie canola, brown mustard (*Brassica juncea*) with canola quality seed and oil. The major metabolites produced by Thlaspi isolates and their proposed classification are summarized in the following table 2.12.

Table 2.12 Classification of Thlaspi isolates based on the secondary metabolite profiles

Isolates	Origin of the isolates	Polanrazines	Phomalair-denones	Phoma-pyrones	Proposed grouping
Thl-1	Saskatoon		X		W. virulent
Thl-2	Saskatoon		X		W. virulent
Thl-3	Saskatoon		X		W. virulent
Thl-4	Saskatoon	X	X	X	Polish type
Thl-5	Saskatoon		X		W. virulent
Thl-6	Saskatoon		X		W. virulent
Thl-7	Saskatoon		X	X	W. virulent
Thl-9	Melfort		X	X	W. virulent
Thl-13	Melfort		X		W. virulent
Thl-14	Eastend		X	X	W. virulent
Thl-15	Eastend		X		W. virulent
Thl-20	Eastend		X	X	W. virulent
Thl-21	Eastend	X	X		Polish type
Thl-23	Eastend		X	X	W. virulent
Thl-24	Eastend		X		W. virulent
Thl-28	Eastend		X	X	W. virulent

In addition, the chemistry of avirulent isolates from France (DAOM 229269 and DAOM 229270), which were recently classified as *Leptosphaeria biglobosa* (Shoemaker and Brun, 2001), were investigated to find out their relationship to the avirulent Canadian isolates. These avirulent isolates (DAOM 229269 and DAOM 229270) were purchased from the Canadian Collection of Fungal Cultures, Ottawa. These isolates were grown in minimal medium as well as in PDB medium. Cultures grown in PDB medium were found to produce brownish-yellow pigments, which are characteristic of cultures of avirulent isolates (McGee and Petrie, 1978). Moreover, both DAOM 229269 and DAOM 229270 produced phomapyrones as major metabolites in minimal medium, which is also consistent with previous reports on weakly virulent Canadian isolates (Pedras and Biesenthal, 2000). Therefore, both cultural characteristic and the secondary metabolite profiles clearly suggested that avirulent isolates DAOM 229269 and DAOM 229270 are in the same group as avirulent Canadian isolates.

In conclusion, the Thlaspi strain initially considered as a distinct group in *P. lingam* is in fact comprised of isolates from weakly virulent and Polish type isolates of *P. lingam/L. maculans*. Of the sixteen Thlaspi isolates analyzed, fourteen isolates were found to be weakly virulent isolates, whereas the other two isolates were found to be Polish type isolates. Furthermore, avirulent isolates DAOM 229269 and DAOM 229270 from France were shown to be similar to avirulent Canadian isolates.

2.4 Biosynthetic studies of phomapyrones

Phomapyrones are a group of secondary metabolites produced by isolates of *P. lingam/L. maculans* including weakly virulent Canadian isolates and Polish isolates. In previous reports, it was proposed the biosynthetic origin of phomapyrones is that of a polyketide. However, independent studies suggested that the biosynthetic origin of

related metabolites isolated from mollusks is polypropionate (Vardaro et al., 1992). On the contrary, Avent et al. (1992a) reported that the biosynthetic origin of nectriapyrone and vermopyrone isolated from *Gliocladium vermoesenii* is that of a polyketide derived from C_2 units. To clarify the origin of these metabolites produced by Polish type isolates and weakly virulent isolates, the biosynthetic origin was studied using the following isotopically enriched metabolites: [2-^{13}C] acetate, [1, 2-$^{13}C_2$] acetate, [2-^{13}C] malonate, [3-d_3] propionate and d_3-L-methionine.

Preliminary experiments were carried out to establish the optimum conditions for feeding experiments. Three sets of cultures were used to determine the conditions leading to maximal the production of phomapyrones (see table 2.13). In these three sets of cultures, the culture medium and inoculum were varied. The culture media used were water, glucose solution in water (1.5 g/100 mL) and minimal medium, experimental conditions I, II and III, respectively as shown in table 2.13. The cultures were prepared for experimental condition I and II by inoculating four-day-old mycelia, whereas pycnidiospores were used as inoculum in experimental condition III. Feeding the cultures with natural sodium acetate (100 mg/100 mL medium) did not improve the production of phomapyrones in these sets of experimental conditions; however, the fungal growth and the relative production of phomapyrones were found best under experimental condition III. Thus, conditions III shown in table 2.13 were employed for further feeding experiments. The liquid cultures of isolate Mayfair 2 grown in minimal medium and fed with labeled precursors such as [2-^{13}C] acetate, [1, 2-$^{13}C_2$] acetate, [2-^{13}C] malonate, [3-d_3] propionate and d_3-L-methionine, separately. After incubation, the cultures were filtered and the broth was extracted with EtOAc. The EtOAc extracts were fractionated by multiple chromatography to yield phomapyrone A, which was analyzed by both HRMS and NMR spectroscopy. The incorporation pattern of ^{13}C labeled precursors into enriched phomapyrone A was determined by a comparison of the integrated and normalized carbon signals of enriched phomapyrone A with that of naturally occurring

phomapyrone A (**49**). The ^{13}C NMR data from the carbon-13 labeling experiments are shown in table 2.14. On the other hand, the incorporation level of deuterium labeled precursors was determined from HREI-MS analysis of enriched phomapyrone A. Other phomapyrones including phomapyrone D (**100**), E (**101**), F (**102**) and G (**104**) were obtained in insufficient amount for analysis.

Table 2.13 Conditions for feeding labeled precursors to cultures of Mayfair 2

Experiment	Medium	Inoculum	Additives (0 h, 24 h, 48h, 72h)	Incubation period
I	Water	Four-day-old mycelia	NaOAc (100mg/100 mL)	120h
	Water	Four-day-old mycelia	None	120h
II	Water	Four-day-old mycelia	Glucose (200 mg/100 mL) NaOAc(100 mg/100 mL)	120h
	Water	Four-day-old mycelia	Glucose (200 mg/100 mL)	120h
III	Minimal medium	Pycnidiospores	NaOAc (100mg/100 mL)	120h
	Minimal medium	Pycnidiospores	None	120h

The proton decoupled ^{13}C NMR spectrum of phomapyrone A (**49**) from the feeding experiment with [2-^{13}C] acetate displayed fourteen signals, which were assigned by comparison with the ^{13}C NMR data of naturally occurring **49**. The intensity of carbon

signals of C-3, C-5, C-7, C-9 and C-11, were found enhanced by more than 50% relative to those of other carbons (see table 2.14), suggesting that C-3, C-5, C-7, C-9 and C-11 were enriched carbons. Therefore, the pattern of incorporation suggested that a pentaketide is the starter unit in the biosynthesis of phomapyrone A (**49**). In agreement with this, the results from a feeding experiment with [1,2-$^{13}C_2$]acetate showed incorporation of five intact C_2 units into phomapyrone A. The ^{13}C NMR spectrum displayed doublets for carbons C-2 to C-11, each flanked by the respective carbon signal of natural abundance. Furthermore, no incorporation was observed for the methyl groups C-12, C-13, C-14 and OMe. Additionally, the study of the biosynthetic origin of phomapyrone A (**49**) was conducted employing [2-^{13}C] malonate as a precursor. As expected, the C-13 labeling was incorporated into enriched phomapyrone A (**49**) at C-3, C-5, C-7, and C-9, but there was no incorporation at C-11. The lack of incorporation at C-11 is strongly suggestive that C-10-C-11 is the starter unit of the pentaketide backbone of phomapyrone A (**49**). Therefore, the results from the feeding experiment with [2-^{13}C] malonate complemented those of the feeding experiments with [2-^{13}C] acetate and [1,2-$^{13}C_2$] acetate in showing phomapyrone A (**49**) is a polyketide derived from five C_2 units.

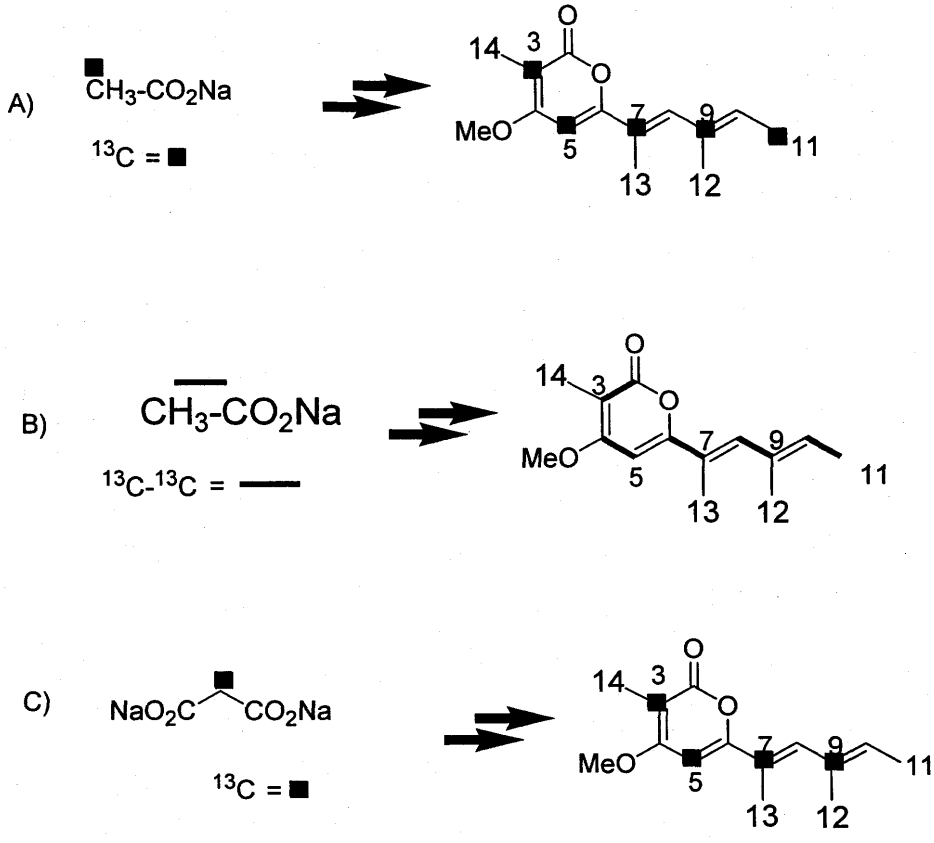

Figure 2.29: Biosynthesis of phomapyrone A (**49**): A) incorporation of sodium [2-^{13}C]acetate, B) incorporation of sodium [1,2-$^{13}C_2$]acetate, C) incorporation of sodium [2-^{13}C]malonate

As shown from the feeding experiments with [1, 2-^{13}C] acetate, [2-^{13}C] acetate and [2-^{13}C] malonate indicated, there were three methyl groups [(δ_C 16.5, C-12), (δ_C 14.0, C-13) and (δ_C 8.6, C-14)] and a methoxy group (δ_C 56.1, OMe) without incorporation (Table 2.14). To investigate the source of the methyl groups and the methoxy group in the biosynthesis of phomapyrone, the liquid culture was fed with d_3-L-methionine (99%) and the phomapyrone obtained from the culture was analyzed by HREI-MS. The results showed the incorporation of 19%, 3%, 1% and 0.9% for M^++3, M^++6, M^++9 and M^++12, respectively. These data indicated the incorporation of CD_3 groups into phomapyrone, suggesting further that the source of the C_1 units in the biosynthesis of phomapyrone A is S-adenosyl methionine. An additional study on the biosynthetic origin of phomapyrones was carried out employing 3,3,3-d_3-propionic acid precursor. Since some reports showed

that polypropionate is the biosynthetic origin of pyrones from marine mollusks, the need to clarify further the biosynthetic origin of pyrones from the blackleg fungus prompted this study. The liquid culture of isolate Mayfair 2 was fed with 3,3,3-d_3-propionic acid, and phomapyrone A (**49**) was isolated and analyzed by HREI-MS. The results showed the absence of any incorporation, suggesting polypropionate is not the biosynthetic origin of phomapyrone A (**49**) from the blackleg fungus.

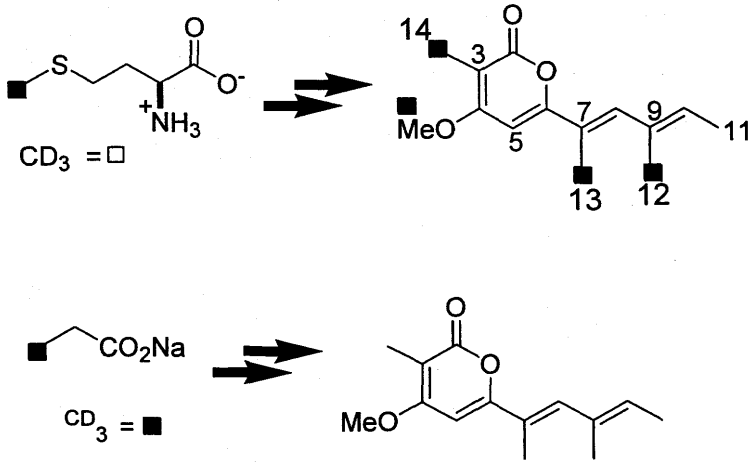

Figure 2.30: Biosynthesis of phomapyrone A (**49**): A) incorporation of [Me-$^2H_3$]methionine; B) incorporation of 3,3,3-d_3-propionic acid

The results of this study were consistent with the previous report by Avent et al. (1992a) on the biosynthetic origin of pyrones from *Gliocladium vermoesenii*. The biosynthetic origin of pyrones such as nectriapyrone (**106**) and vermopyrone (**107**) from *G. vermoesenii* was studied by feeding labeled sodium [1,2-^{13}C]acetate, [Me-^{13}C]methionine, [2-$^2H_3$]acetic acid and [Me-$^2H_3$] methionine to cultures of *G. vermoesenii*. The labeling pattern was indicative of a tetraketide biosynthesis with C-alkylations and O-alkylation originating from [Me-$^2H_3$]methionine (Avent et al., 1992a). However, when nectriapyrone (**106**) was first isolated from *Thyronectria missouriensis*, it was reported that **106** incorporated 2-^{14}C mevalonic acid and was therefore considered a monoterpene (Nair and Carey, 1975). Similar studies on the biosynthetic origin of

fusalanipyrone (**108**), a metabolite of *Fusarium salani*, were conducted by feeding d_3-methionine into cultures of *Fusarium salani*. Incorporation of CD_3 groups suggested that the branched methyl groups and the methoxy group originate from SAM in the biosynthesis of **108** (Abraham et al., 1990). On the other hand, the biosynthetic origin of 2-pyrone and 4-pyrone compounds from marine mollusks was reported to be polypropionate (Vardaro et al., 1992). The polypropionate biogenetic origin of 2-pyrone and 4-pyrone compounds was determined from feeding experiments conducted with [1-^{14}C]sodium propionate. In conclusion, the biosynthetic origin of pyrones from terrestrial organisms appears to be polyketide derived from acetate and malonate units, whereas they are from polypropionate in marine organisms.

Table 2.14 Incorporation data from sodium [2-^{13}C] acetate and sodium [2-^{13}C] malonate feeding experiments based on the ^{13}C NMR (125 MHz) of phomapyrone A (49).

Carbon	Phomapyrone A (Natural)		Phomapyrone A Enriched, [2-^{13}C] acetate			Phomapyrone A Enriched, [2-^{13}C] malonate		
	I_N	I_N*	I_E	I_E*	I_E*/I_N*	I_E	I_E*	I_E*/I_N*
C-2	2.09	0.22	1.89	0.31	1.40	0.47	0.18	0.82
C-3	2.54	0.26	3.25	0.54	2.08	1.49	0.56	2.15
C-4	3.10	0.32	2.34	0.39	1.22	0.77	0.29	0.91
C-5	8.94	0.92	8.14	1.34	1.46	5.46	2.05	2.23
C-6	3.88	0.40	2.52	0.42	1.05	1.01	0.38	0.95
C-7	3.58	0.37	3.29	0.54	1.46	2.25	0.85	2.29
C-8	8.28	0.86	5.76	0.95	1.10	2.47	0.93	1.08
C-9	4.53	0.47	4.39	0.72	1.53	3.66	1.38	2.94
C-10	6.92	0.71	4.96	0.82	1.15	1.78	0.67	0.94
C-11	7.21	0.74	9.26	1.53	2.06	3.06	1.15	1.55
C-12	7.12	0.74	5.47	0.90	1.22	2.34	0.88	1.19
C-13	10.14	1.04	6.40	1.05	1.00	2.65	1.00	0.96
C-14	8.63	0.89	5.85	0.96	1.08	2.30	0.86	0.97
OMe	9.68	1.00	6.07	1.00	1.00	2.66	1.00	1.00

I_N = Integrated signal intensity of natural sample; I_N* = Normalized signal intensity of enriched sample

I_E = Integrated signal intensity of enriched sample; I_E* = Normalized signal intensity of enriched sample

2.5 HPLC analysis of metabolites produced in infected plants

The pathogenic fungus-plant interactions are complex processes and dynamic in nature. From these interactions, the outcome could be either plant disease development or plant resistance to the pathogen depending upon the antagonism between fungal virulence and plant defense (Hadacek, 2002, Schulz et al., 2002). During the interactions, pathogenic fungi produce host-selective toxins to infect plants; plants, in contrast, release phytoalexins to stop the fungal invasion and colonization. One of the objectives of my work was to investigate the secondary metabolites produced *in vivo* both by the fungus Mayfair 2 and plants from the species *Brassica napus* (resistant), *Brassica juncea* (susceptible) and *Sinapis alba* (resistant).

In this study, stem tissues of *B. napus*, *B. juncea*, and *S. alba* were infected with the fungus Mayfair 2 and incubated as described in the experimental part. The infected stem tissues were extracted with methanol, and the methanol extracts were fractionated by FCC. The analysis of the fractions by HPLC equipped with a photodiode array detector led to the detection of both phytoalexins and phytotoxins (see table 2.15). The phytotoxins phomalairdenone A (**55**) and depsilairdin (**122**) were found in the methanol extracts of infected stem tissues of *S. alba* and *B. juncea*. In fact, the detection of these toxins was not consistent in subsequent analysis; for instance, sometime only one of these toxins was detected. The reason seems to be the production of such toxins only in small amounts in infected plant tissues eluding detection by HPLC. In similar analyses of methanol extracts of infected *B. napus*, these phytotoxins were not even detected. Interestingly, only host-selective toxins are found to be produced *in vivo* by Mayfair 2 among all other metabolites produced in liquid cultures. On the other hand, the

phytoalexins present in the infected plant tissues were variable and depended upon the plant tissues used. Hence, rutalexin (**137**), brassinin (**35**), and spirobrassinin (**138**) in *B. napus*, sinalexin (**140**) and brassilexin (**139**) in *S. alba*, and brassilexin (**139**) in *B. juncea* were detected (Pedras et al., 2000; Pedras et al., 2004b). These phytoalexins were not detected in the methanol extracts of control plant tissues, suggesting that their production is in fact due to fungal infection.

Table 2.15 Secondary metabolites detected in infected *B. napus*, *B. juncea* and *S. alba*

Plant	Weight of fresh stem tissue/ MeOH extracts	Fractions /phytotoxins detected	Fractions /Phytoalexin detected
Sinapis alba	80 g/227 mg	F9 /depsilairdin (**122**)	F3/5 /sinalexin (**140**) F5/7 /brassilexin (**139**)
	128 g/300 mg	F7 /phomalairdenone A (**55**)	F3/6 /sinalexin (**140**) F5/6 /brassilexin (**139**)
Brassica juncea	84 g/260 mg	F7 /phomalairdenone A (**55**) F7/8 /depsilairdin (**122**)	F5 /brassilexin (**139**)
	78 g/234 mg	F7 /phomalairdenone A (**55**)	F5/6 /brassilexin (**139**)
Brassica napus	50 g/200 mg	no phytotoxin detected	F6 /spirobrassinin (**138**) F3/4 /rutalexin (**137**) F4/6 /brassinin (**35**)
	105 g/400 mg	no phytotoxin detected	F6 /spirobrassinin (**138**) F3/4 /rutalexin (**137**) F4/6 /brassinin (**35**)

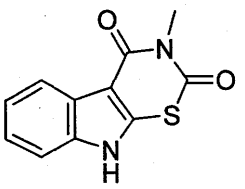

137

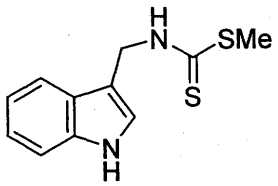

35

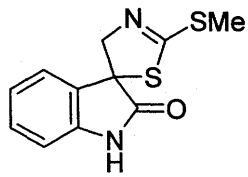

138

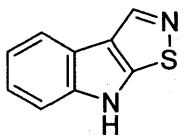

139

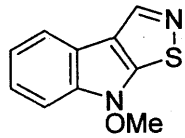

140

In conclusion, the investigation for secondary metabolites produced in infected plant tissues allowed the detection of both host-selective toxins and phytoalexins. Though the roles of host-selective toxins phomalairdenone A (**55**) and depsilairdin (**122**) in infection and disease development are not yet known, their production in infected tissues from all other metabolites determined from liquid cultures suggest the importance of them in the fungal-plant interactions. Similarly, the detection of phytoalexins in the infected plant tissues also suggests their involvement in the interactions between the fungus Mayfair 2 and *Brassica* species. Since phytoalexins are antifungal metabolites, they appear to have a defensive role for *Brassica* species. Moreover, phytoalexins were found to be produced by species which were both susceptible (*B. juncea*) and resistant (*S. alba* and *B. napus*). Finally, the detection of both host-selective toxins and phytoalexins in infected plant tissues suggests that these metabolites take part in complex fungal-plant interactions as mediators.

2.6 Phytoalexins from the wild species *Thlaspi arvense*

Phytoalexins are secondary metabolites synthesized *de novo* by plants in response to diverse forms of stress arising from biotic and/or abiotic factors (Bailey and Mansfield, 1982). Phytoalexins play important roles in plant defenses against pathogenic fungi. One of the objectives of this work is to determine chemical traits contributing to the resistance of some crucifers to blackleg disease. Therefore, it was of great interest to investigate phytoalexin production by *Thlaspi arvense* (stinkweed), a wild crucifer resistant to the virulent strain of blackleg fungus (*Leptosphaeria maculans*/*Phoma lingam*). This section describes and discusses the results of elicitation, isolation and chemical structure determination of phytoalexins as well as a constitutive metabolite from *T. arvense*.

2.6.1 Elicitation, isolation and chemical structure determination of metabolites from Thlaspi arvense (stinkweed)

Preliminary experiments were carried out to establish the time-course response of *T. arvense* (stinkweed) upon abiotic elicitation with $CuCl_2$. Thus, three-week-old *T. arvense* plants were sprayed with $CuCl_2$ every 24h for four consecutive days, and both treated and control plants were incubated under the conditions described in the experimental section. Leaves of both treated and control were excised at 24, 48, 72 and 96h, crushed in liquid nitrogen, extracted with EtOAc, and analyzed by high performance liquid chromatography (HPLC). The chromatogram of extracts of elicited leaves showed two new peaks at 22.6 and 29.5 min, which were not observed in the chromatogram of control extracts (Figure. 2.31). These results indicated that production of elicited metabolites was highest at 72-96h as shown in Table 2.16. Additionally, inoculation of *T. arvense* (stinkweed) with the spores of fungal isolates Mayfair 2 (weakly virulent on canola) or Thlaspi 9 (virulent on stinkweed) elicited the same metabolites at 22.6 and 29.5 min as

with $CuCl_2$. For isolation of elicited metabolites, the experiment was scaled up, three-week-old plants were treated with $CuCl_2$ solution, the leaves (182 g) were collected after 72h of incubation and extracted with EtOAc. The extract (0.74 g) was dried, concentrated and separated by FCC (CH_2Cl_2-MeOH) as described in the experimental section. Fractions F2- F4 were combined and further subjected to multiple chromatography to yield the elicited compound **142** with HPLC retention time of 22.8 min (1 mg). Fractions F9-F12 were combined and further subjected to multiple RP-FCC to afford another elicited compound **38** with a HPLC retention time of 29.5 min (3 mg) and a constitutive metabolite **143** with HPLC retention time of 4.9 min.

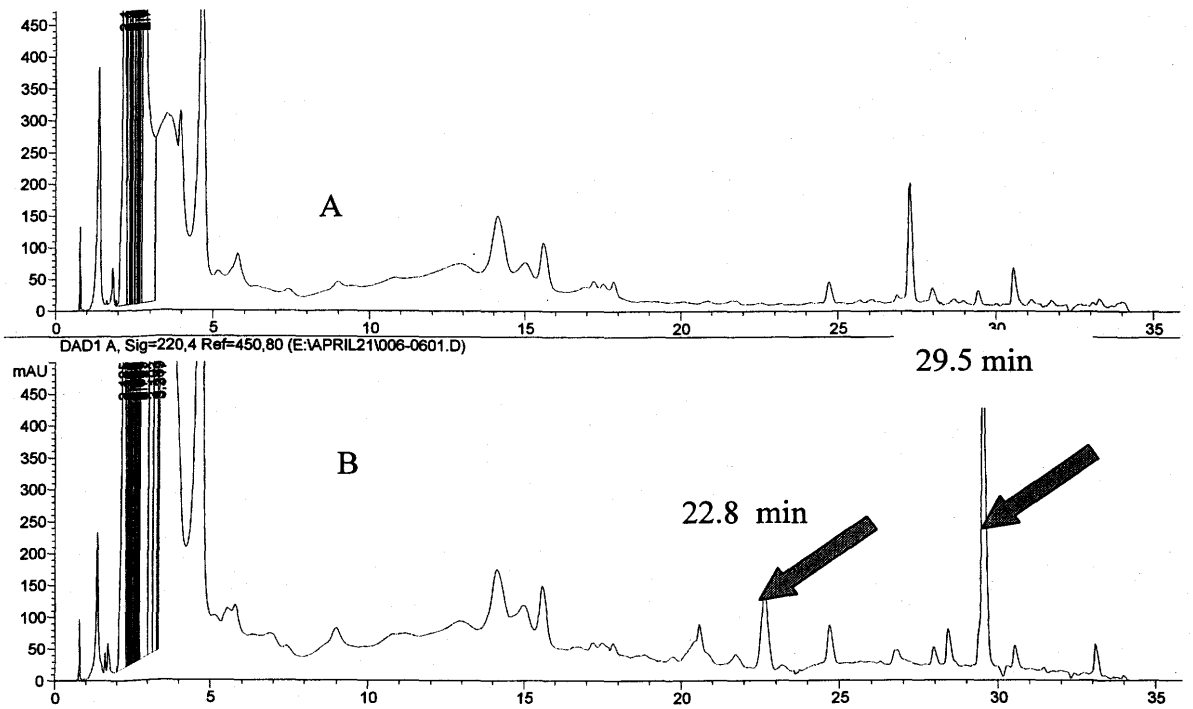

Figure 2.31: HPLC profile of extracts of elicited leaves of *Thlaspi arvense*, A: control extract; B: extract from elicited leaves (elicitation performed with $CuCl_2$, arrows indicate peaks of elicited compounds)

Table 2.16 Elicitation of phytoalexins in leaf tissue of *Thlaspi arvense* using $CuCl_2$ as elicitor

Phytoalexin	HPLC retention time	Concentration (μmol/100g of fresh leaves)			
		24h	48h	72h	96h
Arvelexin (**142**)	22.8 min	0.65 ± 0.05	1.5± 0.3	1.8 ± 0.2	2.6 ± 0.2
Wasalexin A (**38**)	29.5 min	3.7 ± 0.5	7.1 ± 0.3	10.3± 0.8	9.1 ± 0.6

The compound with HPLC retention time of 29.5 min was identified as wasalexin A (**38**) by comparison of its NMR, HRMS, FTIR, UV, and HPLC data with those of an authentic sample available in our laboratory. Wasalexin A (**38**) was a phytoalexin isolated previously from wasabi (*Wasabia japonica*), a crucifer resistant to virulent isolates of the blackleg fungus, after elicitation with $CuCl_2$ and of *P. lingam*/*L. maculans* (Pedras et al., 1999b).

The molecular formula of the elicited compound **142** was determined as $C_{11}H_{10}ON_2$ (HREI-MS), indicating eight degrees of unsaturation. The ^1H NMR spectrum of this metabolite displayed signals for four aromatic protons, two methylene protons and three methoxy protons. The proton decoupled ^{13}C NMR spectrum displayed signals for eleven carbons, of which four were for sp^2 hybridized methine carbons, one for an sp^3 hybridized methylene carbon, one for a methoxy carbon and five for sp^2 hybridized quaternary carbons. The spin systems of the aromatic protons showed that the proton at δ_H 7.14 (H-6, dd, J = 7.5, 7.5 Hz) was coupled to the protons at δ_H 7.04 (H-7, d, J = 7.5 Hz) and 6.57 (H-5, d, J = 7.5 Hz), suggesting H-6 to be *ortho* relative to both H-7 and H-5. Moreover, the ^1H NMR spectrum showed a broad singlet proton at δ_H 7.14 (H-2) and an exchangeable proton at δ_H 8.26 (N-H). The ^1H NMR spectral data as well as the UV spectrum indicated the presence of an indolyl moiety. The most down field carbon at δ_C 154.6 correlating with methoxy protons at δ_H 3.93 was assigned to C-4. In the HMBC

spectrum, a carbon at δ_C 120.2 (C-9) showing only a long-range correlation with methylene protons at δ_H 4.07 (H_2-8) was assigned to the carbon of a nitrile group. Further, the presence of this nitrile was confirmed by a weak IR band shown at 2251 cm^{-1}. The long-range correlations of methylene protons at δ_H 4.07 (H_2-8) with carbons at δ_C 112.6 (C-2), 105.0 (C-3) and 117.7 (C-3a), together with long-range correlations of a proton at δ_H 7.14 (H-2) with carbons at δ_C 105.0 (C-3) and 117.7 (C-3a) suggested an acetonitrile moiety connected to C-3. Therefore, structure **142** was assigned to this elicited metabolite with a HPLC retention time of 22.8 min. This structure of metabolite **142** was confirmed by synthesis. 4-Methoxyindole (**141**) was allowed to react with bromoacetonitrile under Grignard conditions to yield 4-methoxyindolyl-3-acetonitrile (**142**), in 52% overall yield (scheme 2.8), as described in the experimental section.

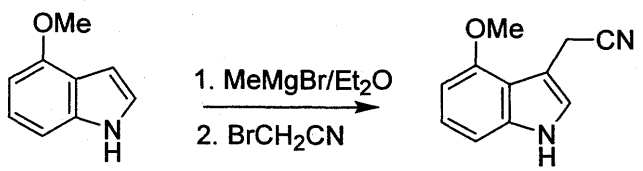

141 **142**

Scheme 2.8 Synthesis of arvelexin (**142**)

Together with elicited metabolites, a constitutive bright yellow compound (**143**) with R_t = 4.9 min., and $[\alpha]^{22°}$= 17.2 (*c* 0.37, ethanol) was isolated. The HRMS-FAB spectrum of the compound gave a molecular ion at m/z 433.1134 (M^++1) which together with NMR data indicated a molecular formula of $C_{21}H_{21}O_{10}$. The ^{1}H NMR spectrum displayed seven protons at sp^3 carbons and six protons at sp^2 carbons. Moreover, the ^{1}H NMR spectrum showed a spin system containing protons at δ_H 6.90 (2H, d, J = 8 Hz, H-3' and H-5') coupling with protons at δ_H 7.80 (2H, d, J = 8 Hz, H-2' and H-6'), in which the coupling constant suggested an *ortho* relationship of H-2' to H-3' and H-5' to H-6'. In

addition, the HMBC data analysis of this spin system suggested the presence of a *para* - hydroxyphenyl moiety. Further analysis of the HMBC data revealed the existence of a flavonoid moiety. The ^{1}H NMR spectrum displayed another spin system connecting five methine protons at δ_H 4.59 (H-1", d, J = 9 Hz), 4.88 (H-2", dd, J = 9, 9 Hz), 3.21 (H-3", dd, J = 9, 9 Hz), 3.68 (H-4", d, J = 11 Hz), 3.41 (H-5", dd, J = 5, 11 Hz) and methylene protons at δ_H 3.16 (H_2-6", m), in which case all are attached to oxygenated sp^3 hybridized carbons. These, together with coupling constants also suggested the presence of a glucose moiety. The anomeric proton at δ_H 4.61 (H-1", d, J = 9 Hz) and the remaining $^{3}J_{H\text{-}H}$ suggested that the glycoside moiety was β-glucopyranoside. The anomeric proton at δ_H 4.61 (H-1") showed long-range correlations with carbons at δ_C 161.0 (C-5), 163.9 (C-7) and 108.2 (C-6), suggestive of its attachment to an aromatic nucleus. Furthermore, the unusual chemical shift of the anomeric carbon at δ_C 74.3 (C-1") as well as the resistance of the glycoside to acid hydrolysis was suggestive of a C-C linked β- glucopyranoside moiety. Hence, the structure **143** was unambiguously assigned to the metabolite with HPLC retention time of 4.9 min. The literature survey led to the identification of compound (**143**) as isovitexin (apigenin 6-C-β-glucopyranoside). Comparison of the ^{1}H and ^{13}C NMR (MeOD), UV, and $[\alpha]_D$ (17.2, *c* 0.37, EtOH, lit. 16.21, Briggs and Cambie, 1958) spectroscopic data of **143** with those reported for isovitexin showed good agreement. Isovitexin (**143**) was first isolated from *Vitex lucens* (Briggs and Cambie, 1958; Horowitz and Gentili, 1964), and later on isovitexin was reported to exhibit potent anti-oxidant activity (Ramarathnam et al., 1989).

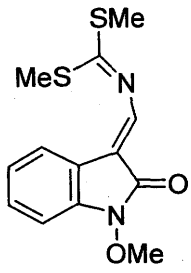

38

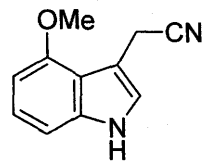

142

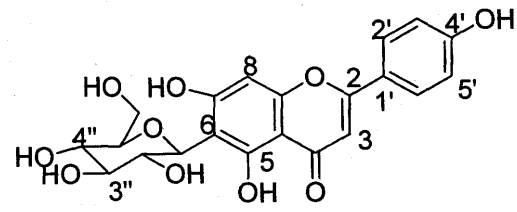

143

Table 2.17 ^{1}H NMR and ^{13}C NMR of 4-methoxyindole-3-acetonitrile (142)

Carbon #	Carbon (δ_C)	δ_H, m, J	Carbon #	Carbon (δ_C)	δ_H, m, J
2	112.6	7.14, bs	7	105.3	H-7 (7.04, d, 7.5 Hz)
3	105.0	-	7a	138.5	-
4a	117.7	-	8	15.6	H-8 (4.07, s)
4	154.6	-	9	120.2	-
5	100.0	6.57, d, 7.5	10	55.3	H-10 (3.93, s)
6	123.7	7.11, dd, 7.5			

Table 2.18 ^{1}H NMR and ^{13}C NMR data in DMSO-d_6 of isovitexin (143)

C #	δ_C	δ_H, m	C#	δ_C	δ_H, m
2	161.1	-	2', 6'	128.4	7.90, d, J = 8 Hz, 2H
3	102.9	6.74, s, 1H	4'	161.8	-
4	183.0	-	3', 5'	116.0	6.91, d, J = 8 Hz, 2H
5	161.0	-	1"	74.3	4.59, d, J = 9 Hz, 1H
6	108.2	-	2"	71.6	4.08, dd, J = 9 Hz, 9 Hz, 1H
7	163.9	-	3"	79.1	3.21, dd, J = 9 Hz, 9 Hz, 1H
8	94.2	6.46, s, 1H	4"	70.8	3.68, s, J = 11Hz, 1H
9	157.7		5"	81.6	3.41, dd, J = 5 Hz, 11 Hz, 1H
10	104.2		6"	61.9	3.16, m, 1H
1'	122.1				

2.6.2 Antifungal bioassays of elicited metabolites

Antifungal bioassays of the metabolites isolated from *Thlaspi arvense* were conducted against three isolates of *L. maculans/P. lingam* BJ 125 (virulent on canola), Mayfair 2 (virulent on brown mustard) and Thlaspi 9 (virulent on stinkweed). The results of antifungal bioassays showed that 4-methoxyindole-3-acetonitrile had antifungal activity at a concentration of 5×10^{-4} M against *L. maculans/P. lingam* (table 2.19). Because 4-methoxyindole-3-acetonitrile (**142**) is an elicited metabolite produced under biotic and abiotic stress and is antifungal, it satisfies the criteria to be a phytoalexin, thus it was named Arvelexin (Pedras et al., 2003a). Arvelexin (**142**) was first isolated from the roots of Chinese cabbage (*B. pekinensis*) infected with *Plasmodiophora brassica* (Nomoto and Tamura, 1970), but was never reported as a phytoalexin. Another phytoalexin from *Thlaspi arvense* (stinkweed) isolated was wasalexin A, which was reported previously from wasabi (*Wasabi japonica*, syn. *Eutrema wasabi*) (Pedras et al., 1999b). Wasalexin A (**38**) showed little inhibition of mycelial growth but inhibits completely the spore germination for 30h (see table 2.20). Interestingly, wasabi and stinkweed are cruciferous plants resistant to the blackleg fungus (Petrie et al., 1995; Pedras and Sorensen, 1998). Besides these two phytoalexins, isovitexin was isolated from stinkweed but it was produced both in control and treated plants. The antifungal bioassay results of isovitexin indicated that it is not antifungal.

Table 2.19 Antifungal activity of metabolites isolated from *Thlaspi arvense* (stinkweed)

Compound	Concentration (M)	% inhibition (mycelium diameter)[a]		
		BJ 125	Mayfair 2	Thlaspi 9
Arvelexin (**142**)	1×10^{-4}	no inhibition	no inhibition	no inhibition
	3×10^{-4}	11 (18 ± 1)	33 (15 ± 1)	no inhibition
	5×10^{-4}	73 (8 ± 1)	53 (12 ± 1)	59 (11 ± 1)
Wasalexin A (**38**)	1×10^{-4}	no inhibition	no inhibition	no inhibition
	3×10^{-4}	17 (15 ± 1)	20 (11 ± 1)	no inhibition
	5×10^{-4}	42 (12 ± 1)	28 (10 ± 1)	30 (11 ± 1)
Indole-3-acetonitrile	1×10^{-4}	no inhibition	no inhibition	no inhibition
	3×10^{-4}	77 (8 ± 1)	13 (18 ± 1)	11 (18 ± 1)
	5×10^{-4}	complete inhibition	25 (16 ± 1)	57 (11 ± 1)
Isovitexin (**143**)	5×10^{-4}	no inhibition	no inhibition	no inhibition

[a] The percentage of inhibition was calculated using the formula: % inhibition = 100-[(growth on treated/growth in control) × 100]; results are the mean of at least three independent experiments (mm ± standard deviation).

Table 2.20 Spore germination bioassay results on *Leptosphaeria maculans/Phoma lingam* (BJ 125 and Thl 9) with wasalexin A (38) after 30 hr incubation

L. maculans/P. lingam	Concentration of wasalexin A (M)	% inhibition of spore germination
BJ 125	1×10^{-4}	complete inhibition
	5×10^{-4}	complete inhibition
Thl 9	1×10^{-4}	84 ± 1
	5×10^{-4}	95 ± 1

CHAPTER THREE

3. Conclusions and Future Work

The chemical investigation of cultures of Mayfair 2 isolate led to the isolation of several secondary metabolites and phytotoxins of diverse biosynthetic origins including phomapyrones, phomalairdenones and phomalairdenols, polanrazines and depsilairdin. These were also produced by isolate Laird 2. The secondary metabolite profile of Mayfair 2 isolate established from this chemical investigation was found to be different from those of avirulent (*P. wasabiae/L. biglobosa*) and virulent isolates of *P. lingam/L. maculans*. Mayfair 2 and Laird 2 are closer genetically to avirulent isolates, however, unlike avirulent isolates, they are pathogenic to *B. juncea* (Taylor et al., 1995), a traditionally blackleg resistant species (Keri et al., 1997). These new blackleg isolates, Mayfair 2 and Laird 2, were not found to produce detectable amounts of sirodesmins or phomalide, which are chemical markers for virulent isolates of *P. lingam*. However, the secondary metabolite profiles of Mayfair 2 and Laird 2 isolates were found to be quite similar to those of weakly virulent Polish isolates. As a result, isolates Mayfair 2 and Laird 2 were classified into a group of weakly virulent Polish type isolates of *P. lingam*. Mayfair 2 and Laird 2 as well as Polish isolates produce polanrazines, which serve as chemical markers for the group. Additionally, the differences in pathogenicity, genetic and cultural characteristics of Mayfair2/Laird 2 from virulent and avirulent isolates support this proposed classification of Mayfair 2 and Laird 2 isolates (Taylor et al., 1995; Keri et al., 1997).

The phytotoxic activity assays against *B. napus*, *B. juncea* and *S. alba* showed depsilairdin (**122**) to be a strong and very selective phytotoxin to *B. juncea*. Depsilairdin (**122**) showed selectivity even at a concentration of 3×10^{-3} M. The lesions formed by **122** were quite similar to those caused by blackleg disease. Interestingly, the selectivity

range of depsilairdin was found to mimic the pathogenicity range of the Mayfair 2 and Laird 2 isolates. Therefore, depsilairdin (**122**) is a host-selective phytotoxin, and appears to have a role in fungal-plant interactions. In addition, only few phomalairdenones and phomalairdenols exhibited moderate phytotoxicity at higher concentrations (*e.g.* 1×10^{-3} M). However, the phomapyrones and most of the phomalairdenones and phomalairdenols were non-phytotoxic metabolites.

The study of the biosynthetic origin of phomapyrones using [2, ^{13}C] acetate, [1, 2-$^{13}C_2$] acetate, [2-^{13}C] malonate, [3-d_3] propionate, and d_3-L-methionine revealed that the phomapyrones are polyketides. The incorporation pattern of carbon-13 in the feeding experiments with [2, ^{13}C]acetate, [1, 2-^{13}C]acetate, and [2-^{13}C]malonate showed that the polyketide is derived from $5C_2$ units. Additionally, the methyl groups at C-3, C-7 and C-9 and methoxy group at C-4 of phomapyrone A (**49**) come from S-adenosylmethionine (SAM) as shown from the results of a feeding experiments with d_3-L-methionine. Contrary to what was reported for pyrones from marine mollusks by Vardaro et al. (1992), we never observed any incorporation of a propionate units into pyrones. Therefore, the biosynthetic origin of phomapyrones is not propionate.

The investigation of elicited metabolites produced by *Thlaspi arvense* led to the isolation of two phytoalexins, **38** and **142**. Antifungal bioassays conducted against Thl 9 (avirulent isolate of *P. lingam*), Mayfair 2 (Polish type isolate), and BJ 125 (virulent isolate of *P. lingam*) showed that these compounds are antifungal, which make them qualify as phytoalexins. Compound **142** was shown for the first time to be a phytoalexin, and therefore was named arvelexin (Pedras et al., 2003a). Compound **38** was identified as wasalexin A. Wasalexin A (**38**) is a phytoalexin first isolated from wasabi (*Wasabia japonica*, syn. *Eutrema wasabi*), which is a crucifer resistant to virulent isolates of *P. lingam* (Pedras et al., 1999b). The production of wasalexin A (**38**) by both *Thlaspi arvense* and *Wasabia japonica* needs further investigation if in fact it has a correlation to their resistance to virulent isolates of *P. lingam*.

Finally, the analysis of chemical substances produced during the infection of plant tissues from *Brassica species* with Mayfair 2 isolate indicated the production of both phytoalexins and phytotoxins. The phytoalexins detected were rutalexin (**137**), brassinin (**35**), and spirobrassinin (**138**) from infected tissues of *B. napus*, brassilexin (**139**) and sinalexin (**140**) from infected tissues of *S. alba*, and brassilexin (**139**) from infected tissues of *B. juncea* (Pedras et al., 2000; Pedras et al., 2004b). In the infected tissues, the phytotoxins detected were depsilairdin (**122**) and phomalairdenone A (**55**), which are both host-selective toxins. Further the detection of depsilairdin (**122**) and phomalairdenone A (**55**) revealed their production *in planta* as well. These host-selective toxins mimic the pathogenicity range of Mayfair 2/Laird 2 isolates as shown by phytotoxicity assays in section 2.2. The pathogen most likely produces these host-selective toxins at an early stage of infection to facilitate invasion and colonization of plant tissues. In response to fungal attack, plants produce phytoalexins, which appear to have defensive roles for plants in these plant-fungal interactions. From these results, it appears that host-selective toxins and phytoalexins have a role in mediating these interactions.

Future Work

1. Study of the fate of depsilairdin (**122**) in resistant *Brassica* species using radioactive isotope labeled depsilairdin.
2. Establishment of secondary metabolite profiles of fungal isolates originating from cruciferous weeds such as *Sisymbrium* spp., *Descurania* spp., *Lepidium* spp. and *Erysimum* spp. to assist the reclassification of *Phoma lingam/Leptosphaeria maculans*.
3. Determine absolute stereochemistry of sesquiterpenes from Mayfair 2 isolate.

CHAPTER FOUR

4. Experimental

4.1 General methods

All chemicals were purchased from Sigma-Aldrich Canada Ltd., Oakville, Ont. except isotope-labeled compounds which were purchased from Cambridge Isotope Laboratories, St. Lenard, Quebec. All solvents were used as such except chloroform and dichloromethane, which were redistilled. Solvents used in syntheses were dried over the following drying agents prior to use: hexane over activity grade I alumina, Et_2O and THF over Na/benzophenone, and CH_2Cl_2 over CaH_2.

Analytical thin layer chromatography (TLC) was carried out on precoated silica gel TLC plates (Merck, 60 F_{254} 2.5 × 5.0 cm, 0.25 mm layer thickness). After elution with a suitable solvent system, compounds were visualized under UV light (254/366 nm) and by dipping the plates in a 5% (w/v) aqueous phosphomolybdic acid solution containing 1% (w/v) ceric sulfate and 4% (v/v) H_2SO_4, followed by heating on a hot plate.

Preparative thin layer chromatography (PTLC) was performed on silica gel plates (Merck, 60 F_{254} 20 × 20 cm, 0.25 or 0.5 mm thickness). Compounds were visualized under UV light (254/366 nm) and/or by dipping the plates along the edge in a 5% (w/v) aqueous phosphomolybdic acid solution containing 1% (w/v) ceric sulfate and 4% (v/v) H_2SO_4, followed by charring of the plate on a hot plate. All solvent mixtures used were volume/volume (v/v) mixtures.

Flash column chromatography (FCC) was performed on silica gel, Merck grade 60, mesh size 230-400, 60 A° or on J. T. Baker reversed phase C-18 silica gel, 40 μm.

High performance liquid chromatography (HPLC) analysis was carried out with a high performance Hewlett Packard liquid chromatograph equipped with a quaternary pump, an automatic injector, and a photodiode array detector (wavelength range 190-600 nm), degasser, and a Hypersil ODS column (5 μm particle size silica, 200 mm × 4.6 mm internal diameter), equipped with an in-line filter. An isocratic elution [80% H_2O-20% CH_3CN for 10 min, followed by gradient elution, 80% H_2O-20% CH_3CN to 60% H_2O-40% CH_3CN for 10 min, 60% H_2O-40% CH_3CN to 25% H_2O-75% CH_3CN for 10 min, and finally 25% H_2O-75% CH_3CN to 100% CH_3CN for 10 min, and flow rate 1.0 mL/min, Laird 2 method] was used. HPLC semi-preparative separations were carried out with a column of 5 μM particle size silica, 200 mm × 10 mm internal diameter. Samples were dissolved in CH_3CN and filtered through a tight cotton wool plug.

Infrared spectra were recorded on a Bio-Rad FTS-40 spectrometer. Spectra were measured by the diffuse reflectance method on samples dispersed in KBr.

Ultraviolet (UV) spectra of metabolites isolated were recorded on a Varian Cary 100 spectrophotometer using a 1 cm cell.

NMR spectra were recorded on Bruker Avance 500 spectrometers. For ^1H NMR (300 or 500 MHz), chemical shift (δ) values are reported in parts per million (ppm) relative to the internal standard TMS. The δ values were referenced to $CDCl_3$ ($CHCl_3$ at 7.26 ppm), CD_3CN (CHD_2CN at 1.94 ppm), MeOH (CD_2HOD at 3.31 ppm), or C_6D_6 (C_6D_5H at 7.16 ppm). First-order behavior was assumed in the analysis of ^1H NMR spectra and multiplicities are as indicated by one or more of the following: s = singlet, d = doublet, t = triplet, q = quartet, m = multiplet, br = broad. Spin coupling constant (J) values are reported to the nearest 0.5 Hz. For ^{13}C (125.8 MHz), chemical shift (δ) values were referenced to $CDCl_3$ (77.23 ppm), D_6D_6 (128.4 ppm) or CD_3CN (118.7 ppm).

Mass spectra (MS) [high resolution (HR), electron impact (EI), chemical ionization (CI) with ammonia as ionizing gas or fast atom bombardment (FAB)] were obtained on a VG 70 SE mass spectrometer, employing a solids probe.

X-ray crystallographic analysis was carried out on an Enraf Nonius kappa a CCD area detector.

Specific rotations, $[\alpha]_D$ were determined at ambient temperature on a Rudolph DigiPol DP 781 polarimeter using a 1 mL, 10 cm path length cell; the units are 10^{-1} deg cm^2 g^{-1} and the concentrations (*c*) are reported in g/100 mL.

Plant material. Seeds of Brassica napus (cultivar Westar), Brassica juncea (cultivar Cutlass), Sinapis alba (cultivar Ochre) and Thlaspi arvense were obtained from Agriculture and Agri-Food Canada Research Station, Saskatoon, SK. The seeds were sown in a commercial potting soil mixture, and plants were grown in a growth chamber, with 16 hours light/8 hours dark cycle, at 24 ± 2°C.

Fungal isolates. Mayfair 2, Laird 2 and Thlaspi isolates were provided by Agriculture and Agri-Food Canada Research Station, Saskatoon, SK. Isolates DAOM 229269 and DAOM 229270 were obtained from Canadian Collection of Fungal Cultures, ECORC, Ottawa, Ont. The solid cultures were grown on V8 agar under continuous light, at 23 ± 2°C for 14 days. The liquid cultures were made by inoculating minimal medium (MM) or potatodextrose broth (PDB) medium with fungal spores at a concentration of 5 × 10^8 spores/100 mL culture medium and grown under continuous light, at 23 ± 2°C for six days.

4.2 The Blackleg fungi

4.2.1 Fungal cultures (MM) and extractions

Solid cultures of Mayfair 2 were grown on V8 agar medium under constant cool fluorescent light at 23 ± 2 °C. Mayfair 2 spores were collected after 15 days of incubation. The spores collected were stored in sterile water at -20 °C. The liquid fungal cultures were grown in 250 mL Erlenmeyer flasks containing 100 mL of culture medium.

Minimal medium (MM) was employed to grow the fungal cultures. Spores were inoculated at a concentration of 5×10^8 spores per 100 mL of culture medium. Incubations were carried out on a shaker at 120 rpm for six days under constant cool fluorescent light at 23 ± 2 °C. A total of 122 L of cultures were grown in minimal medium. The cultures (MM) were filtered, and the broth was combined (110 L). The broth (110 L) was concentrated to 22 L, and extracted with EtOAc (800 mL × 3 / 1L broth). The combined EtOAc extracts were dried over anhydrous sodium sulfate and concentrated to dryness under reduced pressure (2.3 g).

4.2.2 Isolation of metabolites

The EtOAc extracts (350 mg per batch, total amount 2.3 g) were subjected to flash column chromatography (silica gel, 2 cm × 15 cm, 50 mL fractions) and eluted first with CH_2Cl_2 (200 mL) followed by CH_2Cl_2-MeOH (97:3, 200 mL) and then with CH_2Cl_2-MeOH (90:10, 200 mL). All fractions collected were concentrated to dryness under reduced pressure. Fractions F3 to F6 were combined, further subjected to prep. TLC and developed with CH_2Cl_2-MeOH (98:2, for three times). This fractionation gave phomalairdenol C (**118**, 12 mg) and phomapyrone F (**102**, 4 mg), together with non-homogenous material. This material was further separated by prep. TLC using hexane-EtOAc (90:10, developed four times) to yield two compounds, 3-oxosilphinene (**115**, 3 mg) and selin-11-en-4α-ol (**121**, 3 mg).

Fraction F7 from FCC of EtOAc extracts was further chromatographed on FCC (2 cm × 15 cm, silica gel, 50 mL fractions), eluted first with CH_2Cl_2-EtOAc (95:5, 200 mL), followed by CH_2Cl_2-EtOAc (90:10, 200 mL), and then with CH_2Cl_2-EtOAc (80:20, 200 mL). Twelve fractions were collected and concentrated to dryness under reduced pressure. Fractions F2 and F3 were combined, subjected to prep. TLC (hexane-EtOAc, 90:10, multiple development) to yield phomapyrone A (**49**, 36 mg) and phomenin B (**105**, 10 mg). Fractions F6 to F9 from FCC of F7 were combined, further subjected to PTLC

and developed with CH_2Cl_2-MeOH (98:2) to obtain phomalairdenone A (**55**, 12 mg) and phomapyrone D (**100**, 10 mg) and a PTLC fraction of non-homogenous material. A non-homogenous PTLC fraction was further subjected to PTLC and developed with hexane-EtOAc (60:40) to yield polanrazine B (**52**, 4.6 mg) and phomalairdenone D (**114**, 8 mg), and a non-homogenous fraction. Further purification of this PTLC fraction by PTLC developed with hexane-Et_2O (50:50) several times yielded phomapyrone G (**104**, 7 mg) and phomapyrone E (**101**, 4 mg).

Fractions F8 to F9 from FCC of EtOAc extracts were combined, chromatographed on RP-FCC (1 cm × 10 cm, RP-C18, 20 mL) and eluted with CH_3CN-H_2O (40: 60, 140 mL). Fractions F5 and F6 from this RP-FCC were combined and further subjected to RP-FCC (0.5 cm × 5 cm, RP-C18, 10 mL fractions) and eluted with CH_3CN-H_2O (30:70, 80 mL) to yield depsilairdin (**122**, 22 mg).

Fractions F10 to F12 from FCC on EtOAc extracts were combined and subjected to prep. TLC (CH_2Cl_2-MeOH, 97:3, developed three times) to give polanrazine C (**9**, 21 mg) and infectopyrone (**103**, 4 mg), together with UV-inactive non-homogenous material. This material was further chromatographed on prep. TLC and developed with CH_2Cl_2-Et_2O (50:50, for four times) to yield two compounds, phomalairdenol B (**116**, 24 mg) and lairdinol A (**120**, 18 mg) together with non-homogeneous material. This material was further chromatographed on PTLC and developed with hexane-EtOAc (70:30) several times to yield phomalairdenol D (**119**, 9 mg) and phomalairdenol A (**117**, 8 mg).

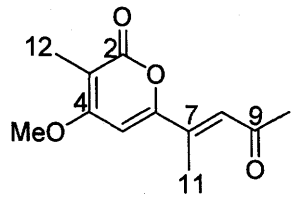

Phomapyrone D (**100**)

^{1}H NMR data in Table 2.1 and ^{13}C NMR data in Table 2.2

HPLC R_t = 18.9 min.

UV λ_{max} 210, 250, 350 nm (photodiode array detector)

FTIR (cm^{-1}) 2996, 1681, 1357, 1013, 746

HREI-MS: *m/z* 222.0893, cal. for $C_{12}H_{14}O_4$ 222.0892, EI-Ms: *m/z* (relative intensity) 222 (100%), 207 (18%), 194 (17%), 179 (19%), 159 (49%), 139 (24%), 57 (56%).

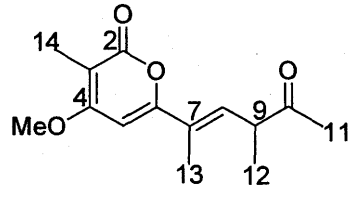

Phomapyrone E (**101**)

^{1}H NMR data in Table 2.1 and ^{13}C NMR data in Table 2.2

HPLC R_t = 22.2 min

UV λ_{max} 230, 335 nm (photodiode array detector)

FTIR (cm^{-1}) 2970, 2927, 1692, 1355, 1170, 1013, 751

HREI-MS: *m/z* 250.1206, cal. for $C_{14}H_{18}O_4$ 250.1205, EI-MS: *m/z* (relative intensity) 250 (13%), 208 (100%), 165 (11%).

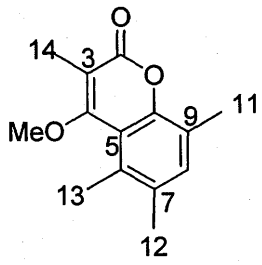

Phomapyrone F (**102**)

^{1}H NMR data in Table 2.1 and ^{13}C NMR data in Table 2.2

HPLC R_t = 30.4 min

UV λ_{max} 210, 290 nm (photodiode array detector)

FTIR (cm^{-1}) 2925, 2855, 1711, 1590, 1202, 1093, 1003

HREI-MS: *m/z* 232.1095, cal. for $C_{14}H_{18}O_4$ 232.1092, EI-MS: *m/z* (relative intensity) 232 (100%), 217 (56%), 189 (63%).

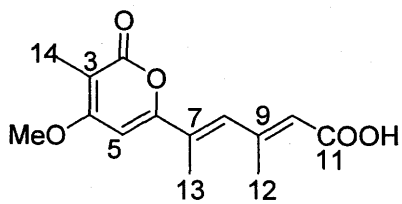

Infectopyrone (**103**)

^{1}H NMR data in Table 2.1 and ^{13}C NMR data in Table 2.2

HPLC R_t = 1.3 min

UVλ_{max} 220, 270, 350 nm (photodiode array detector)

FTIR (cm^{-1}) 3150, 2954, 2925, 1687, 1382, 1251, 1163

HREI-MS: *m/z* 264.1001, cal. for $C_{14}H_{18}O_5$ 264.0997, EI-MS: *m/z* (relative intensity) 264 (45%), 219 (100%), 125 (26%), 83 (25%).

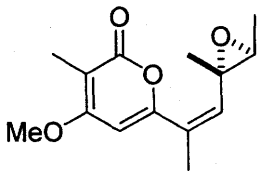

Phomapyrone G (**104**)

^{1}H NMR data in Table 2.1 and ^{13}C NMR data in Table 2.2

HPLC R_t = 23.0 min

UVλ_{max} 230, 330 nm (photodiode array detector)

FTIR (cm^{-1}) 2974, 2929, 1700, 1554, 1247, 1166, 1025

HREI-MS: *m/z* 250.1201, cal. for $C_{14}H_{18}O_4$ 250.1205, EI-MS: *m/z* (relative intensity) 250 (20%), 208 (66%), 139 (49%), 83 (27%).

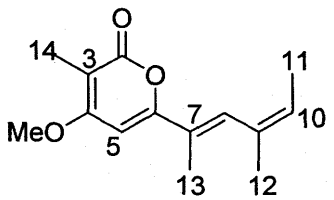

Phomenin B (**105**)

^{1}H NMR data in Table 2.1 and ^{13}C NMR data in Table 2.2

HPLC R_t = 29.6 min

UVλ_{max} 230, 340 nm (photodiode array detector)

FTIR (cm^{-1}) 2956, 2926, 1694, 1556, 1355, 1164, 1013

HREI-MS: *m/z* 234.1262, cal. for $C_{14}H_{18}O_3$ 234.1255, EI-MS: *m/z* (relative intensity) 234 (100%), 219 (67%), 157 (54%), 83 (62%).

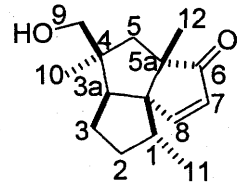

Phomalairdenone D (**114**)

$[\alpha]_D$ = -7.9 (*c* 0.81, CH_2Cl_2)

^1H NMR data and ^{13}C NMR data in Table 2.3

HPLC R_t = 21.7 min

UVλ_{max} 240 nm (photodiode array detector)

FTIR (cm^{-1}): 3454, 2958, 2870, 1697, 1031, 832

HREI-MS: *m/z* 234.1619, cal. for $C_{15}H_{22}O_2$ 234.1619, EI-MS: *m/z* (relative intensity) 234 (81%), 203 (100%), 119 (30%).

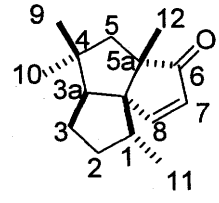

3-Oxosilphinene (**115**)

$[\alpha]_D$ = +0.54 (*c* 0.20, CH_2Cl_2); ^1H NMR data and ^{13}C NMR data in Table 2.3

HPLC Rt = 32.5 min

UVλ_{max} 235 nm (photodiode array detector)

FTIR (cm^{-1}) 2952, 2874, 1708, 1133

HREI-MS: *m/z* 218.1672, cal. for $C_{15}H_{22}O$ 218.1670, EI-MS: *m/z* (relative intensity) 218 (21%), 119 (25), 105 (34%), 77 (41%), 69 (32%), 65 (42%), 91 (100%), 55 (78%); FAB: *m/z* (relative intensity) 219 (16%); CI: *m/z* (relative intensity) 219 (100%);

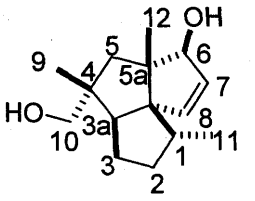

Phomalairdenol B (**116**)

$[\alpha]_D$ = -36 (*c* 1.2, CH_2Cl_2)

^{1}H NMR data in Table 2.4 and ^{13}C NMR data in Table 2.5

FTIR (cm^{-1}) 3287, 2953, 2868, 1373, 1037

HREI-MS: *m/z* 236.1774, cal. for $C_{15}H_{24}O_2$ 236.1776, EI-MS: *m/z* (relative intensity) 236.17 (27.2%), 205.15 (100%), 203.14 (40.5%), 91.05 (48.5%)

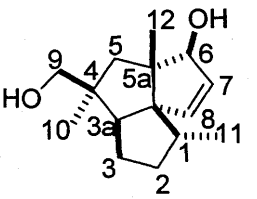

Phomalairdenol A (**117**)

$[\alpha]_D$ = +21 (*c* 0.50, CH_2Cl_2)

^{1}H NMR data in Table 2.4 and ^{13}C NMR data in Table 2.5

FTIR (cm^{-1}) 3352, 2951, 2871, 1375, 1024, 996

HREI-MS: *m/z* 236.1773, cal. for $C_{15}H_{24}O_2$ 236.1776, EI-MS: *m/z* (relative intensity) 236 (19%), 205 (100%), 122 (35%).

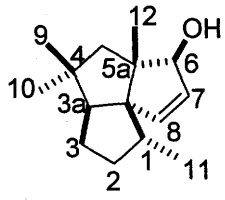

Phomalairdenol C (**118**)

$[\alpha]_D$ = +32 (*c* 1.2, CH_2Cl_2)

^1H NMR data in Table 2.4 and ^{13}C NMR data in Table 2.5

FTIR (cm^{-1}) 3323, 2925, 2873, 1373, 1021

HREI-MS: *m/z* 220.1830, cal. for $C_{15}H_{24}O_1$ 220.1827, EI-MS: *m/z* (relative intensity) 220(100%), 205 (62%), 163 (55%), 123 (92%).

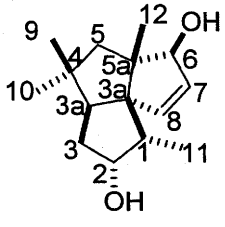

Phomalairdenol D (**119**)

$[\alpha]_D$ = +45 (*c* 0.40, CH_2Cl_2)

^1H NMR data in Table 2.4 and ^{13}C NMR data in Table 2.5

FTIR (cm^{-1}) 3323, 2952, 1459, 1076, 1025

HREI-MS: *m/z* 236.1773, cal. for $C_{15}H_{24}O_2$ 236.1776, EI-MS: *m/z* (relative intensity) 236 (60%), 218 (100%), 203 (85%), 163 (49%), 107 (61%).

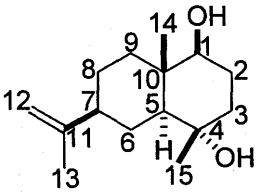

Lairdinol A (**120**)

$[\alpha]_D$ = +18 (*c* 0.40, CH_2Cl_2)

^1H NMR data and ^{13}C NMR data in Table 2.6

FTIR (cm^{-1}) 3379, 2932, 2856, 1382, 1073

HREI-MS: *m/z* 238.1936, cal. for $C_{15}H_{26}O_2$ 238.1932, EI-MS: *m/z* (relative intensity) 238 (27%), 220 (41%), 179 (49%), 162 (66%), 72 (100%).

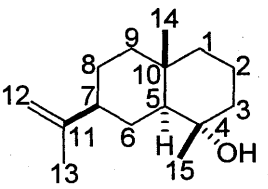

Selin-11-en-4α-ol (**121**)

$[\alpha]_D$ = +1.1 (*c* 0.25, CH_2Cl_2)

^1H NMR data and ^{13}C NMR data in Table 2.6

FTIR (cm^{-1}) 3366, 2926, 2851, 1381, 1057

HREI-MS: *m/z* 222.1997, cal. for $C_{15}H_{26}O$ 222.1983, EI-MS: *m/z* (relative intensity) 222 (27%), 149 (100%), 137 (50%), 95 (42%), 81 (91%).

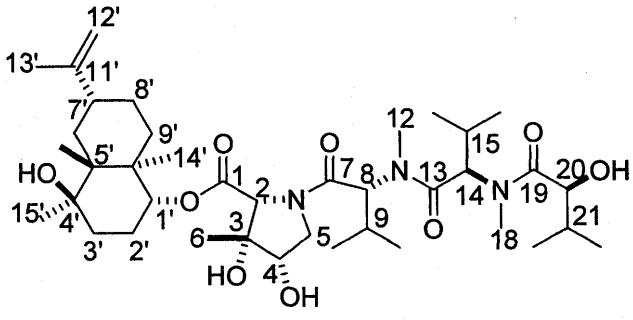

Depsilairdin (**122**)

$[\alpha]_D$ = -65 (*c* .90, CH_2Cl_2); λ_{max} (log ε) 207 (3.6) nm;

^1H NMR data and ^{13}C NMR data in Table 2.7;

FTIR (cm^{-1}) 3449, 2962, 2931, 1753, 1635, 1455, 1385, 1199;

HREI-MS: *m/z* 707.4703, cal. for $C_{12}H_{14}O_4$ 707.4702, EI-Ms: *m/z* (relative intensity) 707 (11%), 634 (49%), 578 (45%), 521 (39%), 465 (100%).

4.2.3 Hydrolysis of depsilairdin

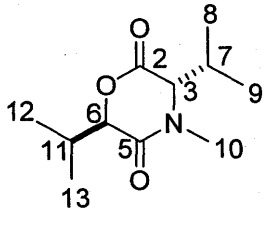

123

Depsilairdin (6 mg) was dissolved in MeOD (400 μL) and added into an NMR tube. This was followed by addition of 100 μL DCl (37%), and then the reaction mixture was kept at room temperature. The reaction progress was monitored employing ^1H NMR spectroscopy. The reaction was run for two weeks until the reference proton signals at δ_H

5.29 and at δ_H 5.34 disappeared completely in the ^1H NMR spectrum of the reaction mixture. After completion of the reaction, the reaction mixture was neutralized and concentrated to dryness on a rotary evaporator. The residue was chromatographed on prep. TLC (0.25 mm, silica gel, 10×20 cm^2) and developed several times with CH_2Cl_2-methanol (90:10) to yield **123**. Further, **123** was purified by HPLC using Laird 2 method (0.4 mg). ^1H NMR (C_6D_6): δ_H 4.37 (d, J = 2 Hz, 1H-6), 3.22 (d, J = 6 Hz, 1H-3), 2.66 (m, 1H-11), 2.38 (s, 3H-10), 1.60 (m, 1H-7), 0.99 (d, J = 7 Hz, 3H-12), 0.98 (d, J = 7 Hz, 3H-13), 0.73 (d, J = 7 Hz, 3H-8), 0.61 (d, J = 7 Hz, 3H-9); ^{13}C NMR (C_6D_6): δ 165.4 (s), 165.3 (s), 81.7 (d), 67.2 (d), 33.5 (q), 31.8 (d), 30.97 (d), 19.4 (q), 18.7 (q), 18.2 (q), 15.7 (q)

4.2.4 Determination of the absolute stereochemistry of 123 by synthesis

Preparation of (R)-2-hydroxy-3-methylbutanoic acid from (R)-valine

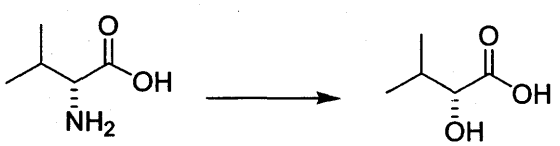

124 **125**

(*R*)-valine (**124**, 200 mg, 1.7 mmol) was placed into a 25 mL round bottom flask, fitted with a septum, and water (4 mL) was added. The reaction vessel was cooled to 0 °C, and sulfuric acid (2N, 1.2 mL) was added dropwise by using a syringe while the mixture was being stirred. After the (R)-valine (**124**) was dissolved in the acidic mixture, addition of sodium nitrite solution (2N, 1.2 mL) was started dropwise at the same rate as addition of 2N sulfuric acid. After the addition was complete, the reaction was stirred at 0 °C for 3 h and then allowed to stir at room temperature for 12 h. The reaction mixture was extracted with EtOAc (5 × 30 mL), and the combined extracts were dried over

Na_2SO_4, filtered, and concentrated (167.5 mg). The resulting crude solid was recrystallized from ether-hexane (40:60) to afford (*R*)-2-hydroxy-3-methylbutanoic acid (**125**, 77%) (Li et al., 1990). $[\alpha]_D$ = -19 (*c* 1.8, $CHCl_3$). ^1H NMR ($CDCl_3$): δ_H 0.95 (d, *J* = 7 Hz, 3H), δ_H 1.08 (d, *J* = 7 Hz, 3H), δ_H 2.17 (m, 1H), δ_H 4.17 (d, *J* = 3 Hz, 1H); ^{13}C NMR ($CDCl_3$): δ_C 16.3 (s), 70.3 (d), 32.8 (d), 19.1 (q), 16.3 (q)

Preparation of (*S*)-2-hydroxy-3-methylbutanoic acid from (*S*)-valine

132 **133**

(*S*)-valine (**132**, 500 mg, 4.0 mmol) was placed into a 50 mL round bottom flask, fitted with a septum, and water (6 mL) was added. The reaction vessel was cooled to 0°C, and sulfuric acid (2N, 3 mL) was added dropwise by using the syringe while the mixture was being stirred. After (*S*)-valine (**132**) was dissolved in the acidic mixture, sodium nitrite solution (2N, 3 mL) was added dropwise at the same rate as the addition of sulfuric acid solution. Following this, the reaction was stirred at 0 °C for 3 h and then at room temperature for another 12 h. The reaction was stopped and the mixture was extracted with EtOAc (5 × 50 mL). The combined extracts were dried over Na_2SO_4, filtered, and concentrated (446 mg). The resulting crude solid was recrystallized from ether-hexane (40:60) to afford (*S*)-2-hydroxy-3-methylbutanoic acid (**133**, 72%) (Li et al., 1990). $[\alpha]_D$ = +18 (*c* 1.5, $CHCl_3$). ^1H NMR ($CDCl_3$): δ_H 0.95 (d, *J* = 7 Hz, 3H), δ_H 1.08 (d, *J* = 7 Hz, 3H), δ_H 2.17 (m, 1H), δ_H 4.17 (d, *J* = 3 Hz, 1H); ^{13}C NMR ($CDCl_3$): δ_C 16.3 (s), 70.3 (d), 32.8 (d), 19.1 (q), 16.3 (q)

Protection of the amino group of (*R*)-valine

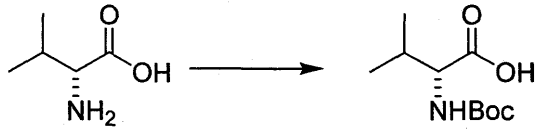

124 **144**

A solution of di-*tert*-butyldicarbonate [$(Boc)_2O$] (1.12 g, 5.1 mmol) in dioxane (4 mL) was added to an ice-cold solution of (*R*)-valine (**124**, 55 mg, 4.3 mmol) in 1N sodium hydroxide (8.9 mL) by means of an addition funnel under stirring. The two-phase mixture was stirred at 5 °C for 30 min, then allowed to warm to room temperature over 6 h at which time TLC analysis showed the completion of the reaction. The dioxane was evaporated and then the aqueous layer was washed with Et_2O (30 mL). EtOAc (50 mL) was then added to the aqueous layer, and the mixture was stirred while 1M H_2SO_4 was added to give pH of 2-3. Following the separation of the organic layer, the aqueous layer was then saturated with NaCl and extracted with EtOAc (4 × 40 mL). The combined organic extracts were dried over Na_2SO_4, filtered and the solvent was removed under vacuum to give Boc-valine (**144**) quantitatively as a thick oil (Campbell et al., 1998).

Preparation of (*R*)-Boc-Me-Valine

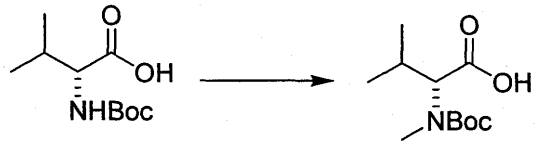

144 **129**

The *tert*-butyloxycarbonylamino acid (**144**, 933 mg, 4.3 mmol) and methyl iodide (2.2 mL, 35.0 mmol) were dissolved in THF (12 mL), and sodium hydride dispersion (567 mg, 12.9 mmol) was added cautiously with gentle stirring to the solution at 0 °C. The suspension was stirred under an argon atmosphere (balloon) at room temperature for 24 h. The reaction was quenched with the addition of EtOAc (50 mL), followed by dropwise addition of water. The mixture was evaporated to dryness, and the oily residue was partitioned between ether (20 mL) and water (50 mL). The ether layer was washed with aqueous $NaHCO_3$ (50 mL), and the combined aqueous extracts acidified to pH 3 with 5% aqueous citric acid. The product was extracted into EtOAc (2 × 30 mL), and the EtOAc extract was washed first with water (2 × 30 mL), followed by with 5% aqueous sodium thiosulfate solution (2 × 30 mL) and then with water (30 mL). Next the EtOAc extract was dried over Na_2SO_4 and evaporated to give a pale yellow oil, Boc-N-MeValine (**129**, 76 %) (Cheung and Benoiton, 1977).

Coupling of (*R*)-2-hydroxy-3-methylbutyric acid and (*S*)-Cbz-MeValine

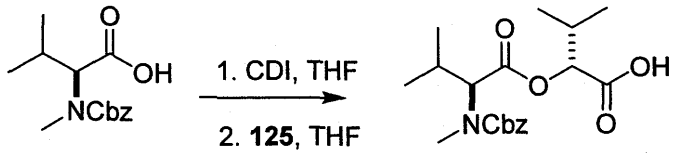

126 **145**

A solution of N,N'-carbonyldiimidazole (CDI) (67 mg, 0.4 mmol) in THF (1 mL) was added to a solution of Cbz-Me-Valine (**126**, 110 mg, 0.4 mmol) in THF (1 mL) and the mixture was stirred under an argon atmosphere at room temperature for 4 h. This was followed by the addition of (*R*)-2-hydroxy-3-methylbutyric acid (**125**, 24.0 mg, 0.2 mmol) in THF (1 mL). After the mixture had been stirred for another 30 h at room temperature the solvent was removed *in vacuo*. The residue was subjected to FCC and eluted with hexane-EtOAc-HOAc (20:6:1) to obtain eight fractions. The combined fractions F5-to-F7 were further subjected to PTLC and developed with hexane-EtOAc-HOAc (20:10:1; for four times) to yield **145** (74%) (Koch et al., 2003).

Deprotection of the amino group by hydrogenolysis of 145

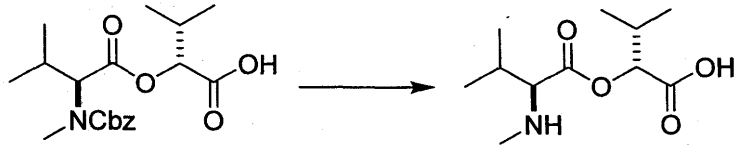

145 **127**

Compound **145** (54 mg, 0.24 mmol) was dissolved in 2 mL of methanol, followed by the addition of Pd/C (10%, 12 mg) and the mixture was vigorously stirred under an H_2 atmosphere (balloon) for 2 h to 2 1/2 h. Then the mixture was filtered with the aid of

Celite, and the combined filtrate and washings were concentrated on a rotary evaporator to yield **127** quantitatively (Ward et al., 1999).

Synthesis of (3*S*,6*R*)-3,6-diisopropyl-4-methyl-2,5-dioxomorpholine (128)

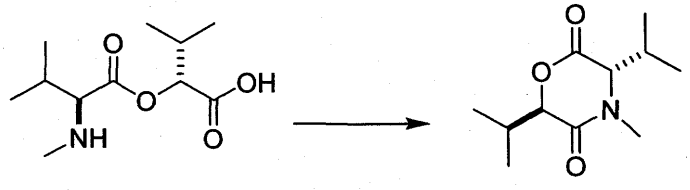

127 **128**

Compound **127** (16 mg, 0.06 mmol) was suspended in CH_2Cl_2 (4 mL) and treated with 2-chloro-1-methylpyridinium iodide (26 mg, 0.10 mmol). After addition of triethylamine (24 μL, 0.18 mmol), the reaction mixture was kept under reflux for 4 h. Finally the solvent was removed *in vacuo*. The residue was purified by subjecting to PTLC and developing with CH_2Cl_2-MeOH (95:5, for two times) to obtain **128** (69.7%) (Koch et al., 2003). $[\alpha]_D$= +168 (*c* 0.94, CH_2Cl_2); ^{1}H NMR ($CDCl_3$): δ_H 0.94 (d, J = 7 Hz, 3H), 1.07 (d, J = 7 Hz, 3H), 1.14 (d, J = 7 Hz, 3H), 1.17 (d, J = 7 Hz, 3H), 2.30 (m, 1H), 2.64 (m, 1H), 3.05 (s, 3H), 3.87 (d, J = 6 Hz, 1H), 4.73 (d, J = 2 Hz, 1H); ^{13}C NMR ($CDCl_3$): δ_C 15.7 (q), 18.6 (q), 19.2 (q), 20.0 (q), 30.8 (q), 32.2 (d), 34.7 (d), 67.8 (d), 82.3 (d), 165.9 (s), 166.3 (s).

Coupling reaction between (*R*)-2-hydroxy-3-methylbutyric acid and (*R*)-Boc-MeVal

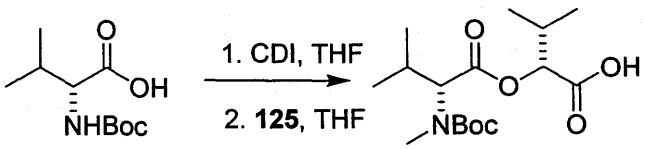

129 **130**

A solution of N,N'-carbonyldiimidazole (CDI) (74 mg, 0.45 mmol) in THF (1 mL) was added to a solution of (*R*)- Boc-Me-Valine (**129**, 105 mg, 0.4 mmol) in THF (1 mL) and the mixture was stirred under an argon atmosphere at room temperature for 4 h. This was followed by the addition of (*R*)-2-hydroxy-3-methylbutyric acid (**125**, 24.0 mg, 0.2 mmol) in THF (1 mL). After the mixture had been stirred for another 30 h at room temperature, the solvent was removed *in vacuo*. The residue was subjected to FCC and eluted with hexane-EtOAc-HOAc (20:6:1) to obtain eight fractions. The combined fractions F2-to-F4 were further subjected to PTLC and developed with hexane-EtOAc-HOAc (20:6:1; for four times) to yield **130** (74%) (Koch et al., 2003).

Synthesis of (3*R*,6*R*)-3,6-diisopropyl-4-methyl-2,5-dioxomorpholine (131*)*

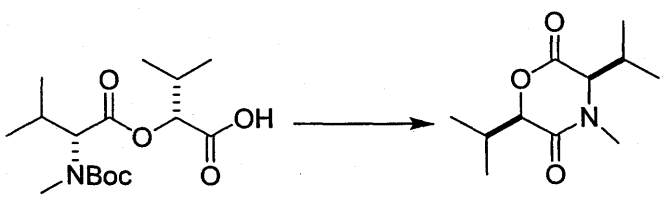

130 **131**

Compound **130** (43 mg, 0.13 mmol) was dissolved in formic acid (5 mL, 98 %) and the solution was kept at room temperature for 2 h. The excess formic acid was removed on a rotary evaporator (<30°C). The residue obtained was suspended in CH_2Cl_2 (4 mL), and followed by the addition of 2-chloro-1-methylpyridinium iodide (68 mg, 0.26 mmol) and triethylamine (52 μL, 0.39 mmol). The reaction mixture was kept under reflux for 8 h. Finally, the solvent was removed *in vacuo*. The residue was subjected to PTLC and developed with CH_2Cl_2-MeOH (95:5, two times) to obtain **131** (70%). $[\alpha]_D = +31$ (*c* 0.95, CH_2Cl_2) ^1H NMR ($CDCl_3$): δ_H 1.06 (d, J = 7 Hz, 3H), 1.08 (d, J = 7 Hz, 3H), 1.15 (d, J = 7 Hz, 3H), 1.2 (d, J = 7 Hz, 3H), 2.30 (m, 1H), 2.33 (m, 1H), 3.04 (s, 3H), 3.85 (d, J = 6 Hz, 1H), 4.53 (d, J = 6 Hz,1H); ^{13}C NMR ($CDCl_3$): δ_C 18.6 (q), 19.4 (q), 20.0 (q), 20.4 (q), 32.7 (d), 32.8 (q), 34.7 (d), 66.8 (d), 84.0 (d), 165.4 (s), 165.7 (d)

Coupling reaction between (*S*)-2-hydroxy-3-methylbutyric acid (133) and (*R*)-Boc-Me-Val (129)

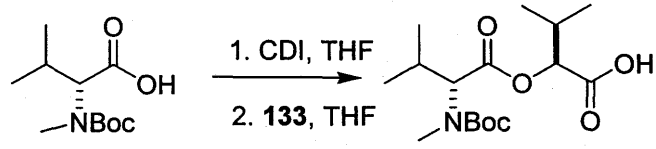

129 **134**

A solution of N,N'-carbonyldiimidazole (CDI) (74 mg, 0.45 mmol) in THF (1 mL) was added to a solution of (*R*)- Boc-Me-Valine (**129**, 105 mg, 0.4 mmol) in THF (1 mL) and the solution was stirred under an argon atmosphere at room temperature for 4 h. This was followed by the addition of (*R*)-2-hydroxy-3-methylbutyric acid (**133**, 24.0 mg, 0.2 mmol) in THF (1 mL). After the mixture had been stirred for another 30 h at room temperature the solvent was removed *in vacuo*. The residue was subjected to FCC and eluted with hexane-EtOAc-HOAc (20:6:1) to obtain eight fractions. The combined

fractions F5-to-F7 were further subjected to PTLC and developed with hexane-EtOAc-HOAc (20:10:1; for four times) to yield **134** (74%).

Synthesis of (3R,6S)-3,6-diisopropyl-4-methyl-2,5-dioxomorpholine (135)

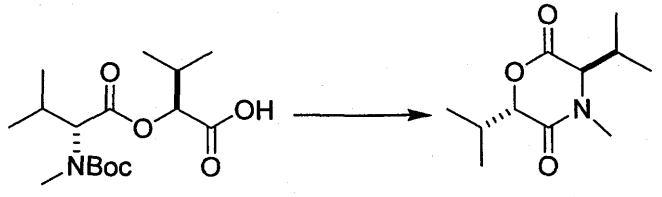

134 **135**

Compound **134** (62 mg, 0.19 mmol) was dissolved in formic acid (5 mL, 98 %) and the solution was kept at room temperature for 2 h. The excess formic acid was removed on a rotary evaporator (<30°C), then the residue was suspended in CH_2Cl_2 (4 mL) and treated with 2-chloro-1-methylpyridinium iodide (95 mg, 0.38 mmol). After addition of triethylamine (76 μL, 0.57 mmol), the reaction mixture was kept under reflux for 4 h. Finally the solvent was removed in vacuo. The residue was purified by subjecting to PTLC and developing with CH_2Cl_2-MeOH (95:5, two times) to obtain **135** (69.7%). $[\alpha]_D$ = -179 (*c* 1.15, CH_2Cl_2); ^1H NMR ($CDCl_3$): δ_H 0.94 (d, *J* = 7Hz, 3H), 1.07 (d, *J* = 7 Hz, 3H), 1.14 (d, *J* = 7 Hz, 3H), 1.17 (d, *J* = 7 Hz, 3H), 2.30 (m, 1H), 2.64 (m, 1H), 3.05 (s, 3H), 3.87 (d, *J* = 6 Hz, 1H), 4.73 (d, *J* = 2 Hz, 1H); ^{13}C NMR ($CDCl_3$): δ_C 15.7 (q), 18.6 (q), 19.2 (q), 20.0 (q), 30.8 (q), 32.2 (d), 34.7 (d), 67.8 (d), 82.3 (d), 165.9 (s), 166.3 (s).

4.3 Metabolites from the cultures of Mayfair 2 in PDB medium

Cultures of Mayfair 2 isolate were grown in PDB medium under constant cool fluorescent light at 23 ± 2 °C for six days. The cultures (PDB) were filtered, and the broth was combined (30 L) and extracted with EtOAc (800 mL × 3/1L broth). The combined EtOAc extracts were dried over anhydrous sodium sulfate and evaporated to dryness on a rotary evaporator (5.4 g). EtOAc extracts (PDB) was fractionated on RP-FCC (1 cm × 10 cm, RP-C18, 50 mL fractions) and eluted with CH_3CN-H_2O (80:20, 300 mL) followed by CH_3CN-H_2O (30:70, 100 mL) and then CH_3CN (100 mL). Fractions collected were concentrated to dryness under reduced pressure. All phytotoxic fractions were further subjected to more elaborate chromatography as follows. F7 (24.0 mg) from RP-FCC of EtOAc extracts was further subjected to PTLC (CH_2Cl_2-EtOAc, 70:30, multiple elution) to give non-homogeneous material. The non-homogenous PTLC fraction was subjected to HPLC (semi-prep. TLC) and eluted with a gradient solvent system: from 25% CH_3CN-75% H_2O to 38% CH_3CN-62% H_2O for 15 min and then from 38% CH_3CN-62% H_2O to 100% CH_3CN for 5 min. Fraction F3 containing the compound (R_t = 12.4 min) was subjected repeatedly to HPLC (semi-PTLC) for purification, and yielded non-homogenous fractions.

Fractions F2 and F3 from RP-FCC of EtOAc extracts were combined (76.4 mg), further subjected to FCC (1 cm × 10 cm, silica gel, 25 mL fractions). The column was eluted first with CH_2Cl_2-EtOAc (70:30, 100 mL), and followed by CH_2Cl_2-EtOAc (60:40, 75 mL). All fractions were evaporated under reduced pressure. Fractions F2 and F3 from this FCC were combined (24 mg) and chromatographed on P TLC (CH_2Cl_2-EtOAc, 60:40, developed twice) to give compound A (6.5 mg). Compound A (6.5 mg) was further purified by semi-prep. HPLC using gradient solvent system (75% H_2O - 25% CH_3CN to 100% CH_3CN over 25 minutes) to yield 3.5 mg.

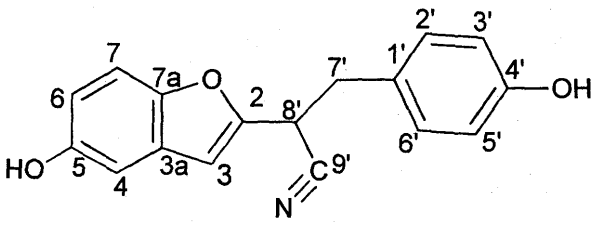

Compound A (**136**)

^{1}H NMR data and ^{13}C NMR data in Table 2.9

$[\alpha]_D = +1.8$ (*c* 0.25, CH_3OH)

HPLC R_t = 12. 4 min

UV λ_{max} 230, 290 nm (photodiode array detector)

FTIR (cm^{-1}): 3375, 2928, 2256, 1610

HREI: *m/z* 279.0896, cal. for $C_{17}H_{13}O_3N$ 279.0895, EI-MS: *m/z* (relative intensity) 279 (8%), 107 (100%)

4.4 Biosynthetic studies of Phomapyrones

4.4.1 A preliminary study

a) Condition I

The liquid culture of Mayfair 2 isolate was grown in minimal medium under constant cool fluorescent light at 23 ± 2 °C. The four-day-old culture was filtered, and the mycelia obtained were further used for inoculating 100 mL sterile distilled water in 250 mL Erlenmeyer flasks. The culture was fed with sodium acetate at a concentration of 100 mg/L at 24 and 48h. The culture was incubated for six days under constant cool fluorescent light at 23 ± 2 °C. The control culture was made by inoculating mycelia in 100 mL sterile distilled water in 250 mL Erlenmeyer flasks. In the course of the experiment, samples (15 mL) were withdrawn from the treated culture as well as from the control at 48, 96 and 144 h, and extracted with EtOAc (3 × 10 mL). The combined extracts were dried, concentrated to dryness on a rotary evaporator, and then analyzed by HPLC.

b) Condition II

The liquid culture of Mayfair 2 isolate was grown in minimal medium under constant cool fluorescent light at 23 ± 2 °C. The four-day-old culture was filtered, and the mycelia were employed to inoculate 100 mL of a solution of glucose (200 mg) in sterile distilled water in 250 mL Erlenmeyer flasks. The culture was fed with sodium acetate at a concentration of 100 mg/L at 24 and 48 h. Control culture was prepared by inoculating 100 mL of a solution of glucose (200 mg) in sterile distilled water with mycelia. The culture was kept on a shaker at 110 rpm under constant cool fluorescent light at 23 ± 2 °C for a total of six days of incubation. In the course of the experiment, samples (15 mL) were withdrawn from the treated culture as well as from the control at 48, 96 and 144 h, and extracted with EtOAc (3 × 10 mL). The combined extracts were dried over

anhydrous Na_2SO_4, concentrated to dryness on a rotary evaporator, and then analyzed by HPLC.

c) Condition III

The sterile minimal medium was inoculated with pycnidiospores of Mayfair 2 isolate at a concentration of 5×10^8 spores/100 mL of culture medium. The culture was fed with sodium acetate at a concentration of 100 mg/L at 48 and 72 h. Similarly, the control culture was made by inoculating the minimal medium with pycnidiospores of Mayfair 2 isolate at a concentration of 5×10^8 spores/100 mL of culture medium. Both treated and control cultures were kept on a shaker at 110 rpm under constant cool fluorescent at 23 ± 2 °C for six days of the incubation. During the course of the experiment, samples (15 mL) were withdrawn from treated culture as well as from the control at 48, 96 and 144 h, and extracted with EtOAc (3 × 10 mL). The combined extracts were dried over anhydrous Na_2SO_4, concentrated to dryness on a rotary evaporator, and then analyzed by HPLC.

4.4.2 Feeding experiment using [2-^{13}C]acetate

Minimal medium (2 L) was prepared and autoclaved. The culture was prepared by inoculating the medium at a concentration of 5×10^8 spores per 100 mL of culture medium in 250 mL Erlenmeyer flasks. Incubations were carried out on a shaker at 120 rpm under fluorescent light for six days. The culture was fed twice with [2-^{13}C]acetate at a concentration of 25 mg [2-^{13}C]acetate per 100 mL of culture at 48 and 72 h. After six days of the incubation period, the culture was removed and filtered, and the broth was extracted with EtOAc (800 mL × 3/1 L broth). The EtOAc extracts were dried over anhydrous Na_2SO_4 and concentrated to dryness under reduced pressure to give 32 mg residue. EtOAc extract (32 mg) were chromatographed on the RP-FCC (1 cm × 10 cm, RP- C18, 20 mL fractions) and eluted first with CH_3CN-H_2O (40-60, 160 mL) followed

by CH_3CN (40 mL). Ten fractions were collected and concentrated to dryness under reduced pressure. Fractions F5 and F6 were combined (5.0 mg) and further subjected to PTLC (hexane-EtOAc, 90:10, multiple elution) to yield phomapyrone A (3 mg).

4.4.3 Feeding experiment using [1,2-$^{13}C_2$]acetate

Minimal medium (5 L) was prepared and autoclaved. The culture medium was added in 100 mL portions into 250 mL Erlenmeyer flasks and inoculated at a concentration of 5 × 10^8 spores per 100 mL of culture medium. Incubations were carried out on a shaker at 120 rpm under fluorescent light at 23 ± 2 °C. The culture was fed twice with [1,2-^{13}C]acetate at a concentration of 25 mg [1,2-^{13}C]acetate per 100 mL of culture at 48 and 72 h. The culture was removed after six days of incubation period and filtered, and the broth was extracted with EtOAc (800 mL × 3/1 L broth). The EtOAc extract was dried over anhydrous $NaSO_4$ and concentrated to dryness under reduced pressure to give 120 mg residue. EtOAc extract (32 mg) was chromatographed on the RP-FCC (1 cm ×10 cm, RP- C18, 20 mL fractions) and eluted first with CH_3CN-H_2O (40-60, 160 mL) followed by CH_3CN (40 mL). Ten fractions was collected and concentrated to dryness under reduced pressure. Fractions F5 and F6 were combined (20.0 mg) and further subjected to prep. TLC (hexane-EtOAc, 90:10, multiple elution) to yield phomapyrone A (4 mg).

4.4.4 Feeding experiment using sodium[2-^{13}C]malonate

Minimal medium (10 L) was prepared and autoclaved. The culture medium was added in 100 mL portions into 250 mL Erlenmeyer flasks and inoculated at a concentration of 5 × 10^8 spores per 100 mL of culture medium. Incubations were carried out on a shaker at 120 rpm under fluorescent light. The culture was fed twice with sodium[2-^{13}C]malonate at a concentration of 25 mg sodium[2-^{13}C]malonate per 100 mL of culture at 48 and 72 h. The culture was removed after six days and filtered, and the broth was extracted with EtOAc (800 mL × 3/1 L broth). The EtOAc extract was dried

over anhydrous Na_2SO_4 and concentrated to dryness under reduced pressure to give 210 mg of residue. EtOAc extract (210 mg) of broth from the cultures fed with [2-^{13}C]malonate was chromatographed on the RP-FCC (1 cm × 10 cm, RP- C18, 20 mL fractions) and eluted first with CH_3CN-H_2O (40-60, 160 mL) followed by CH_3CN (40 mL). Ten fractions were collected and concentrated to dryness under reduced pressure. Fractions F5 and F6 were combined (22 mg) and further subjected to prep. TLC (hexane-EtOAc, 90:10, multiple elution) to yield phomapyrone A (7 mg).

4.4.5 Feeding experiment using [3,3,3-d_3]propionate

Minimal medium (5 L) was prepared and autoclaved. The culture medium was added in 100 mL portions into 250 mL Erlenmeyer flask and inoculated at a concentration of 5×10^8 spores per 100 mL of culture medium. Incubations were carried out on a shaker at 120 rpm under fluorescent light. The culture was fed twice with [3,3,3-d_3] propionate at a concentration of 50 mg per 100 mL of culture at 48 and 72 h. The culture was removed after six days of the incubation and filtered, and the broth was extracted with EtOAc (800 mL × 3/1 L broth). The EtOAc extract was dried over anhydrous Na_2SO_4 and concentrated to dryness under reduced pressure to give 140 mg residue. EtOAc extract (140mg) was subjected to FCC (2 cm × 15 cm, silica gel, 50 mL fractions) and eluted first with CH_2Cl_2 (200 mL) followed by CH_2Cl_2-MeOH (40:60, 200 mL). Eight fractions were collected and concentrated to dryness under reduced pressure. Fractions F5 and F6 were combined (39.0 mg) and further subjected to prep. TLC (hexane-EtOAc, 90:10, multiple elution) to yield phomapyrone A (5 mg).

4.5 Phytotoxicity assays

Canola (*Brassica napus*) cv.Westar, white mustard (*Sinapis alba*) cv.Ochre and brown mustard (*Brassica juncea*) cv.Cutlass plants were grown in a growth chamber,

with 16 h light (fluorescent and incandescent, 450-530 μ mol / s m^2) / 8 h dark at 24 ± 2 °C. The phytotoxicity assays of fractions and isolated compounds from Mayfair 2 cultures grown both in minimal medium and PDB medium were conducted on leaves of two-week-old canola plants (*B.napus*, *B.juncea* and *S. alba*). Samples of the fractions were prepared at a concentration of 1 mg/ml in 50% aqueous methanol. For isolated compounds, the concentrations of samples were 5×10^{-4} M and 1×10^{-3} M in 50% aqueous methanol. To carry out the phytotoxicity assays, two-week-old plant leaves, two leaves from each plant, were punctured at four places with a needle and inoculated at each spot with 10 μl sample. Control leaves were treated similarly employing 50% aqueous methanol. Plants were incubated in a growth chamber and the diameter of the lesions was measured after 7 days incubation period. Results were recorded using a digital camera and lesions were also measured utilizing the following scale: 0=1-2 mm, 1=3-4 mm, 2=4-7 mm, 3=8-10 mm, 4=11-14 mm

4.6 Brine shrimp Lethality assay

The eggs of brine shrimp (*Artemia salina*) were incubated in a Petri dish containing saline water (3.8 g sodium chloride per litre of water) under constant cool fluorescent light at 23 ± 2 °C for 48 h. The test solution was prepared by dissolving the compound in 25 μL methanol followed by addition of saline water to make the final concentration 5×10^{-4} M in 5 mL saline water. The control solution was prepared by adding 25 μL methanol into 5 mL saline water. This was followed by addition of 10 brine shrimp larvae into vials containing 5 ml test and control solutions. The vials were stoppered and kept under constant cool fluorescent light at 23 ± 2 °C for 24 h. After 24 hours, the live brine shrimp larvae in each vial were counted. Each compound was assayed in triplicate.

4.7 HPLC analysis of cultures of Thlaspi isolates

A total of sixteen Thlaspi isolates were obtained from Agriculture and Agri-Food Canada. Solid cultures of Thlaspi isolates were grown on V8 agar medium under constant cool fluorescent light at 23 ± 2 °C. The spores were collected after 14 days of incubation. The spores collected were stored in sterile water at –20°C. The fungal culture for each Thlaspi isolate was grown in triplicate in 250 mL Erlenmeyer flasks containing 100 mL of culture medium. Minimal medium was employed to grow the fungal cultures. Spores were inoculated at a concentration of 5×10^8 spores per 100 mL of culture medium, and the culture was incubated under constant cool fluorescent light at 23 ± 2 °C on a shaker at 110 rpm. During the time course of the experiment, the production of a metabolite was examined by taking 15 mL broth from each flask at 72, 96, and 144 h, and extracted twice with EtOAc (15 mL). The EtOAc extract was dried over anhydrous Na_2SO_4, concentrated to dryness, and analyzed by HPLC.

4.8 Phytoalexins from *Thlaspi arvense*

4.8.1 Time-course study for the production of phytoalexins

Thlaspi arvense plants were grown in a growth chamber with a 16 h photoperiod (20 ± 0.5 °C) at ambient humidity. Four week old *Thlaspi arvense* plants were sprayed with a $CuCl_2$ (2 mmol) solution at 0, 24 and 48 h, and incubated for two more days. Three leaves were excised at the petiole from treated and control plants at 24, 48, 72 and 96 h. The fresh leaves were frozen in liquid nitrogen, crushed, and then extracted with EtOAc. The EtOAc extract was dried over anhydrous Na_2SO_4, and evaporated under reduced pressure. The residues from both elicited and control leaves were weighted and then analyzed by HPLC.

4.8.2 Elicitation of phytoalexins with Laird 2 and Thlaspi isolates

Leaves from *Thlaspi arvense* plants were cut, and the petiole of each leaf was rubbed with cotton wool. Sample leaves were damaged slightly by scraping with sharps and dipped into Laird 2 spore suspension (10^6 spores/mL). Sample leaves as well as control leaves were placed into a Petri dishes with 3-5 mL of water, and then sealed with parafilm. The culture was incubated with a 16 h photoperiod (20 ± 0.5 °C) for seven days. After the incubation, the leaves were frozen, crushed, and extracted with EtOAc. The EtOAc extract was filtered and concentrated under reduced pressure. The EtOAc extracts from treated leaves and control leaves were analyzed by HPLC.

4.8.3 Elicitation, extraction and isolation of phytoalexins from *T. arvense* plants

Four week old *Thlaspi arvense* plants were sprayed with $CuCl_2$ solution (2×10^{-3} M) after every 24 h for three consecutive days. All leaves were collected (182 g) at 72 h, frozen in liquid nitrogen, crushed, and extracted twice with EtOAc. The EtOAc extracts were combined, filtered and concentrated to dryness under reduced pressure. The residue (0.74 g) was column chromatographed (2 cm × 15 cm, silica gel, 100 mL fractions) and eluted first with CH_2Cl_2 (400 mL) followed by CH_2Cl_2/MeOH (97:3, 400 mL) and then with CH_2Cl_2/MeOH (94:6, 400 mL). All fractions collected were concentrated to dryness under reduced pressure.

Fractions F2-F4 from FCC on EtOAc extracts were combined (39 mg), subjected to FCC (1 cm × 10 cm, 50 mL silica gel) and eluted with CH_2Cl_2/hexane (30:70, 200 mL) followed by CH_2Cl_2/hexane (50:50, 200 mL) and finally with CH_2Cl_2 (200 mL). The twelve fractions collected were concentrated to dryness under reduced pressure. Fractions F10-to-F12 containing the elicited metabolite of R_t = 22.9 min were combined (18 mg)

and further subjected to PTLC (0.25 cm, 20 × 20 cm, silica gel). It was developed twice with CH_2Cl_2/MeOH (98:2) to yield **142** (1 mg).

Fractions F7 and F8 from FCC of EtOAc extracts were combined (60.5 mg), and subjected to FCC and eluted first with CH_2Cl_2/MeOH (99:1, 200 mL) followed by CH_2Cl_2/MeOH (97:3, 200 mL). All fractions collected were concentrated to dryness under reduced pressure. Fractions F4 and F5 were combined and further subjected to RP-FCC (0.5 cm × 5 cm, 10 mL, RP-C18) and eluted with CH_3CN/H_2O (30:70, 10 mL) to obtain **38** (1.5 mg).

Fractions F9-F12 were combined, further subjected to RP-FCC (1 cm × 10 cm, 10 mL, RP-C18), and eluted with CH_3CN/H_2O (35:65, 20 mL) to obtain eight fractions. F2 and F3 were combined, further purified by subjecting to another RP-FCC (CH_3CN/H_2O, 25:75, 10 mL) to obtain **143**.

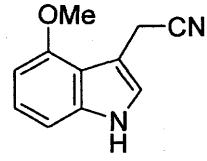

arvelexin (**142**)

^{1}H NMR data and ^{13}C NMR data in Table 2.17

HPLC t_R = 22.8 min

λ_{max} (log ε) 220 (3.5) nm; 266 (3.4) nm

FTIR (cm^{-1}) 3396, 2955, 2850, 2251, 1619, 1590, 1259, 1089

HREI-MS: *m/z* 186.0788, cal. for $C_{11}H_{10}ON_2$ 186.0793, EI-MS: *m/z* (relative intensity) 186(99%), 171 (100%).

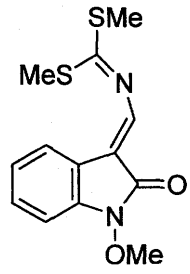

wasalexin A (**38**)

HPLC t_R = 29.2 min

λ_{max} (log ε) 205 (3.6) nm; 285(4.0) nm; 368(3.9) nm

^{1}H NMR (CD_2Cl_2): δ_H 2.73 (s, 2×3H), 4.05 (s, 3H), 7.00 (d, *J* = 7.5 Hz, 1H), 7.07 (ddd, *J* = 7.5, 7.5, 1 Hz, 1H), 7.30 (ddd, *J* = 7.5, 7.5, 1 Hz, 1H), 7.89 (d, *J* = 7.5 Hz).

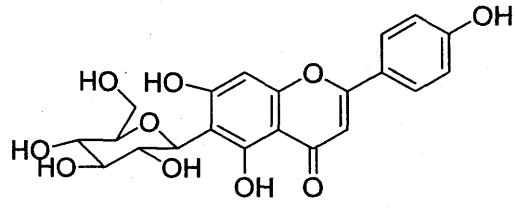

isovitexin (**143**)

HPLC R_t = 4.7 min

$[\alpha]_D$ = 17.2 (*c* 0.37, MeOH)

λ_{max} (log ε) 204 (3.3) nm; 273 (3.6) nm; 302 (3.5) nm, 331 (3.6) nm

HREI-FAB: *m/z* 433.1128 (M^++1), cal. for $C_{21}H_{21}O_{10}$ 433.1134, EI-FAB: *m/z* (relative intensity) 433(100%), 299 (18%).

4.8.4 Preparation of 4-methoxyindole-3-acetonitrile

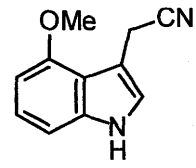

142

Methylmagnesium iodide-diethyl ether complex was prepared by treating magnesium turnings (20 mg, 0.83 mmol) in diethylether with excess methyl iodide. The reaction was stopped when all of the magnesium was consumed. A solution of 4-methoxyindole (25 mg, 0.16 mmol) in 500 µl Et_2O was added dropwise into the reaction mixture containing methylmagnesium iodide. The reaction mixture was stirred for 15 min. Bromoacetonitrile (90 µL, 1.3 mmol) was added dropwise into the mixture and the reaction was allowed to stir for an hour at room temperature under argon. Then the reaction mixture was concentrated to dryness and the residue was suspended in 40 mL of distilled water. The mixture was quenched with 0.5 mL of 2M HCl solution. The aqueous phase was extracted twice with CH_2Cl_2 (20 mL), dried over $MgSO_4$, and concentrated to dryness (54 mg). The purification of 4-methoxyindole-3-acetonitrile (**142**) was effected by FCC with CH_2Cl_2/hexane (40:60) to give 52% yield. 4-Methoxyindole-3-acetonitrile (**142**): ^1H NMR data and ^{13}C NMR data in Table 2.17; FTIR (cm^{-1}) 3396, 2955, 2850, 2251,1619, 1590, 1259, 1089; HREI-MS: *m/z* 186.0788, cal. for $C_{11}H_{10}ON_2$ 186.0793, EI-MS: *m/z* (relative intensity) 186.07 (99.5%), 171.05 (100%).

4.8.5 Mycelial radial growth bioassays

The antifungal bioassay was conducted on BJ 125 (virulent isolate), Mayfair 2 (avirulent Polish type isolates), and Thl-9 (weakly virulent isolates) with 4-methoxyindole-3-acetonitrile and wasalexin A using a mycelial radial growth bioassay. The phytoalexin dissolved in DMSO (5×10^{-2} M) was used to mix with PDA to make treatment mixtures of 5×10^{-4} M, 3×10^{-4} M, and 1×10^{-4} M. The control was PDA containing 0.1% DMSO. The treatment mixtures and control were poured onto a twelve-well-Petri plate, each mixture in three wells, and allowed to solidify. Each well was inoculated by placing an agar plug (4 mm) cut from the edges of 5-day-old solid cultures of the isolates upside down at the center of each well. The Petri plate was sealed with parafilm, and incubated under constant light at 23 ± 2 °C for 96 h. The radius of the mycelial area was measured at 24 h intervals starting at 48 h until full growth of mycelia in the control wells was observed. Each assay was repeated twice.

4.8.6 Spore germination bioassays

The spore germination bioassays were carried out on BJ 125 with wasalexin A. A solution of wasalexin A in DMSO (5×10^{-2} M) was used to make treatment mixtures of 5×10^{-4} M and 1×10^{-4} M by mixing with the control mixture (PDA + 2% DMSO + 3% Tween 80). Each treatment mixture and control were added into the wells of a four-well-Petri plate, and inoculated with 10 μL of 10^7spores/mL. Spore germination was examined under an inverted microscope at the magnification of 10 × 40 (400×). Spores germinated were counted after 30 h of incubation in at least 10 view fields for each well.

4.9 Plant-fungal interaction studies

Canola (*Brassica napus*) cv.Westar, white mustard (*Sinapis alba*) cv.Ochre and brown mustard (*Brassica juncea*) cv.Cutlass plants were a grown in growth chamber, with 16 hrs light (fluorescent and incandescent, 450-530 μ mol / s m^2) / 8 hr dark at 24 ± 2 °C. Stems (10-15 cm length) from three-week-old plants, stripped of all leaves and upper bud, were cut into 2 cm pieces, each piece was cut in half longitudinally and then placed in a transparent dish with the cut surface up and inoculated with Mayfair 2 spore suspension (10 μL, 10^7 spores per mL). The control stems were treated with distilled water. The stem pieces were incubated for a week under light at 23 °C. Then stem pieces were grinded using mortar and ground plant tissue was extracted with methanol for 48 h. The methanol was decanted and concentrated to dryness on a rotary evaporator. The resulting residue was fractionated by FCC (2 cm, silica gel, 50 mL) using as eluent CH_2Cl_2 (200 mL), followed by CH_2Cl_2-MeOH (97:3, 200 mL) and finally CH_2Cl_2-MeOH (94:6) to obtain twelve fractions. The fractions from extracts of infected tissue as well as control were analyzed by HPLC equipped with a photodiode array detector.

5. References

Akimitsu, K., Kohmoto, K., Otani, H., Nishimura, S., 1989. Host-specific effects of toxin from the rough lemon pathotype of *Alternaria alternata* on mitochondria. Plant Physiol. 89, 925-31.

Abraham, W. R., Knoch, I., Witte, L., 1990. Biosynthesis of the terpenoidic polyketide fusalanipyrone. Phytochemistry 29, 2877-8.

Avent, A. G., Hanson, J. R., Truneh, A., 1992a. The biosynthesis of nectriapyrone and veropyrone. Phytochemistry 31, 3447-3449.

Avent, A. G., Hanson, J. R., Truneh, A., 1992b. Two pyrones from *Gliocladium vermoesenii*, Phytochemistry 31, 1065-1066.

Ayer, W. A., Pena-Rodriguez, L. M., 1987. Metabolites produced by *Alternaria brassicae*, the black spot pathogen of canola. Part I, the phytotoxic components. J. Nat. Prod. 50, 400-407.

Bailey, J. A.; Mansfield, J. W. Eds., in *Phytoalexins*. Blackie and Son, Glasgow, U.K., 1982, p. 334.

Bains, P. S., Tewari, J. P., 1987. Purification, chemical characterization and host-specificity of the toxin produced by *Alternaria brassicae*. Physiol. Mol. Plant P. 30, 259-271.

Bais, H. P, Vepachedu R., Gilroy S., Callaway R. M., Vivanco J. M., 2003. Allelopathy and exotic plant invasion: from molecules and genes to species interactions. Science 301, 1377-80.

Bais, H. P., Walker, T. S., Stermitz, F. R., Hufbauer, R. A., Vivanco, J., M., 2002. Enantiomeric-dependent phytotoxic and antimicrobial activity of (±)-catechin. A rhizosecreted racemic mixture from spotted knapweed. Plant Physiol. 128, 1173-1179.

Balesdent, M. H., Jedryczka, M., Jain, L., Mendes-Pereira, E., Bertrandy, J., Rouxel, T., 1998. Conidia as a substrate for internal transcribed spacer-based PCR identification of members of the *Leptosphaeria maculans* species complex. Phytopathology 88, 1210-1217.

Bennett, R., Wallsgrove, R. M., 1994. Secondary metabolites in plant defense mechanisms. New Phytol. 127, 617-633.

Bohlmann, F., Jakupovic, J., 1980. Naturally occurring terpene derivatives. 238. New sesquiterpene hydrocarbons with anomalous carbon skeletons from *Silphium* species. Phytochemistry 19, 259-65.

Bohlmann, F., Misra, L. N., Jakupovic, J., Robinson, H., King, R. M., 1984. New sesquiterpene lactone type from *Dugaldia hoopesii*. J. Nat. Prod. 47, 658-662.

Bohm, B. A., Stuessy, T. F., 2001. Flavonoids of the sunflower family (Asteraceae). Springer, Vienna.

Bottini, A. T., Bowen, J. R., Gilchrist, D. G., 1981. Phytotoxins. II. Characterization of a phytotoxic fraction from *Alternaria alternata* f. sp. lycopersici. Tetrahedron Lett. 22, 2723-6.

Bouarab, K., Melton, R., Peart, J., Baulcombe, D., Osbourn, A., 2002. A saponin-detoxifying enzyme mediates suppression of plant defenses. Nature 418, 889-892.

Briggs, L. H., Cambie, R. C., 1958. Extractives of *Vitex lucens*. I. Tetrahedron 3, 269-73.

Brosch, G., Ransom, R., Lechner, T., Walton, J. D., Loidl, P., 1995. Inhibition of maize histone deacetylases by HC toxin, the host-selective toxin of *Cochliobolus carbonum*. Plant Cell 7, 1941-50.

Browne, L. M., Conn, K. L., Ayer, W. A., Tewari, J. P., 1991. The camalexins: new phytoalexins produced in the leaves of *Camelina sativa*. Tetrahedron 47, 3909-14.

Buchwaldt, L., Green, H., 1992. Phytotoxicity of destruxin B and its possible role in the pathogenesis of *Alternaria brassicae*. Plant Pathol. 41, 55-63.

Buchwaldt, L., Jensen, J. S., 1991. HPLC purification of destruxins produced by *Alternaria brassicae* in culture and leaves of *Brassica napus*. Phytochemistry 30, 2311-2316.

Caldas, E. D., Jones, A. D., Ward, Barney, W., Carl, K., Gilchrist, D. G., 1994. Structural characterization of three new AAL toxins produced by *Alternaria alternata* f. sp. lycopersici. J. Agric. Food. Chem. 42, 327-33.

Campbell, A. D., Raynham, T. M., Taylor, J. K., 1998. A simplified route to the (R)-garner aldehyde and (S)-vinyl glycinol. Synthesis 1707-1709.

Cane, D. E., Oliver, J. S., Harrison, P. H. M., Abell, C., Hubbard, B. R., Kane, C. T., Lattman, R., 1990. Biosynthesis of pentalenene and pentalenolactone. J. Am. Chem. Soc. 112, 4513-24.

Cheng, Yi. -Q., Le, L. D., Walton, J. D., Bishop, K. D., 1999. ^{13}C labeling indicates that the epoxide-containing amino acid of HC-toxin is biosynthesized by head-to-tail condensation of acetate. J. Nat. Prod. 62, 143-145.

Cheung, S. T., Benoiton, N. L., 1977. N-Methylamino acids in peptide synthesis. v. the synthesis of N-*tert*-butyloxycarbonyl, N-methylamino acids by N-methylation. Can. J. Chem. 55, 906-910.

Churchill, A. C. L., Dunkle, L. D., Silbert, W., Kennedy, K. J., Macko, V., 2001. Differential synthesis of peritoxins and precursors by pathogenic strains of the fungus *Periconia circinata*. Appl. Environ. Microbiol. 67, 5721-5728.

Ciuffetti, L. M., Pope, M. R., Dunkle, L. D., Daly, J. M., Knoche, H. W., 1983. Isolation and structure of an inactive product derived from the host-specific toxin produced by *Helminthosporium carbonum*. Biochemistry 22, 3507-10.

Comstock, J. C., Scheffer, R. P., 1973. Role of host-selective toxin in colonization of corn leaves by *Helminthosporium carbonum*. Phytopathology 63, 24-9.

Corbett, R. E., Smith, R. A. J., 1967. Selin-11-en-4α-ol from the essential oil of *Podocarpus dacrydioides*. Tetrahedron Lett. 1009-1012.

Curtis, P. J., Greatbanks, D., Hesp, B., Forbes, C. A., Freer, A. A., 1977. Sirodesmins A, B, C, and G, antiviral epipolythiopiperazine-2,5-diones of fungal origin: x-ray analysis of sirodesmin A diacetate. J. Chem. Soc., Perkin Trans. 1: Organic and Bio-Organic Chemistry 2, 180-9.

Cutignano, A., Fontana, A., Renzulli, L., Cimino, G., 2003. Placidenes C-F, novel α-pyrone propionates from the Mediterranean sacoglossan *Placida dendritica*, J. Nat. Prod. 66, 1399-1401.

Danko, S. J., Kono, Y., Daly, J. M., Suzuki, Y., Takeuchi, S., McCrery, David A., 1984. Structure and biological activity of a host-specific toxin produced by the fungal corn pathogen *Phyllosticta maydis*. Biochemistry 23, 759-66.

De March, G., Séguin-Swartz, G., Petrie, G. A., 1986. Virulence and culture filtrate phytotoxicity in *Leptosphaeria maculans*: perspectives for in vitro selection. Can. J. Plant Pathol. 8, 422-428.

De Marzo, V., Marin, A., Vardaro, R. R., De Petrocellis, L., Villani, G., Cimino, G., 1993. Histological and biochemical bases of defense mechanisms in four species of polybranchiodea ascoglossan mollusks. Mar. Biol. 117, 367-380.

Delserone, L. M., McCluskey, K., Matthews, D. E., VanEtten, H. D., 1999. Pisatin demethylation by fungal pathogens and nonpathogens of pea: association with pisatin tolerance and virulence. Physiol. Mol. Plant P. 55, 317-326.

Dewey, R. E., Siedow, J. N., Timothy, D. H., Levings, C. S., 1988. III. A 13-kilodalton maize mitochondrial protein in E. coli confers sensitivity to *Bipolaris maydis* toxin. Science 239, 293-5.

Dubick, J. P., Daly, J. M., Kratky, Z., Macko, V., Acklin, W., Arigoni, D., 1984. Biological activity of the isomeric forms of *Helminthosporium sacchari* toxin and of homologs produced in culture. Plant Physiol. 74, 117-22.

Dunkle, L. D., Macko, V., 1995. Peritoxins and their effects on sorghum. Can. J. Botany 73, S444-S452.

Feng, B., Nakatsuka, S., Goto, T., Tsuge, T., Nishimura, S., 1990. Biosyntheses of host-selective toxins produced by *Alternaria alternata* pathogens. I: (8R,9S)-9,10-epoxy-8-hydroxy-9-methyl-deca-(2E,4Z,6E)-trienoic acid as a biological precursor of AK-toxins. Agr. Biol. Chem. 54, 845-8.

Férézou, J. P., Quesneau-Thierry, A., Servy, C., Zissmann, E., Barbier, M., 1980. Sirodesmin PL biosynthesis in *Phoma lingam* Tode. J. Chem. Soc. Perk. T. 1: Org. Bioorg. Chem. 8, 1739-46.

Férézou, J. P., Riche, C., Quesneau-Thierry, A., Pascard-Billy, C., Barbier, M., Bousquet, J. F., Boudart, G., 1977. Structures of two toxins isolated from cultures of the fungus *Phoma lingam* Tode: sirodesmin PL and deacetylsirodesmin PL. Nouveau Journal de Chimie1, 327-34.

Gabrielson, R. L., 1983. Blackleg disease of crucifers caused by *Leptosphaeria maculans* (Phoma lingam) and its control. Seed Sci. and Technol. 11, 749-780.

Gall, C., Balesdent, M. H., Desthieux, I., Robin, P., Rouxel. T., 1995. Polymorphism of Tox° *Leptosphaeria maculans* isolates as revealed by soluble protein and isozyme electrophoresis. Mycol. Res. 99, 221-229.

Gardner, J. M., Kono, Y., Chandler, J. L., 1986. Bioassay and host-selectivity of *Alternaria citri* toxins affecting rough lemon and mandarins. Physiol. Mol. Plant P. 29, 293-304.

Gardner, J. M., Kono, Y., Tatum, J. H., Suzuki, Y., Takeuchi, S., 1985. Plant pathotoxins from *Alternaria citri*: Part 1. The major toxin specific for rough lemon plants. Phytochemistry 24, 2861-7.

Gardner, J. M., Mansour, Isis S., Scheffer, R. P., 1972. Effects of the host-specific toxin of *Periconia circinata* on some properties of sorghum plasma membranes. Physiol. Plant Pathol. 2, 197-206.

George, H. L., VanEtten, H. D., 2001. Characterization of pisatin-inducible cytochrome P450s in fungal pathogens of pea that detoxify the pea phytoalexin pisatin. Fungal Genet. Biol. 33, 37-48.

Gilchrist, D. G., Grogan, R. G., 1975. Production and nature of a host-specific toxin from *Alternaria alternata* f. sp. lycopersici. Physiology and Biochemistry 66, 165-171.

Gnanamanickam, S. S., 1979. Isolation of isoflavonoid phytoalexins from seeds of *Phaseolus vulgaris* L. Specialia 323.

González-Coloma, A., Valencia, F., Martín, N., Hoffmann, J. J., Hutter, L., Marco, J. A., Reina, M., 2002. Silphinene sesquiterpenes as model insect antifeedants. J. Chem. Ecol. 28, 117-129.

Graniti, A., 1991. Phytotoxins and their involvement in plant diseases. Introduction. Experientia 47, 751-5.

Gugel, R.K., Petrie, G.A., 1992. History, occurrence, impact, and control of blackleg of rapeseed. Can. J. Plant Pathol. 14, 36–45.

Hadacek, F., 2002. Secondary metabolites as plant traits: current assessment and future perspectives. Crit. Rev. Plant Sci. 21, 273-322.

Haëgele, B. F., Wildi, E., Harmatha, J., Pavlik, M., Rowell-Rahier, M., 1998. Long-term effects on food choice of land snail *Arianta arbustorum* mediated by petasin and furanopetasin, two sesquiterpenes from *Petasites hybridus*. J. Chem. Ecol. 24, 1733-1743.

Hain, R., Reif, H. -J., Krause, E., Langebartels, R., Kindl, H., Vornam, B., Wiese, W., Schmelzer, E., Schreier, P. H., Stöcker, R. H., Stenzel, K., 1993. Disease resistance results from foreign phytoalexin expression in a novel plant. Nature 361, 153-156.

Hammerschmidt, R., 1999. Phytoalexins: what have we learned after 60 years? Annu. Rev. Phytopathol. 37, 285-306.

Hammond, K. E., Lewis, B. G. 1987. The establishment of systemic infection in leaves of oilseed rape by *Leptosphaeria maculans*. Plant Pathol. 36, 135-147.

Hanna, G. M., Lau-cam, C. A., 1993. Determination of the optical purity and absolute configuration of *threo*-methylphenidate by proton nuclear magnetic resonance spectroscopy with chiral solvating agent. J. Pharmaceut. Biomed. 11, 665-670.

Harborne, J. B., 1988. The Flavonoids. Advances in research since 1980. Chapman and Hall, London.

Harborne, J. B., Heywood, V. H., Saleh, N. A. M., 1970. Chemosystematics of the compositae: flavonoid patterns in the Chrysanthemum complex of the tribe *Anthemideae*. Phytochemistry 9, 2011-17.

Harborne, J. B., T. J. Mabry, H, Mabry, 1975. The Flavonoids. Chapman and Hall, London.

Harborne, J. B., Turner, B. L. 1984. *Plant Chemosystematics*. Academic Press Inc., London, United kingdom, pp.50-51.

Hatta, R., Ito, K., Hosaki, Y., Tanaka, T., Tanaka, A., Yamamoto, M., Akimitsu, K., Tsuge, T., 2002. A conditionally dispensable chromosome controls host-specific pathogenicity in the fungal plant pathogen *Alternaria alternata*. Genetics 161, 59-70.

Hayashi, N., Tanabe, K., Tsuge, T., Nishimura, S., Kohmoto, K., Otani, H., 1990. Determination of host-selective toxin production during spore germination of Alternaria alternata by high-performance liquid chromatography. Phytopathology 80, 1088-1091.

Hochlowski, J. E., Faulkner, D. J., 1983. Antibiotics from the marine pumonate Siphonaria diemenensis, Tetrahedron Lett. 24, 1917-1920.

Horowitz, R. M., Gentili, B., 1964. Structure of vitexin and isovitexin. Chem. Ind. 12, 498-9.

Howlett, B.J., Idnurm, A., Pedras, M.S.C., 2001. *Leptosphaeria maculans* the causal agent of blackleg disease of Brassicas. Fungal Genet. Biol. 33, 1–14.

Humpherson-Jones, F. M., 1983. Pathogenicity studies on isolates of *Leptosphaeria maculans* from brassica seed production crops in south-east England. Ann. Appl. Biol. 103, 37-44.

Ingham, J. L., 1973. Disease resistance in higher plants. Concept of preinfectional and postinfectional resistance. Phytopathologische Zeitschrift 78, 314-335.

Ingham, J. L., 1978. Phaseollidin, a phytoalexin of *Psophocarpus tetragonolobus.* Phytochemistry 17, 165.

Ingham, J. L., 1979. Phytoalexin production by flowers of garden pea (*Pisum sativum*). J. Bioscience 34, 296-8.

Ito, K., Tanaka, T., Hatta, R., Yamamoto, M., Akimitsu, K., Tsuge, T., 2004. Dissection of the host range of the fungal plant pathogen *Alternaria alternata* by modification of secondary metabolism. Mol. Microbiol. 52, 399-411.

Johal, G. S., Briggs, S. P., 1992. Reductase activity encoded by the HM1 disease resistance gene in maize. Science 258, 985-7.

Johnson, L. J., Johnson, R. D., Akamatsu, H., Salamiah, A., Otani, H., Kohmoto, K., Kodama, M., 2001. Spontaneous loss of a conditionally dispensable chromosome from the *Alternaria alternata* apple pathotype leads to loss of toxin production and pathogenicity. Curr. Genet. 40, 65-72.

Johnson, R. D., Johnson, L., Itoh, Y., Kodama, M., Otani, H., Kohmoto, K., 2000. Cloning and characterization of a cyclic peptide synthetase gene from *Alternaria alternata* apple pathotype whose product is involved in AM-toxin synthesis and pathogenicity. Mol. Plant Microbe In. 13, 742-753.

Johnson, R. D., Lewis, B. G., 1990. DNA polymorphism in *Leptosphaeria maculans.* Physiol. Mol. Plant P. 37, 417-424.

Kato-Noguchi, H., 2004. Allelopathic substance in rice root exudates: rediscovery of momilactone B as an allelochemical. J. Plant Physiol. 161, 271-276.

Kato-Noguchi, H., Tanaka, Y., Murakami, T., Yamamura, S., Fujihara, S., 2002. Isolation and identification of an allelopathic substance from peel of *Citrus junos*. Phytochemistry 61, 849-853.

Kenfield, D. S., Strobel, G. A., 1981. Selective modulation of helminthosporoside binding by alpha-galactoside-binding proteins from sugar cane clones susceptible and resistant to *Helminthosporium sacchari*. Physiol. Plant Pathol. 19, 145-52.

Keri, M., van den Berg, C. G. J., McVetty, P. B. E., Rimmer, S. R., 1997. Inheritance of resistance to *Leptosphaeria maculans* in *Brassica juncea*. Phytopathology 87, 594-598.

Kim, S. D., Knoche, H. W., Dunkle, L. D., 1987. Essentiality of the ketone function for toxicity of the host-selective toxin produced by *Helminthosporium carbonum*. Physiol. Mol. Plant P. 30, 433-40.

Knogge, W., 1996. Fungal infection of plants. Plant cell 8, 1711-1722.

Koch, C., Simonyiová, S., Pabel, J., Kärtner, A., Polborn, K., Wanner, K. T., 2003. Asymmetric synthesis with 6-*tert*-butyl-5-methoxy-6-methyl-3,6-dihydro-2H-1,4-oxazin-2-one as a new chiral glycine equivalent: preparation of enantiomerically pure α-tertiary and α-quaternary α-amino acids. Eur. J. Org. Chem. 1244-1263.

Koch, E., Badawy, H. M., Hoppe, H. H., 1989. Differences between aggressive and non-aggressive single spore lines of *Leptosphaeria maculans* in cultural characteristics and phytotoxin production. J. Phytopathol. 124, 52-62.

Koch, E., Song, K., Osbourn, T. C., Williams, P. H., 1991. Relationship between pathogenicity and phylogeny based on restriction fragment length polymorphism in *Leptosphaeria maculans*. Mol. Plant Microbe In. 4, 341-349.

Kodama, M., Rose, M. S., Yang, G., Yun, S. H., Yoder, O. C., Turgeon, B. G., 1999. The translocation-associated Tox1 locus of *Cochliobolus heterostrophus* is two genetic elements on two different chromosomes. Genetics 151, 585-596.

Kohmoto, K, Itoh, Y., Shimomura, N., Kondoh, Y., Otani, H., Kodama, M., Nishimura, S., Nakatsuka, S., 1993. Isolation and biological activities of two host-specific toxins from the tangerine pathotype of *Alternaria alternata*. Phytopathology 83, 495-502.

Kohmoto, K., Khan, I. D., Renbutsu, Y., Taniguchi, T., Nishimura, S., 1976. Multiple host-specific toxins of *Alternaria mali* and their effect on the permeability of host cells. Physiol. Plant Pathol. 8, 141-53.

Kohmoto, K., Otani, H., 1991. Host recognition by toxigenic plant pathogens. Experientia 47, 755-64.

Kohmoto, K., Scheffer, R. P., Whiteside, J. O., 1979. Host-selective toxins from *Alternaria citri*. Phytopathology 69, 667-671.

Kong, C., Liang, W., Xu, X., Hu, F., Wang, P., Jiang, Y., 2004a. Release and activity of allelochemicals from allelopathic rice seedlings. J. Agr. Food Chem. 52, 2861-2865.

Kong, C., Xu, X., Zhou, B., Hu, F., Zhang, C., Zhang, M., 2004b. Two compounds from allelopathic rice accession and their inhibitory activity on weeds and fungal pathogens. Phytochemistry 65, 1123-1128.

Kono, Y, Danko, S. J., Suzuki, Y., Takeuchi, S., Daly, J. M., 1983. Structure of the host-specific pathotoxins produced by *Phyllosticta maydis*. Tetrahedron Lett. 24, 3803-3806.

Kono, Y., Daly, J. M., 1979. Characterization of the host-specific pathotoxin produced by *Helminthosporium maydis*, race T, affecting corn with Texas male sterile cytoplasm. Bioorg. Chem. 8, 391-7.

Kono, Y., Gardner, J. M., Suzuki, Y., Takeuchi, S., 1985. Plant pathotoxins from *Alternaria citri*: Part 2. The minor ACRL toxins. Phytochemistry 24, 2869-74.

Kono, Y., Gardner, J. M., Takeuchi, S., 1986. Structure of the host-selective toxins produced by a pathotype of *Alternaria citri* causing brown spot disease of mandarins. Agr. Biol. Chem. 50, 801-4.

Kono, Y., Takeuchi, S., Kawarada, A., Daly, J. M., Knoche, H. W., 1980. Studies on the host-specific pathotoxins produced by *Helminthosporium maydis*, race T. Agr. Biol. Chem. 44, 2613-22.

Kono, Y., Takeuchi, S., Kawarada, A., Daly, J. M., Knoche, H. W., 1981. Studies on the host-specific pathotoxins produced in minor amounts by *Helminthosporium maydis*, race T. Bioorg. Chem. 10, 206-18.

Larsen, T. O., Perry, N. B., Anderson, B., 2003. Infectopyrone, a potential mycotoxin from *Alternaria infectoria*. Tetrahedron Lett. 44, 4511-4513.

Leather, G. R., 1987. Weed control using allelopathic sunflowers and herbicide. Plant Soil 98, 17-23.

Li., W., Ewing, W. R., Harris, B. D., Joullié, M. M., 1990. Total synthesis and structural investigations of didemnins A, B, and C. J. Am. Chem. Soc. 112, 7659-7672.

Liakopoulou-Kyriakides, M., Lagopodi, A. L., Thanassoulopoulos, C. C., Stavropoulos, G. S., Magafa, V., 1997. Isolation and synthesis of a host-selective toxin produced by *Alternaria alternata*. Phytochemistry 45, 37-40.

Liebermann, B., Ellinger, R., Gunther, W., Ihn, W., Gallander, H., 1997. Tricycloalternarenes produced by *Alternaria alternata* related to ACTG-toxins. Phytochemistry 46, 297-303.

Liebermann, B., Ellinger, R., Ihn, W., 1994. ACTG-toxins produced by a strain of *Alternaria alternata* that does not originate from *Citrus* species. J. Phytopathol. 140, 385-8.

Liebermann, B., Nussbaum, R.-P., Gunther, W., 2000. Bicycloalternarenes produced by the phytopathogenic fungus *Alternaria alternata*. Phytochemistry 55, 987-992.

Livingston, R. S., Scheffer, R. P., 1984. Selective toxins and analogs produced by *Helminthosporium sacchari*. Production, characterization, and biological activity. Plant Physiol. 76, 96-102.

Logan, B. A., Monson, R. K., Potosnak, M. J., 2000. Biochemistry and physiology of foliar isoprene production. Trends Plant Sci. 5, 477-81.

Macías, F. A., Varela, R. M., Torres A., Molinillo, J. M. G. Heliespirone A., 1998. The first member of a novel family of bioactive sesquiterpenes. Tetrahedron Lett. 39, 427-430.

Macko, V., Acklin, W., Hildenbrand, C., Weibel, F., Arigoni, D., 1983. Structure of three isomeric host-specific toxins from *Helminthosporium sacchari*. Experientia, 39, 343-7.

Macko, V., Goodfriend, K., Wachs, T., Renwick, J. A. A., Acklin, W., Arigoni, D., 1981. Characterization of the host-specific toxins produced by *Helminthosporium sacchari*, the causal organism of eyespot disease of sugar cane. Experientia, 37, 923-4.

Macko, V., Stimmel, M. B., Wolpert, T. J., Dunkle, L. D., Acklin, W., Baenteli, R., Jaun, B., Arigoni, D., 1992. Structure of the host-specific toxins produced by the fungal pathogen *Periconia circinata*. Proc. Natl. Acad. Sci. USA 89, 9574-8.

Macko, V., Wolpert, T. J., Acklin, W., Jaun, B., Seibl, J., Meili, J., Arigoni, D., 1985. Characterization of victorin C, the major host-selective toxin from *Cochliobolus victoriae*: structure of degradation products. Experientia 41, 1366.

Mann, J. 1994. *Chemical aspects of biosynthesis*. Oxford University Press, Oxford, UK, p 2-4.

Marco, J. A., Sanz-Cervera, J. F., Morante, M. D., García-Lliso, V., Vallès-Xirau, J., Jakupovic, J., 1996. Tricyclic sesquiterpenes from *Artmisia chamaemelifolia.* Phytochemistry 41, 837-844.

Masunaka, A., Tanaka, A., Tsuge, T., Peever, T. L., Timmer, L. W., Yamamoto, M., Yamamoto, H., Akimitsu, K., 2000. Distribution and characterization of AKT homologs in the tangerine pathotype of *Alternaria alternata.* Phytopathology 90, 762-768.

McGee, D.C., Petrie, G.A., 1978. Variability of *Leptosphaeria maculans* in relation to blackleg of oilseed rape. Phytopathology, 68, 625–630.

Meeley, R. B., Johal, G. S., Briggs, S. P., Walton, J. D., 1992. A biochemical phenotype for a disease resistance gene of maize. Plant Cell 4, 71-7.

Meeley, R. B., Walton, J. D., 1991. Enzymic detoxification of HC-toxin, the host-selective cyclic peptide from *Cochliobolus carbonum.* Plant Physiol. 97, 1080-6.

Mendes-Pereira, E., Balesdent, M., Brun, H., Rouxel, T., 2003. Molecular phylogeny of the *Leptosphaeria maculans-L. biglobosa* species complex. Mycol. Res. 107, 1287-1304.

Mengistu, A, Rimmer, S. R., Koch, E., Williams, P. H., 1991. Pathogenicity grouping of isolates of *Leptosphaeria maculans* on *Brassica napus* cultivars and their disease reaction profiles on rapid-cycling brassicas. Plant Dis. 75, 1279-1282.

Mesbah, L. A., van der Weerden, G. M., Nijkamp, H. J. J., Hille, J., 2000. Sensitivity among species of Solanaceae to AAL toxins produced by *Alternaria alternata* f.sp. lycopersici. Plant Pathol. 49, 734-741.

Mirov, N. T., 1965. 'The Genus *Pinus.*' Ronald Press, New York.

Morales, V. M., Pelcher, L. E, Taylor, J. L., 1993. Comparison of the 5.8*s* *r*DNA and internal transcribed spacer sequences of isolates of *Leptosphaeria maculans* from different pathogenicity groups. Curr. Genet. 23, 490-495.

Morrissey, J. P., Osbourn, A. E., 1999. Fungal resistance to plant antibiotics as a mechanism of pathogenesis. Microbiol. Mol. Biol. R. 63,708-724.

Müller, M. M., Hallaksela, A. M. A., 1998. Chemotaxonomical method based on FAST-profiles for the determination of phenotypic diversity of spruce needle endophytic fungi. Mycol. Res. 102, 1190-1197.

Nair, M. S. R., Carey, S. T., 1975. Metabolites of pyrenomycetes. II. Nectriapyrone, an antibiotic monoterpenoid. Tetrahedron Lett. 19, 1655-8.

Nakashima, T., Ueno, T., Fukami, H., 1982. Structure elucidation of AK-toxins, host-specific phytotoxic metabolites produced by *Alternaria kikuchiana* Tanaka. Tetrahedron Lett. 23, 4469-72.

Nakashima, T., Ueno, T., Fukami, H., Taga, T., Masuda, H., Osaki, K., Otani, H., Kohmoto, K., Nishimura, S., 1985. Isolation and structures of AK-toxin I and II, host-specific phytotoxic metabolites produced by *Alternaria alternata* Japanese pear pathotype. Agr. Biol. Chem. 49, 807-15.

Nakatsuka, S., Feng, B. N., Goto, T., Tsuge, T., Nishimura, S., 1990. Biosynthesis of host-selective toxins produced by *Alternaria alternata* pathogens. Part 2. Biosynthetic origin of (8R,9S)-9,10-epoxy-8-hydroxy-9-methyldeca-(2E,4Z,6E)-trienoic acid, a precursor of AK-toxins produced by *Alternaria alternata*. Phytochemistry 29, 1529-31.

Nakatsuka, S., Ueda, K., Goto, T., Yamamoto, M., Nishimura, S., Kohmoto, K., 1986. Structure of AF-toxin II, one of the host-specific toxins produced by *Alternaria alternata* strawberry pathotype. Tetrahedron Lett. 27, 2753-6.

Navarre, D. A., Wolpert, T. J., 1999. Victorin induction of an apoptotic/senescence-like response in oats. The Plant Cell 11, 237-249.

Nomoto, M., Tamura, S., 1970. Isolation and identification of indole derivatives in clubroots of Chinese cabbage. Agr. Biol. Chem. 34, 1590-2.

Ohno, S., Tomita-Yokotani, K., Kosemura, S., Node, M., Suzuki, T., Amano, M., Yasui, K., Goto, T., Yamamura, S., Hasegawa, K., 2001. A species-selective allelopathic substance from germinating sunflower (*Helianthus annuus* L.) seeds. Phytochemistry 56, 577-581.

Ohtani, K., Yamamoto, H., Akimitsu, K., 2002. Sensitivity to *Alternaria alternata* toxin in citrus because of altered mitochondrial RNA processing. Proc. Natl. Acad. Sci. USA 99, 2439-2444.

Osbourn, A. E., 1996. Preformed antimicrobial compounds and plant defense against fungal attack. Plant Cell 8, 1821-1831.

Osbourn, A. E., Clarke, B. R., Lunness, P., Scott, P. R., Daniels, M. J. 1994. An oat species lacking avenacin is susceptible to infection by *Geaeumannomyces graminis* var. tritici. Physiol. Mol. Plant P. 45, 457-467.

Otani, H., Kodama, M., Kohmoto, K., 2002. Infection mechanism of black spot pathogen in Japanese pear. Acta Horticulturae 587, 623-630.

Page, J. E., Madrinan, S., Towers, G. H. N., 1994. Identification of a plant growth inhibiting iridoid lactone from Duroia hirsuta, the allelopathic tree of the "Devil's Garden". Experientia 50, 840-2.

Papadopoulou, K., Melton, R. E., Leggett, M., Daniels, M. J., Osbourn, A. E., 1999. Compromised disease resistance in saponin-deficient plants. P. Natl. Acad. Sci. USA 96, 12923-12928.

Park, P., Ohno, T., Nishimura, S., Kohmoto, K., Otani, H., 1987. Leakage of sodium ions from plasma membrane modification, associated with permeability change, in host cells treated with a host-specific toxin from a Japanese pear pathotype of *Alternaria alternata*. Can. J. Bot. 65, 330-339.

Patterson, N. A., Kapoor, M., 1995. Detection of additional restriction fragment length polymorphisms among the weakly virulent (nonaggressive) and highly virulent

(aggressive) isolates of *Leptosphaeria maculans*. Can. J. Microbiol. 41, 1135-1141.

Paxton, J. D., 1981. Phytoalexins-a working redefinition. Phytopathol. Z. 101, 106-209.

Pedras, M. S. C., 1997. Determination of the Absolute Configuration of the Fragments Composing Phomalide. Can. J. Chem. 75, 314-317.

Pedras, M. S. C., 1998. Towards an understanding and control of plant fungal diseases in Brassicaceae. Recent Res. Devel. Agr. Food. Chem. 2, 513–532.

Pedras, M. S. C., 2001. Phytotoxins from fungi causing blackleg disease on crucifers: isolation, structure determination, detection, and phytotoxic activity. Recent Res. Devel. Phytochem. 5, 109-117.

Pedras, M. S. C., Abrams, S. R., Seguin-Swartz, G., 1988. Isolation of the first naturally occurring epimonothiodioxopiperazine, a fungal toxin produced by *Phoma lingam*. Tetrahedron Lett. 29, 3471-4.

Pedras, M. S. C., Abrams, S. R., Seguin-Swartz, G., Quail, J. W., Jia, Z., 1989. Phomalirazine, a novel toxin from the phytopathogenic fungus *Phoma lingam*. J. Am. Chem. Soc. 111, 1904-5.

Pedras, M. S. C., Biesenthal, C. J., 1998. Production of the host-selective toxin phomalide by isolates of *Leptosphaeria maculans* and its correlation with sirodesmin PL production. Can. J. Microbiol. 44, 547–553.

Pedras, M. S. C., Biesenthal, C. J., 2000. HPLC analyses of cultures of *Phoma spp.*: differentiation among groups and species through secondary metabolite profiles. Can. J. Microbiol. 46, 685-691.

Pedras, M. S. C., Biesenthal, C. J., 2001. Isolation, structure determination, and phytotoxicity of unusual dioxopiperazines from the phytopathogenic fungus *Phoma lingam*, Phytochemistry 58, 905-909.

Pedras, M. S. C., Chumala, P. B., Quail, J. W., 2004a. Chemical mediators: the remarkable structure and host-selectivity of depsilairdin, a sesquiterpenic depsipeptide containing a new amino acid. Org. Lett. 6, 4615-4617.

Pedras, M. S. C., Chumala, P. B., Suchy, M., 2003a. Phytoalexins from *Thlaspi arvense*, a wild crucifer resistant to virulent *Leptosphaeria maculans*: structures, syntheses and antifungal activity. Phytochemistry 64, 949-956.

Pedras, M. S. C., Erosa-López, C. C., Quail, J. W., Taylor, J. L., 1999a. Phomalairdenone: a new host-selective phytotoxin from a virulent type of the blackleg fungus *Phoma lingam*. Bioorg. Med. Chem. Lett. 9, 3291–3294.

Pedras, M. S. C., Jha, M., Ahiahonu, P. W. K., 2003b. The Synthesis and Biosynthesis of Phytoalexins Produced by Cruciferous Plants. Curr. Org. Chem. 7, 1635-1647.

Pedras, M. S. C., Montaut, S., Suchy, M., 2004b. Phytoalexins from the crucifer rutabaga: structures, syntheses, biosyntheses, and antifungal activity. J. Org. Chem. 69, 4471-6.

Pedras, M. S. C., Montaut, S., Zaharia, I. L., Gai, Y., Ward, D. E., 2003c. Biotransformation of the Host-selective Toxin Destruxin B by Wild Crucifers: Probing a Detoxification Pathway. Phytochemistry 64, 957-963.

Pedras, M. S. C., Morales, V. M., Taylor, J. L., 1993a. Phomaligols and phomaligadiones: new metabolites from the blackleg fungus. Tetrahedron 49, 8317-8322.

Pedras, M. S. C., Morales, V. M., Taylor, J. L., 1994. Phomapyrones: three metabolites from the blackleg fungus. Phytochemistry 36, 1315-1318.

Pedras, M. S. C., Nycholat, C. M., Montaut, S., Xu, Y., Khan, A. K., 2002. Chemical defenses of crucifers: elicitation and metabolism of phytoalexins and indole-3-acetonitrile in brown mustard and turnip. Phytochemistry 59, 611-625.

Pedras, M. S. C., Okanga, F. I., Zaharia, I. L, Khan, A. Q., 2000. Phytoalexins from crucifers: synthesis, biosynthesis, and biotransformation. Phytochemistry 53, 161-176.

Pedras, M. S. C., Séguin-Swartz, G., 1990. Rapid high-Performance liquid chromatographic analysis of phytotoxins from *Phoma lingam*. J. Chromatogr. 519, 383-386.

Pedras, M. S. C., Séguin-Swartz, G., Abrams, S. R., 1990. Minor phytotoxins from the blackleg fungus *Phoma lingam*. Phytochemistry 29, 777-782.

Pedras, M. S. C, Séguin-Swartz, G., 1992. The blackleg fungus: phytotoxins and phytoalexins. Can. J. Plant Pathol. 14, 67-75.

Pedras, M. S. C., Smith, K. C., 1997. Sinalexin, a phytoalexin from white mustard elicited by destruxin B and *Alternaria Brassicae*. Phytochemistry 46, 833-837

Pedras, M. S. C., Smith, K. C., Taylor, J. L., 1998. Production of 2,5-dioxopiperazine by a new isolate type of the blackleg fungus *Phoma lingam*. Phytochemistry 49, 1575-1577.

Pedras, M. S. C., Sorensen, J. L., Okanga, F. I., Zaharia, I. L., 1999b. Wasalexins A and B, new phytoalexins from wasabi: isolation, synthesis, and antifungal activity. Bioorg. Med. Chem. Lett. 9, 3015-3020.

Pedras, M. S. C., Taylor, J. L., Morales, V. M., 1995. Phomaligin A and other yellow pigments in *Phoma lingam* and *P. wasabiae*. Phytochemistry 38, 1215-1222.

Pedras, M. S. C., Taylor, J. L., Morales, V. M., 1996. The blackleg fungus of rapeseed: how many species?. Acta Horticulturae 407, 441–446.

Pedras, M. S. C., Taylor, J. L., Nakashima, T. T., 1993b. A novel chemical signal from the blackleg fungus: beyond phytotoxins and phytoalexins. J. Org. Chem. 58, 4778-4780.

Pedras, M. S. C., Zaharia, I. L., Gai, Y., Smith, K. C., Ward, D. E., 1999c. Metabolism of the host-selective toxins destruxin B and homodestruxin B: probing a plant disease resistance trait. Org. Lett. 1, 1655-1658.

Pedras, M. S. C., Zaharia, I.L., Gai, Y., Zhou, Y., Ward, D.E., 2001. In *planta* sequential hydroxylation and glycosylation of a fungal phytotoxin: avoiding cell death and overcoming the fungal invader. Proc. Natl. Acad. Sci. USA 98, 747-752.

Pedras, M.S.C., Sorensen, J.L., 1998. Phytoalexin accumulation and production of antifungal compounds by the crucifer wasabi. Phytochemistry 49, 1959-1965.

Petrie, G. A., Vanterpool, T. C., 1968. The occurrence of *Leptosphaeria maculans* on *Thlaspi arvense*. Can. J. Botany 46, 869-871.

Pope, M. R., Ciuffetti, L. M., Knoche, H. W., McCrery, D., Daly, J. M., Dunkle, L. D. 1983. Structure of the host-specific toxin produced by *Helminthosporium carbonum*. Biochemistry 3505-3506.

Pringle, R. B., Scheffer, R. P., 1963. Purification of the selective toxin of *Periconia circinata*. Phytopathology 53, 785-7.

Pringle, R. B., Scheffer, R. P., 1967. Multiple host-specific toxins from *Periconia circinata*. Phytopathology 57, 530-4.

Purwantara, A., Barrins, J. M., Cozijnsen, A. J., Ades, P. K., Howle, B. J., 2000. Genetic diversity of isolates of the *Leptosphaeria maculans* species complex from Australia, Europe and North America using amplified fragment length polymorphism analysis. Mycol. Res. 104, 772-781.

Ramarathnam, N., Osawa, T., Namiki, M., Kawakishi, S., 1989. Chemical studies on novel rice hull antioxidants. 2.Identification of isovitexin, a C-glycosyl flavonoid. J. Agr. Food Chem. 37, 316-19.

Reddy, P. V., Patel, R., White, J. F., Jr.,1998. Phylogenetic and developmental evidence supporting reclassification of cruciferous pathogens *Phoma lingam* and *Phoma wasabiae* in *Plenodomus*. Can. J. Bot. 76, 1916-1922.

Roberts, M. F., Wink, M.,1998. Alkaloids. Biochemistry, ecology, and medicinal applications. Plenum Press, New York.

Romano, I., Bellitti, M. R., Nicolaus, B., Lama, L., Manca, M. C., Pagnotta, E., Gambacorta, A., 2000. Lipid profile: a useful chemotaxonomic marker for classification of a new cyanobacterium in *Spirulina* genus. Phytochemistry 54, 289-294.

Rose, M. S., Yun, S.-H., Asvarak, T., Lu, S.-W., Yoder, O. C., Turgeon, B. G., 2002. A decarboxylase encoded at the *Cochliobolus heterostrophus* translocation-associated Tox1B locus is required for polyketide (T-toxin) biosynthesis and high virulence on T-cytoplasm maize. Mol. Plant Microbe In. 15, 883-893.

Scheffer, R. P. 1997. *The nature of disease in plants*. Cambridge University Press, Cambridge, United Kingdom. pp 179-209.

Scheffer, R. P., Livingston, R. S., 1980. Sensitivity of sugarcane clones to toxin from *Helminthosporium sacchari* as determined by electrolyte leakage. Phytopathology 70, 400-4.

Scheffer, R. P., Livingston, R. S., 1984. Host-selective toxins and their role in plant diseases. Science 223, 17-21.

Scheffer, R. P., Nelson, R. R., Ullstrup, A. J., 1967. Inheritance of toxin production and pathogenicity in *Cochliobolus carbonum* and *Cochliobolus victoriae*. Phytopathology 57, 1288-91.

Scheffer, R. P., Pringle, R. B., 1961. A selective toxin produced by *Periconia circinata*. Nature 191, 912-13.

Scheffer, R. P., Pringle, R. B., 1963. Respiratory effects of the selective toxin of *Helminthosporium victoriae*. Phytopathology 53, 465-8.

Scheffer, R. P., Ullstrup, A. J., 1965. A host-specific toxic metabolite from *Helminthosporium carbonum*. Phytopathology 55, 1037-8.

Schulz, B., Boyle, C., Draeger, S., Römmert, A. K., Krohn, K., 2002. Endophytic fungi: a source of novel biologically active secondary metabolites. Mycol. Res. 106, 996-1004.

Shoemaker, R. A., Brun, H., 2001. The telemorph of the weakly aggressive segregate of *Leptosphaeria maculans*. Can. J. Bot. 79,412-419.

Siler, D. J., Gilchrist, D. G. 1983. Properties of host specific toxins produced by *Alternaria alternata* f. sp. *lycopersici* in culture and in tomato plants. Physiol. Plant Pathol. 23, 265-74.

Sippell, D. W., Hall, R., 1995. Glucose phosphate isomerase polymorphisms distinguish weakly virulent from highly virulent strains of *Leptosphaeria maculans*. Can. J. Plant Pathol. 17, 1-6.

Smith, C. J., 1996. Accumulation of phytoalexins: Defense mechanism and stimulus response system. New Phytol. 132, 1-45.

Soga, O., 1976. Isolation of flaviolin from the potato culture solution of *Phoma wasabiae* Yokogi.Zeitschrift fuer Naturforschung, Teil B: Anorganische Chemie, Organische Chemie 31B, 124-5.

Somda, I., Renard, M., Brun, H., 1996. Morphology, pathogenicity and isozyme variation amongst French isolates of *Leptosphaeria maculans* recovered from *Brassica juncea* cv. Picra. Plant Pathol. 45, 1090-1098.

Steiner, G. W., Byther, R. S., 1971. Partial characterization and use of a host-specific toxin from *Helminthosporium sacchari* on sugarcane. Phytopathology, 61, 691-5.

Strobel, G. A., 1973. Biochemical basis of the resistance of sugarcane to eyespot disease. P. Natl. Acad. Sci. USA 70, 1693-6.

Strobel, G. A., Hess, W. M., 1974. Evidence for the presence of the toxin-binding protein on the plasma membrane of sugarcane cells. P. Natl. Acad. Sci. USA 71, 1413-17.

Strobel, G. A., Steiner, G. W., 1972. Runner lesion formation in relation to helminthosporoside in sugarcane leaves infected by *Helminthosporium saccharin.* Physiol. Plant Pathol. 2, 129-32.

Strobel, G. A., Steiner, G. W., Byther, R., 1975. Deficiency of toxin-binding protein activity in mutants of sugarcane clone H54-775 as it relates to disease resistance. Biochem. Genet. 13, 557-65.

Suzuki, Y., Coleman, L. W., Daly, J. M., Kono, Y., Knoche, H. W., Takeuchi, S., 1987. Synthesis and biological activity of mimics of PM-toxins, the host-specific corn pathotoxin produced by *Phyllosticta maydis*. Phytochemistry 26, 687-696.

Suzuki, Y., Danko, S. J., Kono, Y., Daly, J. M., Knoche, H. W., Takeuchi, S., 1988. Studies on the conformations of PM-toxin, the host-specific corn pathotoxin produced by *Phyllosticta maydis*. Agr. Biol. Chem. 52, 15-24.

Suzuki, Y., Kono, Y., Takahashi, Y., Suenaga, K., Daly, J. M., Knoche, H. W., Sakurai, A., 1991. Toxic activity of mimics of the host-specific pathotoxin PM-toxin on corn carrying Texas male-sterile cytoplasm. Agr. Biol. Chem. 55, 1061-70.

Suzuki, Y., Tegtmeier, K. J., Daly, J. M., Knoche, H. W., 1982. Analogs of host-specific phytotoxin produced by *Helminthosporium maydis,* race T. II. Biological activities. Bioorg. Chem. 11, 313-21.

Takasugi, M., Katsui, N., Shirata, A., 1986. Isolation of three novel sulfur-containing phytoalexins from the Chinese cabbage *Brassica campestris* L. ssp. *pekinensis* (Cruciferae). J. Chem. Soc., Chem. Comm. 14, 1077-8.

Tanaka, A., Shiotani, H., Yamamoto, M., Tsuge, T., 1999. Insertional mutagenesis and cloning of the genes required for biosynthesis of the host-specific AK-toxin in the Japanese pear pathotype of *Alternaria alternata*. Mol. Plant Microbe In. 12, 691-702.

Taylor, J. L., Borgmann, I., Séguin-Swartz, G., 1991. Electrophoretic karyotyping of *Leptosphaeria maculans* differentiates highly virulent from weakly virulent isolates. Curr.Genet., 19, 273-277.

Taylor, L., Pedras, M. S. C., Morales, V. M., 1995. Horizontal transfer in the phytopathogenic fungal genus *Leptosphaeria* and host-range expansion. Trends Microbiol. 3, 202–206.

Thappa, R. K., Dhar, K. L., Atal, C. K., 1979. Isointermedeol, a new sesquiterpene alcohol from *Cymbopogon flexuosus*. Phytochemistry 18, 671-2.

Tomiyama, K., Sakuma, T., Ishizaka, N., Sato, N., Katsui, N., Takasugi, M., Masamune, T., 1968. New antifungal substance isolated from resistant potato tuber tissue infected by pathogens. Phytopathology 58, 115-16.

Tringali, C., Parisi, A., Piattelli, M., Magnano Di San Lio, G. 1993. Phomenins A and B, bioactive polypropionate pyrones from culture fluids of *Phoma tracheiphila*. Nat. Pro. Lett. 3, 101-106.

Ueda, K., Xiao, J. Z., Doke, N., Nakatsuka, S., 1992. Structure of BZR-cotoxin II produced by *Bipolaris zeicola* race 3, the cause of leaf spot disease in corn. Tetrahedron Lett. 33, 5377-5380.

Ueda, K., Xiao, J. Z., Doke, N., Nakatsuka, S., 1994. Structure of BZR-cotoxin I produced by *Bipolaris zeicola* race 3, the cause of leaf spot disease in corn. Tetrahedron Lett. 35, 7033-7036.

Ueda, K., Xiao, J. Z., Doke, N., Nakatsuka, S., 1995a. Isolation and structure of BZR-cotoxin IV produced by *Bipolaris zeicola* race 3, the cause of leaf spot disease in corn. Tetrahedron Lett. 36, 741-744.

Ueda, K.; Xiao, J. Z.; Doke, N.; Nakatsuka, S.-I., 1995b. Structure of BZR-cotoxin III produced by *Bipolaris zeicola* race 3, the cause of leaf spot disease in corn. Nat. Pro. Lett. 6, 43-48.

Ueno, T., 1990. Secondary metabolites related to host selection by plant pathogenic fungi. Pure and Appl. Chem. 62, 1347-1352.

Ueno, T., Hayashi, Y., Nakashima, T., Fukami, H., Nishimura, S., Kohmoto, K., Sekiguchi, A., 1975a. Isolation of AM-toxin I, a new phytotoxic metabolite from *Alternaria mali*. Phytopathology 65, 82-3.

Ueno, T., Nakashima, T., Hayashi, Y., Fukami, H., 1975b. Structures of AM-toxin I and II, host specific phytotoxic metabolites produced by *Alternaria mali*. Agr. Biol. Chem. 39, 1115-22.

Van Dam, N. M., Vuister, L. W. M., Bergshoeff, C., De Vos, H., van der Meijden, E., 1995. The "RAISON D'ÊTRE" of pyrrolizidine alkaloids in *Cynoglossum officinale*: deterrent effects against generalist herbivores. J. Chem. Ecol. 21, 507-523.

VanEtten, H. D., Mansfield, J. W., Bailey, J. A., Farmer, E. E., 1994. Two classes of plant antibiotics: phytoalexins versus "phytoanticipins". Plant Cell 6, 1191-2.

VanEtten, H. D., Matthews, D. E., Matthews, P. S., 1989. Phytoalexin detoxification: importance for pathogenicity and practical implications. Annu. Rev. Phytopathol. 27, 143-64.

Vardaro, R. R., De Marzo, V., Marin, A., Cimino, G., 1992. α-and γ-pyrone-polypropionates from the Mediterranean ascoglossan mollusk *Ercolania funereal* Tetrahedron 48, 9561-9566.

Vyvyan, J. R., 2002. Allelochemicals as leads for new herbicides and agrochemicals. Tetrahedron 58, 1631-1646.

Walton, J. D., 1996. Host-selective toxins: agents of compatibility. The Plant Cell 8, 1723-1733.

Walton, J. D., Earle, E. D., 1983. The epoxide in HC toxin is required for activity against susceptible maize. Physiol. Plant Pathol. 22, 371-6.

Walton, J. D., Earle, E. D., Gibson, B. W., 1982. Purification and structure of the host-specific toxin from *Helminthosporium carbonum* race 1. Biochem. Bioph. Res. Co. 107, 785-94.

Ward, D. E., Vazquez, A., Pedras, M. S. C., 1996. Understanding host-Selective phytotoxicity: synthesis and biological discrimination of phomalide and its (Z)-isomer. J. Org. Chem. 61, 8008-8009.

Ward, D. E., Vazquez, A., Pedras, M. S. C., 1999. Probing host-selective phytotoxicity: synthesis and biological activity of phomalide, isophomalide, and dihydrophomalide. J. Org. Chem. 64, 1657-1666.

Waterman, P. G. *Chemical taxonomy of alkaloids*. M. F. Roberts & M. Wink (Eds.), Alkaloids: Biochemistry, Ecology, and Medicinal Applications, Plenum Press, New York, USA, 1998, pp. 87-105.

Weston, L. A., Duke, S. O., 2003. Weed and crop allelopathy. Crit. Rev. Plant Sci. 22, 367-389.

Weyerstahl, P., Marschall-Weyerstahl, H., Schröder, M., Brendel, J., Kaul, V. K., 1991. Functionalised silphiperfolenes from *Artemisia laciniata*. Phytochemistry 30, 3349-3352.

Williams, C. A., Greenham, J., Harborne, J. B., 2001. The role of lipophilic and polar flavonoids in the classification of temperate members of the *Anthemideae*. Biochem. Syst. Ecol. 29, 929-945.

Williams, P. H., 1992. Biology of Leptosphaeria maculans. Can. J. Plant Pathol. 14, 30-35.

Williams, R. H., Fitt, B. D., 1999. Differentiating A and B groups of *Leptosphaeria maculans*, causal agent of stem canker (blackleg) of oilseed rape. Plant Pathol. 48, 161–175.

Wink, M., 2003. Evolution of secondary metabolites from an ecological and molecular phylogenetic perspective. Phytochemistry 64, 3-19.

Wolpert, T. J., Macko, V., 1989. Specific binding of victorin to a 100-kDa protein from oats. Proc. Natl. Acad. Sci. USA 86, 4092-4096.

Wolpert, T. J., Macko, V., Acklin, W., Jaun, B., Arigoni, D. 1986. Structure of minor host-selective toxins from *Cochliobolus victoriae*. Experientia 42, 1296.

Wolpert, T. J., Navarre, D. A., Moore, D. L., Macko, V., 1994. Identification of the 100-kD victorin binding protein from oats. Plant Cell 6, 1145-55.

Xiao, J. Z., Tsuge, T., Doke, N., 1992. Further evaluation of the significance of BZR-toxin produced by *Bipolaris zeicola* race 3 in pathogenesis on rice and maize plants. Physiol. Mol. Plant P. 40, 359-370.

Xiao, J. Z., Tsuge, T., Doke, N., Tsuda, M., Nishimura, S., 1991. Rice-specific toxins produced by *Bipolaris zeicola*, race 3, evidence for role as pathogenicity factors for rice and maize plants. Physiol. Mol. Plant P. 38, 67-82.

Yoder, O. C., 1973. A selective toxin produced by *Phyllosticta maydis*. Phytopathology 63, 1361-1366.